Defining a Role for Prostanoid Receptor EP_4 in the Developmental Programming of the Ductus Arteriosus

By

Michael Thomas Yarboro

Dissertation

Submitted to the Faculty of the

Graduate School of Vanderbilt University

In partial fulfillment of the requirements

for the degree of

DOCTOR OF PHILOSOPHY

In

Cell and Developmental Biology

December 16th, 2023

Nashville, Tennessee

Approved:

Jeff Reese M.D.

Andrea Page-McCaw Ph.D.

Ken Lau Ph.D.

Michelle Southard-Smith Ph.D.

Ambra Pozzi Ph.D.

Dedication

For a mother who always comforted me when I fell.

For a father who taught me to never stop getting back up.

Finally, for those who lost their struggles to congenital heart disease.

If I could give you my heart I would,

but I suppose my labor will have to do.

Acknowledgments

I thought this would be easier. Not easy, but easier. I was wrong. But learning to not take being wrong personally is perhaps the most practical lesson science can teach us. That and the value of teamwork. I couldn't have accomplished any of this alone. There are too many people who have touched this project and my growth through it to be fully listed here, but I certainly plan to try.

There are two people who have had the greatest steering impact on my progression as a scientist and my personal growth in the last few years. Jeff Reese, and I have spent so much time together working through experiments, data, conferences, career opportunities. He has devoted so much time to my growth as a scientist and as an individual. I will never be able to thank him enough. I have endured horrible health issues during my training, and he has always been understanding and compassionate beyond what was required. He has stuck up for me when I needed it, but also recognized the moments I needed to stick up for myself. He has been the best mentor I could have imagined. I absolutely could not have made it through this without him, and I hope we continue to collaborate as I move further into the world of vascular biology. The second person is Naoko Boatwright. Naoko is the engine that keeps our lab and several others running. She is an absolute expert at her craft and has mastered so many techniques I don't think I could list them. But more importantly, she is always attentive and understanding to other members of our group. If someone needs help with an experiment, or coverage when they are ill, Naoko is there without hesitation. She is one of the most impressive people I have ever known, and humble enough that sentence will make her squirm. She deserves half of this doctorate. Jeff and Naoko welcomed me into their lab like a family and have treated me as such ever since. I cannot thank them enough.

With the aforementioned health issues, constant complications with my project, and my own brand of stubborn self-reliance, I have been a difficult student. My committee has been incredibly patient with me throughout it all, especially Andrea, my chair. I have not always followed instructions, and you could have made my life so much harder for it. Thank you for recognizing I was always working towards my goals, even if I wasn't vocal about it. The shear amount of expertise on my committee is hard to fathom, and still, everyone has always been willing to help me when I needed it. Andrea, Michele, Ambra, Ken; thank you all so much for seeing me through this. You have shaped me into the scientist I am today.

He may not know this, but the person who convinced me to come to Vanderbilt was Chris Wright. The program in developmental biology that Chris leads is the most amazing program I've seen at Vanderbilt, with involvement and training opportunities rivaling most departments. The program in developmental biology training grant supported me for two years, but once you become one of Chris's trainees, he aggressively supports you forever. The PDB journal club is absolutely what allowed me to work through my anxiety about presenting science, and the discussion at the journal club has shaped the critical eye with which I view everything. Thankyou Chris, for always seeing potential in me, even in the moments I didn't see it in myself.

My project was also supported by an American Heart Association predoctoral fellowship. The mission of the AHA has a lot of personal meaning to me for reasons that will become clear later. It means the world to me for this particular organization to see potential in me as an investigator.

While I may be a student in the Department of Cell and Developmental Biology which deserve their own thanks, my daily interactions have mostly been within the division of neonatology. I have been supported, trained, and had the opportunity to train a slew of rising

faculty, technicians, and undergrads. At the center of this are a few people who really helped me through my project. Mark Hunt is an amazing coordinator for the division. He always has the answers you need and is always willing to lend a hand. Courtney Berger and I made an excellent team, wonderful friends, and I'm so glad to have had the opportunity to work with her. Deanna Sekulich is a recent addition to the lab, but has picked up technical skills at an amazing pace. I'm glad to have worked with her and am certain she will make an amazing scientist if that is what she chooses to do (no pressure). Elaine Shelton taught me many of the techniques I use on a daily basis and has been an absolutely amazing sounding board for experimental ideas and writing over the years. She has genuinely made me stronger as a scientist.

I have been blessed with an amazing family, especially two amazing parents. I was a challenging kid, but they met those challenges with a tempered hand and well-reasoned word. I'm the son of a draftsman and a master machinist. My parents taught me early that you could make anything you wanted from nothing with the right application of thought and effort. That you could be whatever you wanted as long as you were willing to take the good with the bad. They encouraged me at an early age to explore anything that interested me; or rather, they supported me because they knew good and well they couldn't stop me. To this day, they are always here when I need them and provide absolutely unwavering support. They are good, humble people, and they taught me to be the same. I love them with all I am and am proud to be their son. When I was little, there was no way they could have known this is what I would choose to do with my life. I'm sure they had full expectations I would live a few houses down and be around for Sunday supper. That's just not the case. Leaving home, and them, is still the hardest thing I've ever done. But I'm carrying what they taught me wherever I go, and I wouldn't be there without them.

I also had amazing grandparents. I spent a lot of my childhood standing across an operating table from my grandfather the veterinarian. He instilled in me a love of biology and a sense of stewardship that guides me. I still use what I learned from him daily in my work. My grandmother was the strongest person I've ever known, and it is the resilience I learned from her that has carried me through this. When I was young, my malmal walked me through the woods pointing out all the plants and their uses to heal the sick. She captivated my interest in what nature could show us if we were willing to learn. She also always had my back, even when she probably shouldn't have. I never knew my palpal, but I feel him every time I play his fiddle, and it has comforted me through many long nights of study and writing.

Throughout this tumultuous process I have been blessed with a phenomenal friend group. They have always been caring and understanding of my circumstances and have offered help without ever expecting something in return. Natalya has always leant an ear, and usually taken my side. When I needed a place to live, she said yes without hesitation. Kevin has always offered a hand and a smile. Megan and I were inseparable through most of grad school and always found the best concerts. Ashley provides a spark of life and levity to everything no matter the circumstances and she has always been able to eek a smile out of me on the longest days. Whitney is always there, without question, no matter the hour, and she knows I'm always there too. My friends from back home have also kept me sane. Ruffin has always been willing to fight harder for me than I am for myself, and I'm not exactly a pushover. Erik consistently brings the creative spark of a fresh perspective to every conversation and is who I go to when I need to think outside the box. Kyle keeps me in check, always providing a dose of critical thought and global perspective. When I need to make sure my head is in the right place; that I'm headed the right direction, these three are my compass. I am so proud of all of you. Thank you for sticking with me.

Four donors provided human tissue for transcriptional analysis as a part of this project. They deserve our thanks, our respect, and our remembrance.

It is no mistake I found myself in a lab studying congenital heart defects. I was born with several severe congenital heart defects myself. I went through surgery as a toddler, and medical observation until I was 17. During my procedure, I was legally dead for 70 minutes. I came very close to not being here and have already surpassed my pre-surgery life expectancy. It was hard, painful, embarrassing, and uncomfortable, but I was lucky. Others weren't. Many of the kids I remember playing with in the waiting rooms of my clinics didn't make it. I still remember their faces. More than anyone or anything else, they are the reason I am here. I feel a deep connection with them and want to do anything in my power to try and prevent others from meeting the same fate or enduring the same struggle. It's the thought of them that kept me writing on long nights. It's the thought of them that keeps me moving forward. This is for you. I wish it was more.

Finally, I'd like to acknowledge the publishers that have allowed reprint of published work for the purposes of this dissertation.

Table of Contents

List of Tables

List of Figures

phenotype.....144

Abbreviations

(Lp)PLA2) – platelet activating factor acetyl hydrolase/oxidized lipid lipoprotein associated phospholipase A2

AC – adenylyl cyclase

ACE – angiotensin-converting-enzyme

AGTR1 – angiotensin II receptor type 1

Akt – protein kinase B

ALK1 – activin receptor-like kinase 1

AMPK – adenosine mono-phosphate activated protein kinase

Ao – ascending aorta

Asxl2 – additional sex combs like 2

ATP – adenosine tri-phosphate

BMP – Bone morphogenetic protein

BRET – bioluminescence resonance energy transfer

BRG1 – brahma-related gene 1

BRM – brahma

cAMP – cyclic adenosine mono-phosphate

CGMP – cyclic guanosine mono-phosphate

CHD – congenital heart disease

CHF – congestive heart failure

CO – carbon monoxide

COX - cyclooxygenase

cPGES – cytosolic prostaglandin E synthase

cPLA2 – cytosolic phospholipase A2

CREB – cyclic adenosine mono-phosphate response element binding protein

CRISPR – clustered regularly interspaced short palindromic repeats

cSrc – tyrosine-protein kinase Src

CX – connexin

CYP – cytochrome P450

CYPOR – cytochrome p450 reductase

DA – ductus arteriosus

DAG – diacyl glycerol

DEG – differentially expressed gene

DPC – days post-coitus

ECM – extracellular matrix

eNOS – endothelial nitric oxide synthase

EP4 – prostanoid receptor EP4

EPAC – exchange factor activated by cAMP

EPRAP – EP4 receptor associated protein

ERK – extracellular signal-regulated kinase kinase

ET1 – endothelin 1

ETA – endothelin 1 A-type receptor

ETC – electron transport chain

FBLN1 – fibulin 1

FDR – false discovery rate

FGF – fibroblast growth factor

FPKM – fragments per kilobase of transcripts per million

FRET – Förster resonance energy transfer

GC – guanylate cyclase

GEF – guanine nucleotide exchange factor

GIVA PLA2 – group IV cytosolic phospholipase A2

GO – gene ontology

GO BP – gene ontology biological process

GO CC – gene ontology cellular component

GO MF – gene ontology molecular function

Gpc3 – glypican 3

GPCR – G protein coupled receptor

GTP – guanosine tri-phosphate

Hand2 – heart and neural crest derivatives-expressed protein 2

HAS – hyaluronic acid synthase

HFOV – high frequency oscillatory ventilation

HIF2a – hypoxia inducible factor 2a

HPGD/PGDH– 15-hydroxy-prostaglandin dehydrogenase

HPV – hypoxic pulmonary vasoconstriction

ICER – inducible cyclin adenosine mono-phosphate repressor

IEL – internal elastic lamina

ILK – integrin-linked kinase

iNOS – inducible nitric oxide synthase

IP3 – inositol tri-phosphate

iPLA2 – calcium-independent phospholipase A2

IUGR – intrauterine growth restriction

KO – knockout

LA – ligamentum arteriosum

LOX – lysyl oxidase

MAPK – mitogen activated protein kinase

MATR3 – matrin 3

MEK – mitogen activated protein kinase kinase

MF1 - mesodermal/mesenchymal forkhead 1

MFH1- mesenchymal forkhead 1

MHC – myosin heavy chain

MLC – myosin light chain

MLCK – myosin light chain kinase

MLCP – myosin light chain phosphatase

MMP – matrix metalloproteinase

mPGES – microsomal prostaglandin E synthase

MTHFR – elastin methylenetetrahydrofolate reductase

mtNOS – mitochondrial nitric oxide synthase

MYH11 – myosin heavy chain 11

NAD+/ NADH – nicotinamide adenine dinucleotide

NFE2 – nuclear factor erythroid 2

NICU – neonatal intensive care unit

nNOS – neuronal nitric oxide synthase

NO – nitric oxide

NOS – nitric oxide synthase

NSAID – non-steroidal anti-inflammatory drugs

NT3 – neurotrophin 3

O2 – diatomic oxygen

PDA – persistent patency of the ductus arteriosus

PDE - phosphodiesterase

pGC – particulate guanylate cyclase

PGD – prostaglandin D

PGDS – prostaglandin D synthase

PGE – prostaglandin E

PGF – prostaglandin F

PGFS – prostaglandin F synthase

PGG – prostaglandin G

PGH – prostaglandin H

PGI – prostaglandin I

PGT – prostaglandin transporter

PKA – protein kinase A

PKC – protein kinase C

PKG – protein kinase G

PLA2 – phospholipase A2

PLC – phospholipase C

pO2 – partial pressure of oxygen

POSTN – periostin

PPHN – persistent pulmonary hypertension of the newborn

PPI – protein-protein interaction

PTGER – prostaglandin E receptor

PTGS – prostaglandin-endoperoxide synthase

qRT-PCR – quantitative reverse-transcription polymerase chain reaction

RBPJ – recombinant signal binding protein for immunoglobulin κ J

Rim4 – recombinant-induced mutation 4

ROS – reactive oxygen species

RTK – receptor tyrosine kinase

RT-PCR – reverse-transcription polymerase chain reaction

SGBS – Simpson-Golabi-Behmel syndrome

sGC – soluble guanylate cyclase

SMC – smooth muscle cell

SNP – single nucleotide polymorphism

SNP – sodium nitroprusside

SNP – sodium ntroprusside

sPLA2 – secreted phospholipase A2

SSRI – selective serotonin reuptake inhibitor

TAAD – thoracic aortic aneurysm and dissection

Tagln – transgrelin

TFAP2B – transcription factor AP2β

TGFβ – transforming growth factor β

TNF – tumor necrosis factor

TP – thromboxane receptor

TRAF1 – tumor necrosis factor receptor associated factor 1

TXA2 – thromboxane A2

TXS – thromboxane synthase

UP Keywords – UniProt Keywords

VNCC – vagal neural crest cells

VSMC – vascular smooth muscle cell

WT - wildtype

XOR – xanthine oxidoreductase

Chapter 1

INTRODUCTION

Abstract:

The ductus arteriosus (DA) is a muscular artery which helps to define the fetal pattern of the circulatory system. After birth, the DA undergoes muscular constriction and remodeling which establish the adult division between the pulmonary and systemic circulation. Fetal DA patency requires *acute* vasodilatory signaling via the prostaglandin (PGE_2) receptor EP_4. However, in humans and mice, disrupted PGE_2-EP_4 signaling *in utero* causes unexpected persistent patency of the DA (PDA) after birth, suggesting another *chronic* role for EP_4 during development. It is likely that sustained PGE_2 signaling via EP_4 is responsible for directing the proper development of the DA to enable its closure after birth. This is mediated through highly ordered developmental processes, likely representing a developmental program that is heretofore an unstudied paradigm for DA formation and function.

Introduction:

The DA is a fetal vessel which shunts blood right-to-left past the lungs *in utero* to protect the developing pulmonary vasculature and direct freshly oxygenated blood from the placenta into the systemic circulation (**Figure 1A**). Compared to the large elastic arteries which it interconnects (aorta, pulmonary artery), the DA is a large muscular artery with dynamic vasoactive properties. While DA

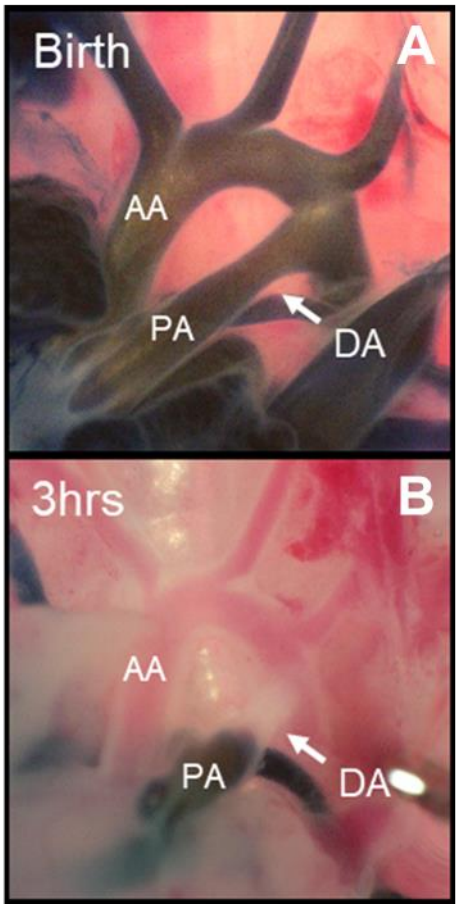

Figure 1. DA closure in the mouse. A) dye perfused outflow tracts of a term CD1 WT pup at birth displaying a patent DA and free flow of dye in a right-to-left fashion from the pulmonary circuit (pulmonary artery) to the systemic circuit (aortic arch). **B)** at 3hrs after birth, the DA has constricted preventing flow of dye from right-to-left and establishing the divided pulmonary and systemic circuits of the adult circulatory system. DA – ductus arteriosus, AA – aortic arch, PA – pulmonary artery.

patency, or openness, is essential during fetal development, its rapid postnatal closure is critical for circulatory transition to neonatal life. DA constriction is an elegant cascade of biological processes requiring acute changes in vascular tone,

transcriptional profiles, fluidity in cell phenotypes, and both prenatal and postnatal structural remodeling (1, 2). Frequently, disruptions in these genetic, environmental, and developmental processes result in failure of the DA to close, termed PDA. Risk for PDA is multifactorial, consisting of genetic, environmental, immunological, and as of yet unexplained factors. Regardless of cause, PDA poses serious challenges for affected infants, especially more fragile preterm infants. Treatment options are limited, and all convey their own risks of severe side effects. For this reason, an emphasis on preventative medicine, and to that end a deep understanding of the mechanistic underpinnings of DA formation, closure, and transcriptional identity is critical.

Role of DA in Transition to Neonatal Life/Embryology:

The specifics of the DA's anatomical position and function result from the complex evolutionary transition from water-based respiration to air-based respiration. In the majority of fish species, the circulatory system exists as a singular loop where deoxygenated blood returns from the body, passes through the sinus venosus, through a single atria, and into a single ventricle, which expels it through the aortic arch arteries associated with the gills (3). As blood passes through these arch arteries, it is reoxygenated via gas transfer with the surrounding water. The development of primitive lungs in some fish species allowed them to shift back and forth between water-breathing and air-breathing, but required further modification of the cardiovascular system. In order to separate gill-based water breathing from lung-based air breathing, separate vascular circuits were required. Thus, aquatic

species with terrestrial habits developed hearts with septations dividing the atria and ventricles into left and right sides. The most proximal, sixth aortic arch artery to the heart became a muscular shunt which could alternate blood flow between the lungs and other arch arteries, depending on environmental context. This system of alternating between gills and lungs survives in some extant fish such as the lung fishes, gouramis, bichirs, and some species of climbing perch. These should not be confused with other fish species which rely on labyrinthine organs (arapima, beta fish) or highly vascularized swim bladders (alligator gar) for air breathing, as these rely on different circulatory adaptations (4).

Due to the necessity of the DA structure for adaptation to air breathing, it is conserved in five vertebrate classes; amphibians (5), reptilians (6, 7), birds (8, 9), mammals (10), and of course the lobed fin fishes in which they evolved (11). Of note, these groups span all terrestrial life. While there is variation in structure amongst these classes, the unilateral DA of mammals arise from the left sixth arch artery, and the bilateral DA of birds arise from both the left and right sixth arch arteries (12). Specifically, the vascular smooth muscle cells (VSMCs) of the DA arise from neural crest cells which migrate via aortic arch arteries down the DA and ascending Ao on their way towards the heart where they will contribute to cardiac development (13-15). Endothelium of the DA and ascending Ao are contributed by migration from the second heart field (16). This combination of cellular origins makes the DA and Ao unique amongst the central vasculature, despite their different phenotypes. For this reason, the ascending Ao provides an exceptional control for studies of DA development and physiology. The DA has likely been evolutionarily conserved as a structure due to its indispensable role during embryonic development. Whether a bird embryo developing in an egg or a mammal developing *in utero*, the fluid-filled environment prevents the use of lungs for respiration. As a result, whether a bird embryo through its chalaza and air cell (17), or a mammal through its umbilical cord and placenta, oxygenation of fetal blood is obtained independent of the underdeveloped, unaerated

lungs. As previously mentioned, the vascular and alveolar structures of the lungs develop very slowly, and have high vascular resistance *in utero* (18, 19), thus a full hemodynamic load is injurious (20). To prevent this, the DA shunts the majority of oxygenated right ventricular outflow ~60% in humans (21), past the developing lungs.

After birth, closure of the mammalian DA is initiated by a cascade of signals arising in part from the newly inflated lungs. The fetal environment is markedly hypoxic, with oxygen (O_2) tensions equal to 20-30% of normal adult values (22). Increasing O_2 tension exerts a constrictive effect on the DA while also helping to stimulate metabolism of circulating dilatory prostaglandins (23-25). As the DA closes and remodels, the adult circulatory pattern of wholly divided pulmonary and systemic circuits is established (**Figure 1B**). While some animals do maintain either an open (tortoises (26)) or reversible DA (lungfish (12)), this is not the case with humans or mice. In humans, functional DA closure occurs in 12-24hrs and permanent anatomic closure will occur over the course of 2-3 weeks (27). In mice, functional DA closure occurs in 3-6hrs (**Figure 1**) and permanent anatomic closure in 2-3 days (28). PDA disrupts the transition of the cardiovascular system to neonatal life and may have severe hemodynamic consequences. Excessive left-to-right shunting results in pulmonary over-circulation with oxygenated blood being mixed with deoxygenated blood and recirculated through the lungs. This over-circulation can result in pulmonary edema, as well as enlargement of the left side of the heart and a decrease in delivery of oxygenated blood to peripheral tissues known as “ductus steal” (1). Together, these effects burden the development of the infant and contribute to poor outcomes.

Clinical Relevance/Human Epidemiological Data:

Despite decades of research, the exact mechanistic underpinnings of PDA are still poorly understood. Risk factors for PDA have been thoroughly catalogued and provide important insights into DA biology (**Table 1**). There is evidence for a genetic basis in some forms of PDA, but in most cases, PDA likely results from a combination of prematurity, environmental conditions, or cardiovascular comorbidities. PDA comprises 5-10% of congenital heart disease (CHD) cases in the US (29). While PDA is relatively rare in healthy term infants, it is disproportionately common in preterm (64% at 27-28 weeks) and very preterm infants (87% at 24 weeks) (30, 31). Most at risk are those with particularly low birth weights (80% in infants <1000 grams) (32). It should be noted that low birth weight is itself likely not the causeof PDA or its increased severity. Instead, it is likely that birth weight is a more reliable predictor of gestational maturity than timing in medically complicated pregnancies. With this consideration, prematurity appears to be the most important indicator of PDA prevalence and severity in the newborn. Premature infants also tend to have a high incidence of comorbidities. While extremely premature infants (<28 weeks) comprise only 0.7% of births in the United States (33) together with slightly more mature infants (28-32 weeks) they account for more than half of all infant deaths (34). Without limiting by PDA or other comorbidities, extremely premature infants have a 26% mortality rate during their initial birth hospitalization with each lost week of gestation correlating to lower survival (35, 36). While instances of extremely premature infants have been relatively consistent since 2000 (33), the frequency of the less severe late preterm infants (28-32 weeks) which historically accounted for ~75% of preterm births, are increasing (37). With preterm infants currently comprising 11.4% of live births in the United States (33) PDA incidence may be increasing not decreasing. With treatment, an isolated PDA has a good prognosis (27), but adverse outcomes can be severe, especially in preterm and low-birth weight neonates where comorbidities tend to define outcomes (38).

Established Risk Factors for PDA	Other Factors Associated with PDA	
Early gestational age	IUGR	**Maternal drugs:**
Low birth weight	Delay in indocin treatment	Antihistamine
RDS	Furosemide treatment	Magnesium
Persistence of DA flow	Use of HFOV	ACE inhibitors
Sepsis	Race:	Anticonvulsants
Excess fluid administration	Caucasian (PT)	Ca channel blockers
Antenatal NSAID exposure	African American (T)	Cocaine
Initial hypotension	Gender:	Maternal PKU
Need for intubation/airway pressure	Male (PT)	
Lack of antenatal betamethasone	Female (T)	**Genetic Conditions** (T)
Maternal diabetes (T)	Prolonged ROM	(trisomy 21, 18, 13, Char, Holt-Oram, DiGeorge, Noonan, CHARGE, TAAD/PDA)
Birth at high altitude (T)	Twins	
Congenital rubella (T)	Perinatal stress	Genetic Susceptibility
Hypothyroidism (T, PT)	Antenatal hemorrhage	Familial PDA
	Breech	
	Phototherapy	

Table 1. Factors associated with PDA. Risk factors for PDA were considered to be well-established if they were identified by studies that sought causative factors for PDA, remained significant after multivariate analysis, or were consistently observed in multiple controlled trials in different patient populations. Other factors that have been shown to have an association with PDA were drawn from single studies, epidemiologic surveys, birth defect registry reports, case reports, or small studies that did not control for confounding variables. PDA at term (T) gestation is regarded as a congenital malformation, but these risk factors may also occur in preterm (PT) infants. Conflicting studies that did not detect an association of PDA with these factors are not presented. Genetic conditions were considered separately. Only a subset of representative citations are shown for risk factors that were consistently identified in numerous studies. (IUGR, intrauterine growth restriction; HFOV, high frequency oscillatory ventilation; ACE, angiotensin-converting-enzyme) *Adapted with permission from Reese et al. (39)*

Contributors to PDA:

The environment of the womb has a profound effect on the developing tissues of the fetus, including the DA. One historical example of this was the observation of an increased incidence of PDA in the offspring of mothers infected with rubella (40). Congenital rubella syndrome, infection of the fetus with rubella during gestation, has not only been found to increase PDA, but to increase pulmonary hypertension-dependent mortality associated with PDA (41). This increased mortality could be abated via closure of the DA. Interestingly, the congenital rubella syndrome-associated PDA features a tubular-type PDA configuration which makes the DA significantly harder to close via transcatheter occlusion compared to cone-type PDAs (42). While various PDA configurations have been described in detail via echocardiography (43) and a classification system has been adopted to categorize them (44), this is primarily relevant for catheter-based occlusion.

Pharmacological treatments administered to mothers during pregnancy have also been associated with PDA. The importance of developmental timing in fetal PGE_2 signaling was first supported by observations that maternal exposure to cyclooxygenase (COX) inhibitors, given as a tocolytic to arrest preterm labor by blocking production of PGE_2, results in *fetal DA constriction* after 30-32 weeks of gestation, but not earlier in pregnancy (45, 46). In contrast, mothers who received COX inhibitors as tocolytics during late- but not mid-gestation had an increased risk of PDA in their offspring (47). This particular finding revolutionized the understanding of the DA and will be expanded on throughout this dissertation. Similarly, the treatment of antenatal depression using selective serotonin reuptake inhibitors such as sertraline or fluoxetine (48) is very common, with prescriptions written in 2-6% of all pregnancies (49-51). Illustrating an important aspect of these maternal-fetal interactions, selective serotonin reuptake inhibitors (SSRIs) readily cross the placenta resulting in fetal levels of 70-80% those of the maternal blood. Maternal SSRI administration, while not directly linked to PDA in infants, was found to predispose neonates to persistent pulmonary hypertension of

the newborn (PPHN) (52, 53), a condition promoted by *in utero* constriction of the DA (54). In one of the first projects I worked on during my Ph.D., our group performed studies on the DA of neonatal mice, finding dose dependent constriction in response to SSRIs, as well as *in utero* constriction of the DA in SSRI treated pregnant dams (55). Together these findings suggest SSRIs likely contribute to PPHN in humans through *in utero* constriction of the DA. As another example, antenatal betamethasone, despite being associated with decreased PDA in observational (56-58) and controlled (59) studies increases the vasoconstrictive potential of the DA across all tested timepoints, likely through regulation of genes associated with O_2 sensing and muscle contraction (60). This may be problematic in pregnancy, as it could lead to *in utero* constriction, despite being a powerful strategy to accelerate maturation of other organ systems and decrease comorbidities.

Cardiovascular comorbidities also predispose an infant to PDA, or increased symptoms from PDA. PDA exists as a secondary disorder in ~10% of other congenital heart defects (27). While PDA and the primary defect may arise from a similar genetic or developmental disruption, severe congenital heart defects are often reliant on a patent DA to be compatible with life. Further, many of the more critical congenital heart defects display no outward symptoms until the DA begins to close after birth (4). Specifically, hypoplastic left heart syndrome, transposition of the great arteries, and tetralogy of Fallot are examples of life-threatening conditions which require maintenance of a patent DA (5). These medically induced PDAs are maintained with prostaglandins such as PGE1 until the primary defect can be surgically corrected, at which point the DA is usually ligated or excised, depending on the repair.

Maternal treatment is not the only way that drug exposures can affect PDA. It is now becoming more clear that pharmacological interventions performed in the neonatal intensive care unit (NICU) can affect DA tone, both positively and negatively. It was previously believed that fetal and neonatal sepsis contributed to PDA, as the conditions correlate clinically. However, our group found that while

the inflammatory pathways associated with sepsis had little or no effect on tone in the mouse DA, the aminoglycoside antibiotics administered to treat that sepsis resulted in dilation of the DA (61). This is likely through the depression of calcium (Ca^{2+}) flux that mediates gentamicin's myocardial depressant effects (39, 62-64). Trials using cimetidine, an H_2 receptor antagonist generally used as an antacid, in an attempt to decrease lung injury in extremely premature infants failed to decrease lung injury and increased incidence of PDA (65). Our group found this was caused by cimetidine-mediated cytochrome P450 inhibition (CYP), which may disrupt the O_2 sensing mechanisms of the DA (39, 66). Similar effects were found for ranitidine, an H_2 receptor antagonist with similar CYP inhibitor properties. Phosphodiesterase (PDE) 3 inhibitors milrinone, amrinone, and the PDE5 inhibitor sildenafil have all been found to have vasodilatory effects on the DA despite their continued use in the NICU (67-69).

Clinical Options to Treat PDA:

The first-line treatment for PDA is administration of COX inhibitors, usually indomethacin or ibuprofen. Indomethacin is relatively COX-1 selective, and tends to have vasoconstrictive effects on the cerebral, renal, and mesenteric vasculature (70). Decreased cerebral blood flow is accompanied by reduced cerebral oxygenation (71) and potentially cerebral ischemia (72). Reduced renal blood flow results in decreased creatinine clearance (73), higher blood urea nitrogen levels (74), decreased urine output (75), and overall decreased kidney function. While there are conflicting reports as to whether prophylactic indomethacin is associated with increased risk for necrotizing enterocolitis (76) or not (77-80), gut hypoperfusion and subsequent mucosal hypoxia provide a route for potential ischemia, ulceration, and bacterial invasion (81, 82). Gastrointestinal perforation has been reported (81). While many of these effects may be abated by the use of ibuprofen, this treatment may be associated with pulmonary issues such as an increased susceptibility to chronic lung disease

(requiring supplemental O_2 at 28 days of age) or persistent pulmonary hypertension of the newborn, though these findings are hotly debated (83). It is worth noting that while necrotizing enterocolitis, chronic lung disease, and persistent pulmonary hypertension are all common amongst infants with PDA, this may be due to these conditions being more prevalent in extremely premature neonates.

Therapeutically, indomethacin has a closure rate of 80-90% (27), but pharmacologically unresponsive PDAs will require surgical ligation or catheter-based occlusion. Any cardiothoracic surgery comes with extreme risk, but this risk is increased for premature and low birth weight neonates. Unfortunately, it is the extremely premature neonates who are most likely to fail pharmacological treatment. Overall, surgical ligation conveys a mortality rate of 2-20% depending on comorbidities. Ligation is also associated with increased neurodevelopmental impairment, retinopathy of prematurity, and chronic lung disease (84). Additionally, 30-44% of all PDA ligations are followed by acute respiratory and hemodynamic instability in the initial 24hrs post procedure (85, 86). This condition is referred to as post-ligation cardiac syndrome, and it is associated with systemic hypotension, (85, 86) chronic lung disease (87), and by some reports, up to 33% mortality (88). A less fatal but common side effect of ligation is the accidental severing of the left recurrent laryngeal nerve which wraps around the DA *in situ*, resulting in partial vocal paralysis (89, 90). A relatively new alternative to surgical ligation is percutaneous closure using a catheter-based occlusion device such as the Amplatzer Piccolo (91). In this procedure, a catheter delivers a deployable mesh device which will be placed into the patent lumen of the DA under ultrasound or fluoroscopic guidance, occluding flow and providing a scaffold for surrounding tissue ingrowth to achieve permanent, secure closure. Clinical trials and multi-center studies are still in progress, so it is difficult to thoroughly evaluate the risk factors of percutaneous closure (92-94). While treatment options all convey risk, the bottom line is an open DA must eventually be closed. Left untreated, pulmonary hypertension may develop, and the mortality rate for untreated PDA increases with age (95-97). All cases of PDA in the adult are

unresponsive to COX inhibitors and will likely need treatment with riskier surgical options. Because treatment options for PDA are limited, with such severe side effects, and such a vulnerable population, preventative medicine, and therefore a thorough understanding of the underlying biology is required. The breadth and severity of side effects associated with disrupting the prostanoid pathway further emphasizes the importance of prostanoid signaling in the DA.

Genetic Landscape of the DA:

Developmental programs are sequential cascades of gene and protein expression with subsequent pathway regulation which direct a developmental process. Grasping the genetic and transcriptional landscapes of the DA are critical to identifying potential constituents or regulators of such a program. This starts with understanding the heritability of PDA and what genes/transcripts may affect PDA risk or severity. Both term and preterm PDAs may have a genetic component, with a 5% sibling recurrence rate (98, 99) and a higher correlation between monozygotic twins compared to dizygotic twins (100, 101). While reports have varied, one twin study found that genetic factors and a common gestational environment contributed up to 76% of this variance. Studies on familial PDA and the offspring of consanguineous parentage provide genetic information on chromosome regions that confer risk for PDA (102, 103). In addition, candidate gene studies have identified genetic loci which contribute to syndromic forms of PDA such as transcription factor AP2β (*TFAP2B)*, or whose sequence variants can contribute to isolated non-syndromic cases of PDA (104, 105). Although the genetic predisposition for most PDAs is unknown, a robust understanding of the genes whose perturbation results in PDA may provide key insights into the development and function of the DA critical to the designing new and improved therapies. To this end, many mouse models of PDA have been described. These will be discussed in-depth in chapter 3. Of note, few mouse models of PDA originated as attempts to generate a PDA phenotype. PDA was generally an incidental finding among

other cardiovascular anomalies. Knockouts (KOs) of several key genes involved in prostaglandin signaling, including prostaglandin-endoperoxide synthase 1 (*Ptgs1*);*Ptgs2* double KO (106, 107), prostaglandin E receptor 4 (*Ptger4*) KO (108-110), and the *Pgdh* KO (24, 111) resulted in PDA. *Ptger4* (EP_4) expression was also found to be downregulated in the *Prdm6* KO mouse (112), emphasizing the importance of PG signaling pathways in the DA. Microarray studies have also been performed on mouse (113, 114), rat (115-120), sheep (121), chicken (122), and human (123, 124) tissues in efforts to elucidate the transcriptional landscape of the DA. Methodologies varied greatly between these studies with their findings varying in kind. The state of this understanding is, to borrow a phrase, 'as clear as mud at night.' Recent studies utilizing next-gen sequencing have attempted to remedy this, and even identified new KO models in the process (125), but a global and comprehensive understanding of this landscape is required to advance the state of PDA treatment.

Preparation of the DA for Closure and Remodeling:

DA closure occurs in three primary steps. Soon after birth, the first stage, "functional closure" in response to acute signaling changes, occurs. This process takes about 1-3 days in humans or 3-6hrs in mice and results in a DA that is completely but reversibly occluded by muscular constriction of the vessel wall. Next, a rapid wave of remodeling and "anatomic closure" begins within the lumen and wall of the constricted DA, leaving it irreversibly closed. This generally takes up to a week in humans and about 24-48hrs in mice. Finally, a second wave of neonatal remodeling occurs resulting in fibrosis and necrosis, leaving a new structure, the *ligamentum arteriosum* (LA), as a remnant of the DA structure. This process can take quite a while, several weeks in humans, and multiple days in mice. It is clear that tissue remodeling, and to that effect cell phenotype, play significant roles in effective DA closure. An underappreciated preliminary stage precedes the others and consists of several key remodeling steps that occur in late gestation and prepare the DA for eventual closure.

Critically, in cases of PDA none of these pre- or post-birth remodeling steps occur (126), therefore these processes are likely critical for proper DA function.

DA structural remodeling, and in some ways the process of DA closure, actually begin in the immediate antenatal period. During late development, the DA undergoes a process of extensive remodeling of its extracellular matrix (ECM) and tissue structure which is necessary to prepare the vessel for closure after birth. At the beginning of this process, during mid-gestation, the DA exists as three discrete layers; an adventitia of fibroblasts and myofibroblasts, a continuous muscular media of VSMCs aligned perpendicular to the direction of flow, and an intima composed of a single layer of endothelium, separated from the medial layer by a contiguous sheet of elastin designated the internal elastic lamina (IEL) (**Figure 2A**). VSMCs such as those in the medial layer of the DA, display a spectrum of phenotypes (127-129), though this is usually simplified as an axis with a sedentary, contractile phenotype on one side and a secretory, migratory, synthetic phenotype on the other. In literature from the 1970s-80s, before the variable smooth muscle cell (SMC) phenotype was fully understood, contractile SMCs are referred to as ‘mature’ with any other phenotypic characteristics deemed ‘immature.’ The exact phenotypic state of DA VSMC populations at this preparatory point in DA development is somewhat unknown. Microarray analysis of laser micro-dissected VSMCs from preterm rat DAs revealed the presence of some mature muscle markers associated with the contractile phenotype, but also extensive expression of synthetic or non-muscle markers (119). This suggests a mixed phenotypic population of DA VSMCs, containing both contractile cells

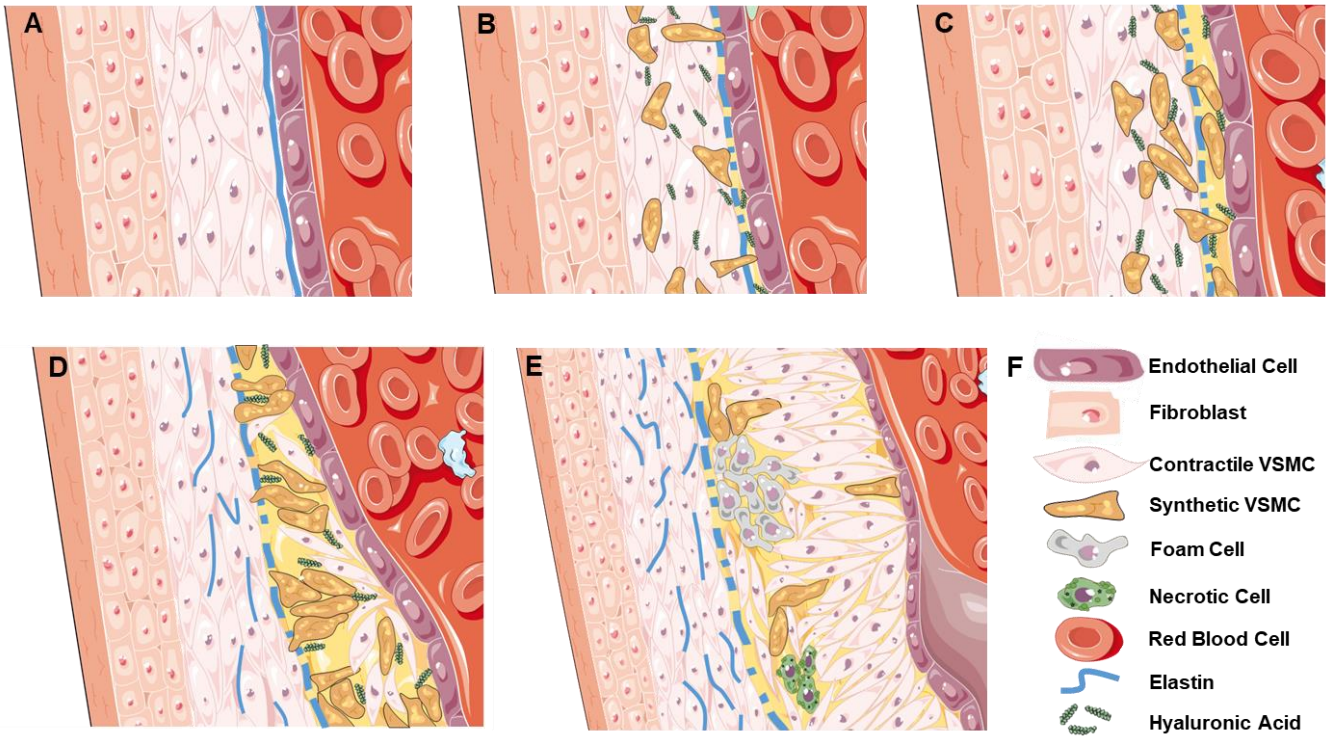

Figure 2. EP_4-mediated late gestational remodeling prepares the DA for closure. **A)** The developing DA, with (right to left) an open lumen, intima composed of a single layer of endothelial cells attached to an intact IEL, media composed of several layers of circumferentially oriented contractile VSMCs, and an adventitia composed of several layers of fibroblasts and thick extracellular matrix. **B)** Synthetic VSMCs from the DA media begin to secrete hyaluronic acid facilitating migration, disrupt LOX mediated crosslinking of elastin leading to a fragmented IEL, and migrate inward towards the IEL; all reportedly EP_4 mediated processes. Endothelial cells begin to detach from the IEL in a possibly hyaluronic acid mediated mechanism. **C)** Synthetic VSMCs begin to invade the subendothelial space created by complete detachment of endothelial cells from the IEL. **D)** Intimal thickening progresses as VSMC numbers in the subendothelial space continue to increase, due primarily to migration not replication. Synthetic VSMCs begin to transition back into contractile VSMCs which assume a radial orientation perpendicular to the lumen. Continued disruption of LOX leads to the formation of disorganized partial sheets of elastin throughout the media. **E)** Intimal thickening is complete, characterized by a thick layer of radially reoriented contractile VSMCs dividing the highly fragmented IEL from the intimal endothelial cells. Endothelial cells may begin breaking basal polarity and growing on top of each other. Fragmented elastin sheets are common in the medial layer with human DA forming a secondary discontinuous elastic lamina in the mid-media. In larger species such as humans, full intimal cushions form, protruding into the lumen of the vessel and disrupting perfusion to the vessel wall. This results in the formation of deposits of fat-rich macrophages called foam cells, and cores of necrotic cells in the subendothelial space. **F)** Legend. Figure created using images and assets from Servier Medical Art. Servier Medical Art by Servier is licensed under a Creative Commons Attribution 3.0 Unported License (https://creativecommons.org/licenses/by/3.0/).

which maintain DA tone, and a migratory, synthetic subpopulation. At this stage, synthetic VSMCs begin to disrupt the cross-linking of elastin required to maintain the IEL. This is possibly achieved through the EP_4-mediated inhibition of lysyl oxidase (LOX) (130, 131).

Upregulation of matrix metalloproteinases (MMPs) by some unknown mechanism and subsequent matrix degradation is also a potential explanation. Unable to adequately maintain itself, the IEL becomes fragmented, with large openings forming across its surface (132, 133). Disorganized patches of elastin begin to form throughout the medial layer, with a second highly fenestrated IEL forming in the middle of the medial layer in humans (132, 134). The endothelial cells of the intimal layer begin to break their bonds with the IEL creating a subendothelial space (**Figure 2B**) (135, 136) though not in some species, such as dogs (126, 137). Proper regulation of elastin is critical to DA closure after birth, and an intact IEL is associated with PDA in both humans and dogs (137-140). Natural genetic disruption of elastin assembly in the brown Norway rat (141) produces several vascular disorders (142) including PDA (143). VSMCs migrate through the fragmented IEL into the subendothelial space (**Figure 2C**) (144). These VSMCs contain large amounts of rough endoplasmic reticulum and were found throughout the subendothelial space and media, lending support to the notion these migratory cells are of the secretory synthetic phenotype. Further, areas of the vessel rich in ‘odd looking’ VSMCs contain less elastin, suggesting these synthetic VSMCs are responsible for elastin degradation in the DA (145).

VSMC migration is facilitated by the EP_4-mediated production of hyaluronic acid, a hygroscopic matrix component by the secretory synthetic VSMCs (146-148). This hyaluronic acid is readily detected in the subendothelial region, and may contribute to endothelial cell detachment from the IEL, expansion of the subendothelial space, and migration of synthetic VSMCs into this space (135). EP_4-mediated activation of AC increases cyclic adenosine mono-phosphate (cAMP), which activates the serine/threonine protein kinase A (PKA), and subsequently hyaluronic acid synthase (HAS). This has

been shown to promote cell migration in cells cultured from rat DA (146). The process of amassing VSMCs in the subendothelial space is called intimal thickening, which is present in most species (**Figure 2D**). A more extreme version of this occurs in larger species such as humans, with the formation of large intimal cushions which serve to partially occlude the lumen of the DA (**Figure 2E**)

(132, 136, 149, 150). These intimal cushions are large enough they may prevent complete perfusion into the vessel wall, leading to antenatal cytolytic necrosis, immune recruitment in the formation of mucoid lakes, and necrotic cores of dying SMCs (134). Endothelial cell detachment from the IEL does not occur in some species, including dogs, explaining why some species may lack intimal cushion formation (126, 137). The severity of intimal thickening and disruption of the IEL increases with gestational age (132, 144). The VSMCs within the subendothelial space undergo radial realignment, assuming a contractile phenotype and organizing themselves pointing inward towards the lumen, perpendicular to their normal orientation (144, 151). Large amounts of amorphous extracellular material is also present in glycogen pockets throughout the media at this stage, and may represent un-crosslinked matrix proteins staged for post birth fibrosis of the vessel (144). At this point, the DA is ready for birth and subsequent constriction.

Mechanisms of Postnatal DA Closure:

After birth, a complex cascade of signals and processes lead to the initial, functional closure of the DA. As soon as the neonate leaves the hypoxic environment of the womb, their airway opens, and breathing is initiated. The sudden increase in partial pressure of oxygen (pO_2) begins to relax the hypoxic pulmonary vasoconstriction (HPV) mechanism that has been constricting the pulmonary vasculature *in utero*. Separation from the placenta cuts off a key source of prostaglandins, with remaining PGE_2 being rapidly metabolized by 15-hydroxy-prostaglandin dehydrogenase (HPGD)

which is highly expressed in the lungs (23). Decrease in PGE_2 activation of EP_4 leads to a gradual decline in cAMP and reduced activation of myosin light chain phosphatase (MLCP), allowing the cycling of myosin light chain (MLC) in the contractile apparatus. This is further facilitated by internalization of EP_4 which reduces the rate of signaling. Simultaneously, O_2-sensing mechanisms act to increase internal Ca^{2+}, triggering calmodulin-dependent activation of myosin light chain kinase (MLCK) and increasing MLC cycling. O_2 displacement of CO attachment to circulating hemoproteins alleviates another dilatory mechanism, decreasing cyclic guanosine mono-phosphate (cGMP) production and further decreasing activation of MLCP. With MLC free to cycle and MLCK active, the DA VSMCs rapidly constrict, completely occluding the vessel, and establishing the adult circulatory pattern. At this stage, blood may still be present in the lumen of the DA, but the vessel is hemodynamically insignificant, and the systemic and pulmonary circuits no longer mix.

The processes belying the permanent closure of the DA are still unclear. Recent sequencing analysis shows that certain transcripts become upregulated during this window, specifically those associated with matrix and cytoskeletal components (125). It is unclear what role the radially realigned VSMCs in the subendothelial space play. It is thought that intimal cushions serve to occlude the lumen of vessels in species which are too large for lumen obliteration by muscular closure alone. The need for these cushions is likely dictated by the ratio of circumference to area of the vessel cross section. VSMCs themselves take up space, and it is logical there would be limits to how much they can compress the vessel wall. Once the vessel is completely closed, the endothelial cells begin to necrose. VSMCs which have likely transitioned to a synthetic myofibroblast-like phenotype, begin to produce large amounts of matrix proteins, leading to fibrosis of the tissue. This permanently seals the vessel and prevents medication-induced reopening, or mechanical reopening under pressure.

Finally, following permanent anatomic closure of the DA, the VSMCs undergo necrosis and apoptosis, leaving behind a fibrotic tether between the pulmonary artery and aortic arch. This

structure is termed the LA and it will persist through adulthood. The LA is an overlooked structure which provides some support to the positioning of the outflow tracts, but does not appear to serve other functions, although it may remain partially responsive to stimuli (152). Though the process of DA degradation likely begins immediately after permanent closure, this can take some time, with SMCs present two months after birth in the pig DA (153, 154). Though these SMCs are in the process of degenerating, with lipid vacuoles, lysosomes, dilated rough endoplasmic reticulum, and Golgi bodies found in their cytoplasm. Early endothelial cell degeneration was characterized by aggregates of Weibel-Palade bodies; elongated secretory organelles which mediate inflammation and tissue repair in vascular endothelium (155). Fibrosis and lipid vacuole production by degenerating SMCs increases by six months of age. Fibromuscular connective tissues fill the lumen and the boundary between intima and media becomes indiscernible (144). Aforementioned amorphous extracellular material is reduced throughout the media, replaced by crosslinked matrix including collagen fibers (144). Interestingly, the remodeling process of the DA reproduces many characteristics of pathologic atherosclerosis (144, 149, 154). These include intimal thickening-mediated stenosis of the vessel, expansion of intimal VSMCs, degradation of the IEL, and the generation of lipid-filled vacuoles. There are also similarities in immune recruitment to the vessel wall, though this has not been thoroughly studied in the DA (156).

Vascular Smooth Muscle Cells in DA function:

In order to understand the complex cascade of factors that leads to DA closure at birth, it is critical to understand the mechanisms underlying the contraction and relaxation of SMCs. Smooth muscle cells compose the cylindrical walls of many tissues throughout the digestive system, respiratory tract, and reproductive systems (157). We are interested specifically in the VSMCs that compose the medial layers of blood vessels. SMCs lack the striated pattern created by repeating

contractile apparatuses in skeletal and cardiac muscle. Instead, SMCs possess a crosshatch pattern of contractile proteins that allow them to shorten and widen on contraction, decreasing the luminal diameter of their given structure. In the vasculature, this equates to vasoconstriction. The contractile apparatus of VSMCs is composed of long actin filaments and myosin chains which span the cell connecting intermediate junctions on opposite faces (157). The formation of cross bridges between the heads of myosin dimers allows them to exert force. These myosin dimers are composed of two heavy chains (MHC) with prominent heads that interact with actin. At the base of these heads are the myosin light chains whose phosphorylation state allows the interaction of MHC and actin. Specifically, phosphorylated MLC activates the actomyosin Mg-ATPase portion of the MHC, allowing cross bridge cycling (158, 159). The phosphorylation state of MLC is generally controlled by receptor signaling, detection of stretch by specialized ion channels, or neuronal signaling. Some muscular arteries, like the DA, maintain a baseline level of MLC phosphorylation giving them vascular tone, or the maintenance of a partially contracted lumen (160). The state of the contractile apparatus in SMCs is largely determined by a balance between MLCK which phosphorylates MLC facilitating contraction, and MLCP which dephosphorylates MLC preventing contraction (161-163). Dilatory factors generally act to increase the activity of MLCP and decrease the activity of MLCK. This points to the most critical factor for muscle contraction of any kind, intracellular Ca^{2+}. The activity of MLCK is largely governed by calmodulin, which binds and activates MLCK following activation by intracellular Ca^{2+} (162, 164). This makes Ca^{2+} critical for significant contraction of SMCs. This Ca^{2+} can either be imported through the cell membrane, or released from intracellular Ca^{2+} stores like the sarcoplasmic reticulum (165). MLCP is also subject to regulation by inhibitors such as RhoA (166), or activators such as its own M110 regulatory subunit (167). 7 transmembrane G protein coupled receptors (GPCRs) can mediate both relaxation and constriction in SMCs, depending on their G protein subunits. The GPCRs discussed here function through heterotrimeric G protein complexes, or large GTPases composed of an α subunit and a β/γ complex (168). Each receptor contains a guanine nucleotide exchange factor

(GEF), which exchanges the GDP bound to the alpha subunit for a GTP (169). This elicits a conformational change which leads to the dissociation of the G proteins from the receptor. The activated α subunit will then go on to illicit G protein-specific downstream effects. For instance, the EP_1 receptor is bound to a $G_q\alpha$ subunit, which once activated, will activate membrane bound phospholipase C (PLC) to produce inositol triphosphate (IP3) and diacylglycerol (DAG). This IP3 will then bind IP3 receptors on the sarcoplasmic reticulum, initiating the release of Ca^{2+} into the cell, fostering contraction. DAG on the other hand, activates protein kinase C (PKC) which phosphorylates targets such as L-type Ca^{2+} channels which import more Ca^{2+} into the cell. As with all kinases discussed here, kinase isoforms are often tissue specific and illicit specific functions based on context. It is not safe to assume kinases do the same thing in different places. The specific mechanism of each signal will be discussed in detail.

Prostaglandin E2 and the DA:

A critical pathway for maintaining DA patency *in utero* is prostaglandin signaling, specifically PGE_2 activation of the prostanoid receptor EP_4. This ligand-receptor interaction is part of a large family of lipid signaling molecules known as eicosanoids, which are produced by the activity of the COX isozymes, and their corresponding receptors. Eicosanoid signals are generally paracrine in nature and mediate communication between cell types within a tissue. PGE specifically was first suggested to exist in 1930 as a blood pressure lowering substance found in prostate homogenate (170, 171). PGE_1 was isolated from sheep vesicular glands in 1959 (172) with PGE_2 and PGE_3 identified in the prostate in 1964 (173). In the early 1970's, eicosanoids were shown to dilate the DA (174), including PGE_2 in 1973 (175). Non-steroidal anti-inflammatory drugs (NSAIDs) were shown to close the DA in 1974 (176) and as early as 1976, clinical trials had shown the potential of indomethacin, a COX inhibitor, to treat PDA in human preterm infants (177). In the 1980's,

prostaglandins were found to dilate the DA in rabbits (178, 179). Additionally, blocking the production of prostaglandins with COX inhibitors such as indomethacin was found to prevent this dilation. Shortly after its discovery, in 1994 EP_4 was found to mediate PGE_2 based dilation of the rabbit DA (180). PGE_2 is the most important prostaglandin mediator of DA tone (10) and has been widely shown to dilate the rodent DA (108, 176, 181, 182). As previously mentioned, clinical administration of PGE_2 can be used to keep a closing DA patent, or COX inhibitors used to close a patent DA. But COX inhibitors administered during pregnancy can result in DA based complications. Interestingly, COX inhibitors, given as a tocolytic to arrest preterm labor, results in *fetal DA constriction* after 30-32 weeks of gestation, but not earlier in pregnancy (45, 46). In contrast, multiple reports suggest that indomethacin tocolysis is associated with postnatal PDA (47, 183-191), although this has not been a consistent finding (192-194). This discrepancy is likely due to variations in the timing, dosage, and length of tocolytic treatments. In general tocolytic treatments later in pregnancy (47, 185), closer to delivery (188), with higher dosage (190), or longer duration (189, 190) promote PDA. Incidence aside, tocolysis has also been associated with failed pharmacological treatment and an increased need for ligation (47, 186, 187, 189, 191). For some mothers, PDA risk was linked to receiving COX inhibitors as tocolytics during late- but not mid-gestation, hinting at a developmental trend (47). This maturation-dependent response was confirmed pharmacologically in mice (195-197) and COX-1;COX-2 double KO mice were generated which consistently produced a PDA phenotype coupled with congestive heart failure and early neonatal death (106, 107). This makes sense, as the importance of PGE_2 for DA tone seems to change throughout gestation. It was previously shown that PGE_2 is more critical for DA patency in late-gestation whereas NO is more critical in mid-gestation (198-201).

For the purpose of maintaining DA patency, PGE_2 production is considered to take place in either the placenta, acting as an endocrine mediator (10) or within the DA wall, acting in autocrine or paracrine fashion (202, 203). Eicosanoid biosynthesis begins with hydrolysis of the sn-2 position of

membrane phospholipids by phospholipase A2 (PLA_2). This frees a fatty acid precursor for use by the COX isozymes. Currently, there are 15 identified groups of PLA_2 isoforms subdivided into four types: cytosolic $cPLA_2$, secreted $sPLA_2$, Ca^{2+}-independent $iPLA_2$, and platelet activating factor acetyl hydrolase/oxidized lipid lipoprotein associated (Lp)PLA_2 (204). These isoforms perform diverse biological roles from mediating inflammation to promoting necrosis in old world snake venoms, but our primary focus is on the cytosolic group. $cPLA_2$s, specifically the group IV cytosolic (GIVA) PLA_2 was originally identified from human platelet cells in 1986 (205), with its transcript cloned and sequenced in 1991 (206, 207). GIVA PLA_2 is Ca^{2+} dependent, has a preference for arachidonic acid in the sn-2 position (206, 208), and is the primary PLA_2 responsible for eicosanoid biosynthesis and subsequent inflammation (209-211). Several additional $sPLA_2$s (groups IIA, IID, V, and X) also contribute (212). COX isozymes act primarily on three fatty acid precursors: dihomo-γ-linolenic acid, arachidonic acid, and timnodonic acid, corresponding to the products PGE_1, PGE_2, and PGE_3 respectively, where the subscript refers to the number of carbon-carbon double bonds (213). The relative ratio of fatty acid precursors corresponds to their rate of mobilization by PLA_2. Due to the weighted ratio of arachidonic acid in animal cells, PGE_2 is the predominant product. There are two COX isozymes, COX-1 and COX-2, both of which contain two active sites; a cyclooxygenase site and a peroxidase site (214). For example, the cyclooxygenase site may utilize an arachidonic acid and 2x O_2 to generate a five-carbon ring with a separate endoperoxide bridge, and a peroxide group, a fatty acid intermediary called prostaglandin G_2 PGG_2 (214-216) (**Figure 3**). The peroxidase site then reduces the peroxide group to a hydroxide converting PGG_2 to prostaglandin H_2 (PGH_2). PGH_2 is then released into the cytosol where it can associate to a synthase and be converted into one of five signaling compounds: prostaglandin D_2 (PGD_2), prostaglandin I_2 (PGI_2), prostaglandin $F_2\alpha$ ($PGF_2\alpha$), thromboxane A_2 (TXA_2), or the focus of my work, PGE_2. Conversion to PGE_2 is mediated by PGE synthases, of which there are three; two microsomal (mPGES1 and mPGES2) which are membrane associated and one cytosolic (cPGES) (217).

Regulation of PGE_2 production is a primary mechanism of controlling EP receptor activity. This is achieved by control of the expression, activation, and proximity of PLA_2, the COX isozymes, or the pathway-specific synthases. These relationships exist because of the recruitment of isozymes and synthases to particular subcellular microdomains which facilitate the efficient movement of products from one component to another. PLA_2 activation is

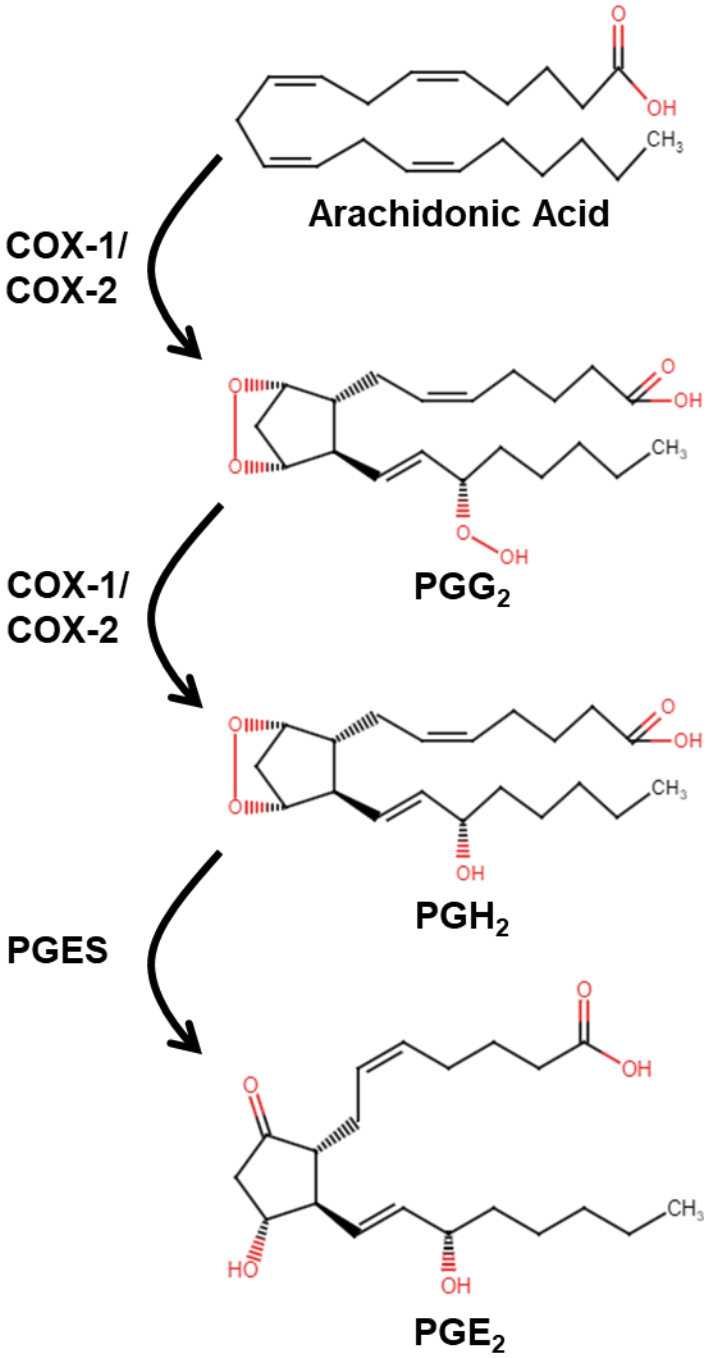

Figure 3. Eicosanoid synthesis of PGE_2 from arachidonic acid. Arachidonic acid is liberated from the phospholipids in the cell membrane by PLA_2. Arachidonic acid is then acted on by the cyclooxygenase site of either COX-1 or COX-2 producing PGG_2. PGG_2 is then acted on by a separate endoperoxide site of either COX-1 or COX-2 producing PGH_2. PGH_2 is then converted to PGE_2 by one of three PGE synthases: mPGES1, mPGES2, and cPGES. *Structures created in the RCSB PDB Sketch Tool CC0 1.0 Universal (CC0 1.0) Public Domain Dedication*

mediated primarily by phosphorylation by mitogen activated protein kinase (MAPK) (218) and the activation of inflammatory receptors such as bradykinin (219). The COX isozymes each have their own affinities for fatty acid precursors (220) and peroxide requirements (221-223) controlled by the shape of their active sites (224), though these differences are minor and their active sites highly conserved (214). They also differ in how far the isozyme sits down into the membrane it is attached to (224). Further, these isozymes exist as homodimers and occasionally as heterodimers (50, 225) with these groupings exhibiting specificity to subcellular microdomains, though this localization is contested (226). Generally, both isozymes are found in the luminal surface of the endoplasmic reticulum and both inner and outer surfaces of the nuclear envelope (226, 227). The COX isozymes also exhibit cell type-specific expression with COX-1 being found in most tissues, but not every cell of those tissues (228), whereas COX-2 is undetectable in most mammalian tissues until being rapidly induced by immune or inflammatory insult (229-234). This has led COX-1 to be called the constitutive isoform and COX-2 the inducible isoform, though COX-2 is constitutively expressed in certain tissues such as brain (235), testes (236), and kidney (237). All these factors, specific affinities, depth in the membrane, homo- or heterodimerization, affect the relative affinities and efficiencies of a particular isozyme. In general, COX-1 is the isozyme responsible for the immediate, constitutive production of PGH_2 in most cell types (215, 228) and responds to Ca^{2+} stimulation on a minute scale, whereas COX-2 is critical for the continued, delayed production of inflammation-associated PGH_2 with production lasting for several hours after activation (238-243). It is possible that these specific roles for the COX isozymes result from their functional coupling with particular PLA_2 isozymes (219). Both $cPLA_2$ and $sPLA_2$ isoforms can generate the free fatty acid precursors to fuel PGH_2 synthesis by the COX isozymes. COX-1 seems to be functionally coupled to $cPLA_2$, whereas COX-2 seems primarily functionally coupled to the secretory $sPLA_2$ isoforms (219). Localization to subcellular microdomains also allows the COX isozymes to couple to pathway specific synthases (244, 245). Specifically, COX-1 is functionally coupled with the cytosolic PGES, PGF synthase (PGFS), and thromboxane synthase

(TXS), whereas COX-2 is coupled with the microsomal PGES isoforms, and PGI synthase (PGIS) (243-246). PGD synthase (PGDS) couples to both COX isozymes and exhibits its own system of immune based regulation (244). Through the activity of the three PGE synthases, mPGES1, considered inducible, and the constitutively expressed mPGES2 and cPGES, fibroblasts, epithelial, endothelial, and certain immune cells are able to produce large amounts of PGE_2 (247). Eicosanoid biosynthesis displays a complex landscape of regulatory complexity. While, for our purposes, we are only concerned with PGE_2, it is critical to understand how many levels of regulation precede its synthesis. As with any biological process, there are, of course tissue-specific exceptions to these rules.

PGE Receptors and the DA:

PGE_2 acts primarily through one of four prostanoid receptors, EP1, 2, 3 or 4. The EP receptors are 7 transmembrane GPCRs which each have their own G protein preferences, subsequent downstream signaling cascades, and expression patterns. Prostanoid receptors were gradually defined and named throughout the 1980's, with the designation 'EP' being chosen to avoid confusion with purinergic receptors (248). Receptor identification was done primarily through the use of selective agonists and antagonists, with early EP_1 agonists such as SC-19220 being critical to this process (213). EP_4 was the last of these receptors to be identified from piglet saphenous vein in 1994 (249). EP_4 had been previously cloned in 1993, but it's distinctions from EP_2 were not apparent and it was initially labeled EP_2, with papers of the time reflecting this (249-253). Prostanoid receptors are classified into clusters based on molecular evolution and G protein preference (254). For the sake of simplicity, we will focus only on the four EP receptors and the TP receptor here. EP_2 and EP_4 are both within the first cluster, and act through $G_s\alpha$ proteins to stimulate adenylyl cyclase (AC) and increase cAMP. EP_1 and TP are both in cluster 2 and act through $G_q\alpha$ to increase intracellular Ca^{2+} through the

activation of PLC/PKA (168, 213). Finally, EP_3 falls within cluster 3, and acts through $G_i\alpha$ to decrease cAMP by inhibiting AC (255). Though attempting to understand the properties of EP receptors strictly by their clusters fails to account for splice variants. EP_3, for example, has 7 splice variants, some of which couple with $G_s\alpha$ or $G_q\alpha$ instead of $G_i\alpha$, completely inverting their signaling effects (256, 257). This means that expression analysis, or studies of PGE_2 response alone will never be sufficient to determine what G proteins are being utilized or which downstream pathways are active.

EP_4 was found to be the primary EP receptor in the DA of rats (146) (qRT-PCR), rabbits (258) (qRT-PCR), lambs (259) (Northern blot) (260) (qRT-PCR), pigs (261, 262) (Western blot), baboons (260) (qRT-PCR), and humans (263) (RT-PCR) (264) (immunohistochemistry). In addition, EP_4 is differentially expressed between the DA and Ao in mice (114), rodents, and humans (265). EP_4 expression in the human rises over gestation and is limited to the media and intima of the DA (264). EP_4 expression has also been found to decrease in the neonatal period (258). The EP_4 KO mice were created by three independent labs using distinct transgenic strategies, though all utilizing an excision of exon 2 (108-110). Nguyen et al, reported the first example of a mouse model of PDA in 1997. EP_4 KO mice (129/SvEv background) had neonatal lethality accompanied by a widely patent DA and pulmonary edema (108). This phenotype was observed by all three groups with varying penetrance. When the null allele was crossed into a mixed genetic background (B6D2 F1, C57BL/6 (unspecified sub-strain) and DBA/2 cross) the uniformly lethal phenotype changed to 5% survival after 1 backcross and to 21% survival after 4 crosses (108) representing a strain dependent sensitivity to the PDA phenotype which is diluted in an increasingly mixed genetic background. Despite the fact that KO models have been produced for all prostaglandin receptors (266-271), only EP_4 KO mice have a PDA phenotype, and all global EP_4 KO models have PDA (108-110). The EP_4 KO PDA phenotype has been termed the ‘paradoxical PDA’ due to its counterintuitive signaling, since the removal of a vasodilatory receptor is expected to foster constriction, not an inability to constrict (272) (**Figure 4**).

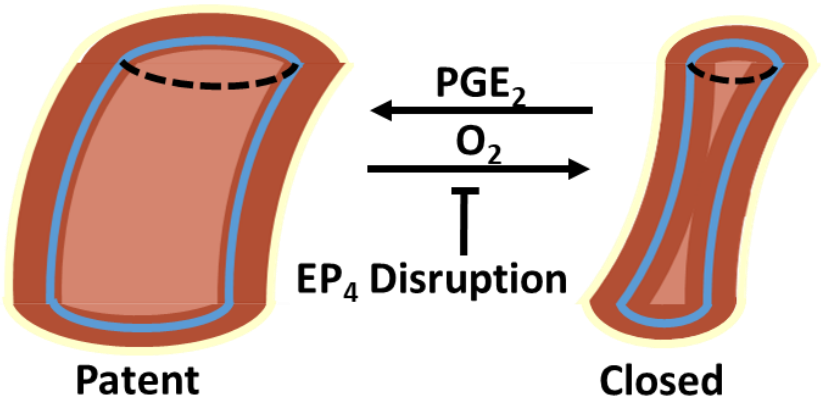

Figure 4. Disruption of EP_4 during gestation results in a 'paradoxical' PDA. While PGE_2 stimulation of EP_4 is generally vasodilatory, supporting DA patency *in utero*, chronic disruption of EP_4 during gestation prevents the O_2 mediated constriction of the DA after birth, leading to PDA.

For this reason, our group speculated that EP_4 may play an additional role in the DA, guiding vessel formation and remodeling.

Both EP_4 and EP_2 couple through $G_s\alpha$ to activate AC and increase cAMP in a vasodilatory fashion (**Figure 5**). In the DA this is mediated primarily through coupling with type 2 and type 6 AC isoforms (147). The mechanisms of cyclic nucleotide-mediated vasodilation

are diverse and rely entirely on the expressed cellular machinery in a given cell. Despite this, the general scheme of vasodilation is principally the same for both GPCR signaling derived cAMP or NO/CO signaling derived cGMP. The cyclic nucleotide acts through one of three classes of molecules: cyclic nucleotide-dependent ion channels, cyclic nucleotide binding PDE, or cyclic nucleotide dependent protein kinases. Both cAMP and cGMP are hydrolyzed by PDE isoforms, neutralizing their vasodilatory activity. Critically, PDE isoforms exhibit some level of cAMP or cGMP specificity in their action (273-275). Multiple PDE isoforms have been identified as important in the DA and will be discussed in detail later. Canonically, cAMP is thought to function through the PKA and cGMP through the serine/threonine protein kinase G (PKG). Despite this, cAMP-mediated transactivation of PKG is thought to be more relevant in vasodilation (276-279). One proposed mechanism for this transactivation is the PKA-mediated activation of eNOS (endothelial nitric oxide synthase) and subsequent cGMP production (168). Once active, PKA or PKG act to relax SMCs through two synergistic mechanisms; the reduction of intracellular Ca^{2+} and the desensitization of the contractile apparatus to remaining Ca^{2+}. In order to import Ca^{2+} without hyperpolarizing the cell membrane, Ca^{2+} activated K^+ channels (K_{Ca}) export K^+ proportionally to imported Ca^{2+}. Activation of K_{Ca} channels by either PKA or PKG prevents this efflux of K^+ impeding the ability of the cell to increase Ca^{2+} concentrations, resulting in relaxation (279-284). Additionally, phosphorylation of certain Ca^{2+}

channels reduces the influx of Ca^{2+} (285). PKG also phosphorylates Ca^{2+}/ATPase pumps in both the plasma membrane (outward directing) (286) and sarcoplasmic reticulum (inward directing) (287) facilitating the movement of Ca^{2+} either out of the cell or into the sarcoplasmic

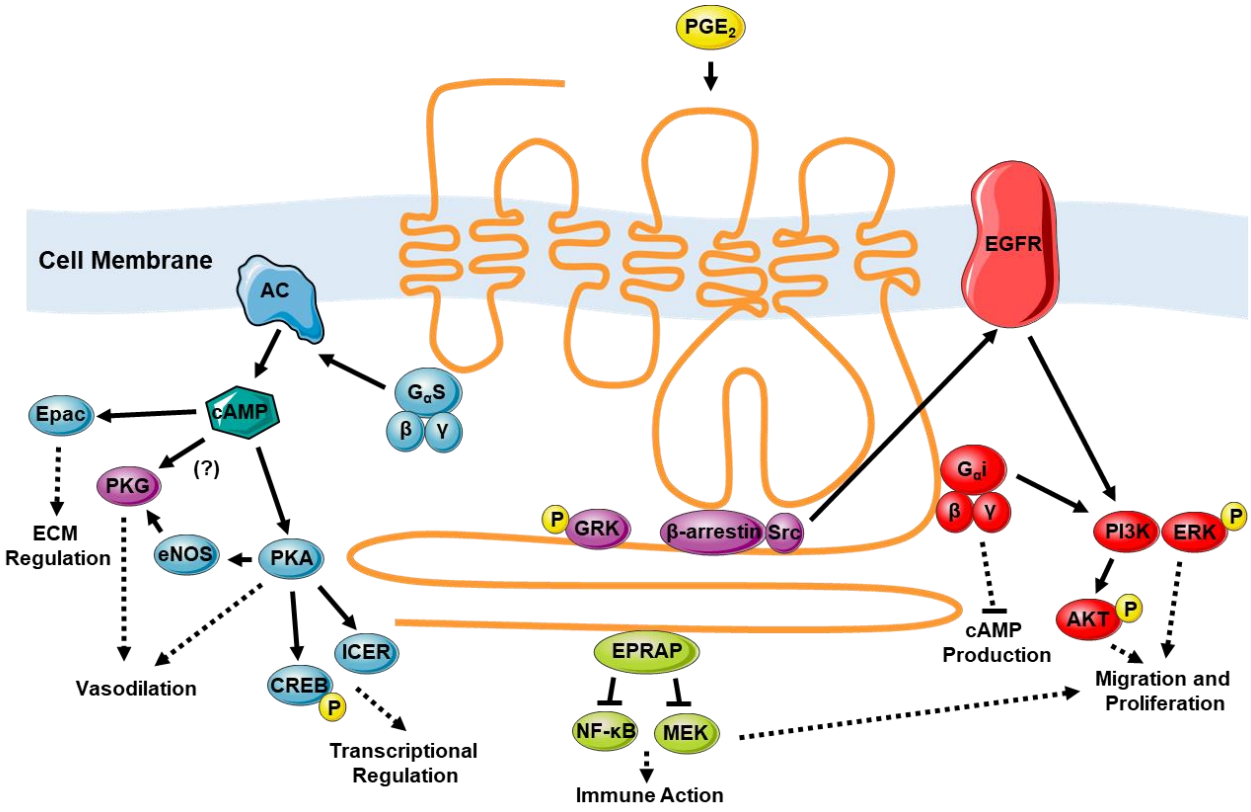

Figure 5. Downstream signaling mechanisms of the EP_4 receptor potentially relevant to the DA. Position of pathway constituents approximate where they interact with the transmembrane loops and tail domain of the EP_4 receptor. EP_4 acts primarily through the $G_s\alpha$ G protein in vasculature leading to adenylyl cyclase (AC)-mediated cAMP production. cAMP activates the exchange protein activated by cAMP (EPAC) and subsequent regulation of extracellular matrix (ECM) components such as hyaluronic acid in the DA. cAMP activation of protein kinase A (PKA) facilitates context-dependent transcriptional regulation through the cAMP response element binding protein (CREB) and the inducible cAMP early repressor (ICER). EP_4 stimulation increases protein kinase G (PKG)-mediated vasodilation in a cAMP-dependent fashion. This may occur through PKA-mediated increases in endothelial nitric oxide synthase (eNOS) activity, or some unknown mechanism. PKA and PKG both mediate vasodilation through the phosphorylation-based regulation of ion channels and regulatory components of the contractile apparatus. EP_4 can also act through the $G_i\alpha$ G protein, antagonizing cAMP production through AC, as well as stimulating the Ras-ERK pathway through activation of PI3K/ERK/AKT promoting migration and proliferation. Activation of G protein-coupled receptor kinase (GRK) leads to rapid desensitization of the receptor, which phosphorylates serine residues facilitating the binding of β-arrestin and subsequent receptor internalization. β-arrestin also promotes c-SRC and transactivation of receptor tyrosine kinases such as EGFR. Transactivation of EGFR further activates the Ras-ERK pathway. EP_4 possesses a long tail domain enabling it to interact with the EP_4 receptor-associated protein (EPRAP) which elicits various immune actions in a cAMP-independent way. Solid lines represent direct interactions. Dashed lines represent connections to processes. Figure created using images and assets from Servier Medical Art. Servier Medical Art by Servier is licensed under a Creative Commons Attribution 3.0 Unported License (https://creativecommons.org/licenses/by/3.0/). *Modified with permission from Konya et al. (168)*

reticulum, lowering intracellular content. Finally, PKG is capable of phosphorylating PLC and preventing the production of IP3 and the subsequent release of intracellular Ca^{2+} stores (273, 288, 289). It should be noted that an inverted version of this mechanism, by which cGMP

activates PLC activity and subsequent IP3 production increasing intracellular Ca^{2+} is proposed in pancreatic acinar cells (290). Additional regulation of K_{Ca} channels may occur through cAMP independent interactions with G protein-activated AC (291-293). Within smooth muscle, the cycling of MLC is regulated by a balancing act of MLCK which phosphorylates MLC, activating it, and MLCP which dephosphorylates MLC, deactivating it. Essentially, inhibiting MLCP increases MLC activation in a Ca^{2+} independent fashion sensitizing the cell, whereas inhibiting MLCK desensitizes the cell, even in the presence of Ca^{2+} (167, 294). cGMP-PKG activity has been shown to increase MLCP activity without a change in MLCK activity, shifting the balance of MLC cycling resulting in relaxation (167, 294). This is possibly achieved through the PKG-mediated phosphorylation of an MLCP activating residue, the M110 regulatory subunit or inhibition of an as yet unknown inhibitor (167).

Activation of PKA can also lead to transcriptional changes through the activation of the cAMP response element binding protein (CREB), or the inducible cAMP repressor (ICER), a truncated form of CREB which binds the same cAMP response element, but is strictly inhibitory (295). CREB promotes the transcription of *c-fos* and various neuropeptides while ICER antagonizes this. Increased cAMP also activates the exchange factor activated by cAMP, (EPAC). EPAC 1 and 2 interact with members of the Ras superfamily leading to proliferation, migration, differentiation, and inflammation (296). PKA-mediated cAMP production can also lead to a feed-forward expression of COX-2 through AMP activated protein kinase (AMPK) (297). This feed-forward cycle of EP_4 activation and COX-2 expression has been noted by several investigators (298-300) and is likely only kept in check by internalization of the EP_4 receptor (301). Regardless, in most vascular beds, PGE_2 acts through EP_2 or EP_4 and is generally vasodilatory. This is in contrast to EP_3, which, being coupled to an inhibitory G

protein, reduces cAMP and leads to vasoconstriction. EP_3 is prevalent in human internal mammary arteries, as well as rat mesenteric arteries, both of which constrict in response to PGE_2 (302, 303). While EP_2 and EP_4 share a primary signaling mechanism, EP_4 has a significantly more complicated downstream cascade. Unlike EP_2, EP_4 has also been shown to associate with $G_i\alpha$ like EP_3, meaning that it can mediate context-dependent vasoconstriction (**Figure 5**) (304). $G_i\alpha$ also supports activation of PI3K and extracellular signal-regulated kinase kinase (ERK) which fosters migration through phosphorylation of proteins which promote protrusion, adhesion, and contraction (305-308). ERK activation is generally promigratory and prometastatic in cancers (309), and was associated with *in vivo* neurovascularization and endothelial migration (310).

Additionally, EP_4 possesses a long, c-terminal tail domain absent in other EP receptors which enable two highly consequential signaling mechanisms. First, G protein coupled receptor kinase (GRK) can associate to the c-terminus where it rapidly phosphorylates residues desensitizing the receptor and attracting βarrestin (**Figure 5**). βarrestin then initiates receptor internalization, the binding of tyrosine-protein kinase Src (cSrc), and the transactivation of neighboring receptor tyrosine kinases. These receptor tyrosine kinases include growth factor receptors which can further increase signaling through ERK, protein kinase B (Akt), and support migration. Interestingly, due to a lack of this elongated tail domain, EP_2 does not undergo the same process of desensitization and internalization (311), making it a much more potent vasodilator, albeit one that is usually present at much lower expression levels. The role of the EP_4 C-terminal tail in receptor desensitization was determined by sequential truncation experiments where the tail was gradually shortened until desensitization was lost and the receptor persisted at the cell surface (312). EP_2 also possess four N-glycosylation sites compared to two in EP_4, with N-glycosylation playing a key role in maintaining the receptor at the cell surface (313). Additionally, the elongated c-terminus of the EP_4 tail domain allows it to interact with the EP_4 receptor associated protein (EPRAP), stabilizing subunit p105 of its complex

(314). This prevents the activation of NF-κB and mitogen-activated protein kinase kinase (MEK)/ERK which act to block transcription of proinflammatory cytokines (**Figure 5**) (315). Comprehensive studies on what downstream pathways EP_4 acts through in various body tissues are elusive, and it is largely assumed that these potential signaling mechanisms are active simultaneously.

A major factor governing the function of each EP receptor is their tissue-specific expression. EP_1 is fairly ubiquitously expressed (316) (qRT-PCR). EP_2 is expressed at low levels and found in bone marrow (317) (qRT-PCR), female reproductive tissues (318) (qRT-PCR), and the airways (319) (qRT-PCR). EP_3 is expressed in fatty tissues (316) (qRT-PCR), kidney (320) (*in situ* hybdridization), pancreas (316) (qRT-PCR), and vena cava (316) (qRT-PCR). EP_4 is expressed in the gastrointestinal tract (321, 322) (*in situ* hybridization), uterus (318) (qRT-PCR), bone marrow (317) (qRT-PCR), and skin (316) (immunohistochemistry). As previously mentioned, EP_4 expression is high in the DA and conserved amongst various species (146).

EP_4 is consistently the largest of the EP receptors, with sizes of 402, 358, 390, and 488 amino acids in humans (323), and 405, 362, 366, and 513 amino acids in mice (256, 324), for EP_1, EP_2, EP_3, and EP_4 respectively. The four receptors are coded as separate genes within the genome, *Ptger1*, *Ptger2*, *Ptger3*, and *Ptger4* respectively. Interestingly, instead of sharing common evolutionary lineage with each other, the receptors evolved within their clusters. For example, the EP_3 receptor is more closely related to the TXA_2 receptor than to any other EP receptor. This is reflected in the sequence homology of the EP receptors, with EP_4 sharing only 30% and 37% homology with EP_1 and EP_3 respectively. EP_4 and EP_2 both associate with the same G protein and still only share 38% homology (256, 323). The most conserved region is within the membrane helices that form the PGE_2 binding pocket, with a single threonine residue, T168, in the second extracellular loop essential (325). Within EP_4 specifically, 7 residues likely mediate PGE_2 binding: S103, T168, Y168, F191, L195, S285, and 311 (326). Possibly as a testament to how indispensable these receptors are, amino acid

homology within a given receptor isoform is fairly high across species ranging from 88-99% amongst various mammals, with mice and humans sharing 88% (213). Despite high levels of amino acid conservation in the final protein products, the *Ptger4* gene varies significantly between humans and mice. The Human *PTGER4* gene is a 7 exon, 86,952nt gene located on chromosome 5 (Ensemble). The mouse *Ptger4* gene by comparison, is 3 exons, 14,025nt, located on chromosome 15 in a region composed of other genes also found in the human chromosome 5 (Ensemble). The increase in exons in the human *PTGER4* gene allows it to code for 5 splice variants, as opposed to only three in the mouse (Ensemble, MGI). While the majority of these variants are nonprotein coding, mice produce both the standard 513 amino acid Ptger4-201 as well as a 488 amino acid variant, Ptger4-202. Practically no research has been done on this particular variant, its expression pattern, or its receptor kinetics.

Nitric Oxide Signaling in DA Vasodilation:

While PGE_2-EP_4 signaling is critical for maintaining DA patency in late gestation, the dilator responsible for maintaining DA patency in early gestation is nitric oxide (NO). Pharmacological inhibition studies in rats revealed that while blocking the production of PGE_2 in term pups (D21; 21 DPC, days post-coitus) resulted in strong constriction, a significantly weaker constriction was observed in preterm pups (D19) (199). Inhibition of NO synthesis found the exact opposite, with term pups experiencing little constriction, while preterm pups showed severe constriction. These results were replicated in mice for both term (D19) and preterm (D16) with similar findings (200). The story in lambs is more complicated, with inhibitors of nitric oxide synthase (NOS) exhibiting little effect in mounted DA rings, but sodium nitroprusside (SNP), an NO donor, producing a stronger dilation in preterm vessels than term (198). While both NO and cGMP were found to dilate the ovine DA, prostaglandins seem to exert more control over DA tone (327).

NO is produced by the degradation of L-arginine into L-citrulline, and then NO alongside O_2 and nicotinamide adenine dinucleotide phosphate (NAPDH) (328). NO is produced by three NOS isoforms, one inducible, (iNOS), and two constitutive, neuronal NOS (nNOS) and the endothelial eNOS. While iNOS is limited to immune action and regulated via expression, nNOS and eNOS are activated by increasing intracellular Ca^{2+} and calmodulin. While all three isoforms of NOS have been detected in large vessels (329-332) unsurprisingly, eNOS is the primary NO source for the vasculature. Examination of NOS isoforms in mice revealed that eNOS was the predominant isoform in the DA, and that it localized to the endothelium via *in situ* hybridization (200). Studies in lambs found that both eNOS and nNOS were found in the endothelium of the DA (198, 327). Interestingly, dilatory effects of both NOS and cGMP were not endothelium-dependent in the lamb DA (333). A fourth, debated NOS is thought to reside within the mitochondrial matrix and generate nitrogen species there (mtNOS) (334, 335). The existence of mtNOS is omitted in the current DA literature, but such a molecule could interplay with one of the potential O_2 sensing mechanisms in the DA. Non-enzymatic routes of NO production are also possible, with cytochrome P450 reductase (CYPOR) and xanthine oxidoreductase (XOR) both capable of reducing nitrite. NO can also be stored and transported in the blood as S-nitrosylated proteins, iron-nitrosylhemoglobin, and the local heme-mediated reduction of nitrite. In the vasculature, NO generally acts in a paracrine fashion, diffusing outward through the vessel wall from the endothelium, eliciting VSMC relaxation and local vasodilation in response to decreased perfusion. NO mediates its vasodilatory effects by activating soluble guanylate cyclase (sGC) in VSMCs which in turn produces cGMP (328). Similar to cAMP, cGMP then acts through one of three classes of molecules, cGMP-dependent ion channels, cGMP binding phosphodiesterases, or cGMP dependent protein kinases (336). The downstream effects of NO on a particular tissue are directly dependent on the expression levels of these proteins. It is worth noting that a membrane-bound particulate guanylate cyclase (GC) isoform (pGC) exists, which is capable of producing cGMP in response to carbon monoxide (CO) (336). CO production has been

detected in the lamb DA and was found to play a minor dilatory role in DA tone (337). cGMP-dependent ion channels are prevalent in both vision and olfaction (273) but don't appear important for VSMC relaxation. Most actions of NO seem to be mediated by the activation of PKG, which is expressed at high levels in smooth muscle cells and few other tissues (338).

NO also depresses mitochondrial respiration by competing with O_2 for binding with cytochrome c oxidase in the mitochondria. Seeing as the byproducts of mitochondrial redox are considered a potential O_2 sensing mechanism for regulation of DA tone, NO may play an additive vasodilatory role; exerting vasodilatory force through the production of cGMP, but also impeding O_2 sensing and subsequent vasoconstriction. This is supported by the capacity of NO to decrease O_2 consumption in the vessel wall (339, 340)

Oxygen Sensing in DA Vasoconstriction:

Key to the process of DA closure after birth is O_2-mediated constriction of the DA. After birth, increasing pO_2 from the newly inflated lungs provides the initial muscular constriction of the DA and begins the process of flushing and metabolizing circulating PGE_2. Despite ample research, the exact mechanism of O_2 sensing in the DA is unclear. O_2 sensing may occur through a combination of three potential mechanisms; the production of isoprostanes, the generation of byproducts from mitochondrial redox, the activation of endothelin 1 (ET1) by a CYP-mediated mechanism (**Figure 6**).

F-2 isoprostanes are eicosanoid signals produced by the free radical peroxidation of arachidonic acid without enzymatic action (341). Isoprostanes are established markers of oxidative stress shown to be vasoconstrictive in various vascular beds (342, 343), including in the isolated

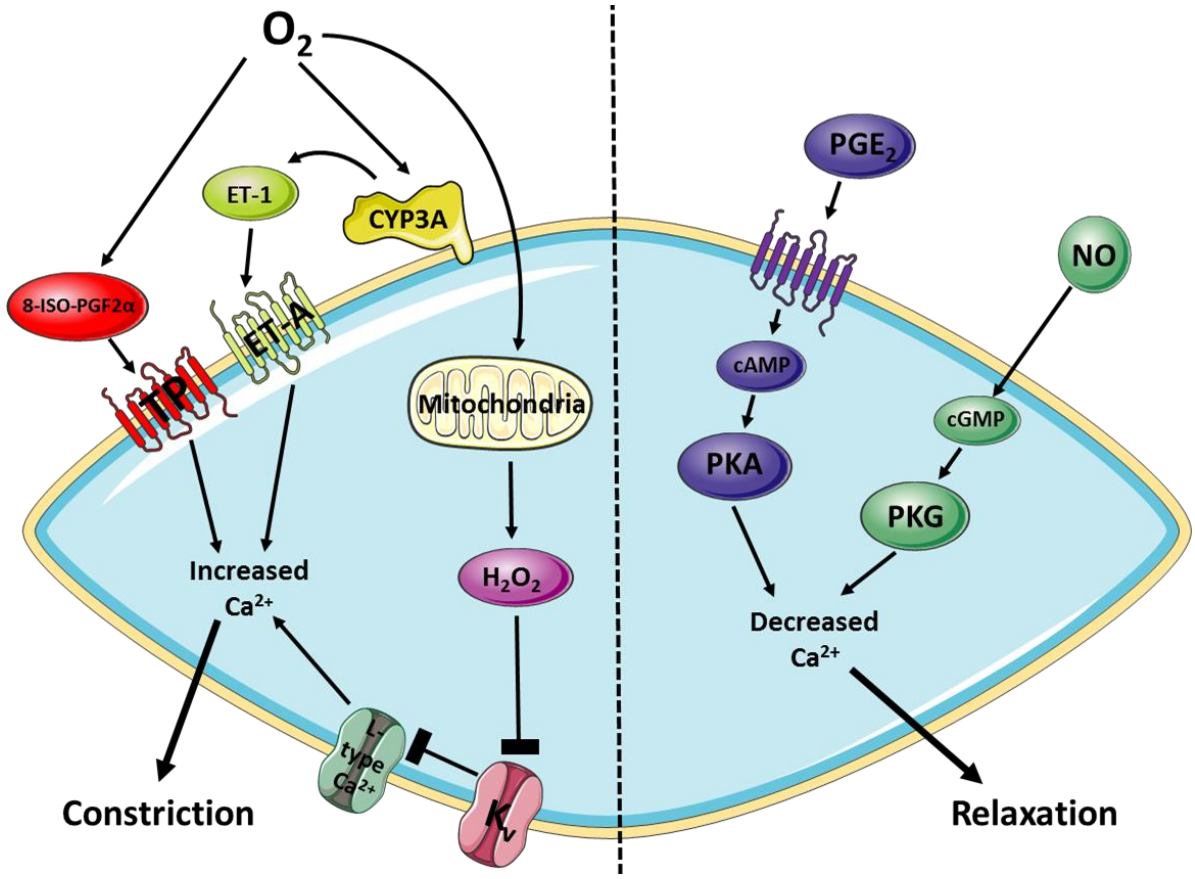

Figure 6. Three proposed mechanisms mediate O_2 sensing in the DA. 1) Isoprostanes such as 8-ISO-PGF2α are produced by the metabolism of circulating eicosanoids following inflation of th lungs. Isoprostanes bind thromboxane (TP) receptors increasing Ca^{2+} and facilitating constriction. 2) Increasing O_2 tension leads to increased cycling of mitochondrial redox pairs, resulting in increased production of reactive oxygen species such as H_2O_2. H_2O_2 inhibits the voltage gated potassium channels (K_v) allowing depolarization of the membrane and activation of L-type Ca^{2+} channels, increasing intracellular Ca^{2+}. 3) O_2-mediated CYP450 activity, specifically that of CYP3A results in the downstream production of endothelin 1 (ET-1). ET-1 activates endothelin A (ET-A) receptors increasing intracellular Ca^{2+}. 4) O_2-mediated VSMC constriction is antagonized by the dilatory action of both PGE_2 through the EP receptors, and NO which both act to decrease intracellular Ca^{2+}.

chicken DA (344, 345). O_2 exposure results in increases in 8-iso-$PGF_{2\alpha}$ in rats (346) as well as 8-iso-$PGF_{2\alpha}$ and 8-iso-PGE_2 in mice (347). Pharmacological studies on isolated DA found that 8-iso-$PGF_{2\alpha}$ mediates potent vasoconstriction through stimulation of the TXA_2 receptor whereas 8-iso-PGE_2 mediates a much weaker vasodilatory effect through stimulation of EP_4 (347). TXA_2 expression increases at term, which may explain the strength of vasoconstriction.

In addition to DA patency, constriction of the branch pulmonary arteries and resistance pulmonary arteries contribute to the hemodynamic shunting past the lungs and through the DA *in utero*. This process, called HPV is mediated by a system of O_2 sensors (348) and ion channels (349, 350) which act to maximize oxygenation of the blood by limiting flow to damaged or unproductive sections of alveoli. This functions exactly the opposite of the peripheral (351, 352) or cerebral vasculature (353), which dilate in response to hypoxia in an attempt to guarantee adequate perfusion. The mitochondria of VSMCs are proposed to act as one of these sensors in specific vessels. Mitochondria are the power houses of the cell, generating adenosine tri-phosphate (ATP) an energetic intermediary, through a successive redox cascade referred to as the electron transport chain (ETC). This chain begins with electron donors produced through metabolic cycles such as nicotinamide adenine dinucleotide (NADH) which are oxidized (NAD^+) to build a proton gradient and ends with the reduction of O_2 to H_2O. The initial substrate of each successive Complex of this process and its corresponding oxidized molecule, for example NADH/NAD^+, form a redox couple. Additionally, Complexes I and III of the ETC generate reactive oxygen species (ROS). Together, redox couples and ROS act to regulate transporters, ion channels, and enzymes, resulting in changes to intracellular Ca^{2+} and Ca^{2+} sensitivity (354). Because O_2 is generally the rate-limiting component of mitochondrial function, mitochondrial networks fuse and slow production of ATP during hypoxia. This results in a decrease in ROS production as well as a relative shift in redox couples from the oxidized partner (NAD^+) to the reduced (NADH). After birth, when the DA shifts from the hypoxic environment of the

womb to room air, the mitochondrial network of its SMCs begin to fission, ATP production increases, and Complex I and III begin to produce more ROS (355), specifically H_2O_2. Studies in rabbits revealed that O_2-mediated DA constriction was dependent on inhibiting voltage gated potassium channels (K_V) (349, 356). Once inhibited, K_V channels allow the depolarization of the cell membrane, activation of L-type voltage gated Ca^{2+} channels (Ca_L) which increase intracellular Ca^{2+} via influx (357, 358). Inhibition of Ca_L channels prevents constriction of the human DA in normoxia (359). O_2-mediated DA constriction is endothelium independent (360) indicating the O_2 sensing mechanism is intrinsic to DA SMCs. Studies of hypoxic human DA rings further link vasoconstriction to ROS, showing constriction in response to oxidizing agents and relaxation in response to antioxidants (361). Further, inhibitors of the ETC reproduce findings in hypoxic vessels, increasing K^+ efflux, decreasing ROS production, and producing vasodilation (362). Tying these factors exclusively to mitochondrial dynamics, mitochondrial fusion has been shown to be necessary for O_2-mediated DA constriction (355).

An extensive search for an O_2 sensor and effector within the DA has taken place for decades. Due to several characteristics of the DA O_2 response, such as an uneven distribution within the vasculature, and developmental regulation that doesn't coincide with the maturation of contractile function, it was suggested the DA O_2 response was receptor mediated (363, 364). Initial observations that suppression of a vasoconstrictive peptide secreted from the endothelium, ET1, prevented O_2-mediated constriction flagged it as a potential effector (365-367). It has been proposed that a cytochrome P-450 hemoprotein of the CYP3A subfamily acts as the O_2 sensor. This CYP3A functions as the catalytic element of a monooxygenase reaction producing an intermediary which activates ET1 (364). It is also possible that CYP450-associated epoxygenase and 12(S)-lipoxygenase play a role in the production of this intermediary (368). This is further supported by an increase in 12(S)-lipoxygenase expression in the DA at birth (115). While the exact connection between CYP450-

mediated O_2 sensing and endothelin activation remains unclear, ET1 acting through its A-type receptor (ET_A) is the most potent constrictor of the DA in some laboratory contexts (366, 369). ET1 is expressed in the DA muscle, is upregulated at birth (115, 116), and increases its expression with increasing O_2 tension (365, 370). O_2-mediated DA constriction is also disrupted through the deletion or inhibition of either ET_A (8, 365-367, 371, 372) or disruption of CYP450 function (373).

Summary:

A thoughtful examination of the basic biology of DA closure leads to several key conclusions and subsequent questions. The process of DA closure does not begin at birth, but with key remodeling changes that occur during late gestation. These changes, which prepare the DA for closure after birth seem to suggest the existence of a time-dependent developmental program. Many of these processes appear to be tied to PGE_2 signaling through EP_4. Further, the seemingly paradoxical PDA phenotypes produced by the time-sensitive disruption of the COX isozymes in humans and mice, as well as deletion of EP_4 suggest that prostaglandin signaling must play some additional role in DA development beyond acute vasodilation. What exactly does EP_4 do during development to prepare the DA for closure after birth? How does the absence of EP_4 disrupt the O_2-mediated closure of the DA at birth? I hypothesized that PGE_2 signaling through EP_4 mediates a time-dependent developmental program responsible for establishing the mature contractile capabilities and O_2 sensing mechanisms of the term DA. Through this dissertation, I will describe my logic, experiments, and findings related to EP_4 and its role in proper DA development.

Aims

Gap in Knowledge

While it is understood that acute PGE_2-EP_4 signaling is required to maintain a patent DA *in utero*, PDA phenotypes in both COX-1/COX-2 double KO (106, 107, 374) and EP_4 KO mice (108-110) suggest a chronic developmental role for PGE_2-EP_4 signaling in establishing the mature, term DA. While this developmental role for EP_4 has been speculated in the literature (272, 375), the cause of the EP_4 KO phenotype and the underlying mechanisms through which chronic EP_4 stimulation matures the DA remain unclear. Specifically, PDA may result from deficits in DA contractile potential or failure of the DA to respond to specific signals such as O_2, neither of which have been explored in the EP_4 KO DA. Additionally, it is unclear exactly when during development EP_4 is required for proper DA development. While it has been suggested that EP_4 exerts its developmental role in the DA through a developmental program (272), this has not been clearly demonstrated and downstream constituents of such a program have not been effectively identified.

Questions

Is DA development mediated by an EP_4-associated developmental program?

When is EP_4 required for proper DA development?

What features of DA function are established by chronic EP_4 stimulation in the DA?

Hypothesis

We hypothesize that prostaglandin signaling mediates a **time-dependent** developmental program crucial for the establishment of the DA's **contractile potential**, and/or **O_2 sensing capabilities**.

Aims

Aim 1: Establish the presence of a developmental program within the DA. *This aim will address the hypothesis that DA development is mediated by a distinct set of effector genes, potentially regulated by EP_4*. Analysis of both murine and human transcriptomic data sets will identify genes important for DA identity. Collation of mouse models and comparison to human single gene syndromes associated with PDA will identify genes crucial for DA development.

Aim 2: Define the developmental window in which EP_4 is required for proper DA development. *This aim will address the hypothesis that EP_4 plays distinct roles as an acute regulator of DA tone and a chronic regulator of DA development*. Pharmacological inhibition studies will be used to identify the acute contributions of EP receptors to DA tone and the timing in which EP_4 is required for proper DA development.

Aim 3: Determine whether the EP_4 KO PDA phenotype results from deficits in contractile potential. *This aim will address the hypothesis that EP_4 is responsible for establishing the contractile properties of the term DA*. Pressurized vessel myography and mice lacking EP_4 receptors will be used to determine the developmental contribution of EP_4 to DA tone.

Aim 4: Determine whether the EP_4 KO PDA phenotype results from deficits in O_2 sensing and constriction. *This aim will address the hypothesis that EP_4 is responsible for establishing the O_2 sensing capabilities of the term DA*. Pressurized vessel myography will assess the O_2 response of the

DA from mice lacking EP_4 receptors *ex vivo*. Exposure of mice lacking EP_4 receptors to hyperoxia after birth will assess O_2 response *in vivo*.

Significance

EP_4 is the most prevalent EP receptor in the human DA (263, 264) and disruption of PGE_2 production through the administration of COX inhibitors as a tocolytic contributes to PDA (47). Further, treatment with COX inhibitors is the first line pharmacological treatment for PDA. The importance of PGE_2-EP_4 for DA development seems highly conserved and provides an incredibly useful therapeutic target for clinical management of the DA. While we understand the importance of PGE_2-EP_4 in the DA, we do not understand the developmental timing of this importance or the developmental processes affected. A deeper understanding of the developmental role of EP_4 in the DA may inform better treatment of infants suffering PDA, and of prospective mothers to prevent potential PDA in their newborns.

Chapter 2

TRANSCRIPTIONAL PROFILING REVEALS PUTATIVE TARGETS OF A DEVELOPMENTAL PROGRAM IN THE DUCTUS ARTERIOSUS

Adapted with permission from Michael T. Yarboro, Matthew D. Durbin, M.D., Jennifer L. Herington, Ph.D., Elaine L. Shelton, Ph.D., Tao Zhang, M.D., Ph.D., Cris G. Ebby, Jason Z. Stoller, M.D., Ronald I. Clyman M.D., Jeff Reese, M.D. (2017) Transcriptional Profiling of the Ductus Arteriosus: Comparison of Rodent Microarrays and Human RNA Sequencing. Semin Perinatol. DOI: 10.1053/j.semperi.2018.05.003

Abstract:

DA closure is crucial for the transition from fetal to neonatal life. This closure is supported by changes to the DA's signaling and structural properties that distinguish it from neighboring vessels. Examining transcriptional differences between these vessels is key to identifying genes or pathways responsible for DA closure. Such transcripts are likely targets of a developmental program which guides DA function after birth. Several microarray studies have explored the DA transcriptome in animal models but varied experimental designs have led to conflicting results. Thorough transcriptomic analysis of the human DA has yet to be performed. A clear picture of the DA transcriptome is key to guiding future research endeavors, both to allow more targeted treatments in the clinical setting, and to understand the basic biology of DA function. In this chapter, I use a cross-

species cross-platform analysis to consider all available published rodent microarray data and novel human RNAseq data in order to identify high priority candidate genes which may constitute the developmental program of the DA.

Introduction:

The DA is an essential vascular shunt connecting the pulmonary artery and aorta, allowing oxygenated blood from the placenta to bypass the developing lungs *in utero*. After birth, DA closure is required for a proper transition to neonatal life. Often, the postnatal DA fails to close, resulting in PDA. PDA accounts for nearly 10% of congenital heart defects (38, 376), including more than 30% of preterm infants with a birth weight of <1500g (377, 378).

Effective DA closure is dependent on a combination of signaling and structural changes which support constriction and eventual remodeling of the vessel (25, 148, 379). Despite the proximity and common neural crest lineage of their smooth muscle cells (15), the ascending aorta (Ao) doesn't undergo these changes, suggesting transcriptional differences between these vessels may define the DA's function. Numerous attempts to understand these differences at the transcriptome level have provided insight but varied experimental design and statistical analyses have created contradictions and ambiguity in the literature. Further, the transcriptome of the human DA has not been explored with the advanced genomic techniques now available, such as RNA-seq. A clear picture of the DA's transcriptional profile is key to guiding future research endeavors, both to allow more targeted treatments in the clinical setting, and to understand the basic biology underlying DA function.

The goals of this study were to: 1) define differentially expressed genes (DEGs) in DA versus Ao samples that were commonly identified in previously published microarray datasets using rodent models, 2) identify human DA-enriched transcripts using RNA-seq analysis, and 3) explore

transcriptional commonalities between the rodent and human DA. Although cross-species and cross-platform comparisons are fraught with limitations, identification of robust markers of DA identity or novel DA-enriched pathways promises to provide unique insights into DA development and function.

Results:

Comparison of Published Rodent Microarrays:

Our microarray meta-analysis focused on studies containing DA to Ao comparisons in term animals, since there were too few preterm studies for comparison. Comparison of DA to Ao expression allowed DA-specific genes to be distinguished from temporally-regulated genes that are important for generalized vessel development. Differential expression was recalculated from raw data using a uniform statistical approach. Array data from three mammalian species (rat, mouse, sheep) were available, but differences in experimental design and genome annotation limited the use of data from sheep (121). Four rodent studies met pre-specified criteria (vessel type, gestational stage) and were included for analysis (114, 117, 119, 120) (**Table 1**). There were 444 genes identified as differentially expressed in at least three of four arrays. Of these, 87 genes were consistently increased in DA versus Ao (DA enriched), while 189 genes were consistently decreased in DA versus Ao (Ao enriched) (**Figure 1**). Complete gene lists are provided for both DA enriched (**Table S1**) and Ao enriched (**Table S2**) gene sets. Interestingly, many of the genes that were common to at least 3 studies, such as *Abcc9* (380-383), *Cacna1c* (384), *Edn1* (10, 117, 383), *Pde4b* (69, 121), *Ptger4* (108-110, 113, 383, 385, 386), and *Tfap2b* (104, 383, 387-392), have previously been identified as significant for DA function (**Table S1**, blue typeface). A more thorough listing of previously identified genes

Table 1 **Summary of Included and Excluded Studies using Microarray to Compare DA and Ao**

Study (ref)	Species	Strain	Description	GSE#	Platform	Probe#	Analysis	Samples	Age	Genes UP	Genes DOWN
Jin 2011[13]	*Rattus norwegicus*	Wistar	Term and preterm DA	3422	Affy Rat U34 A Array	8799	ANOVA	2 DA vs 2 Ao	E21	328	366
Bokenkamp 2014[9]	*Rattus norwegicus*	Wistar	Isolated SMC vs endothelium	51248	Affy Rat 230 2.0 Array	12088	ANOVA	6 DA vs 6 Ao	E21	2453	2347
Hseih 2014[10]	*Rattus norwegicus*	F344	PDA in Brown-Norway rat	40534	Affy Rat 1.0 ST Array	29215	ANOVA	2 DA vs 2 Ao	E21	2027	2336
Shelton 2014[14]	*Mus musculus*	CD1 WT	Term DA expression	51664	Affy Mouse 430 2.0 Array	45101	ANOVA	4 DA vs 4 Ao	E19	1532	1958
Costa 2006[42]	*Rattus norwegicus*	Long-Evans	Oxygen's effect on preterm DA	3290	Affy Rat U34 A,B,C Array	26379	Excluded (preterm only)	_	_	_	_
Yokoyama 2007[43]	*Rattus norwegicus*	Wistar	Vitamin A and DA maturation	3420	Affy Rat U34 A Array	8799	Excluded (Ao data unavailable)	_	_	_	_
Gruzdev 2012[26]	*Mus musculus*	129S6	DA from EP4 null mice	NA	Illumina Mouse Ref8 v1.1 Array	24613	Excluded (Ao data unavailable)	_	_	_	_
Liu 2013[44]	*Rattus norwegicus*	Wistar	Term DA endothelium	40500	Affy Rat 1.0 ST Array	29215	Excluded (endo only)	_	_	_	_
Goyal 2016[12]	*Ovis aries*	_	Term and preterm DA	87840	Agilent 019921 Sheep Array	15068	Excluded (incomplete annotation)	_	_	_	_

*Abbreviations: Affy – Affymetrix, ANOVA – analysis of variance, Ao – aorta, DA – ductus arteriosus, E21 – embryonic day 21, NA – not applicable, PDA – persistent patency of the ductus arteriosus, SMC – smooth muscle cell

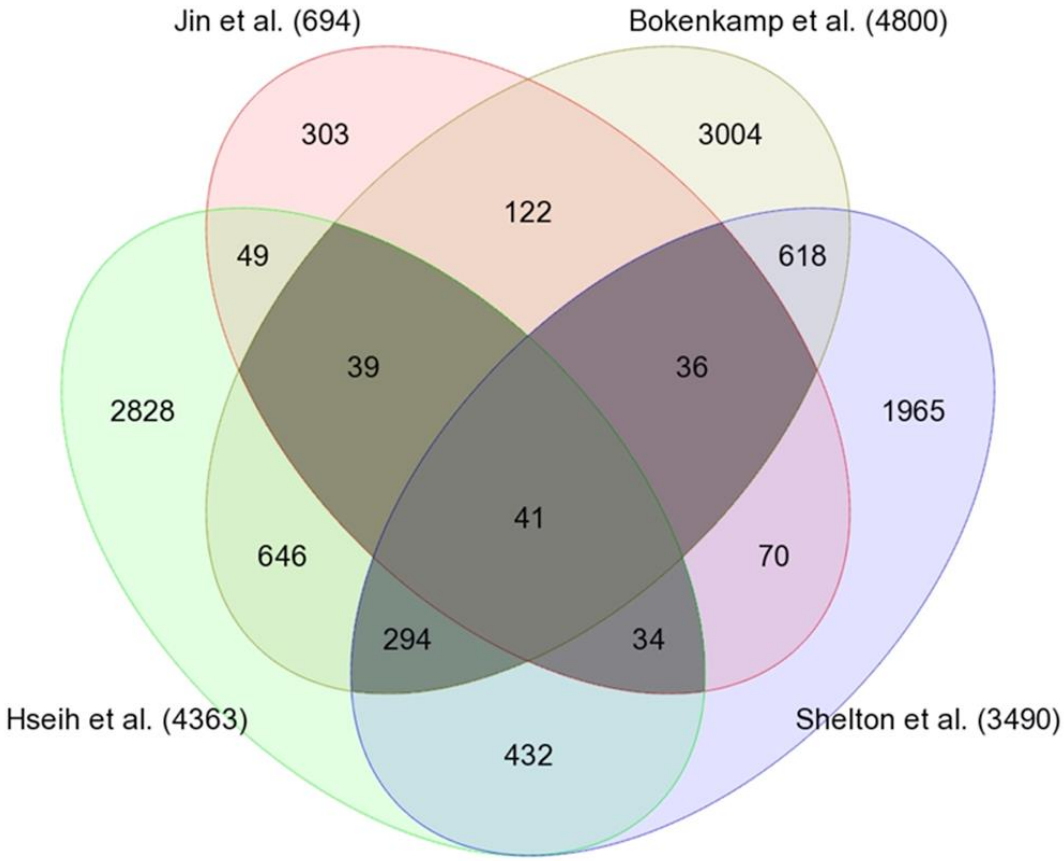

Figure 1. Venn diagram of compared rodent microarray studies. Darkly shaded areas represent 444 DEGs (p-value ≤ 0.05, fold change ≥ 1.2) identified by at least 3 of 4 studies. Of these, 168 genes had conflicting direction of expression and were excluded from further analysis. Of the remaining 276 genes, 87 were consistently increased, while 189 were consistently decreased in DA versus Ao (genes are listed in **Tables S1** and **S2**, respectively).

significant for DA function can be found in Lewis *et al.* (393). Identification of these established genes suggests that this approach was sufficient to detect genes and pathways relevant for DA function.

Human RNA-seq Analysis:

cDNA libraries were prepared for paired DA and Ao samples from 4 subjects. Libraries were sequenced to an average of 60 million genomic reads with an average genomic coverage rate of 67.7% (**Table 2**). Reads were aligned to human genome version 38 and quantified against Refseq Transcripts 83. GSA was then used to detect DEGs from counts normalized to Fragments Per Kilobase of transcript per Million (FPKM)-mapped reads. Hierarchical clustering analysis resulted in a heat map of RNA-seq samples (**Figure 2**). This heat map demonstrates that vessel identity was the primary determinant of clustered expression patterns. Interestingly, 77% of probes selected for hierarchical clustering were DA enriched, compared to 23% Ao enriched, suggesting the DA's phenotype is driven by expression of DA-specific genes, as opposed to suppression of Ao-specific genes. Overall, 2082 genes showed differential expression between DA and Ao with a p-value of 0.05 and fold change of ≥2 (**Figure 3**). 186 of these genes met a permissive false discovery rate (FDR) criteria (Benjamini-Hochberg) of 0.10 or less, with 118 showing increased expression in the DA compared to Ao and 68 showing decreased expression in DA compared to Ao. Complete gene lists from this analysis are provided for both DA enriched (**Table S4**) and Ao enriched (**Table S5**) transcripts. The 20 most highly expressed (by FPKM) DEGs in the human DA were also identified (**Table S6**).

Table 2 **Summary of Genome[1] and Transcriptome[2] Reads and Alignment**

Sample	Vessel	Genomic Reads	Genomic Alignments	Unique Alignments	Non-unique Alignments	Avg. Genomic Coverage	Transcript Reads
122	Ao	30428844	63437690 (87.7%)	24463103 (80.4%)	2215202 (7.3%)	38.6%	26761371
122	DA	60595040	97693434 (46.7%)	23044387 (38.0%)	5276853 (8.7%)	73.9%	28415074
134	Ao	52700686	121687422 (92.9%)	43540599 (82.6%)	5419786 (10.3%)	85.8%	49240999
134	DA	48552058	110777274 (91.1%)	40162140 (82.7%)	4064536 (8.4%)	75.6%	44456169
162	Ao	75583943	151451022 (85.6%)	60853248 (80.5%)	3811368 (5.0%)	72.3%	65157040
162	DA	61495042	124335202 (90.9%)	53260107 (86.6%)	2661866 (4.3%)	54.4%	56289111
208	Ao	79155461	160662212 (91.7%)	69096983 (87.3%)	3482646 (4.4%)	65.2%	73200814
208	DA	82789808	169365096 (90.9%)	71228323 (86.0%)	4003913 (4.8%)	75.9%	75899608
	Mean	**60375726**	**124051203 (87.2%)**	**48909215 (80.6%)**	**3764205 (6.6%)**	**67.7%**	**52427523**

[1] Genome reads aligned to hg38
[2] Transcriptome reads aligned to RefSeq Transcripts 83

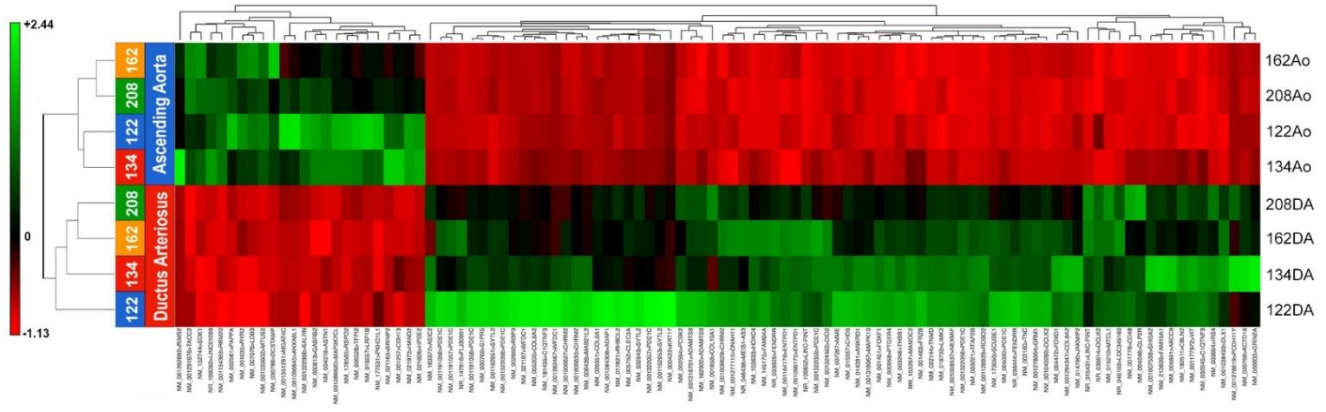

Figure 2. **Dendrogram of Human RNA-seq samples**. Heat map analysis of RNA-seq data showing separation of samples by vessel identity. Gene identities are specified in **Tables S4, S5**.

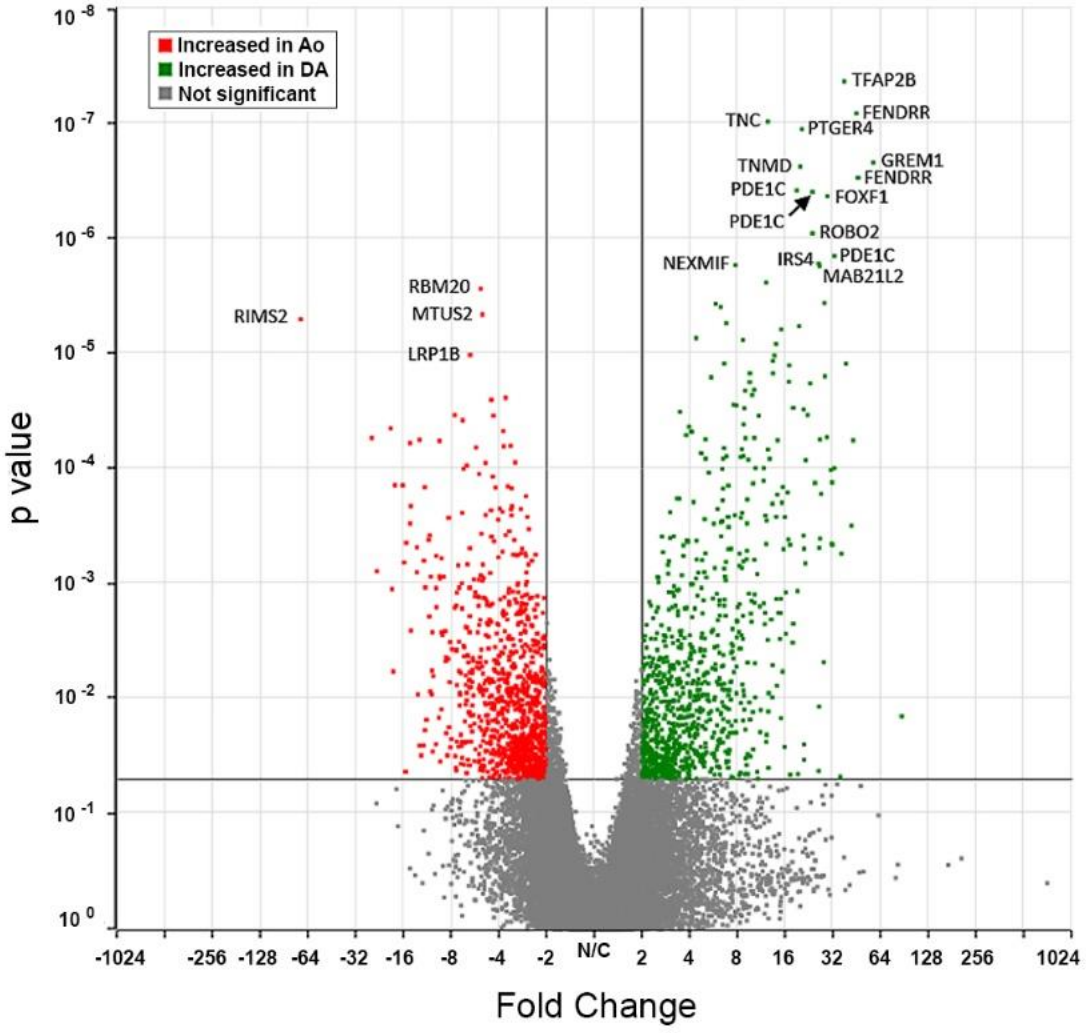

Figure 3. Volcano plot of RNA-seq differentially expressed genes. With p-value 0.05 and fold change >2, 2082 genes showed differential expression in the human DA compared to Ao: 1027 up-regulated, and 1055 down-regulated. Of these, 186 genes had an FDR (Benjamini-Hochberg) of 0.10 or less: 118 up-regulated, and 68 down-regulated (genes are listed in **Tables S4** and **S5**, respectively). Labeled genes represent the highest and lowest differentially expressed findings of this study (the black arrow only serves to connect the label for PDE1C with its respective dot).

Intersection of Human and Rodent DEGs:

To compare the findings of the microarray and RNA-seq studies, rodent gene symbols were converted to human orthologues (bioDBnet). Of the 276 DEGs from the rodent microarray analysis and the 186 DEGs from the human RNA-seq, 11 genes were common to both studies (**Figure 4**). Several of these genes, including *ABCC9* (380-383), *PDE1C* (69, 383, 394), *PTGER4* (108-110, 113, 383, 385, 386), and *TFAP2B* (104, 383, 387-392) have previously been described as significant for DA identity. *TFAP2B* had a notably high fold change (37.9) similar to findings from individual microarray studies (**Table S1**)

Genes differentially expressed between DA and Ao were categorized by functional annotation (DAVID). Overlap between rodent microarray and human RNA-seq was found for GO Biological Process (BP) (48.4%), GO Cellular Component (CC) (63.2%), GO Molecular Function (MF) (47.4%), KEGG (55.6%), and UniProt (UP) Keywords (59.5%) (**Table S7**). Of the top 30 UP Keyword terms from rodent microarray and human RNA-seq, 16 were found in common (**Figure 5**). Terms such as ‘Calcium’, ‘Cell adhesion’, ‘collagen’, ‘extracellular matrix’, and ‘metalloprotease’ align with pathways known to be important for DA constriction and remodeling (136, 145, 146, 148, 149, 389, 395, 396). Diagrams of GO BP and GO CC alignments are also provided **(Figure 6, 7).**

Discussion:

There are currently nine published microarray studies of the DA (113-121), each performed to answer a specific question, and consequently, each with a different experimental design. In order to extract the most meaningful information from these studies, criteria were selected that would include as many studies as possible while only considering comparable

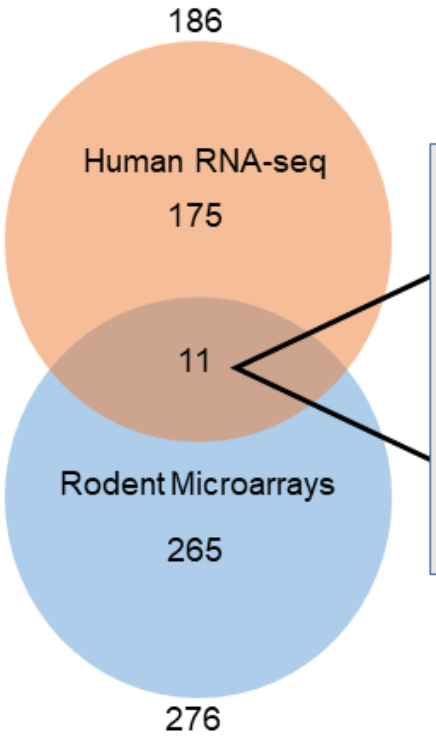

Gene Symbol	Microarray Meta-analysis Direction	Microarray Meta-analysis Studies	RNA-seq Fold Change
TFAP2B	UP	3	37.9
PDE1C	DOWN	3	33.2
MAB21L2	UP	3	25.3
PTGER4	UP	4	20.5
ADAMTS9	UP	3	5.8
ABCC9	UP	4	3.8
POSTN	DOWN	3	-3.2
KCNMA1	DOWN	3	-3.5
RYR2	DOWN	3	-3.7
CDH13	DOWN	3	-4.2
MTUS2	DOWN	3	-5

Figure 4. **Venn diagram of DA vs. Ao genes common between Microarray and RNA-seq analyses**. 11 genes were identified as differentially expressed between DA and Ao in both the human RNA-seq and the rodent microarray comparison. 186 genes from RNA-seq are listed in **Tables S4, S5**; 276 genes from microarray comparisons are listed in Tables **S1, S2**.

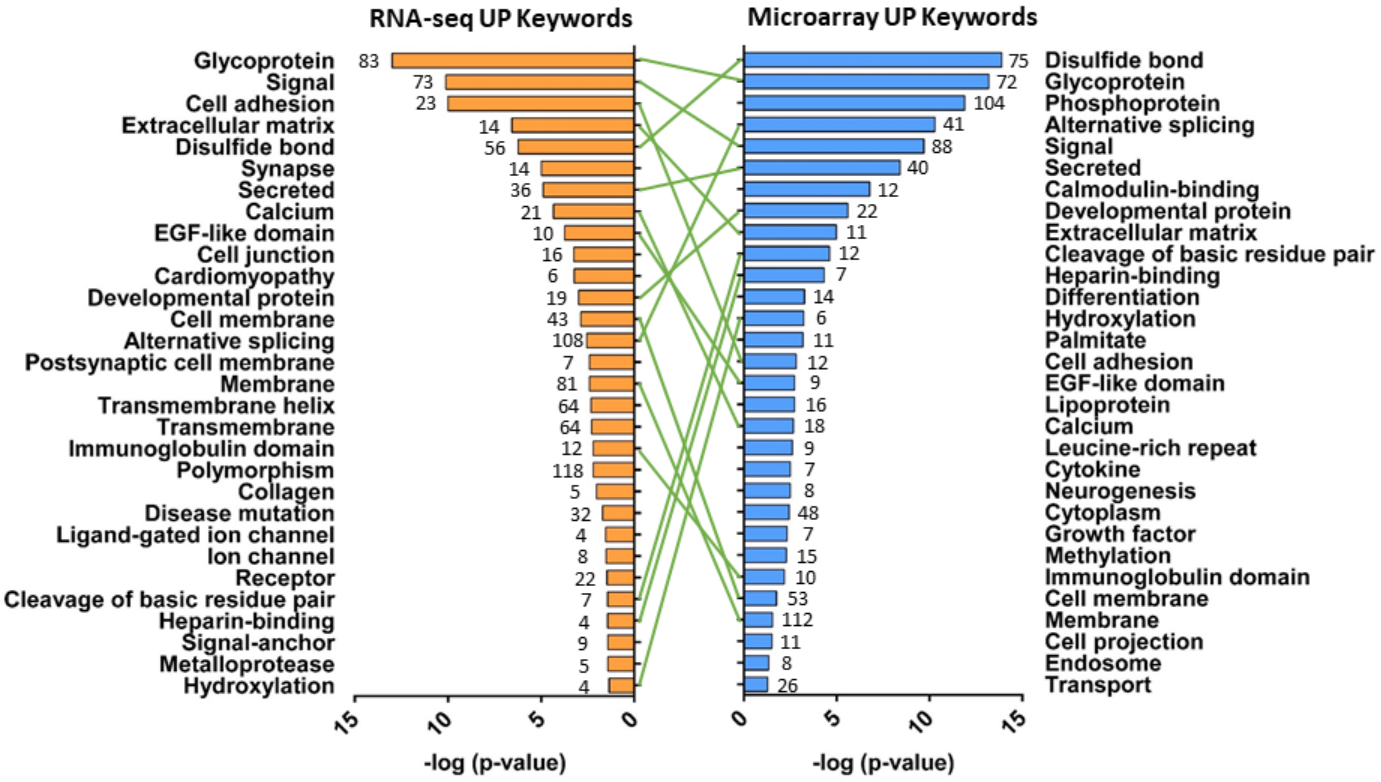

Figure 5. 'Tornadogram' showing top 30 UniProt (UP) Keywords common between Microarray and RNA-seq analyses. Genes differentially expressed in DA vs. Ao were categorized by UP Keywords (DAVID), plotted by p-value, and compared across platforms. Number of genes represented in each category shown at the end of bars.

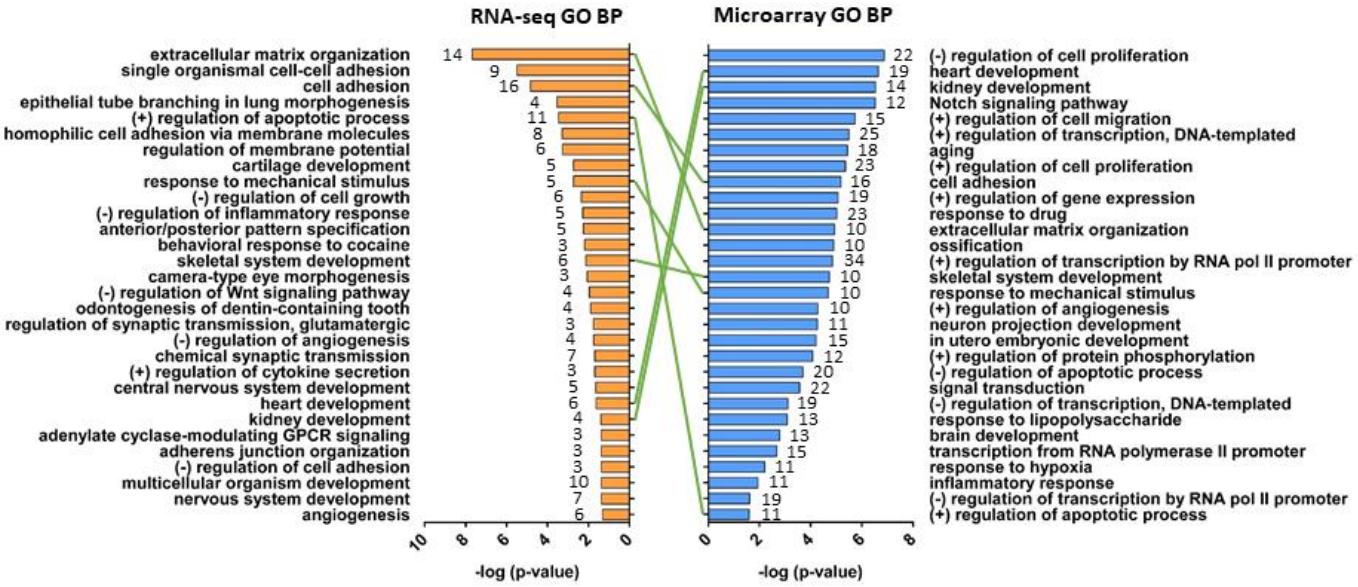

Figure 6. **'Tornadogram' showing top 30 GO Biological Process (BP) terms common between Microarray and RNAseq analyses.** Genes differentially expressed in DA vs. Ao were categorized by functional annotation (DAVID), plotted by p-value, and compared across platforms. Number of genes represented in each category shown at the end of bars.

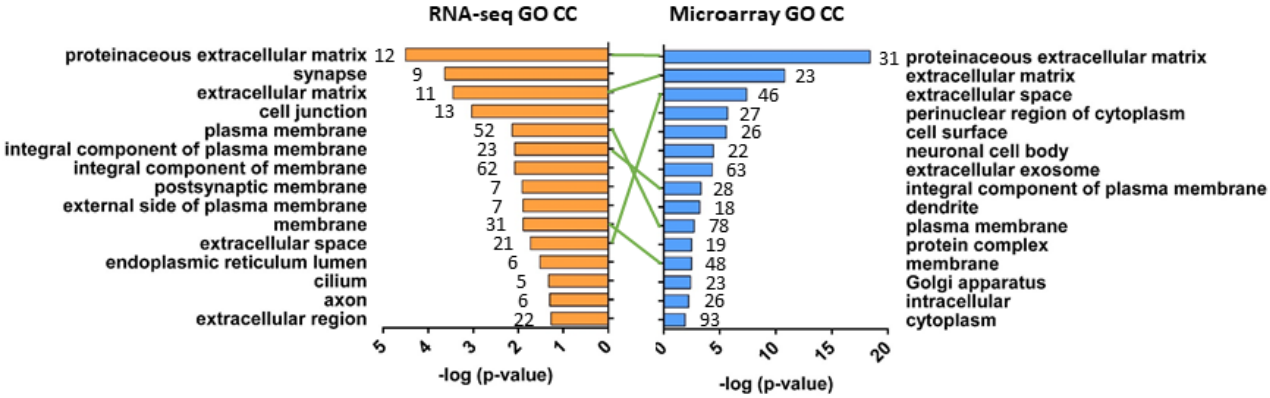

Figure 7. **'Tornadogram' showing top 30 GO Cellular Component** (**CC**) **terms common between Microarray and RNAseq analyses.** Genes differentially expressed in DA vs. Ao were categorized by functional annotation (DAVID), plotted by p-value, and compared across platforms. Number of genes represented in each category shown at the end of bars.

data sets. We focused on studies that included DA to Ao comparisons as they distinguish between DA-specific genes and developmental genes also expressed in neighboring vasculature, while also controlling for biases inherent to each study. In addition, studies that analyzed the term-gestation time point were chosen because this developmental time point was the most represented among available microarray data sets. Although individual array studies have identified differences between term and preterm DAs (117, 119, 121), examination of the available data suggested that differences in study design and consideration of disparate preterm time points would make data alignment unreliable and preclude inter-study comparisons. There is one published microarray study of human DA samples, though it was not considered because it was conducted on abnormal tissue (patients requiring DA stents) and contained no Ao tissue for comparison (123). Overall, 11 genes were differentially expressed in both the preterm human RNA-seq as well as the term rodent microarrays, suggesting that a small subset of genes may define DA identity over a broad developmental time span and between species. This number would be expected to increase in an analysis comparing differential time points in the same species or comparable time points across different species.

Among the DEGs identified as common between rodent microarray data sets and human RNA-seq analysis were several genes which have been previously identified as important for the DA. Two of these, *PTGER4*, which encodes the prostanoid receptor EP_4, and *TFAP2B*, which encodes transcription factor AP-2β, have key roles in DA biology. EP_4 is a G-protein coupled receptor and primary regulator of DA patency. EP_4 is the predominant prostanoid receptor in the mammalian DA (258, 261-264, 397-400). During late gestation, circulating PGE_2 stimulates EP_4 to maintain DA patency (398-400). Catabolism of circulating prostaglandins by HPGD in the newly inflated lungs helps facilitate neonatal DA closure (23, 401). Interestingly, EP_4 KO mice die shortly after birth with a PDA (108-110, 385, 386). Similarly, mice lacking both of the cyclooxygenase enzymes required for PGE_2 production, also die with PDA (106, 107). Normally the removal of a dilatory stimulus would be

expected to result in constriction, but these animals paradoxically present with a widely patent DA. Taken together, these findings suggest that prostaglandins, acting via the EP_4 receptor pathway, may play a role in developmentally programming the DA in addition to their acute vasodilatory function (106, 108, 113, 196, 201). The prevalence of EP_4 among microarray studies and its high fold change in our human RNA-seq data support its role as an important regulator of DA development and function.

TFAP2B is thought to regulate proliferation and differentiation during development. Mutations in *TFAP2B* result in Char syndrome, a neural crest disorder typically associated with developmental abnormalities of the hands and face, as well as PDA (104, 387, 391). Single nucleotide variants in *TFAP2B* have also been linked to non-syndromic PDA (390, 392). *TFAP2B* was highly enriched in DA vs. Ao expression in both human RNA-seq (38-fold increase) and three rodent microarrays (33-fold increase in Shelton *et al.* (114)). *Tfap2b* was not included in the probe set used by Jin *et al.*, and thus was found significant in all possible sources. Interestingly, the array from Bokenkamp *et al.* (119) found *Tfap2b* to be similarly enriched in both DA SMC and DA endothelium, despite only DA SMCs originating from the neural crest (16). These findings are consistent with previous speculation that *Tfap2b* may act as a critical regulator of DA gene expression. Ivey *et al.* showed that *Tfap2b* expression was specific to DA SMCs and that knockout mice lacked proper SMC differentiation (402). They also found that *Tfap2b* expression was required for the sequential expression of hypoxia inducible factor 2α (*Hif2a*) and endothelin-1 (*Et-1)*. These data suggested the hypothesis that Tfap2b is a transcriptional regulator which interacts with *Hif2a* and *Et-1* during development to drive differentiation of DA SMCs. In order to determine the true role of *Tfap2b* in DA development, transcriptional comparisons must be made between the DA of *Tfap2b* null and wild-type mice.

Of the eleven DEGs common to the human RNA-seq and rodent microarrays, one gene, *PDE1C* showed discordant results for DA vs. Ao expression between species. *Pde1c* had

consistently decreased DA/Ao expression in three rodent microarray studies (-1.3, -2.4, and -2.9 fold change), but increased DA/Ao expression in human RNA-seq data (33.2 fold change). PDE1C catalyzes hydrolysis of the second messengers, cAMP and cGMP. Given the importance of both EP_4 and nitric oxide signaling via cAMP and cGMP, respectively, in regulating DA tone (199-201, 403), PDE1C's involvement in the DA is logical. PDE1C activity has been shown to affect DA tone (67, 404, 405) and is thought to do this by attenuating the dilatory effects of EP_4 stimulation and downstream cAMP production in the DA (69). PDE1C is also associated with pathological vascular remodeling, driving proliferation and migration in vascular smooth muscle cells, processes relevant for DA functionality (406, 407). Due to this study's limitations, it is impossible to say conclusively whether this discrepancy arises from gestational differences, species differences, or some unknown experimental factor. That said, there are many phosphodiesterase isoforms which exhibit varying levels of conservation between rodents and humans. It is reasonable to think that specific PDE isoforms may exhibit differences in expression pattern, level, and timing within rodent and human tissues. Additionally, specific PDE isoforms including *Pde1c,* have been shown to exhibit timing specific expression via qRT-PCR during cardiovascular development in mice (408), suggesting the timing difference between our term rodent array data and preterm human data may explain this discrepancy.

Similarly, some genes shown to be relevant for DA function in prior studies were not identified in our combined approach. For example, *KCNMA1*, which encodes a subunit of the BK_{CA} potassium channel, was identified in the microarray study by Shelton *et al.* (114) as enriched in the DA (fold change 2.1). Those results were confirmed by RT-qPCR, *in situ* hybridization and functional analysis (114). Despite these convincing results, *KCNMA1* was enriched in the Ao by other microarrays and our human RNA-seq data. Considering Shelton *et al.* is the only study using mice, this may represent a species-specific difference. These findings highlight the importance of multi-model comparisons in DA research.

There are several limitations in our present analysis. Previous DA microarray studies have raised concerns about the efficacy and appropriateness of directly comparing different microarray data sets (119, 121, 409, 410). This is not field-specific, and there are well-known limitations to this type of comparison (411-413). This is especially true for embryonic and pregnancy-associated tissues which have high internal variability even within tissue type (414, 415). The primary concern is a bias towards type 2 errors, or under-detection of truly differentially expressed and biologically relevant genes.

Direct gene comparison between species also suffers from differences in naming conventions and conservation of specific orthologues. To address this, we focused on functional annotation of our gene lists, to emphasize *pathways* that were in agreement rather than individual gene identity. This strategy has been shown to be more consistent across studies and yield more reproducible, biologically informative results (413, 416). In doing so, several aspects of vessel physiology which may be altered between the DA and neighboring vessels were identified. Genes associated with alterations in ECM organization between DA and Ao were identified by GO biological process, GO cellular component, GO molecular function, and UP keywords in both rodent microarrays and human RNA-seq. Alterations in ECM composition play a critical role in remodeling of the DA in both late gestation and neonatal life (136, 145, 148, 389, 395). Interestingly, several mouse knockout models of ECM-related genes have PDA (417, 418). There was limited direct alignment of ECM-associated genes between the microarray and RNA-seq studies. Only periostin (POSTN), an integrin binding protein which supports cell adhesion and migration, was identified in both rodent microarrays and human RNA-seq. However, both rodent arrays and human RNA-seq studies identified several collagen family members (*Col11a1*, *Col3a1*, *Col5a2*, *Col6a3*) (*COL8A1*, *COL8A2*, *COL9A1*, *COL19A1*) and ADAMTS family genes (*Adamts1*, *Adamts9*, *Adamtsl2*, *Adam33*, *Adamtsl5*)

(*ADAMTS9*, *ADAMT22*, *ADMATS8*). These data suggest that though there are species differences in orthologues, similar pathways are important for both the rodent and human DA.

This study was also hindered by the limited number of preterm datasets. Because the human RNA-seq and rodent microarray data were obtained at different gestational time points, it is difficult to draw clear, unbiased comparisons. For the purposes of identifying effectors related to a developmental program in the DA, it would have been preferable to have multiple comparable time points from both rodent and human datasets. For fairly obvious ethical reasons, this is not the case. Ambiguity still exists concerning the correlation of critical events in DA development between rodents and humans. Thus, at this point, more information on developmental milestones is needed to identify parallel features of DA regulation.

Finally, microarray studies were performed on different platforms, resulting in different sets of transcripts that could possibly be detected for each array. Comparisons between these platforms were then limited to the sets of genes that are represented on all array platforms. This is a minor shortcoming, but is further compounded when comparing microarray results to RNA-seq, which is not restricted by predetermined probe sets as a sequencing-based approach. Thus, our list of genes common to both rodent microarrays and human RNA-seq data sets is capped by the set of genes which is represented on the most limited array platform, predisposing this analysis to under-report significant genes from the RNA-seq which may have been omitted from specific microarray platforms.

In conclusion, comparison of microarray studies from animal models with new information from human RNA-seq data generated high priority candidate genes to consider in future DA studies. The differential expression of these genes between DA and Ao in multiple studies/species suggests they may be key for DA identity, and a part of the developmental program that helps define this vessel from the surrounding vasculature. The conserved enrichment of specific key regulators of DA function, such as *Ptger4* is particularly promising. Clinically, identification of DA-specific or highly

enriched genes in the DA is a requisite step in finding new DA-selective drugs or providing a molecular address for homing of therapeutic agents to the target tissue. Although cross-platform and cross-species transcriptomic comparisons are fraught with limitations, they offer a unique opportunity to visualize pathways of interest to better understand DA development and function.

Supplemental Tables

Table S1 **Genes Enriched in the Rodent DA by Three or More Microarrays** (Fold Change (FC); DA vs Ao)

Gene Symbol[1,2]	Gene Name	Entrez ID	Study #	Jin FC	Hseih FC	Shelton FC	Bokenkamp SMC FC	Bokenkamp Endo FC
Abcc9	ATP binding cassette subfamily C member 9	25560	4	5.6	2.6	2.8	1.7	1.5
Actg2	actin, gamma 2, smooth muscle, enteric	25365	4	2.8	2.3	7.8	2.2	2.0
Dpep1	dipeptidase 1 (renal)	94199	4	6.1	3.7	1.5	3.0	
Edn1	endothelin 1	24323	4	1.4	1.6	1.5		1.7
Fhl2	four and a half LIM domains 2	63839	4	4.9	2.7	1.8	3.0	2.8
Lrba	LPS responsive beige-like anchor protein	361975	4	9.2	2.9	2.0	1.9	1.7
Ncam1	neural cell adhesion molecule 1	24586	4	2.0	1.4	2.3	1.5	
Nr4a1	nuclear receptor subfamily4, group A, member1	79240	4	1.7	1.5	1.5	1.5	
Pcsk5	proprotein convertase subtilisin/kexin type 5	116548	4	4.8	2.5	1.6	3.0	-1.2
Penk	proenkephalin	29237	4	1.8	1.3	2.4	2.2	2.3
Ppp1r12a	protein phosphatase 1, regulatory subunit 12A	116670	4	2.3	1.4	2.4	1.8	
Ptger4	prostaglandin E receptor 4	84023	4	2.6	2.4	3.8	3.8	-1.3
Tnfrsf11b	TNF receptor superfamily member 11B	25341	4	4.8	2.7	3.8	2.8	3.5
Adamts1	ADAM metallopeptidase with thrombospondin type 1 motif, 1	79252	3		3.1	1.8	2.4	
Adamts9	ADAM metallopeptidase with thrombospondin type 1 motif, 9	312566	3		3.9	3.1	2.7	2.7
Adamtsl2	ADAMTS-like 2	311827	3		4.0	3.1	2.0	
Adgrl3	adhesion G protein-coupled receptor L3	170641	3	3.9	1.3	1.4		-1.4
Agtr1a	angiotensin II receptor, type 1a	24180	3	1.4	1.5	-1.8	1.5	4.3
Akap5	A-kinase anchoring protein 5	171026	3		2.1	8.4	1.9	2.1
Atp1b1	ATPase Na+/K+ transporting subunit beta 1	25650	3	2.8	1.5	-1.7	2.6	
Barx1	BARX homeobox 1	364680	3		1.3	1.3	1.2	
Bmp2	bone morphogenetic protein 2	29373	3		1.3	1.5		1.9
Bmp4	bone morphogenetic protein 4	25296	3	2.6	1.5			1.8
Cacna1c	calcium voltage-gated channel subunit alpha1C	24239	3	2.1		1.5	1.2	
Cd55	CD55 molecule, decay accelerating factor for complement	64036	3	6.4		1.5		1.5
Cdk17	cyclin-dependent kinase 17	314743	3	1.4		1.4	1.5	
Celsr2	cadherin, EGF LAG seven-pass G-type receptor 2	83465	3	1.6	1.4	1.5		
Cnn1	calponin 1	65204	3	1.4	1.4	2.7		
Cntn3	contactin 3	54279	3		1.9	3.6		1.3
Cyr61	cysteine-rich, angiogenic inducer, 61	83476	3	2.2	1.4	4.0		
Dab2	DAB2, clathrin adaptor protein	79128	3		1.4	2.3		1.9
Des	desmin	64362	3	6.1	2.6	5.0		
Egr1	early growth response 1	24330	3	-1.2	1.4	1.3	2.0	1.9
Enpp3	ectonucleotide pyrophosphatase/phosphodiesterase 3	54410	3	2.0	2.9	-1.9	1.9	
Fat4	FAT atypical cadherin 4	310341	3		1.4	2.1		1.5
Fgfr2	fibroblast growth factor receptor 2	25022	3	5.8	2.0	3.1		-1.2
Ghr	growth hormone receptor	25235	3	9.5	1.8		2.0	
Gpm6b	glycoprotein m6b	192179	3		6.3	2.8	2.6	
Grem1	gremlin 1, DAN family BMP antagonist	50566	3		1.6	12.3	2.9	
Grm3	glutamate metabotropic receptor 3	24416	3	3.6	1.6	1.4		
Higd1a	HIG1 hypoxia inducible domain family, member 1A	140937	3	7.5	1.5		2.1	1.6
Hoxa4	homeo box A4	100912525	3		1.4	2.8	1.5	
Hspa1a	heat shock 70kD protein 1A	24472	3	18.5	3.3		5.2	
Hspb1	heat shock protein family B (small) member 1	24471	3	2.1	3.0		2.2	
Hspb8	heat shock protein family B (small) member 8	113906	3		1.5	1.3	2.7	
Il15	interleukin 15	25670	3	6.1	1.6	2.5		
Inhba	inhibin beta A subunit	29200	3		3.5	2.2	2.6	2.4
Kcnj8	potassium voltage-gated channel subfamily J member 8	25472	3	2.8	1.8	9.0		
Kcnk3	potassium two pore domain channel subfamily K member 3	29553	3	5.8		2.4	1.8	
Kctd1	potassium channel tetramerization domain containing 1	291772	3		2.3	1.7	2.9	2.5
Lama1	laminin subunit alpha 1	316758	3		2.1	2.2	2.1	2.0
Lrrn3	leucine rich repeat neuronal 3	81514	3		1.4	2.4	1.7	
Ltbp1	latent transforming growth factor beta binding protein 1	59107	3	2.7	1.5	2.3		
Mab21l2	mab-21 like 2	680102	3		7.2		3.7	1.7
Marc2	mitochondrial amidoxime reducing component 2	171451	3	3.1	2.9			1.8
Meis1	Meis homeobox 1	686117	3		1.7	2.2	1.5	1.4
Mfsd2a	major facilitator superfamily domain containing 2A	298504	3		2.0	1.5	1.2	
Mgll	monoglyceride lipase	29254	3	3.2	1.5	1.3		
Nalcn	sodium leak channel, non-selective	266760	3	6.2	1.4	1.7	-2.3	

Nr4a3	nuclear receptor subfamily 4, group A, member 3	58853	3		1.2	3.5	2.4	3.2
Olfml2b	olfactomedin-like 2B	304960	3		1.4	1.8	1.7	
Parm1	prostate androgen-regulated mucin-like protein 1	286894	3		1.8	1.8	1.7	
Pde4b	phosphodiesterase 4B	24626	3	2.1		2.0	2.4	1.6
Prkar2b	protein kinase cAMP-dependent type 2 regulatory subunit beta	24679	3	1.4	1.4		2.0	1.6
Ptbp1	polypyrimidine tract binding protein 1	29497	3	1.4		1.2		1.5
Ptn	pleiotrophin	24924	3	1.7	3.2	1.5		
Rdh10	retinol dehydrogenase 10	353252	3		1.8	1.5	1.7	1.8
Rgs5	regulator of G-protein signaling 5	54294	3		1.5	4.4	3.1	3.3
Runx1	runt-related transcription factor 1	50662	3		1.6	2.9	2.8	2.0
Ryr3	ryanodine receptor 3	170546	3		1.4	1.8	2.5	
Scx	scleraxis bHLH transcription factor	680712	3		1.6	2.3	2.9	
Serinc3	serine incorporator 3	296350	3	1.9		1.4	1.2	
Sfrp1	secreted frizzled-related protein 1	84402	3		2.4	2.3	2.5	2.1
Sfrp2	secreted frizzled-related protein 2	310552	3		1.9	1.4	1.8	
Skap2	src kinase associated phosphoprotein 2	155183	3		1.2	1.6		1.8
Slc2a4	solute carrier family 2 member 4	25139	3	2.7	1.8	2.3		
Slit2	slit guidance ligand 2	360272	3		2.5	3.4	2.3	4.0
Snd1	staphylococcal nuclease and tudor domain containing 1	64635	3	1.2	-1.3	1.3		1.3
Sox9	SRY box 9	140586	3		1.6	3.8	1.3	
Tagln	transgelin	25123	3	1.9	1.4	1.4		
Tfap2a	transcription factor AP-2 alpha	306862	3		1.9	1.5	1.4	
Tfap2b	transcription factor AP-2 beta	301285	3		13.5	33.1	13.9	9.0
Tgfbi	transforming growth factor, beta induced	116487	3		4.3	3.3	2.6	2.4
Tmem150c	transmembrane protein 150C	360916	3		14.1	1.3	21.1	12.4
Tmem26	transmembrane protein 26	309724	3		1.4	1.5		1.9
Tnn	tenascin N	304913	3		5.0	3.4	11.5	3.3
Tom1l1	target of myb1 like 1 membrane trafficking protein	287622	3		1.4	1.3	1.5	

[1]Genes in blue have previously been identified as important for DA function in the literature

[2]Bokenkamp *et al*. is divided by SMC and EC in accordance with this study's experimental design

Table S2 **Genes Enriched in the Rodent Ao by Three or More Microarrays** (Fold Change (FC); DA vs Ao)

Gene Symbol[1,2]	Gene Name	Entrez ID	Study #	Jin FC	Hseih FC	Shelton FC	Bokenkamp SMC FC	Bokenkamp Endo FC
Add3	adducin 3	25230	4	-1.8	-1.9	-1.5	-2.2	
Akap1	A-kinase anchoring protein 1	114124	4	-1.5	-1.3	-1.3		-1.2
Cpq	carboxypeptidase Q	58952	4	-1.8	-1.6	-1.3	-1.8	-1.8
Golgb1	golgin B1	192243	4	-1.2	-1.4	-1.2	-1.7	
Igfbp6	insulin-like growth factor binding protein 6	25641	4	-1.7	-2.1	-2.9	-1.6	
Itga7	integrin subunit alpha 7	81008	4	-1.4	-2.3	-2.3	-1.5	-1.3
Pdgfra	platelet derived growth factor receptor alpha	25267	4	-1.9	-2.2	-1.7	-3.6	
Rrad	RRAD, Ras related glycolysis inhibitor and calcium channel regulator	83521	4	-1.4	-2.0	-2.0		-1.8
Slc6a9	solute carrier family 6 member 9	116509	4	-3.4	-2.1	-1.3		-1.4
Syt7	synaptotagmin 7	59267	4	-1.4	-1.7	-1.5		-1.3
Abhd14a	abhydrolase domain containing 14A	300982	3		-1.2	-1.3	-1.3	-1.3
Acsl5	acyl-CoA synthetase long-chain family member 5	94340	3	-1.7	-1.5	-1.2		
Adam33	ADAM metallopeptidase domain 33	311425	3		-1.6	-1.3		-1.8
Adamtsl5	ADAMTS-like 5	314626	3		-1.2	-1.9		-1.5
Adcy4	adenylate cyclase 4	54223	3	-1.4		-1.4	-1.9	
Adcy9	adenylate cyclase 9	302950	3		-1.3	-1.3		-1.6
Adgrd1	adhesion G protein-coupled receptor D1	689257	3		-1.9	-1.8		-1.5
Agap1	ArfGAP with GTPase domain, ankyrin repeat and PH domain 1	316611	3		-1.3	-1.7		-1.4
Agtr2	angiotensin II receptor, type 2	24182	3	-1.3	-1.6	1.7	-3.8	
Aig1	androgen-induced 1	292486	3		-1.9	-1.8	-1.6	
Akap6	A-kinase anchoring protein 6	64553	3		-1.8	-3.9		-1.3
Alcam	activated leukocyte cell adhesion molecule	79559	3		-1.9	-2.2	-1.7	
Alx1	ALX homeobox 1	25401	3	-1.2		-3.3		-1.3
Amigo2	adhesion molecule with Ig like domain 2	300186	3		-1.2	-3.2		-1.6
Ampd2	adenosine monophosphate deaminase 2	362015	3		-1.4	-1.4	-1.3	
Ank2	ankyrin 2	362036	3		-2.1	-1.3	-2.4	-2.2
Arhgap44	Rho GTPase activating protein 44	303222	3		-1.8	-1.4	-1.6	
B4galt2	beta-1,4-galactosyltransferase 2	313536	3		-1.3	-1.2	-1.3	
Bcar3	breast cancer anti-estrogen resistance 3	310838	3		-1.5	-3.3	-2.1	
Bche	butyrylcholinesterase	65036	3		-2.4	-2.0	-2.0	
Bdkrb2	bradykinin receptor B2	25245	3	-3.4	-1.5			-1.3
C2cd2	C2 calcium-dependent domain containing 2	304055	3		-1.5	-1.6		-1.5
Calml4	calmodulin-like 4	691455	3	-2.1	-2.9			-2.1
Casq2	calsequestrin 2	29209	3	-2.4	-3.5		-2.1	-2.1
Cdh13	cadherin 13	192248	3		-3.0	-3.3	-1.9	-2.5
Cdh6	cadherin 6	25409	3		-2.3	-3.4		-1.4
Cdk6	cyclin-dependent kinase 6	114483	3		-1.3	-1.9		-1.3
Cnnm2	cyclin and CBS domain divalent metal cation transport mediator 2	294014	3		-1.8	-1.5		-1.7
Col11a1	collagen type XI alpha 1 chain	25654	3	-1.7	-2.1	4.1	-3.8	
Col3a1	collagen type III alpha 1 chain	84032	3		-1.6	-1.3	-2.0	
Col5a2	collagen type V alpha 2 chain	85250	3		-1.9	-1.3	-1.3	
Col6a3	collagen type VI alpha 3 chain	367313	3		-1.9	-1.4	-2.5	
Corin	corin, serine peptidase	289596	3		-4.2	-5.1		-2.3
Cpd	carboxypeptidase D	25306	3	-1.8	-1.6	-1.3		
Cped1	cadherin-like and PC-esterase domain containing 1	500046	3		-2.0	-2.6	-1.7	
Cplx2	complexin 2	116657	3	-1.4		-1.3		-1.4
Csf1	colony stimulating factor 1	78965	3		-2.0	-1.9	-1.4	-1.3
Cxcl13	C-X-C motif chemokine ligand 13	498335	3	-5.4	-1.6		-2.7	
Cyth3	cytohesin 3	116693	3		-2.3	-1.4	-1.7	-1.3
Dcn	decorin	29139	3	-1.9		-1.3	-4.1	2.4
Dhtkd1	dehydrogenase E1 and transketolase domain containing 1	361272	3		-1.4	-1.3	-1.7	
Dpysl3	dihydropyrimidinase-like 3	25418	3	-14.2	-1.4	1.7		-1.3
Ebf1	early B-cell factor 1	116543	3		-1.4	-1.5	-2.0	-1.5
Fam13a	family with sequence similarity 13, member A	362378	3		-1.9	-1.4	-1.5	
Fam20c	FAM20C, golgi associated secretory pathway kinase	304334	3		-2.0	-1.4	-1.4	-1.6
Fchsd2	FCH and double SH3 domains 2	308864	3		-1.6	-1.3		-1.3
Fgf2	fibroblast growth factor 2	54250	3		-1.4	-1.5		-1.3
Fmo2	flavin containing monooxygenase 2	246245	3		-2.9	-3.0		-1.8
Foxc1	forkhead box C1	364706	3		-1.4	-1.5		-1.3
Frmd4b	FERM domain containing 4B	252858	3	-2.0	-1.7	-1.9		
Frmd6	FERM domain containing 6	257646	3		-1.7	-1.5	-1.4	
Galm	galactose mutarotase	313843	3		-1.2	-1.5		-1.4
Galt	galactose-1-phosphate uridylyltransferase	298003	3		-1.3	-1.2	-1.3	
Gas7	growth arrest specific 7	85246	3		-2.6	-1.9	-1.8	

Gdf10	growth differentiation factor 10	79216	3	-1.9	-1.4		-1.8	
Gfra2	GDNF family receptor alpha 2	25136	3	-2.0	-3.7	-1.4		
Glis2	GLIS family zinc finger 2	302946	3		-1.3	-1.5	-1.4	-1.2
Glt8d2	glycosyltransferase 8 domain containing 2	366859	3		-1.5	-2.0	-1.2	
Grasp	general receptor for phosphoinositides 1 associated scaffold protein	192254	3		-1.5	-1.9		-1.3
Grb14	growth factor receptor bound protein 14	58844	3		-1.6	-2.3	-1.8	-1.7
Grip2	glutamate receptor interacting protein 2	171571	3	-1.8	-1.7	-2.7		
Gstk1	glutathione S-transferase kappa 1	297029	3		-1.5	-1.8	-1.5	-1.3
Hapln1	hyaluronan and proteoglycan link protein 1	29331	3		-1.4	-2.0		-1.5
Herc3	HECT and RLD domain containing E3 ubiquitin protein ligase 3	362377	3		-1.3	-1.3	-2.0	
Heyl	hes-related family bHLH transcription factor with YRPW motif-like	313575	3		-2.0	-1.9		-1.7
Hmgcs2	3-hydroxy-3-methylglutaryl-CoA synthase 2	24450	3	-10.4	-2.2			-1.3
Hpcal4	hippocalcin-like 4	50872	3	-2.3	-2.4		-2.2	-1.3
Igf1r	insulin-like growth factor 1 receptor	25718	3	-1.5	-1.3		-1.7	-1.4
Igf2bp2	insulin-like growth factor 2 mRNA binding protein 2	303824	3		-1.3	-1.2	-1.3	
Igfbp2	insulin-like growth factor binding protein 2	25662	3	-3.7	-2.6	6.2	-1.9	
Igsf3	immunoglobulin superfamily, member 3	295325	3		-1.7	-1.3	-2.0	
Inpp5k	inositol polyphosphate-5-phosphatase K	287533	3		-1.3	-1.4		-1.2
Kcnma1	potassium calcium-activated channel subfamily M alpha 1	83731	3	-5.9	-2.4	2.1	-2.5	-4.2
Kcnq1	potassium voltage-gated channel subfamily Q member 1	84020	3	-1.8	-2.2			-1.7
Kif3a	kinesin family member 3a	84392	3		-1.2	-1.5	-1.3	
Klf15	Kruppel-like factor 15	85497	3		-1.6	-2.2	-1.7	-1.8
Krt8	keratin 8	25626	3	-2.0	-3.6	-1.8		
Lama4	laminin subunit alpha 4	309816	3		-1.6	-1.5	-1.3	
Lamb1	laminin subunit beta 1	298941	3		-2.0	-2.0	-1.8	
Laptm4b	lysosomal protein transmembrane 4 beta	315047	3		-1.3	-1.7	-1.3	
Lbh	limb bud and heart development	683626	3		-1.3	-2.2	-1.5	
Ldhb	lactate dehydrogenase B	24534	3	-1.4	-1.6		-1.7	
Lhfpl2	lipoma HMGIC fusion partner-like 2	294643	3		-1.6	-1.7	-1.7	
Lifr	leukemia inhibitory factor receptor alpha	81680	3		-1.8	-1.3		-1.3
Limd1	LIM domains containing 1	316101	3		-1.6	-1.6		-1.2
Lingo1	leucine rich repeat and Ig domain containing 1	315691	3		-1.6	-1.7	-1.5	-2.2
Lox	lysyl oxidase	24914	3	-1.8	-1.4		-1.5	
Loxl1	lysyl oxidase-like 1	315714	3	-1.3	-2.0		-2.0	
Lrrfip1	LRR binding FLII interacting protein 1	367314	3		-1.4	-1.3	-1.4	-1.4
Lrtm2	leucine-rich repeats and transmembrane domains 2	680883	3		-1.2	-1.3	-1.4	
Ltbp2	latent transforming growth factor beta binding protein 2	59106	3	-1.9	-2.1	1.7	-1.7	
Map2	microtubule-associated protein 2	25595	3	-3.6	-4.8		-3.7	
Matn2	matrilin 2	299996	3		-2.0	-1.3	-1.7	-1.8
Meis2	Meis homeobox 2	311311	3		-1.5	-1.7	-1.5	
Mfhas1	malignant fibrous histiocytoma amplified sequence1	306508	3		-1.3	-1.7	-1.4	
Mobp	myelin-associated oligodendrocyte basic protein	25037	3	-2.2	-1.6		-1.6	-1.6
Mtdh	metadherin	170910	3	-1.6	-1.4		-1.3	1.2
Mtus1	microtubule associated tumor suppressor 1	306487	3		-2.5	-1.9	-2.4	
Mtus2	microtubule associated tumor suppressor candidate2	498136	3		-2.4	-3.5	-1.9	-3.4
Mycbp2	MYC binding protein 2, E3 ubiquitin protein ligase	290447	3		-1.3	-1.3	-1.3	
Myh10	myosin heavy chain 10	79433	3	-7.5	-1.2	-1.3		
Myo1d	myosin ID	25485	3		-2.2	-1.5	-1.6	
Ndrg2	NDRG family member 2	171114	3		-1.7	-1.5		-1.8
Nf2	neurofibromin 2	25744	3		-1.3	-1.6		-1.2
Nid1	nidogen 1	25494	3		-1.5	-1.8	-1.6	
Nid2	nidogen 2	302248	3		-2.0	-2.3	-2.2	-1.7
Nrarp	Notch-regulated ankyrin repeat protein	499745	3		-1.8	-1.6		-1.4
Ntrk2	neurotrophic receptor tyrosine kinase 2	25054	3		-2.1	-1.2.	-4.3	
Ntrk3	neurotrophic receptor tyrosine kinase 3	29613	3	1.4	-1.3	-2.9	-1.9	-1.8
P4ha2	prolyl 4-hydroxylase subunit alpha 2	360526	3		-1.5	-1.3	-1.5	-1.3
Pck2	phosphoenolpyruvate carboxykinase 2 (mitochondrial)	361042	3		-1.5	-1.4	-1.8	-1.6
Pde1c	phosphodiesterase 1C	81742	3	-2.4	-1.3	-2.9		
Pdlim5	PDZ and LIM domain 5	64353	3	-2.3	-1.3	-1.4		
Phkg1	phosphorylase kinase, gamma 1	29353	3	-4.2		-3.4		-1.2
Pld1	phospholipase D1	25096	3		-1.5	-1.7		-1.7
Plpp3	phospholipid phosphatase 3	192270	3	-1.6	-1.7		-2.0	
Polg	DNA polymerase gamma, catalytic subunit	85472	3		-1.3	-1.2		-1.3
Postn	periostin	361945	3	-2.5	-3.8		-2.7	
Ppp1r9a	protein phosphatase 1, regulatory subunit 9A	84685	3		-1.5	-1.7		-2.1

Prrc1	proline-rich coiled-coil 1	291444	3		-1.3	-1.5	-1.3	
Ptger3	prostaglandin E receptor 3	24929	3	-3.5	-1.9		-2.4	-1.3
Ptprd	protein tyrosine phosphatase, receptor type, D	313278	3		-1.7	-1.6	-2.0	-1.7
Qpct	glutaminyl-peptide cyclotransferase	313837	3	-1.6	-1.3	1.3	-2.4	
Rab3ip	RAB3A interacting protein	29885	3		-3.6	-1.3	-3.6	-3.1
Rab7b	Rab7b, member RAS oncogene family	501854	3		-2.3	-2.8	-1.5	-1.7
Ramp1	receptor activity modifying protein 1	58965	3		-1.7	-3.0	-1.4	
Rarb	retinoic acid receptor, beta	24706	3		-1.3	-1.5	-2.0	
Rarres2	retinoic acid receptor responder 2	297073	3		-1.8	-2.5	-1.7	-1.5
Rasd2	RASD family, member 2	171099	3		-1.3	-2.6		-1.3
Rassf9	Ras association domain family member 9	65053	3	-2.6	-2.4	-1.8		
Rbm6	RNA binding motif protein 6	315997	3		-1.3	-1.2	-1.3	
Rhoj	ras homolog family member J	299145	3		-1.4	-1.2		-1.3
Rif1	replication timing regulatory factor 1	295602	3		-1.5	-1.3	-1.5	
Ryr2	ryanodine receptor 2	689560	3		-1.3	-1.7		-2.5
Sash1	SAM and SH3 domain containing 1	365037	3		-2.1	-1.7	-2.5	
Scarf1	scavenger receptor class F, member 1	303313	3		-1.4	-1.3		-1.3
Scube3	signal peptide, CUB domain and EGF like domain containing 3	294297	3		-2.1	-1.5		-2.3
Sema5a	semaphorin 5A	310207	3		-1.5	-2.0	-1.4	
Sema6d	semaphorin 6D	311384	3		-2.2	-1.4	-1.9	
Sept8	septin 8	303135	3		-1.3		-2.1	-1.3
Sh3pxd2a	SH3 and PX domains 2A	309460	3		-1.6	-1.2	-1.9	-1.9
Sipa1l2	signal-induced proliferation-associated 1 like 2	361442	3		-1.6	-1.3		-1.5
Slc1a4	solute carrier family 1 member 4	305540	3		-1.9	-1.6		-1.6
Slc24a3	solute carrier family 24 member 3	85267	3		-1.5	-2.0	-2.1	-1.8
Slc44a1	solute carrier family 44 member 1	85254	3		-1.5	-1.2	-1.4	
Slc7a3	solute carrier family 7 member 3	29485	3	-2.5	-6.3		-4.1	-2.9
Slc9a3r2	SLC9A3 regulator 2	116501	3		-1.4	-1.8		-1.2
Slx4ip	SLX4 interacting protein	499895	3		-1.4	-1.4	-1.3	
Smarca2	SWI/SNF related, matrix associated, actin dependent regulator of chromatin, subfamily a, member 2	361745	3		-1.7	-1.3		-1.6
Smpd3	sphingomyelin phosphodiesterase 3	94338	3		-2.0	-1.9	-1.7	
Snta1	syntrophin, alpha 1	362242	3		-1.8	-1.9	-1.5	
Sod2	superoxide dismutase 2	24787	3	-1.8	-1.3	-1.3		
Sorbs3	sorbin and SH3 domain containing 3	282843	3		-1.4	-1.4		-1.4
Specc1	sperm antigen with calponin homology and coiled-coil domains 1	303208	3		-2.1	-1.5	-2.3	-1.5
Sphkap	SPHK1 interactor, AKAP domain containing	316561	3		-2.7	-3.8		-2.0
Spock2	SPARC/osteonectin, cwcv and kazal like domains proteoglycan 2	361840	3	-2.8	-1.3	-2.0		
Spon1	spondin 1	64456	3	-1.6	-1.9	-4.2		
St3gal3	ST3 beta-galactoside alpha-2,3-sialyltransferase 3	64445	3	-1.5	-1.2		-1.4	
Stc1	stanniocalcin 1	81801	3		-2.9	-3.9	-2.3	-1.9
Stmn4	stathmin 4	79423	3	-1.6	-3.0			-2.1
Stx1a	syntaxin 1A	116470	3		-1.6	-2.0	-1.7	-1.4
Stx3	syntaxin 3	81802	3		-1.4	-2.1		-1.3
Sult1a1	sulfotransferase family 1A member 1	83783	3	-3.1	-2.6		-2.0	
Tbx18	T-box18	315870	3		-1.2	-1.9	-2.4	
Tet1	tet methylcytosine dioxygenase 1	309902	3		-1.3	-1.6	-1.9	
Tgfbr2	transforming growth factor, beta receptor 2	81810	3		-2.1	-1.6		-1.2
Thbs2	thrombospondin 2	292406	3		-1.7	-1.8	-2.0	
Timp4	tissue inhibitor of metalloproteinase 4	680130	3		-2.8	-5.0	-1.5	-1.7
Tmem117	transmembrane protein 117	500921	3		-1.7	-2.3	-1.6	
Tmx4	thioredoxin-related transmembrane protein 4	296182	3		-1.9	-1.4		-1.4
Traf3	Tnf receptor-associated factor 3	362788	3		-1.5	-1.2	-1.4	
Trim47	tripartite motif-containing 47	690374	3		-1.4	-1.8		-1.3
Tspan5	tetraspanin 5	362048	3		-1.7	-2.3	-1.3	
Tub	tubby bipartite transcription factor	25609	3	-3.3		-1.5	-1.5	
Usp54	ubiquitin specific peptidase 54	408223	3		-1.6	-1.3	-1.6	
Vasn	vasorin	679921	3		-1.5	-1.6	-1.4	
Vstm4	V-set and transmembrane domain containing 4	361112	3		-1.4	-1.6	-2.3	
Xirp1	xin actin-binding repeat containing 1	100910104	3		-2.3	-2.3		-1.7
Zmiz1	zinc finger, MIZ-type containing 1	361103	3	-4.8	-1.2		-1.3	

[1]Genes in blue have previously been identified as important for DA function in the literature
[2]Bokenkamp *et al*. is divided by SMC and EC in accordance with this study's experimental design

Table S3 **Summary of Transcript[1] Reads**

Sample	Vessel	Transcript Reads	Exonic Reads	Intronic Reads	Intergenic Reads
122	Ao	26761371	48.28%	35.60%	6.85%
122	DA	28415074	43.54%	28.42%	18.13%
134	Ao	49240999	58.16%	24.76%	6.51%
134	DA	44456169	49.42%	33.93%	7.36%
162	Ao	65157040	30.93%	52.77%	8.91%
162	DA	56289111	32.26%	51.34%	8.43%
208	Ao	73200814	29.42%	54.20%	8.28%
208	DA	75899608	32.84%	50.83%	8.16%
	Mean	**52427523**	**40.61%**	**41.48%**	**9.08%**

[1] Transcriptome reads aligned to RefSeq Transcripts 83

Table S4 **Genes Enriched in the Human DA by RNA-seq** (Fold Change; DA vs Ao)

Gene Symbol	Gene Name	Fold Change	P-value	FDR	FPKM DA	FPKM Ao	Entrez ID
GRM1	glutamate metabotropic receptor 1	57.9	1.26E-06	3.98E-03	0.97	0.02	2911
FENDRR	FOXF1 adjacent non-coding developmental regulatory RNA	45.1	1.21E-07	1.60E-03	2.47	0.05	400550
WFDC1	WAP four-disulfide core domain 1	40.2	1.64E-05	1.51E-02	0.89	0.02	58189
FSTL5	follistatin like 5	39.4	6.78E-05	3.14E-02	2.74	0.07	56884
TFAP2B	transcription factor AP-2 beta	37.9	1.94E-07	1.73E-03	3.49	0.09	7021
ADAP1	ArfGAP with dual PH domains 1	36.7	9.70E-06	1.24E-02	0.72	0.02	11033
PCDH11Y	protocadherin 11 Y-linked	33.6	1.14E-04	4.04E-02	0.48	0.01	83259
PDE1C	phosphodiesterase 1C	33.2	3.97E-06	7.85E-03	0.43	0.01	5137
NRXN3	neurexin 3	32.7	3.66E-04	7.57E-02	0.58	0.02	9369
VTCN1	V-set domain containing T-cell activation inhibitor 1	31.9	2.63E-04	6.08E-02	0.18	0.01	79679
ASIC2	acid sensing ion channel subunit 2	31.5	3.48E-05	2.24E-02	1.72	0.05	40
GALNT14	polypeptide N-acetylgalactosaminyltransferase 14	29.9	4.76E-04	8.77E-02	0.08	0.00	79623
CLEC3A	C-type lectin domain family 3 member A	29.9	5.92E-05	2.92E-02	1.08	0.04	10143
FOXF1	forkhead box F1	29.4	4.37E-07	2.17E-03	2.74	0.09	2294
SCUBE1	signal peptide, CUB domain and EGF like domain containing1	28.7	1.03E-05	1.28E-02	0.62	0.02	80274
VIT	vitrin	28.5	5.35E-04	9.42E-02	0.63	0.02	5212
IRS4	insulin receptor substrate 4	26.2	1.30E-06	3.98E-03	1.88	0.07	8471
MAB21L2	mab-21 like 2	25.3	2.08E-06	5.51E-03	16.77	0.66	10586
ROBO2	roundabout guidance receptor 2	24.6	1.50E-06	4.26E-03	5.37	0.22	6092
KRT17	keratin 17	24.6	5.31E-05	2.74E-02	10.97	0.45	3872
HECW1	HECT, C2 and WW domain containing E3 ubiquitin protein ligase 1	23.2	1.72E-04	4.76E-02	1.39	0.06	23072
FLJ30901	uncharacterized protein FLJ30901	22.0	6.62E-05	3.14E-02	0.31	0.01	150378
GLP1R	glucagon like peptide 1 receptor	21.9	4.65E-04	8.65E-02	0.85	0.04	2740
FAM19A1	family with sequence similarity 19 member A1, C-C motif chemokine like	20.6	7.37E-06	1.05E-02	8.08	0.39	407738
PTGER4	prostaglandin E receptor 4	20.5	9.38E-08	1.60E-03	21.27	1.04	5734
SYTL2	synaptotagmin like 2	20.4	2.84E-04	6.36E-02	0.48	0.02	54843
TNMD	tenomodulin	19.9	3.43E-07	1.95E-03	2.28	0.11	64102
RBP3	retinol binding protein 3	19.7	4.56E-05	2.57E-02	0.53	0.03	5949
LINC-PINT	long intergenic non-protein coding RNA, p53 induced transcript	19.1	2.67E-05	2.00E-02	0.55	0.03	378805
CD48	CD48 molecule	17.8	2.55E-04	5.96E-02	0.21	0.01	962
ANKRD1	ankyrin repeat domain 1	16.5	1.67E-05	1.51E-02	2.08	0.13	27063
UBL7	ubiquitin like 7	16.2	3.27E-05	2.24E-02	0.36	0.02	84993
ICAM4	intercellular adhesion molecule 4 (Landsteiner-Wiener blood group)	16.1	2.21E-04	5.58E-02	0.12	0.01	3386
ALKAL1	ALK And LTK Ligand 1	16.1	2.22E-04	5.58E-02	0.43	0.03	389658
SCTR	secretin receptor	15.1	1.05E-04	3.90E-02	0.14	0.01	6344
CDH3	cadherin 3	14.0	3.93E-04	7.86E-02	0.33	0.02	1001
C16orf89	chromosome 16 open reading frame 89	14.0	1.23E-04	4.21E-02	2.43	0.17	146556
ICAM3	intercellular adhesion molecule 3	13.8	1.93E-04	5.10E-02	0.10	0.01	3385
LOC349160	uncharacterized LOC349160	13.8	1.62E-05	1.51E-02	1.63	0.12	349160
PCSK2	proprotein convertase subtilisin/kexin type 2	13.6	6.61E-06	1.05E-02	3.24	0.24	5126
GRIN2A	glutamate ionotropic receptor NMDA type subunit 2A	13.3	1.40E-04	4.38E-02	1.41	0.11	2903
PCDH11X	protocadherin 11 X-linked	13.0	2.29E-04	5.67E-02	0.81	0.06	27328
S1PR5	sphingosine-1-phosphate receptor 5	12.9	7.68E-06	1.05E-02	2.15	0.17	53637
COL9A1	collagen type IX alpha 1 chain	12.6	1.61E-04	4.71E-02	2.33	0.18	1297
TNC	tenascin C	12.1	7.76E-08	1.60E-03	99.27	8.22	3371
DGKA	diacylglycerol kinase alpha	12.1	2.49E-04	5.90E-02	0.07	0.01	1606
COL8A2	collagen type VIII alpha 2 chain	11.8	4.14E-06	7.85E-03	2.49	0.21	1296
ICAM5	intercellular adhesion molecule 5	11.8	1.68E-04	4.71E-02	0.62	0.05	7087
DLX1	distal-less homeobox 1	11.5	1.69E-04	4.71E-02	0.63	0.05	1745
DNAH11	dynein axonemal heavy chain 11	9.9	1.15E-04	4.06E-02	0.88	0.09	8701
RHBDL2	rhomboid like 2	9.9	1.33E-04	4.26E-02	0.76	0.08	54933
LOC101927069	uncharacterized LOC101927069	9.6	8.80E-05	3.54E-02	1.07	0.11	101927069
C1QTNF3	C1q and tumor necrosis factor related protein 3	9.5	1.21E-05	1.42E-02	20.52	2.16	114899
CHD5	chromodomain helicase DNA binding protein 5	9.5	3.57E-06	7.75E-03	2.48	0.26	26038
DIO2	iodothyronine deiodinase 2	9.5	1.43E-05	1.47E-02	2.41	0.25	1734
MAPK10	mitogen-activated protein kinase 10	9.4	7.00E-05	3.16E-02	0.80	0.09	5602
KCTD16	potassium channel tetramerization domain containing 16	9.1	5.78E-05	2.91E-02	1.81	0.20	57528
CHRM2	cholinergic receptor muscarinic 2	8.8	3.06E-05	2.17E-02	3.60	0.41	1129
FOXD1	forkhead box D1	8.7	4.48E-05	2.57E-02	0.73	0.08	2297
COL19A1	collagen type XIX alpha 1 chain	8.7	3.70E-05	2.27E-02	2.50	0.29	1310
CSGALNACT1	chondroitin sulfate N-acetylgalactosaminyltransferase 1	8.5	5.09E-04	9.12E-02	0.55	0.06	55790
LINC00643	long intergenic non-protein coding RNA 643	8.2	5.92E-04	9.98E-02	1.06	0.13	646113
PKHD1	polycystic kidney and hepatic disease 1 (autosomal recessive)	8.2	1.62E-04	4.71E-02	0.45	0.06	5314
FOXG1	forkhead box G1	8.1	3.08E-04	6.76E-02	0.18	0.02	2290

MEIS1-AS3	MEIS1 antisense RNA 3	7.9	1.78E-04	4.85E-02	0.35	0.04	730198
NEXMIF	Neurite Extension And Migration Factor	7.8	7.96E-07	3.52E-03	11.00	1.40	340533
DLX2	distal-less homeobox 2	7.4	2.61E-05	2.00E-02	14.15	1.90	1746
MME	membrane metalloendopeptidase	7.3	7.41E-05	3.17E-02	0.89	0.12	4311
WIF1	WNT inhibitory factor 1	7.2	1.11E-04	3.99E-02	0.94	0.13	11197
LOC100130238	uncharacterized LOC100130238	7.1	5.66E-05	2.89E-02	0.84	0.12	100130238
CCDC129	coiled-coil domain containing 129	7.0	3.81E-05	2.29E-02	0.96	0.14	223075
SHISA2	shisa family member 2	6.9	3.70E-06	7.75E-03	6.29	0.91	387914
INMT	indolethylamine N-methyltransferase	6.8	7.89E-05	3.23E-02	23.55	3.47	11185
JAKMIP2	janus kinase and microtubule interacting protein 2	6.7	2.06E-05	1.75E-02	2.20	0.33	9832
HOXC4	homeobox C4	6.7	1.37E-05	1.47E-02	2.72	0.41	3221
MTCL1	microtubule crosslinking factor 1	6.6	7.29E-06	1.05E-02	2.24	0.34	23255
GLP2R	glucagon like peptide 2 receptor	6.6	3.84E-04	7.77E-02	0.37	0.06	9340
HOXA5	homeobox A5	6.5	1.69E-04	4.71E-02	1.65	0.25	3202
FAM84A	family with sequence similarity 84 member A	6.5	7.32E-05	3.17E-02	0.67	0.10	151354
SYT4	synaptotagmin 4	6.2	5.70E-04	9.69E-02	0.50	0.08	6860
GIRK1	glutamate ionotropic receptor kainate type subunit 1	6.2	3.71E-04	7.61E-02	2.88	0.46	2897
LIMK2	LIM domain kinase 2	6.2	2.93E-06	6.85E-03	4.64	0.75	3985
TNNC1	troponin C1, slow skeletal and cardiac type	6.0	4.35E-04	8.33E-02	1.22	0.20	7134
ARHGEF3	Rho guanine nucleotide exchange factor 3	5.9	5.17E-04	9.18E-02	1.72	0.29	50650
EPB42	erythrocyte membrane protein band 4.2	5.9	1.11E-04	3.99E-02	1.46	0.25	2038
ADAMTS9	ADAM metallopeptidase with thrombospondin type 1 motif 9	5.8	1.09E-06	3.98E-03	68.53	11.83	56999
THBS1	thrombospondin 1	5.4	5.19E-06	9.38E-03	60.97	11.20	7057
FREM3	FRAS1 related extracellular matrix 3	5.4	5.21E-04	9.21E-02	1.04	0.19	166752
FRZB	frizzled-related protein	5.3	4.85E-05	2.62E-02	113.24	21.47	2487
PIP5K1B	phosphatidylinositol-4-phosphate 5-kinase type 1 beta	5.2	2.08E-04	5.37E-02	2.84	0.54	8395
ISM1	isthmin 1	5.0	5.45E-04	9.53E-02	0.80	0.16	140862
SERPINB6	serpin family B member 6	5.0	4.34E-04	8.33E-02	0.55	0.11	5269
COL8A1	collagen type VIII alpha 1 chain	4.8	3.72E-05	2.27E-02	5.21	1.09	1295
MAMDC2	MAM domain containing 2	4.8	2.79E-05	2.06E-02	20.56	4.30	256691
CBLN2	cerebellin 2 precursor	4.7	5.94E-05	2.92E-02	31.68	6.68	147381
CD82	CD82 molecule	4.4	4.87E-05	2.62E-02	5.01	1.13	3732
PAMR1	peptidase domain containing associated with muscle regeneration 1	4.3	1.98E-04	5.19E-02	2.37	0.54	25891
DCLK2	doublecortin like kinase 2	4.3	2.83E-06	6.85E-03	158.67	36.98	166614
LINC00672	long intergenic non-protein coding RNA 672	4.2	3.93E-04	7.86E-02	3.51	0.84	100505576
GCNT2	glucosaminyl (N-acetyl) transferase 2, I-branching enzyme (I blood group)	4.2	1.66E-04	4.71E-02	1.13	0.27	2651
APCDD1L	APC down-regulated 1 like	4.1	4.84E-04	8.88E-02	1.42	0.35	164284
ENTPD1	ectonucleoside triphosphate diphosphohydrolase 1	3.9	4.59E-05	2.57E-02	6.62	1.71	953
ABCC9	ATP binding cassette subfamily C member 9	3.8	2.36E-05	1.88E-02	12.06	3.17	10060
HOXB4	homeobox B4	3.8	3.61E-04	7.57E-02	1.12	0.30	3214
CADM1	cell adhesion molecule 1	3.7	3.97E-04	7.90E-02	3.86	1.05	23705
HOXB3	homeobox B3	3.5	6.07E-05	2.94E-02	16.72	4.79	3213
SAMD11	sterile alpha motif domain containing 11	3.5	4.69E-04	8.68E-02	82.12	23.69	148398
DNAH14	dynein axonemal heavy chain 14	3.3	2.80E-04	6.36E-02	5.58	1.67	127602
LINC00607	long intergenic non-protein coding RNA 607	3.3	4.54E-04	8.58E-02	2.71	0.83	646324
HMGA2	high mobility group AT-hook 2	3.2	4.57E-04	8.58E-02	5.04	1.59	8091
LINC00623	long intergenic non-protein coding RNA 623	3.2	2.62E-04	6.08E-02	21.25	6.72	728855
RAI14	retinoic acid induced 14	3.1	9.78E-05	3.79E-02	7.81	2.56	26064
DOK6	docking protein 6	3.0	2.03E-04	5.28E-02	7.04	2.32	220164
HOMER1	homer scaffolding protein 1	3.0	9.81E-05	3.79E-02	5.58	1.85	9456
TENM3	teneurin transmembrane protein 3	2.7	4.97E-04	8.99E-02	19.90	7.41	55714
CAMK1D	calcium/calmodulin dependent protein kinase ID	2.5	2.85E-04	6.36E-02	4.94	1.95	57118
STIM2	stromal interaction molecule 2	2.5	3.31E-04	7.12E-02	5.34	2.16	57620
PRICKLE2	prickle planar cell polarity protein 2	2.3	5.55E-04	9.56E-02	10.20	4.35	166336

Table S5 **Genes Enriched in the Human Ao by RNA-seq** (Fold Change; DA vs Ao)

Gene Symbol	Gene Name	Fold Change	P-value	FDR	FPKM DA	FPKM Ao	Entrez ID
RIMS2	regulating synaptic membrane exocytosis 2	-67.9	2.07E-05	1.75E-02	0.01	0.53	9699
HPSE2	heparanase 2 (inactive)	-24.6	1.21E-04	4.20E-02	0.01	0.17	60495
DCSTAMP	dendrocyte expressed seven transmembrane protein	-20.3	3.26E-05	2.24E-02	0.03	0.68	81501
PPFIBP1	PPFIA binding protein 1	-19.8	5.48E-04	9.53E-02	0.01	0.22	8496
TM6SF1	transmembrane 6 superfamily member 1	-17.8	6.76E-05	3.14E-02	0.01	0.22	53346
MGAT4C	MGAT4 family member C	-16.3	1.30E-04	4.26E-02	0.02	0.34	25834
RAPSN	receptor associated protein of the synapse	-15.7	1.04E-04	3.89E-02	0.03	0.46	5913
TBX20	T-box 20	-14.8	3.34E-04	7.13E-02	0.06	0.88	57057
SPATA6L	spermatogenesis associated 6 like	-14.6	1.27E-04	4.26E-02	0.01	0.15	55064
ANXA8L1	annexin A8-like 1	-14.2	1.58E-05	1.51E-02	0.16	2.30	728113
STAC2	SH3 and cysteine rich domain 2	-13.6	7.47E-05	3.17E-02	0.02	0.27	342667
GAS2	growth arrest specific 2	-13.4	3.66E-04	7.57E-02	0.01	0.07	2620
BRINP2	BMP/retinoic acid inducible neural specific 2	-12.3	1.46E-04	4.44E-02	0.03	0.37	57795
NEIL1	nei like DNA glycosylase 1	-11.4	5.04E-04	9.07E-02	0.00	0.05	79661
RSPO2	R-spondin 2	-11.2	4.25E-04	8.32E-02	0.06	0.69	340419
RBFA	ribosome binding factor A (putative)	-11.1	2.25E-04	5.59E-02	0.01	0.08	79863
SLC26A6	solute carrier family 26 member 6	-9.9	5.70E-04	9.69E-02	0.01	0.08	65010
FCGR3A	Fc fragment of IgG receptor IIIa	-9.9	4.28E-04	8.33E-02	0.01	0.07	2214
MSLN	mesothelin	-9.4	2.18E-04	5.55E-02	0.03	0.25	10232
TFPI2	tissue factor pathway inhibitor 2	-9.2	5.12E-05	2.68E-02	0.74	6.78	7980
A4GALT	alpha 1,4-galactosyltransferase	-8.9	1.48E-04	4.44E-02	0.04	0.38	53947
GABRB2	gamma-aminobutyric acid type A receptor beta2 subunit	-6.7	2.97E-05	2.15E-02	0.40	2.72	2561
LDB3	LIM domain binding 3	-6.6	1.20E-04	4.19E-02	0.14	0.89	11155
LRP1B	LDL receptor related protein 1B	-5.9	1.37E-05	1.47E-02	1.43	8.48	53353
PKHD1L1	polycystic kidney and hepatic disease 1 (autosomal recessive)-like 1	-5.5	7.52E-05	3.17E-02	2.31	12.81	93035
KALRN	kalirin, RhoGEF kinase	-5.3	1.24E-04	4.21E-02	2.36	12.63	8997
RBM20	RNA binding motif protein 20	-5.1	6.84E-06	1.05E-02	1.72	8.76	282996
RIPK4	receptor interacting serine/threonine kinase 4	-5.1	3.27E-04	7.07E-02	0.09	0.44	54101
MTUS2	microtubule associated tumor suppressor candidate 2	-5.0	1.75E-05	1.55E-02	7.97	39.45	23281
HAND2	heart and neural crest derivatives expressed 2	-4.8	5.10E-05	2.68E-02	1.17	5.61	9464
TACC2	transforming acidic coiled-coil containing protein 2	-4.7	1.45E-05	1.47E-02	1.11	5.17	10579
PLD5	phospholipase D family member 5	-4.6	1.82E-04	4.85E-02	0.35	1.64	200150
LINC01099	long intergenic non-protein coding RNA 1099	-4.3	7.38E-05	3.17E-02	0.29	1.23	101928656
CDH13	cadherin 13	-4.2	1.43E-04	4.44E-02	3.69	15.67	1012
MFAP3L	microfibrillar associated protein 3 like	-4.2	2.42E-04	5.86E-02	0.34	1.44	9848
PDE10A	phosphodiesterase 10A	-4.0	1.33E-04	4.26E-02	1.22	4.89	10846
KDELC1	KDEL motif containing 1	-3.8	2.23E-04	5.59E-02	3.06	11.78	79070
PHACTR1	phosphatase and actin regulator 1	-3.7	4.03E-04	7.97E-02	0.70	2.61	221692
PAPPA2	pappalysin 2	-3.7	2.49E-04	5.90E-02	0.69	2.56	60676
RYR2	ryanodine receptor 2	-3.7	1.35E-04	4.28E-02	7.41	27.15	6262
MAP3K7CL	MAP3K7 C-terminal like	-3.7	3.54E-05	2.24E-02	2.64	9.66	56911
SDK1	sidekick cell adhesion molecule 1	-3.6	4.02E-05	2.39E-02	2.89	10.40	221935
FAM19A2	family seq similarity 19 member A2, C-C motif chemokine like	-3.6	2.49E-04	5.90E-02	1.54	5.51	338811
KCNMA1	potassium calcium-activated channel subfamily M alpha 1	-3.5	2.74E-04	6.27E-02	0.49	1.69	3778
DUSP27	dual specificity phosphatase 27 (putative)	-3.5	1.25E-04	4.21E-02	1.17	4.05	92235
ASTN1	astrotactin 1	-3.4	9.73E-05	3.79E-02	0.83	2.77	460
KANK4	KN motif and ankyrin repeat domains 4	-3.3	4.31E-04	8.33E-02	2.30	7.62	163782
TMTC1	transmembrane and tetratricopeptide repeat containing 1	-3.3	9.52E-05	3.79E-02	1.64	5.37	83857
POSTN	periostin	-3.2	1.45E-04	4.44E-02	49.83	161.49	10631
FIGN	fidgetin, microtubule severing factor	-3.2	3.12E-04	6.79E-02	2.64	8.54	55137
RGS17	regulator of G-protein signaling 17	-3.2	4.92E-04	8.97E-02	0.95	3.02	26575
PAPPA	pappalysin 1	-3.1	1.83E-04	4.85E-02	2.57	8.03	5069
DSEL	dermatan sulfate epimerase-like	-3.1	2.38E-04	5.84E-02	33.23	103.24	92126
NOV	nephroblastoma overexpressed	-3.0	3.40E-04	7.23E-02	10.92	32.35	4856
CYFIP2	cytoplasmic FMR1 interacting protein 2	-2.9	1.09E-04	3.99E-02	1.76	5.15	26999
WWP2	WW domain containing E3 ubiquitin protein ligase 2	-2.9	1.62E-04	4.71E-02	1.69	4.90	11060
ADAM22	ADAM metallopeptidase domain 22	-2.9	2.92E-04	6.49E-02	0.72	2.10	53616
ZBTB16	zinc finger and BTB domain containing 16	-2.8	5.48E-04	9.53E-02	0.64	1.80	7704
PAPPA-AS1	PAPPA antisense RNA 1	-2.7	1.48E-04	4.44E-02	5.10	13.89	493913
RNF144A	ring finger protein 144A	-2.7	5.55E-04	9.56E-02	3.67	9.98	9781
FOXCUT	FOXC1 upstream transcript (non-protein coding)	-2.7	5.62E-04	9.64E-02	0.65	1.74	101927703
ERBB4	erb-b2 receptor tyrosine kinase 4	-2.7	1.33E-04	4.26E-02	13.50	35.88	2066
BVES	blood vessel epicardial substance	-2.6	1.67E-04	4.71E-02	3.96	10.32	11149
ADAMTS8	ADAM metallopeptidase with thrombospondin type 1 motif 8	-2.6	6.86E-05	3.14E-02	6.12	15.95	11095
PRELP	proline and arginine rich end leucine rich repeat protein	-2.5	4.60E-04	8.59E-02	1.11	2.75	5549
NPR1	natriuretic peptide receptor 1	-2.5	3.79E-04	7.74E-02	17.33	42.88	4881
ENPP1	ectonucleotide pyrophosphatase/phosphodiesterase 1	-2.3	2.55E-04	5.96E-02	28.96	67.73	5167
ST6GAL2	ST6 beta-galactoside alpha-2,6-sialyltransferase 2	-2.1	5.12E-04	9.14E-02	7.67	16.15	84620

Table S6 **Differentially Expressed Genes Most Highly Expressed in the Human DA by RNA-seq** (Fold Change; DA vs Ao)

Gene ID	Gene Name	Fold change	P-value	FDR	FPKM DA	FPKM Ao	Entrez Gene
DCLK2	doublecortin like kinase 2	4.3	2.83E-06	6.85E-03	158.67	36.98	166614
FRZB	frizzled-related protein	5.3	4.85E-05	2.62E-02	113.24	21.47	2487
TNC	tenascin C	12.1	7.76E-08	1.60E-03	99.27	8.22	3371
SAMD11	sterile alpha motif domain containing 11	3.5	4.69E-04	8.68E-02	82.12	23.69	148398
ADAMTS9	ADAM metallopeptidase with thrombospondin type 1 motif 9	5.8	1.09E-06	3.98E-03	68.53	11.83	56999
THBS1	thrombospondin 1	5.4	5.19E-06	9.38E-03	60.97	11.20	7057
CBLN2	cerebellin 2 precursor	4.7	5.94E-05	2.92E-02	31.68	6.68	147381
INMT	indolethylamine N-methyltransferase	6.8	7.89E-05	3.23E-02	23.55	3.47	11185
PTGER4	prostaglandin E receptor 4	20.5	9.38E-08	1.60E-03	21.27	1.04	5734
LINC00623	long intergenic non-protein coding RNA 623	3.2	2.62E-04	6.08E-02	21.25	6.72	728855
MAMDC2	MAM domain containing 2	4.8	2.79E-05	2.06E-02	20.56	4.30	256691
C1QTNF3	C1q and tumor necrosis factor related protein 3	9.5	1.21E-05	1.42E-02	20.52	2.16	114899
TENM3	teneurin transmembrane protein 3	2.7	4.97E-04	8.99E-02	19.90	7.41	55714
MAB21L2	mab-21 like 2	25.3	2.08E-06	5.51E-03	16.77	0.66	10586
HOXB3	homeobox B3	3.5	6.07E-05	2.94E-02	16.72	4.79	3213
DLX2	distal-less homeobox 2	7.4	2.61E-05	2.00E-02	14.15	1.90	1746
ABCC9	ATP binding cassette subfamily C member 9	3.8	2.36E-05	1.88E-02	12.06	3.17	10060
NEXMIF	Neurite Extension And Migration Factor	7.8	7.96E-07	3.52E-03	11.00	1.40	340533
KRT17	keratin 17	24.6	5.31E-05	2.74E-02	10.97	0.45	3872
PRICKLE2	prickle planar cell polarity protein 2	2.3	5.55E-04	9.56E-02	10.20	4.35	166336

Table S7 **GO, KEGG, and UP Keywords Common in Human RNA-seq and Rodent Microarrays**

	RNA-seq	RNA-seq	Microarray	Microarray
GO Biological Process – Overlap: 30/62 Common 48.4%	**Count**	**PValue**	**Count[1]**	**PValue**
GO:0001501~skeletal system development	6	7.53E-03	10	1.87E-05
GO:0001525~angiogenesis	6	4.88E-02	8	1.79E-02
GO:0001822~kidney development	4	4.11E-02	14	2.86E-07
GO:0006366~transcription from RNA polymerase II promoter	9	8.68E-02	15	2.10E-03
GO:0007155~cell adhesion	16	1.45E-05	16	6.55E-06
GO:0007166~cell surface receptor signaling pathway	6	9.73E-02	10	1.98E-03
GO:0007188~adenylate cyclase-modulating G-protein coupled receptor signaling pathway	3	4.25E-02	3	7.81E-02
GO:0007399~nervous system development	7	4.30E-02	10	2.52E-03
GO:0007420~brain development	5	8.88E-02	13	1.61E-03
GO:0007507~heart development	6	2.36E-02	19	2.22E-07
GO:0008284~positive regulation of cell proliferation	9	5.61E-02	23	4.38E-06
GO:0009612~response to mechanical stimulus	5	1.86E-03	10	2.02E-05
GO:0009952~anterior/posterior pattern specification	5	5.59E-03	7	6.59E-03
GO:0010628~positive regulation of gene expression	6	8.42E-02	19	8.36E-06
GO:0010811~positive regulation of cell-substrate adhesion	3	4.47E-02	4	2.73E-02
GO:0016337~single organismal cell-cell adhesion	9	3.20E-06	6	1.84E-02
GO:0016525~negative regulation of angiogenesis	4	1.77E-02	4	7.07E-02
GO:0021766~hippocampus development	3	8.83E-02	5	4.93E-02
GO:0030198~extracellular matrix organization	14	2.09E-08	10	1.15E-05
GO:0030308~negative regulation of cell growth	6	4.48E-03	9	4.04E-04
GO:0042475~odontogenesis of dentin-containing tooth	4	1.28E-02	5	1.46E-02
GO:0043065~positive regulation of apoptotic process	11	3.50E-04	11	2.57E-02
GO:0045600~positive regulation of fat cell differentiation	3	6.52E-02	4	3.40E-02
GO:0048704~embryonic skeletal system morphogenesis	3	4.68E-02	5	8.76E-03
GO:0050715~positive regulation of cytokine secretion	3	2.05E-02	3	7.81E-02
GO:0051216~cartilage development	5	1.86E-03	6	3.04E-03
GO:0060441~epithelial tube branching involved in lung morphogenesis	4	2.88E-04	4	4.85E-03
GO:0071356~cellular response to tumor necrosis factor	4	7.45E-02	7	1.30E-02
GO:0072210~metanephric nephron development	2	1.77E-02	2	5.67E-02
GO:0097070~ductus arteriosus closure	2	4.36E-02	2	8.38E-02
GO Cellular Component – Overlap: 12/19 Common, 63.2%	**Count**	**PValue**	**Count**	**PValue**
GO:0005576~extracellular region	22	5.39E-02	18	2.87E-02
GO:0005578~proteinaceous extracellular matrix	12	3.19E-05	31	3.83E-19
GO:0005615~extracellular space	21	1.85E-02	46	3.97E-08
GO:0005886~plasma membrane	52	7.34E-03	78	1.91E-03
GO:0005887~integral component of plasma membrane	23	8.29E-03	28	4.81E-04
GO:0009897~external side of plasma membrane	7	1.27E-02	8	8.98E-02
GO:0016020~membrane	31	1.29E-02	48	3.18E-03
GO:0030424~axon	6	5.05E-02	15	7.40E-04
GO:0030425~dendrite	7	8.26E-02	18	5.96E-04
GO:0031012~extracellular matrix	11	3.57E-04	23	1.62E-11
GO:0043005~neuron projection	6	6.34E-02	17	1.82E-04
GO:0045211~postsynaptic membrane	7	1.22E-02	8	2.35E-02
GO Molecular Function – Overlap: 9/19 Common, 47.4%	**Count**	**PValue**	**Count**	**PValue**
GO:0001077~transcriptional activator activity, RNA polymerase II core promoter proximal region sequence-specific binding	6	6.38E-02	11	4.61E-03
GO:0005178~integrin binding	7	3.87E-04	9	1.17E-04
GO:0005201~extracellular matrix structural constituent	4	2.29E-02	6	5.65E-04
GO:0005509~calcium ion binding	17	8.07E-04	23	6.72E-04
GO:0008201~heparin binding	6	1.53E-02	13	1.77E-06
GO:0042803~protein homodimerization activity	12	6.82E-02	29	2.36E-05
GO:0043565~sequence-specific DNA binding	9	9.93E-02	15	4.36E-02
GO:0044325~ion channel binding	4	8.33E-02	9	6.00E-04
GO:0050839~cell adhesion molecule binding	4	1.87E-02	4	8.78E-02
Kegg Pathway – Overlap: 5/9 Common, 55.6%	**Count**	**PValue**	**Count**	**PValue**
hsa04020~Calcium signaling pathway	8	1.13E-03	11	4.17E-04
hsa04024~cAMP signaling pathway	6	3.38E-02	10	2.45E-03
hsa04724~Glutamatergic synapse	4	8.53E-02	5	9.25E-02
hsa04911~Insulin secretion	4	4.21E-02	7	1.72E-03
hsa04924~Renin secretion	4	2.03E-02	5	1.75E-02
UP_Keywords – Overlap: 22/37 Common, 59.5%	**Count**	**PValue**	**Count**	**PValue**
Alternative splicing	108	2.76E-03	41	4.73E-11
Calcium	21	4.63E-05	18	2.18E-03
cAMP	3	3.63E-02	3	4.54E-02
Cell adhesion	23	9.66E-11	12	1.52E-03
Cell junction	16	5.61E-04	11	8.95E-02
Cell membrane	43	1.35E-03	53	1.74E-02
Cleavage on pair of basic residues	7	3.74E-02	12	2.45E-05
Collagen	5	9.26E-03	4	5.19E-02

Developmental protein	19	1.02E-03	22	2.44E-06
Disulfide bond	56	5.71E-07	75	1.21E-14
EGF-like domain	10	1.82E-04	9	1.81E-03
Extracellular matrix	14	2.77E-07	11	1.06E-05
Glycoprotein	83	1.03E-13	72	6.87E-14
Heparin-binding	4	3.76E-02	7	4.75E-05
Hydroxylation	4	4.54E-02	6	5.90E-04
Immunoglobulin domain	12	6.32E-03	10	6.76E-03
Membrane	81	4.02E-03	112	2.91E-02
Metalloprotease	5	3.88E-02	5	4.29E-02
Secreted	36	1.31E-05	40	3.87E-09
Signal	73	7.28E-11	88	1.99E-10
Signal-anchor	9	3.78E-02	7	7.95E-02
Synapse	14	1.02E-05	8	9.50E-02

[1]Number of genes identified within each term

Chapter 3

MOUSE MODELS AND HUMAN SINGLE GENE SYNDROMES ASSOCIATED WITH PATENT DUCTUS ARTERIOSUS (PDA) FURTHER SUPPORT THE CONCEPT OF A DEVELOPMENTAL PROGRAM IN THE DUCTUS ARTERIOSUS

Adapted with permission from: Michael T. Yarboro, Srirupa H. Gopal, M.D., Rachel L. Su, Thomas M. Morgan, M.D. Ph.D., and Jeff Reese, M.D. (2022) Mouse Models of Patent Ductus Arteriosus (PDA) and their Relevance for Human PDA. Dev Dyn. DOI: 10.1002/dvdy.408

Abstract:

After birth, changes in complex signaling pathways lead to constriction and permanent closure of the DA. This process is likely mediated by a coordinated developmental program which acts to mature the DA. Although limits on the availability of human DA tissues prevent comprehensive studies on the mechanisms of DA function, mouse models have been developed that reveal critical pathways in DA regulation. More than 30 different transgenic mouse models exhibiting PDA have been described, each potentially representing a constituent of the DA's developmental program. Additionally, I Identified 224 human single-gene syndromes that are associated with PDA, including a small subset that consistently feature PDA as a prominent phenotype. Comparison and functional analyses of these genes provide insight into DA development and identify key regulatory pathways that may constitute a developmental program within the DA.

Introduction:

The DA is a fetal vessel which shunts blood past the uninflated lungs, providing oxygenated blood from the placenta to the peripheral circulation and protecting the developing pulmonary vasculature *in utero*. At birth, increasing O_2 tension along with a decrease in prostaglandins and other vasodilatory mediators leads to constriction, closure, and subsequent fibromuscular transformation of the DA into the LA. Failure of the postnatal DA closure process may lead to PDA, with potentially harmful consequences in newborns. PDA accounts for up to 10% of CHD and is particularly problematic for preterm and especially low birthweight neonates (38, 376). In preterm infants born at 27 - 28 weeks gestation, 64% retain a patent DA at 7 days after birth, and amongst neonates born at 24 weeks that figure increases to 87% (31). Options for management include pharmacological treatment with cyclooxygenase inhibitors, surgical ligation, interventional catheter-based occlusion, or conservative management, each of which have potential for harm (419).

Normal DA closure consists of a highly ordered series of biological steps involving different cell types, signaling pathways, and mechanical forces (1). Attempts to study these processes in preterm infants, while vital for advancing understanding and treatment of PDA, are limited by tissue availability and quality, as well as the nature of *ex vivo* and *in vitro* experiments. Large animal models have been used for centuries to study the anatomy, physiology and pharmacology of the DA (420, 421). More recent studies on small animal models offer insights into DA embryology and function in more tractable laboratory species (10, 422). Rodent models of PDA have gained popularity due to their high fecundity, short gestation, and large litter sizes. The mouse is a robust and widely used mammalian model which benefits from over a century of genetic methodology (423). The first transgenic models of PDA in mice were reported over 20 years ago (108, 109). Currently, there are over 30

reported genetic mouse models of PDA which provide insight into the role of specific ligands and receptors, structural or hematopoietic elements, and other molecular mediators of DA development and function. While some of these models may not be pertinent to the human DA, comparison to human single-gene syndromes associated with PDA may help identify relevant transcripts that warrant future analysis.

Human PDAs vary widely in their characteristics, severity, and underlying causes. A PDA in infancy may occur as part of a complex CHD or as an isolated anomaly. Isolated PDA occurs frequently in preterm infants, primarily as a result of developmental immaturity which might not affect a given infant born at term. In contrast, a PDA in term infants is more likely to be associated with a genetic syndrome or a defined fetal embryopathy (e.g., congenital rubella syndrome) (25, 419). Both term and preterm PDAs may have a genetic component, with a 5% sibling recurrence rate (98, 99) and a higher correlation between monozygotic twins compared to dizygotic twins (100, 101). While reports have varied, one twin study found that genetic factors and a common gestational environment contributed up to 76% of this variance. Studies on familial PDA and the offspring of consanguineous parentage provide genetic information on chromosome regions that confer risk for PDA (102, 103). In addition, candidate gene studies have identified genetic loci which contribute to syndromic forms of PDA such as *TFAP2B*, or whose sequence variants can contribute to isolated non-syndromic cases of PDA (104, 105). Although the genetic predisposition for most PDAs is unknown, a robust understanding of the genes whose perturbation results in PDA may provide key insights into the developmental program which directs DA identity. A better understanding of this program will support the development of new and improved therapies.

In this chapter I discuss the existing genetic mouse models of PDA and their potential implications for human DA biology. Additionally, I probed multiple digital databases to identify

single-gene syndromes associated with PDA in humans. Gene Ontology (GO) tools identified pathways and processes common between existing mouse models and human single-gene syndromes. Together these genes which are critical for proper DA function in mice and humans, help to further define the presence of a developmental program which defines the DA from surrounding vessels.

Mouse Models of PDA:

Existing mouse models of PDA fall into several categories based on molecule type, localization, or pathway of action: components of the prostaglandin signaling pathway, proteins specific to SMCs, proteins involved in developmental signaling, matrix and cytoskeletal components, platelet function, chromatin modifiers, and transcription factors. Representative images (**Figure 1**) and summary information (**Table S1**) for each model are provided respectively.

Prostaglandin Signaling:

Ptger4 knockout (KO): The prostaglandin E receptor EP_4 is the canonical mediator of PGE_2 effects in the DA. The EP_4 receptor gene, *PTGER4* is consistently enriched in both the mouse and human DA among various expression studies (265). The EP_4 receptor is a GPCR which is capable of signaling through both G-α_s and G-α_i G-proteins giving it the ability to increase or decrease (respectively) the amount of cAMP in a cell, endowing potentially conflicting roles dependent on context (213). The EP_4 KO PDA phenotype was reported by three independent labs using distinct transgenic strategies (108-110). Nguyen et al, reported the first example of a mouse model of PDA in 1997. EP_4 KO mice had neonatal lethality accompanied by a widely

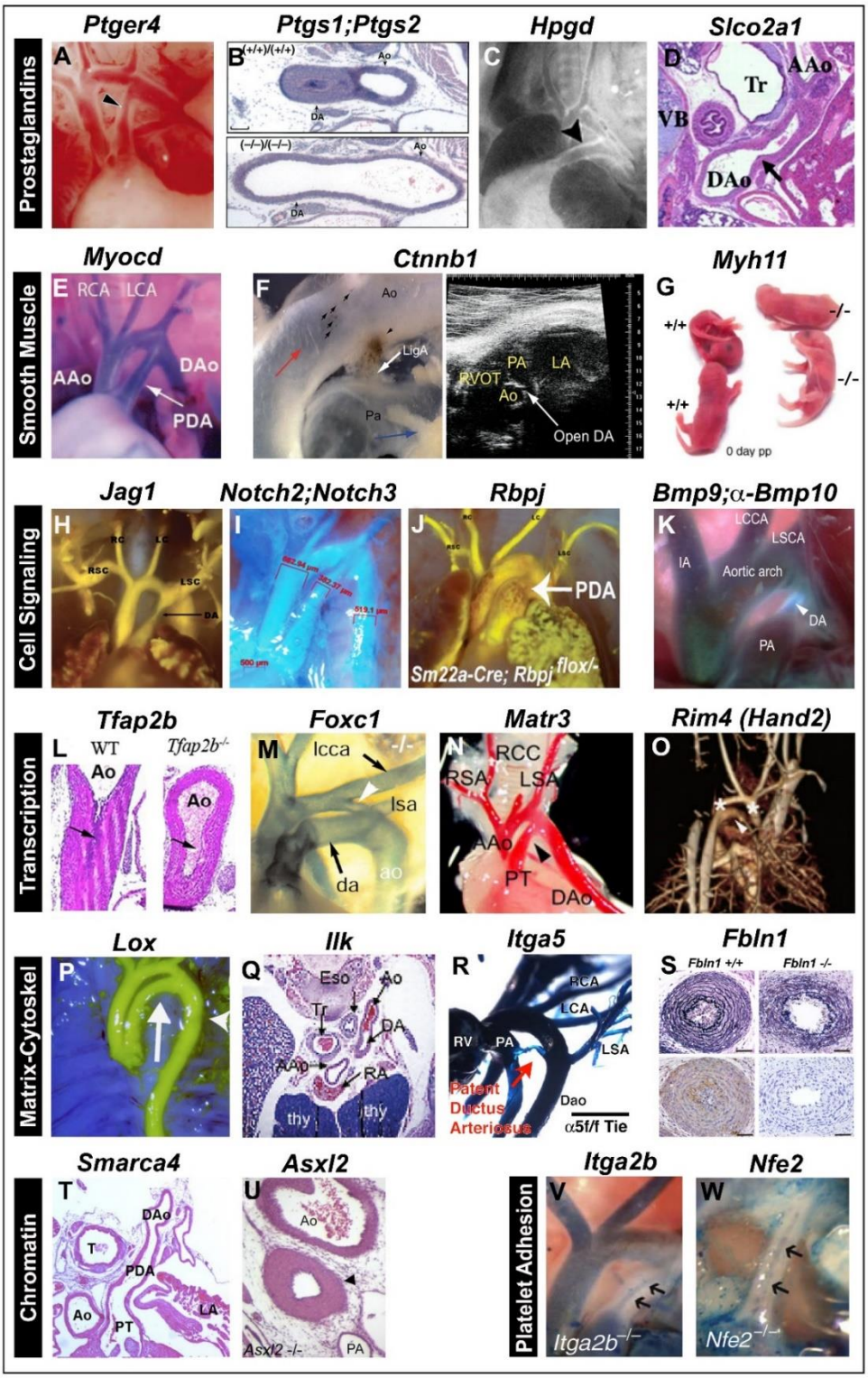

Figure 1. Representative images of various mouse knockout models exhibiting a PDA phenotype. PDA images (arrows, arrowheads) were obtained by whole mount or stained sections, as well as angiography and ultrasound. Images adapted or reproduced with permission. Full citations available in published work (424).

patent DA and pulmonary edema (**Figure 1A**) (108). This phenotype was observed by all three groups with varying penetrance. When the null allele was crossed from a 129/SvEv background into a mixed genetic background (B6D2 F1, C57BL/6 and DBA/2 cross) (background information provided in **Table S1**) the uniformly lethal phenotype changed to 5% survival after 1 backcross and to 21% survival after 4 crosses (108). These data suggest that compensatory mechanisms exist for closing the DA and that genetic diversity may protect against genetic predisposition to PDA. The EP_4 KO PDA phenotype has been termed the 'paradoxical PDA' due to its counterintuitive signaling, since the removal of a vasodilatory receptor is expected to foster constriction, not an inability to constrict (272). *For this reason, it is suspected that EP_4 may play an additional role in the DA, guiding vessel formation and remodeling.* This has been further supported by findings that EP_4 signaling is necessary for the production of hyaluronic acid in the DA, a process key for movement of SMCs into the sub-endothelial space coinciding with permanent DA closure (146).

Ptgs1;Ptgs2 double KO: COX-1 and COX-2 are the enzymes responsible for the production of PGE_2, the primary ligand for the EP receptors, including EP_4 (213). While COX-1 and COX-2 share similar functions, they often differ in localization and expression, and support different processes (425). COX-1 is generally associated with tissue homeostasis and epithelial maintenance whereas COX-2 is typically associated with inflammation. The initial characterizations of mice with targeted mutation of either the COX-1 (*Ptgs1*) or COX-2 (*Ptgs2*) genes did not reveal a PDA phenotype. However, generation of COX-1;COX-2 double KO animals revealed a robust PDA phenotype and neonatal lethality (106). Animals showed signs of congestive heart failure (CHF) similar to other PDA models. PDA was noted in both outbred CD-1 mice (106) and inbred C57Bl/6 mice (**Figure 1B**) (107). While the link between prenatal

exposure to COX inhibitors and PDA is established in both humans (47, 187) and rodents (195-197), it remains paradoxical that removal of a vasodilator results in dilation instead of constriction. *In situ* hybridization and PCR assays suggested that circulating PGE_2 generated in peripheral tissues acts on PGE receptors in the DA via endocrine mechanisms (106). ***Moreover, pharmacologic studies suggest that prostaglandin ligand-receptor signaling via the COX-EP_4 axis during specific gestational windows play a novel role regulating DA development, in addition to their well-known role in DA vasodilation*** (196).

Ptgs2 KO: Following the discovery of a PDA phenotype COX-1;COX-2 double KO mice, the COX-1 and COX-2 KO models were re-examined. A PDA phenotype was found in COX-2 KO pups with 35% penetrance in a 129/Ola and C57BL/6 mixed background (background information provided in **Table S1**). Further, while COX-1 KO offspring showed little or no PDA phenotype, deletion of one COX-1 allele increased penetrance of the COX-2 KO PDA phenotype such that COX-$1^{-/+}$;COX-$2^{-/-}$ mice had 79% penetrance and COX-$1^{-/-}$;COX-$2^{-/-}$ mice displayed 100% penetrance (374). Additional studies utilized a targeted point mutation to generate mice expressing Cox-2 protein defective in COX function but preserving its peroxidase function (*Ptgs2^{Y385F}*). *Ptgs2^{Y385F}* mice exhibited no PDA which suggested the formation of COX-1 and COX-2^{Y385F} heterodimers (225). Despite the loss of COX-2 functionality, *Ptgs2^{Y385F}* mice produce enough PGE_2 to maintain DA function, implying non-catalytic COX-2 heteromers are bound to functional COX-1 partners. These findings suggest COX-2 is the predominant COX isoform required for DA development and function, likely owing to its ten-fold lower activating concentration (222, 426), and it is possible that COX-1 serves an auxiliary role, potentially through heterodimerization.

Hpgd KO: Prostaglandins play key signaling roles in nearly all tissue types. In many contexts, prostaglandin-mediated effects are regulated through catabolism by enzymes such as 15-hydroxyprostaglandin dehydrogenase (PGDH). Mice hypomorphic for the PGDH gene (*Hpgd*) exhibit preterm labor associated with the genotype of both pup and dam. *Hpgd* KO mice die neonatally with PDA (**Figure 1C**) (23, 24), presumably related to elevated levels of PGE_2. In wildtype (WT) mice, following initiation of respiration, pulmonary vascular resistance falls as the DA constricts, redirecting blood through the newborn lungs, which express high levels of PGDH. PGDH catabolizes circulating PGE_2, lowering serum levels leading to further DA closure. As expected, postnatal administration of indomethacin can rescue *Hpgd* KO animals by inhibiting prostaglandin synthesis and allowing PDA closure. Infants with mutations in the *HGPD* gene have multiple phenotypes, including PDA (427) (**Table S2**).

Slco2a1 KO: For PGDH to oxidize circulating prostaglandins, they must be internalized by the prostaglandin transporter (PGT) encoded by the *Slco2a1* gene. PGT is expressed with PGDH in the neonatal lung where it facilitates DA closure through reducing serum PGE_2 (428, 429). *Slco2a1* KO mice are born in a Mendelian ratio but die shortly after birth with PDA and associated CHF (**Figure 1D**) (430). *Slco2a1* hypomorphs survive a day longer, also dying with PDA. Histology of KO animals shows no differences in SMC composition or intimal thickening compared to WT. Similar to *Hpgd* KO mice, both *Slco2a1* KO and *Slco2a1* hypomorphs can be rescued with neonatal indomethacin. Mutations in the human *SLOC2A1* gene result in autosomal recessive hypertrophic osteoarthropathy and PDA in infants (**Table S2**) (430, 431).

Smooth Muscle Cell Specific:

Myocd KO: Myocardin is regarded as a master regulator of cardiac and SMC genes. Myocardin, encoded by the *Mycod* gene, is a transcriptional coactivator of serum response factor (SRF) providing for the spatiotemporal expression of genes critical to cardiac and SMC cell fate (432, 433). Whereas global constitutive *Myocd* KO mice die prior to E10.5, mice with neural crest -selective deletion survive to term but die before P3 with PDA **(Fig.1E)** (111). *Myocd* KO DA tissue was deficient mature SMC markers such as *Acta2*, *Myh11*, and *Tagln*. These findings emphasize the importance of NC derivatives in DA formation and function.

Ctnnb1 KO: Beta catenin is a cell-cell adhesion protein and signal transducer for the Wnt pathway encoded by the *Ctnnb1* gene. Wnt signaling is key for many developmental processes, including the differentiation of vagal neural crest cells (VNCCs) which give rise to the SMCs of the DA (15, 434). Mice expressing constitutively-activated Beta catenin (*Ctnnb1Δex3*) were used to explore VNCCs' role in establishing DA cell populations. These results confirmed that DA SMCs derive from 3 populations, the non-pigmented non-VNCC derived SMC1 (80-90%), the non-pigmented VNCC-derived population SMC2 (10-20%), and a very small number of pigmented VNCC-derived melanoblasts (less than 1%) (435). *Ctnnb1Δex3* mice exhibited shifts in cell population, with virtually all SMC2 cells replaced by melanoblasts and the SMC1 population unaffected. This shift was associated with PDA **(Fig.1F)**. These findings suggest the Wnt-driven phenotype of DA SMCs is key to proper formation and closure.

Myh11 KO: The DA is a muscular artery with tone controlled by the constriction and relaxation of VSMCs. VSMC activity is driven by the contractile apparatus, comprised of specific actins, myosin heavy chains, and myosin light chains responsible for different phases of contraction. Smooth muscle myosin heavy chain 11 (*Myh11*) and other SMC genes are precociously expressed in DA SMCs compared to surrounding vessels (3, 436). *Myh11* KO mice have delayed DA closure, taking 6hrs instead of 3hrs to close, and die as neonates unless their bladders are manually relieved (**Figure 1G**) (437). Interestingly PDA is not the cause of death though the left ventricle experiences hemodynamic overload similar to other models. While the DA was not assessed, isometric force measurements from KO bladder tissue suggest muscle phenotypes, including delayed DA closure, may result from the loss of the transient high-force phase 1 contraction in the KO. The sustained phase 2 contraction was unaffected and may explain the eventual DA closure (437). Infants with monoallelic mutations in *MYH11* can suffer both familial thoracic aortic aneurysm and PDA (**Table S2**) (438), and MYH11 R712Q mutation causes diminished myosin motor elasticity (439).

Developmental Signaling:

Jag1 SMC Conditional KO: JAG1 is a cell surface ligand which binds Notch pathway receptors activating their downstream gene regulatory actions. Notch provides signaling between neighboring cells key for the proliferation, differentiation, and movement necessary for development and maintenance of the body (440). *Jag1* expression is normally limited to the endothelium but is found throughout the medial wall in mouse DAs. Interestingly, endothelial-specific deletion of *Jag1* resulted in embryonic death (~e10.5) with hemorrhages, vascular remodeling and SMC differentiation defects (440). Subsequent studies of SMC conditional *Jag1* KO mice revealed PDA and outflow tract defects (**Figure 1H**). Immunofluorescent

staining revealed decreased expression of mature SMC markers throughout the media of outflow tracts, with only SMCs contacting the endothelium appropriately differentiated. These findings suggest *Jag1*-driven Notch signaling is key to the synthetic-contractile fate of SMCs in the DA and outflow tracts. Further, SMC expression of *Jag1* seems key to the lateral transduction of differentiation signals from the endothelium. This signaling behavior is suggested to be unique to the DA and descending aorta. The PDA phenotype could be partially rescued with indomethacin within 12hrs after birth. Infants with *JAG1* mutations can suffer CHD, tetralogy of Fallot, and the more general Alagille syndrome, all associated with PDA (**Table S2**) (441).

Notch2 KO/Notch3 Het: Notch receptors (1-4) detect surface ligands such as Jag1 on neighboring cells and drive nuclear localization. NOTCH2 and NOTCH3 are the predominant Notch receptors in the vasculature, NOTCH2 being more globally expressed. While deletion of either receptor results in vascular defects, those associated with *Notch2* are considerably more severe (442). *Notch2* KO mice have a partial phenotype, with ~40% dying postnatally with PDA (**Figure 1I**). Interestingly, $Notch2^{-/-};Notch3^{+/-}$ mice all die with PDA. $Notch2^{-/-};Notch3^{+/-}$ mice also have dilated aortic segments and decreased medial expression of mature SMC markers. These data are consistent with the known role of Notch signaling in mature SMC differentiation. $Notch2^{+/-};Notch3^{-/-}$ animals showed no PDA phenotype or neonatal death, indicating *Notch2* may be more critical for SMC differentiation in the DA. Infants with monoallelic NOTCH2 and NOTCH3 mutations may suffer from Hajdu-Cheney syndrome (443) and Lateral Meningocele syndrome (444) respectively, both associated with PDA (**Table S2**).

Rbpj SMC Conditional KO: The recombinant signal binding protein for immunoglobulin κ J region (*Rbpj*) is a key downstream transcriptional regulator of the Notch pathway. RBPJ acts as a repressor of gene expression but becomes an activator when bound to a Notch protein. Following their work on the *Jag1* KO PDA, Gridley and colleagues created SMC-specific conditional *Rbpj* KO mice using the same *Tagln-cre* driver as their previous model (445). As expected, the SMC-specific *Rpbj* KO mice die neonatally with PDA and decreased expression of mature SMC markers in the DA media (**Figure 1J**) (446). Interestingly, whereas *Jag1* KO mice could be rescued with neonatal indomethacin, only 1 of 9 *Rbpj* KO animals were rescued. This stronger phenotype indicates there may be other Notch ligands which contribute to the eventual activation of RPBJ and mature SMC differentiation.

Gdf2 KO anti-Bmp10: Bone morphogenetic proteins (BMPs) are members of the transforming growth factor beta (TGFβ) superfamily and play key roles in guiding tissue architecture throughout the body. BMP9 and BMP10 have both been shown to bind the activin receptor-like kinase 1 (ALK1) on the endothelium of blood vessels, suggesting a role in vascular disease (417). *Bmp10* KO (BMP10) mice die with cardiac defects in mid-gestation, while *Gdf2* KO (BMP9) mice are viable (417). Interestingly, while the *Gdf2* KO DA is occluded enough to prevent flow at P5, its lumen is not completely filled with intimal cells, such as the WT, and red blood cells can be observed. This phenotype is exacerbated by the administration of a neutralizing anti-BMP10 antibody on P1 and P3. *Gdf2* KO anti-BMP10-treated mice achieve temporary DA constriction on P0 and P3, indistinguishable from WT, but show a partially patent lumen at P5 lined with endothelial cells, red blood cells, and an island of intimal cells (**Figure 1K**). These findings were not observed with anti-BMP10 treatment of WT animals, or at later time points (P3, P5), suggesting a narrow window when BMP function is critical for

fibromuscular transformation of the DA into the LA. Recombinant BMP9 and BMP10 were found to increase expression of *Ptgs2* and *Has2* mRNA, which encodes HAS, where hyaluronic acid is a key component for matrix deposition and cell movement. Further, at P3, *Gdf2* KO anti-BMP10 treated mice lacked the matrix deposition key to DA fibrosis and *ligmentum arteriosum* formation. Thus, *Gdf2* KO anti-BMP10-treated mice are one of the few mouse models with abnormalities in the second, anatomical closure phase of permanent DA remodeling.

Gpc3 KO: Glypican-3 (*Gpc3*) is a heparan sulfate proteoglycan (HSPG) which plays a key role in cardiac development. Glypicans attach themselves to cell surfaces through glycophosphatydilinositol linkages, where they bind and modify various ligands, modulating cell signaling. Previous studies suggest that *Gpc3* specifically may interact with BMP, Hedgehog, Wnt, and fibroblast growth factor (FGF) signaling pathways (447) and is widely expressed throughout vertebrate development. However, human loss-of-function *GPC3* mutations result in a rare congenital overgrowth syndrome associated with CHD; Simpson-Golabi-Behmel Syndrome (SGBS). Similarly, when *Gpc3* KO mice were examined, they were found to have multiple defects, including PDA. While *Gpc3* KO mutants exhibited a delay in coronary vascular plexus formation and subsequent reduction in sonic hedgehog mRNA expression consistent with GPC3 acting as a co-receptor for FGF9, it is unclear whether these signaling disruptions could contribute to a PDA phenotype, or even whether the PDA observation in this model is biologically significant. *Gpc3*'s association with both BMP and Wnt signaling family members and the presence of a PDA phenotype in infants suffering SGBS (448), provide plausibility that *Gpc3* plays a role in DA function (**Table S2**).

Transcription:

Tfap2b KO: The importance of the transcription factor AP2 beta (*TFAP2b*) in DA function was first observed in human clinical populations. Mutations in *TFAP2b* lead to Char syndrome, a neural crest disorder associated with craniofacial abnormalities and PDA (104, 387, 391). Similarly, single nucleotide polymorphisms/mutations in *TFAP2b* are associated with non-syndromic PDA (390, 392). Subsequently, a *Tfap2b* KO mouse model revealed kidney disorders, delayed closure of the DA, and neonatal death (**Figure 1L**) (449). These findings were corroborated by a recent CRISPR (clustered regularly interspaced short palindromic repeats) derived *Tfap2b* KO. *In situ* hybridization revealed that *Tfap2b* specifically labels DA SMCs with tight borders until E18.5 (450). Interestingly the vessel wall of *Tfap2b* KO DAs showed no significant changes in morphology or elastin deposition, but *in situ* hybridization revealed a significant decrease in calponin, a robust marker of mature SMCs at E18.5 (402). KO animals were also found to have decreased expression of *Hif2a* and *Et-1* suggesting a *Tfap2b*-driven signaling cascade which plays a key role in DA O_2 sensing mechanisms at birth (**Table S2**) (402).

Foxc1 KO: Mesenchymal forkhead 1 (MFH1 or FOXC2) and mesodermal/mesenchymal forkhead 1 (MF1 or FOXC1) are both forkhead family transcription factors which share a nearly identical DNA binding domain as well as overlapping embryonic expression in the paraxial mesoderm, mesenchyme and endothelium of the branchial arches. MFH1 and MF1 KO mice die prenatally and perinatally with a spectrum of cardiovascular and skeletal defects (451, 452). Interestingly, when *Mfh1*$^{tm1+/-}$ *and Mf1*$^{lacZ+/-}$ mice are crossed to obtain *Mfh1*$^{tm1+/-}$*;Mf1*$^{lacZ+/-}$ double heterozygotes, nonallelic noncomplementation leads to a similar spectrum of cardiovascular defects including PDA (**Figure 1M**) (452) accompanied by prenatal and

perinatal death. While PDA was not detected in *Mfh1* KO mice, it was detected in *Mf1* KO mice. Sectioning of *Mf1* KO mice at D10.5 revealed fully formed and symmetrical aortic arches, indicating that *MF1* expression is not required for aortic arch formation. *Mf1* and *Mfh1* are thought to mediate signaling between the endothelium of the intima and the neural crest-derived mesenchyme of the media, likely related to cell fate determinations. It makes sense that *MF1* expression decreases in the DA following closure, as both of these populations die out. Infants with mutations in *FOXC1* may suffer Axenfeld-Rieger syndrome (453) which is associated with PDA (**Table S2**).

Matr3 KO: Matrin3 is a nuclear matrix protein that is associated with distal myopathy 2, including vocal cord and pharyngeal muscle weakness. Genetic examination of a novel proband exhibiting developmental delay and cardiovascular defects including PDA revealed mutations in both *AHDC1* and Matrin 3 (*MATR3*). While the *AHDC1* mutation is likely the source of developmental delay, creation of a genetrap construct in exon 13 of the mouse *Matr3* gene revealed a key role for *Matr3* in cardiovascular development (454). Homozygous $Matr3^{Gt\text{-}ex13}$ mice show early embryonic death (most by 4.5dpc, all by 8.5dpc). $Matr3^{Gt\text{-}ex13}$ heterozygotes showed a spectrum of cardiovascular defects similar to the human proband including PDA in 12% of heterozygotes (**Figure 1N**). Immunohistochemistry showed localization of *Matr3* in both the SMCs and endothelial cells of the large arteries. These data, considered with Matr3's proposed role in stabilizing select mRNAs, indicate a key role in the proper development of the outflow tracts. Infants with mutations in *MATR3* suffer from various phenotypes, including PDA (**Table S2**) (454).

Hand2 trisomy; Rim4 mouse: The human disorder 4q+ is a syndrome resulting from a triplicated region of the human chromosome 4. 4q+ results in varied phenotypes including delays in growth and cognition, physical deformities and CHD including PDA. Interestingly, a mouse model with an analogous trisomy mutation, the recombinant-induced mutation 4 (Rim4) mouse was discovered allowing studies into which genes might be responsible. Rim4 heterozygous mice and 4q+ humans are both trisomic for the heart and neural crest derivatives-expressed protein 2 (*Hand2*) gene, which codes a member of the basic helix-loop-helix family of transcription factors associated with cardiovascular development and defects. Rim4 mice are generally unwell with 80% of those on a C57Bl/10J background dying neonatally. Additionally, these mice were found to have PDA amongst other deformities (**Figure 1O**) (455). Interestingly, these symptoms were ameliorated when Rim4 mice were crossed with a *Hand2* KO line to correct the genomic dosage of *Hand2*. *Hand2* was generally found to be necessary for proper formation of the ventricles and outflow tracts, consistent with its involvement with neural crest cells, though a mechanism of action is unknown.

Matrix/ Cytoskeleton:

Lox KO: ECM composition is critical for establishing both the mechanical properties and cell identity of blood vessels. *Lox* encodes an enzyme responsible for the crosslinking of elastin and collagen, as well as influencing proliferation and cell fate. *Lox* KO mice are born with abnormally formed outflow tracts, thoracic aortic aneurysm and dissection (TAAD) and die as neonates with ruptured diaphragms, impaired airways, and PDA (22%) (**Figure 1P**) (418). Closer examination of the ascending and descending aortas indicated disrupted elastin fiber formation and region-specific changes in biomechanical properties. Regional changes in

expression of ECM, MMPs, and SMC cell cycle genes within the ascending and descending aorta suggest Lox-mediated matrix crosslinking plays a critical role in DA development and function.

Ilk KO: Integrin-linked kinase (ILK) is a protein which localizes to the integrins of the membrane-associated dense plaques, where it uses its kinase domain to foster downstream signal transduction in response to force transduction signals between the contractile apparatus and ECM. ILK is critical for both polarization of the epiblast and vasculogenesis, resulting in embryonic lethality for *Ilk* KO and endothelial-specific *Ilk* KO mice (456). To investigate lLK's role in vascular signal transduction, SMC-specific *Ilk* KO mice were created (*Sm22-cre*$^{+}$;*Ilk*$^{Fl/Fl}$) which showed extremely dilated thoracic aortic aneurysms (up to 50% of the thorax) and PDA with associated perinatal lethality (**Figure 1Q**) (456). Histological analysis revealed disruptions in the normal spindle-like morphology and circumferential orientation of VSMCs and ablation of the elastin layers characteristic of elastic arteries. Morphogenic changes in outflow tract anatomy could be detected by e12.5. Notably, other neural crest-associated defects were not observed. Immunohistochemical labeling for mature SMC-specific markers indicated a loss in contractile SMC phenotype in the *Sm22-cre*$^{+}$;*Ilk*$^{Fl/Fl}$ KO vessels. Together these data suggest a critical role for *Ilk* in proper outflow tract development.

Itgα5 and Itgαv KOs: Integrins are heterodimeric cell adhesion receptors which mediate responses to ECM ligands. Integrins α5 and αv are the primary receptors for fibronectin and support angiogenesis by allowing endothelial cells to assess their environment. KOs of fibronectin and various integrins result in embryonic lethality, β1 integrin KOs being preimplantation lethal. Interestingly only endothelial-specific KO of *Itgα5* and *Itgαv* produced

severe outflow tract defects. While only 4% of *Itgα5*$^{-/-}$;*Itgαv*$^{-/-}$ animals survived to adulthood one adult displayed PDA. Subsequently, PDA was discovered in several *Itgα5*$^{-/-}$;*Itgαv*$^{+/-}$ animals of mixed genetic background (**Figure 1R**) (457). Of the *Tie2-cre*$^{+}$;*Itgα5*$^{flox/flox}$ WT mice examined at 10-20 weeks, 9/10 had PDA and half succumbed before weaning. Interestingly, these mice were on a C57BL/6 N7 background, whereas *Tie2-cre*$^{+}$;*Itgα5*$^{flox/-}$ mice on a 129S4:C57BL/6 background, lacked PDA. This suggests strain specific modifiers modulate DA phenotypes. Additionally, PDA afflicted adult mice of 10-20 weeks but may also contribute to premature loss of littermates. This suggests the loss of *Itgα5* may result in PDAs of varying severity, some hemodynamically tolerable. This discrepancy may result from background modifiers.

<u>*Fbln1 KO:*</u> Fibulin-1 (FBLN1) is a glycoprotein which binds ECM proteins and participates in directed cell migration during development. Interestingly, *Fbln1* upregulation is reported in rat DA following EP_4 stimulation. *Ptger4* KO mice also have decreased *Fbln1* expression, suggesting EP_4 stimulation may guide *Fbln1* expression. Further, when *Fbln1* KO mice were generated, 7/7 pups showed PDA 6h after birth with complete closure in controls (**Figure 1S**) (458). *Fbln1* KO mice also had decreased intimal thickening, where VSMCs migrate through the IEL into the sub-endothelial space, facilitating DA closure. Thus, disruption of VSMC migration in the *Fbln1* KO DA and potentially the *Ptger4* KO DA may contribute to PDA.

Chromatin:

<u>*Smarca4 KO:*</u> Brahma (BRM), and Brahma-related gene 1 (BRG1; encoded by the *Smarca4* gene) are members of the SWI/SNF complex, an ATP-dependent chromatin remodeling complex thought to play a role in SMC differentiation. While global *Smarca4* KO mice die around implantation, SMC-specific *Smarca4* KO mice revealed ventricular septal defect and

PDA (33% of offspring) resulting in CHF and neonatal death (**Figure 1T**) (459). While *Smarca4*$^{+/-}$ offspring also show PDA (10%), possession of functional *Brm* alleles appears to be protective. Mature SMC gene expression was also lost in the GI tract and bladder. These data support independent roles for *Smarca4* and *Brm* in the differentiation of SMCs relevant for DA function.

Asxl2 KO: The Additional Sex Combs Like 2 (*Asxl2*) gene encodes a putative polycomb group protein likely responsible for maintaining epigenetic gene repression through complex assembly. The exact mechanisms are debated (460). All three ASXL proteins (1, 2, and 3) are expressed in the outflow tracts, ASXL2 being the most enriched. *Asxl2* KO mice in a C57BL/6 background die neonatally with PDA and severe cyanosis (98.2%), and other CHD (22%) (**Figure 1U**) (461). Despite PDA, histology of WT and KO tissues were indistinguishable, suggesting *Asxl2*'s role in DA closure is nonstructural. Interestingly, *Asxl2* KO mice on a mixed C57BL/6;129Sv genetic background lacked PDA and neonatal death, highlighting the strain-dependence of PDA.

Platelet Aggregation:

Itga2b KO: Platelet aggregation is thought to support DA occlusion due to remodeling of endothelial and subendothelial SMCs during permanent DA closure. Disrupted endothelial surfaces provide access to collagen and therefore binding surfaces for activated platelets. The integrin alpha 2b (*Itga2b*) gene encodes a preprotein which is processed to create subunits for the integrin alpha 2b/beta 3 receptor which contributes to platelet aggregation. Interestingly, 31% of *Itga2b* KO mice showed PDA 12h post-delivery (**Figure 1V**) (462). *Itga2b* KO mice also

exhibited a 26% reduction in luminal platelet accumulation neonatally. This decrease seems to disrupt either the thrombotic occlusion of the DA or platelet-derived signaling involved in permanent closure.

Nfe2 KO: The nuclear factor erythroid 2 (*Nfe2*) gene encodes an essential component of the NF-E2 protein complex which regulates megakaryocyte differentiation and subsequently, platelet production. Similar to *Itga2b* KO, *Nfe2* KO mice present with PDA 12hrs after delivery, though more frequently (70%), with 100% closure amongst WT littermates (**Figure 1W**) (462). *Nfe2* KO mice also had reduced platelet accumulation in the neonatal DA and decreased luminal proliferation. The *Nfe2* KO PDA was unresponsive to indomethacin, further complicating prostaglandin's role in DA closure. Together, the *Itga2b* KO and *Nfe2* KO models suggest a role for platelet aggregation in murine DA closure. While studies of platelets and DA closure in mice are limited, extensive clinical research has had mixed findings in humans. Several studies found associations between thrombocytopenia and PDA outcomes (462, 463) or treatment failure (464). Others suggest thrombocytopenia does not contribute to PDA (465), is not associated with an increased incidence of PDA (466, 467), and that transfusions of platelets have no effect on PDA closure (468).

Mouse Models of Premature DA Closure:

Ntf3 KO: Neurotrophin 3 (*Nt3*) is a neuronal growth factor which activates the receptor tyrosine kinase TRKC, supporting survival and differentiation. Interestingly, *TrkC* is expressed in the non-neuronal tissues of the heart and outflow tracts, as well as neural cresy cells, suggesting *Nt3* may contribute to cardiovascular development. *Nt3* KO animals show variable

but severe CHD (469). Interestingly, all *Nt3* KO animals show premature closure of the DA *in utero*. While mechanisms are unknown, this is likely related to changes in survival or differentiation of the DA's neural crest-derived population.

Gja5 KO; Gja1 Heterozygous: Gap junctions like connexins 40 (CX40/ *Gja5*) and 43 (CX43/ *Gja1*) contribute to cardiac conduction by facilitating electrical coupling through the movement of ions. While CX40 and CX43 serve similar functions, they vary in expression and are differentially dispensable for cardiac formation and survival, with *Gja1* KO being nonviable (470, 471). Interestingly, crossing *Gja5* and *Gja1* KO lines indicates additive effects of connexin deficiency on cardiac conduction (471). The $Gja5^{-/-};Gja1^{+/-}$ offspring are particularly interesting, as they are nonviable and show premature constriction of the DA at e18.5, in conjunction with severe CHD.

Pharmacological Models in Mice:

In addition to genetic models, pharmacological models which stimulate or inhibit particular pathways have proven valuable for interrogating PDA. An example is the use of the selective COX-1 and COX-2 inhibitors. Prolonged treatment of dams with COX-1 and COX-2 inhibitors during late gestation (D15-D18) leads to PDA whereas acute treatment in term animals (D19) results in constriction (195-197). Mid-gestational (D11-D15) treatment produced no phenotype (196). These results support clinical findings of PDA following administration of COX inhibitors as tocolytics for women in preterm labor (47, 187, 188), and further suggest the existence of a prostaglandin-mediated developmental program during gestational maturation.

Aminoglycoside antibiotics (gentamicin) (61) and certain antacids which inhibit cytochrome P450 enzymes (cimetidine) (66) also cause PDA in mice. A recent cohort study confirmed the role of gentamicin in human PDA (472) and cimetidine studies originated from human clinical observations (65, 66). Antibiotics, antacids, and COX inhibitors are routinely used in the treatment of pregnant women and neonates emphasizing the utility of these animal models. Pharmacologic models also exist in other rodents, where vasodilatory mediators (PGE_2, atrial natriuretic peptide, $MgSO_4$, furosemide, phosphodiesterase 3 antagonists, endothelin receptor antagonists) or environmental perturbations (hypothermia, hypoxia, copper deficiency, LPS-induced inflammation) result in PDA.

PDA in Human Genetic Syndromes:

Human PDA has a complicated and multi-factorial genetic etiology (379). PDA likely exists as two overlapping disorders, with preterm PDA arising from prematurity, and term PDA from genetic alterations. Further, PDA exists in syndromic and non-syndromic forms, the former being more common in term PDA (473). A genetic basis for PDA is supported by: 1) higher concordance rates of PDA in monozygotic versus dizygotic twins, 2) familial PDA with specific chromosomal deletions/mutations, 3) genetic polymorphisms conferring susceptibility to PDA, and 4) human dysmorphic syndromes with PDA and poly- or monogenic inheritance.

To better understand the genes crucial for DA development and function, we searched multiple databases for single-gene syndromes associated with PDA. Using data from OMIM, GeneCards, Human Phenotype Ontology, DisGeNET, FindZebra, GeneReviews and UniProtKB, a pooled list of n=224 human single-gene syndromes associated with PDA was generated (**Table S2**). PDA associations were verified through original sources (PMIDs

provided). Deletion and duplication syndromes resulting in PDA were also compiled (**Table S3**). 224 candidate effectors were assessed for protein-protein interactions (PPI) using STRING V11.0. 148 proteins were identified as part of a high confidence PPI network (**Figure 2**). Use of a blind vote counting strategy between single-gene syndromes and known mouse models revealed n=10 genes associated with PDA in both mice and man (**Figure 3, Table S4**). This list contained several known PDA regulatory genes, including *HPGD*, *MYH11*, *JAG1-NOTCH*, and *TFAP2B.* Due to irregular naming conventions and incomplete information on cross-species orthologues, the molecular function of mouse and human PDA-associated

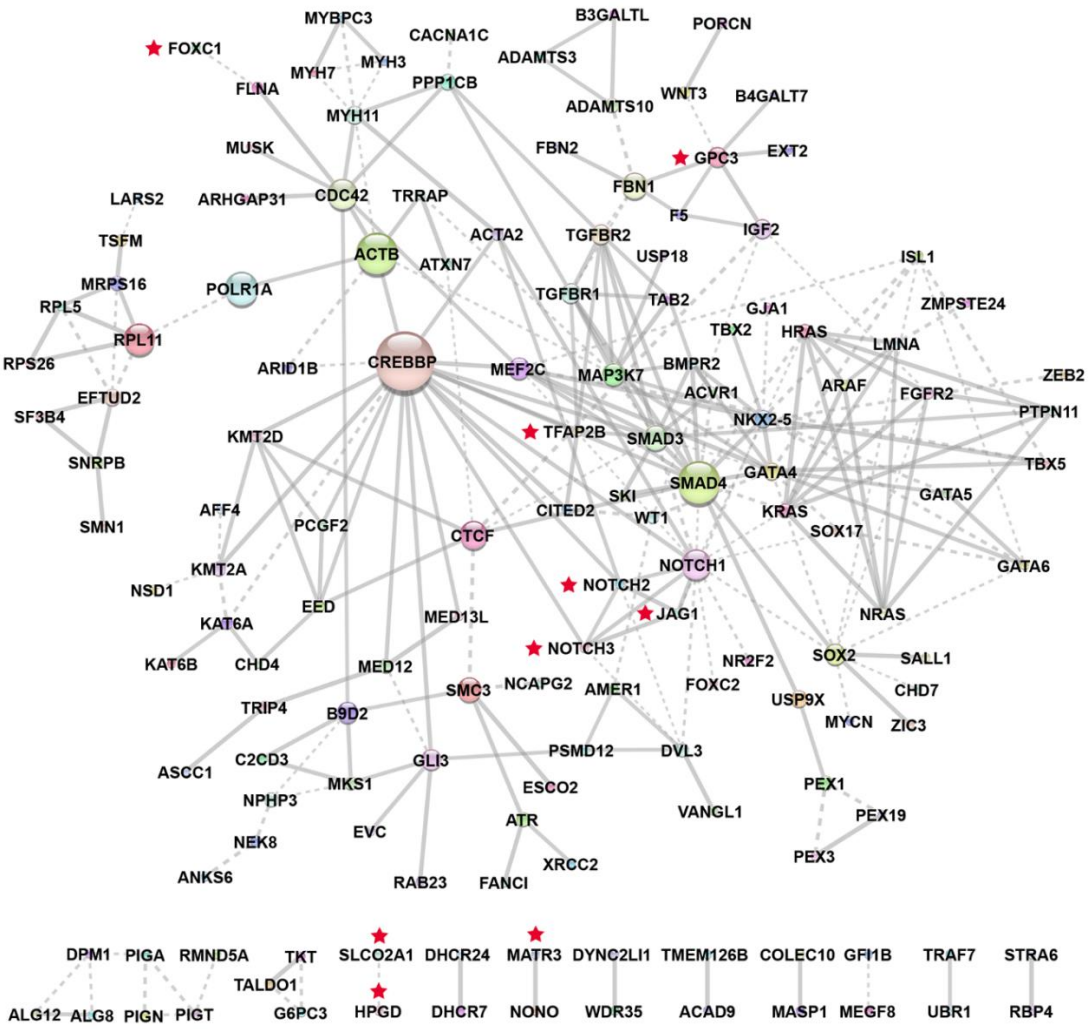

Figure 2. Protein-Protein Interaction (PPI) network of effectors in PDA-associated human single-gene syndromes. Human single-gene syndromes associated with PDA were used to construct a list of 224 potential effectors of DA function. This list was blindly assessed for known and predicted PPI including both direct (physical) and indirect (functional) associations using STRING 11.0. A minimum interaction score of 0.7 was selected representing a high confidence interval. The resulting network contains 219 proteins (nodes) and 256 interactions (edges) with a PPI enrichment P-value of less than 1.0e-16. 71 proteins were removed, as they lacked high confidence interactions. Edge thickness represents the confidence score of the PPI. Red stars indicate proteins with associated mouse models of PDA.

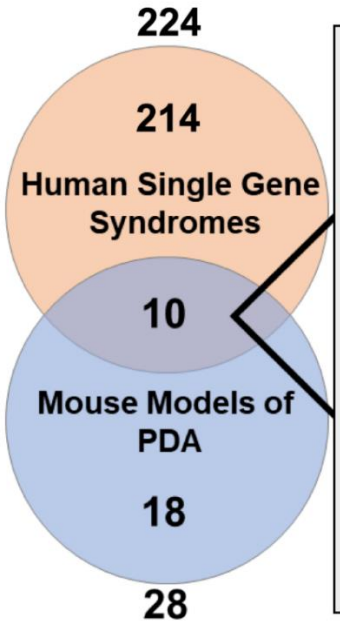

Gene	Phenotype	Phenotype MIM number	PMID
FOXC1	Axenfeld-Rieger syndrome, type 3	602482	11343302
GPC3	Simpson-Golabi-Behmel syndrome, type 1	312870	20950395
HPGD	Hypertrophic osteoarthropathy, primary, autosomal recessive 1	259100	18500342
	Digital clubbing, isolated congenital	119900	9402870
	Cranioosteoarthropathy	259100	
JAG1	Tetralogy of Fallot	187500	9410541
	Alagille syndrome 1	118450	
	?Deafness, congenital heart defects, and posterior embryotoxon	617992	
MATR3	Developmental delay, left ventricular outflow tract defects, bicuspid aortic valve, coarctation of the aorta, PDA		25574029
MYH11	Aortic aneurysm, familial thoracic 4	132900	11249915
NOTCH2	Hajdu-Cheney syndrome	102500	8723560
NOTCH3	Lateral meningocele syndrome	130720	25394726
SLCO2A1	Hypertrophic osteoarthropathy, primary, autosomal recessive 2	614441	22197487
			20083684
TFAP2B	Patent ductus arteriosus 2	617035	18752453
	Char syndrome	169100	8326495

Figure 3. Overlap of mouse models of PDA with associated human single-gene syndromes. 10 of the 28 identified mouse models of PDA were found to have correlates in the compiled list of 224 human single-gene syndromes with PDA. The full table of human single-gene syndromes with PDA is shown in **Table S4**.

genes were compared. For top molecular function categories, 9/20 were common between mouse and human, suggesting higher levels of concordance than by gene name alone. A curated list of n=41 human single-gene syndromes consistently associated with PDA was derived from the GeneReviews database, to gauge the frequency of PDA in each syndrome (**Table 1**). Collectively, these data reveal similarities in the genetic landscape of PDA in mice and humans and identify pathways key for regulation of fetal DA patency and postnatal closure.

Discussion:

PDA is a clinically relevant disorder of impaired circulatory adaptation to newborn life. Despite knowledge of risk factors (39), current PDA treatment options are limited and the decision when or whether to treat remains an ongoing dilemma (474, 475). An understanding of the DA's complex molecular, environmental and genetic regulation would benefit efforts to develop therapies, limit drug exposure, identify patients at risk for drug toxicity or treatment failure, and develop patient-specific pharmacogenomic approaches. *The identification and characterization of a developmental program within the DA would contribute to these goals.* We recently conducted a transcriptomic meta-analysis using published rodent microarrays and human preterm RNAseq data to identify candidate effectors involved in DA development and function (265). Although species and gestation-stage differences of the data limited comparisons, 11 genes were found to be significantly upregulated in the DA compared to the aorta in both rodent and human tissues. Two genes, *PTGER4* and *TFAP2B* have associated mouse models of PDA, supporting the notion that correlation of human single-gene syndromes and rodent models are useful for the study of PDA.

Prostaglandin signaling plays a key role in DA tone. COX-1 and COX-2-derived PGE_2 stimulates DA dilation through EP receptors, chief of which is EP_4.(113, 263, 265) This PGE_2-mediated dilation maintains DA patency throughout late gestation. Upon birth the newly inflated lungs catabolize circulating PGE_2 via HPGD. Decreased circulating PGE_2 and O_2-stimulated constriction lead to the initial muscular DA closure shortly after birth (476). Additional studies implicate the PGE_2-EP_4 axis in remodeling of the fetal DA. EP_4-driven, adenylyl cyclase 6-mediated (147) hyaluronic acid deposition supports the migration of VSMCs from the media, through the IEL, and into the subendothelial space to form intimal cushions, structures potentially key for DA closure in larger animals (146, 213). In addition, EP_4-driven EPAC1 activity promotes VSMC migration into the subendothelial space (477) and an EP_4-mediated inhibition in elastogenesis and LOX expression contributes to remodeling (213, 396). Four mouse models of PDA target key prostaglandin signaling genes, highlighting this pathway's significance for DA development and function. Of note, disruption of the prostaglandin pathway during late- but not mid-gestation, in mice or humans, results in PDA, not premature constriction, contrary to expectations for the removal of a dilatory stimulus. *This suggests a developmental programming role for the PGE_2-EP_4 axis which warrants further investigation.*

Monoallelic mutations in *TFAP2B* are associated with both Char syndrome-associated PDA (104, 387, 391) and single nucleotide mutation-based nonsyndromic PDA (390, 392). TFAP2B likely regulates proliferation and differentiation during DA development, though the lack of defined downstream pathways and KO phenotypes make this difficult to assess. *Tfap2b* expression is required for expression of hypoxia inducible factor 2a (*Hif2a*) and endothelin-1 (*Et-1*). *Tfap2b* KO animals also show decreased maturity in DA SMCs. Notably, *Tfap2b* is highly enriched in the DA vs. Ao and was found significant by every rodent microarray in which

it was assessed (265). TFAP2B's role in the differentiation of DA SMCs via HIF2A, ET-1, and other downstream effectors requires further investigation to fully understand its contribution to DA development and function.

Currently, animal models are the primary means for studying DA regulatory mechanisms. Due to their well-defined genetic composition, manageable size, short life span, ease of breeding, and litter size, mice are perhaps the most widely used of these models. To determine whether PDA-associated genes in KO mice relate to human disease, we used online genetic databases to compile a comprehensive list of 224 single-gene syndromes (**Table S2**) as well as 14 chromosomal deletions, duplications, or additions associated with PDA (**Table S3**). Of these 224 candidate effectors, 148 proteins were found to have high confidence PPI (**Figure 2**) suggesting these proteins may function as a coordinated network to regulate DA function. Several syndromes with associated mouse models such as Char syndrome (*TFAP2B*) and Alagille syndrome (*JAG1*) have well-known associations with PDA. Conversely, *HPGD* and *NOTCH* genes (2 and 3) are more associated with PDA in mice. Only 10/28 known mouse models of PDA have human syndrome correlates (**Figure 3**), but 9 of those correlates showed high confidence PPI in our interaction network (**Figure 2**). Interspecies gene comparison is complicated by irregular naming conventions and orthologue conservation which prevents direct comparisons. However, using functional annotation tools, we observed notable overlap between mouse models and human PDA syndromes in GO Biological Process (41.6%) (**Figure 4**), GO Cellular Component (37.5%), GO Molecular Function (48.0%), KEGG (66.7%), and UP Keywords (37.9%) (**Table S5**). While strong matches in GO Biological Process terms associated with heart and vascular development,

patterning, or morphogenesis were expected, the number of GO terms related to RNA and DNA regulation coupled with ‘nucleoplasm’ and ‘nucleus’ lend more support to the idea that DA closure is a conserved, developmentally programmed event.

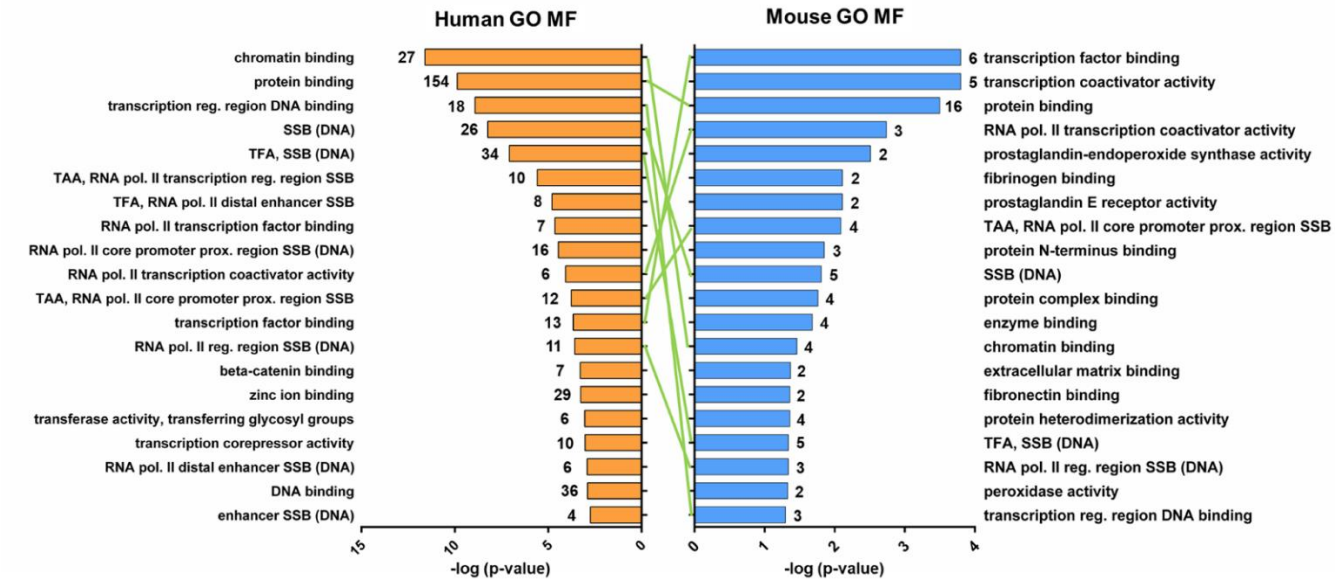

Figure 4. 'Tornadogram' of top 20 GO Molecular Function (MF) terms common between known mouse models of PDA and human single-gene syndromes with PDA. Genes known to be associated with PDA in mouse models (blue) and genes associated with PDA single-gene syndromes in humans (orange) were categorized by GO MF (DAVID), plotted by p-value, and compared across platforms. The number of genes represented in each category is displayed at the end of each bar. Like terms (n=9) are connected by green lines.

Although concordance between mouse and human PDA-associated genes was modest (10/28) (**Table S4**), clinical data suggests the 18 non-correlated mouse models may prove informative for human PDA (**Figure 5**). For example, while no known *PTGS* (1 or 2) or *PTGER4* mutations are associated with human PDA, pharmacologic inhibition of COX enzymes *in utero* is linked to PDA in newborns (47, 187-189, 478). Similarly, while mutations of platelet genes *Itga2b* and *Nfe2* confer PDA in mice but not humans, thrombocytopenia and various platelet indices correlate with PDA in preterm infants (462, 479). Information from some mouse models is even contradictory. While compound mutations in mouse *Gja5*;*Gja1* gap junction genes result in premature DA constriction, humans with *GJA1* mutations have PDA. Despite inconsistencies, deeper examination of candidate genes from mouse models will likely be informative for human PDA.

Our strategy comparing mouse KO models to human single-gene syndromes with PDA has limitations. PDA may be polygenic or occur through epigenetic misregulation. Our search focused on coding region mutations of single genes but recent cardiovascular genetic studies suggest noncoding *de novo* variants may be important for CHD (480). PDA might also be secondary, resulting from the abnormal hemodynamics of complex CHD. Although enumerable human disorders have been modeled with KO mice, genetic dissimilarities exist in DA development between mice and humans (265). Screening strategies based on KO genes may overlook other single-gene regulatory mechanisms. For example, Cantú syndrome patients, frequently affected by PDA, have monoallelic *activating* mutations in *ABCC9* or *KCNJ8* which form K_{ATP} channels. Mouse models mimicking constitutive activation of *Abcc9* and *Kcnj8* have not been evaluated for PDA, although pharmacologic studies in mice correlate to the Cantú PDA phenotype (481). In other cases, a genetically-defined PDA phenotype in humans may be

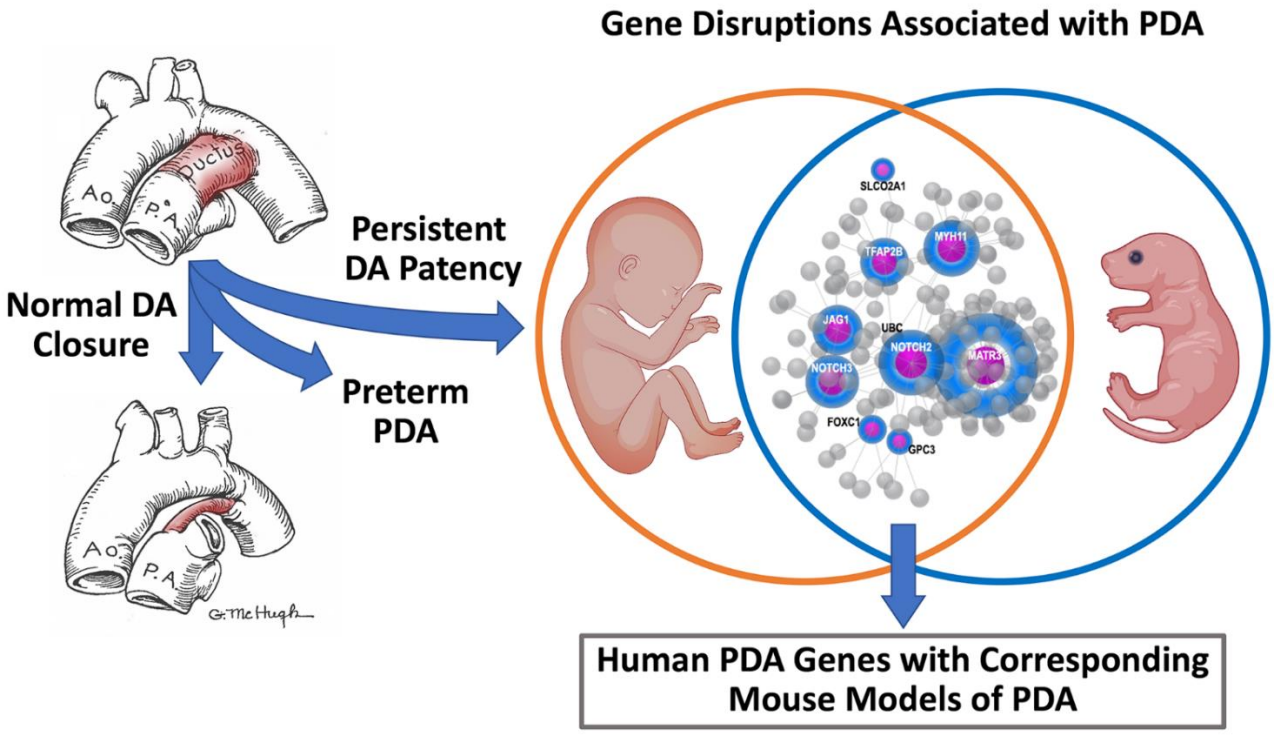

Figure 5. Graphical Abstract. Failure of normal ductus arteriosus (DA) closure occurs in both term and preterm infants. Persistent DA patency and preterm PDA can be assessed in mice through genetic models of PDA and in humans through single gene syndromes associated with PDA. Genes represented in both sets are relevant for human health.

overlooked in mice. *TBX1* mutations associated with 22q11 deletions and DiGeorge or Velocardiofacial syndrome correlate with PDA. However, DA patency was not assessed in *Tbx1* KO mice despite the cyanosis and neonatal lethality common in mouse models of PDA (482). Of the 214 human single-gene syndromes which lack a corresponding mouse PDA model, 68 genes display embryonic lethality when deleted in mice and an additional 61 genes lack mouse models altogether. More importantly, mice with targeted deletion of one of 26 genes corresponding to a human single-gene syndrome exhibit neonatal lethality, consistent with PDA, however their DA status was not reported. We also recognize that compensation for genetic mutations is species-specific and genotype-phenotype correlations may vary in mice and humans. For example, several mouse models lack PDA despite a corresponding human single-gene syndrome with PDA, including ACTA2 (483), MKKS (484), SLC25A24 (485) and others. Furthermore, KO mice created to study PDA sometimes lack a phenotype, including KOs for endothelin ET-A receptor (366), cytochrome P450 enzyme Cyp3a (364), PGE synthetic enzyme mPGES1 (486), Prx1 and Prx2 homeobox genes (487), and others. Our comparisons may also suffer from the limiting nature of database searches. OMIM and other resources are not constantly curated, leading to possible omissions of human single gene syndromes associated with PDA that are too recent for inclusion, precluding an exhaustive compendium.

Our focus on KO mice is also complicated by strain-selective modifiers which alter penetrance or severity of some cardiovascular phenotypes (488), possibly including PDA. Further, 4/ 28 mouse models of PDA had decreased phenotype severity on different backgrounds (*Ptger4* KO*, Itgα5*$^{-/-}$*;Itgαv*$^{+/-}$*, Hand2* KO *, and Asxl2* KO). For unknown reasons, mice on C57Bl/6 backgrounds seem particularly susceptible to PDA phenotypes (**Table S1**). Lack of reporting for sub-strains within the original mouse model publications further

complicates this picture. Many KO mice are never outcrossed to wholly different backgrounds, concealing potential PDA phenotypes. Finally, our comparison of mouse KO models to human single-gene syndromes does not separate isolated PDA from PDA coexisting with complex CHD since our goal was a broad-based and inclusive screen.

In addition to single-gene syndromes, single nucleotide polymorphisms (SNPs) and single-gene variants can indicate susceptibility to PDA. SNPs in TFAP2B, tumor necrosis factor (TNF) receptor associated factor 1 (TRAF1) (489), Angiotensin II receptor type 1 (AGTR1) (490), elastin (491), methylenetetrahydrofolate reductase (MTHFR) (492) and multiple other genes predispose infants to PDA. In addition, genetic variants in the CYP2C9 enzyme are associated with increased risk of indomethacin treatment failure in preterm neonates (493). SNPs, generally defined as occurring in >1% of the population, and rare variants occurring in <1% of the population certainly contribute to syndromic disorders, though distinctions between these are contentious and vary between populations (494). The involvement of SNPs and variants in PDA is a rapidly evolving field of research (495). While our search for single-gene syndromes did identify several SNPs and rare variants, there is insufficient information to interpret their contributions to DA biology or pharmacogenomics (496) at this time.

In summary, the expanding number of mouse models of PDA, while not a perfect proxy for human vascular development, provide valuable information on vascular transition at birth and much-needed research tools to study the mechanisms of DA development (497). *Mouse models of PDA implicate important gene networks and multiple pathways that may be involved in a developmental program which defines DA identity. The prevalence of prostanoid genes amongst mouse models of PDA further suggests a guiding role for PGE_2-EP_4 in DA*

development. Comparison and functional analyses of mouse and human PDA-associated genes will provide a better understanding of key regulatory steps that may serve as potential therapeutic targets for management of PDA.

Supplemental Tables:

Table S1	Genetic Models of Patent Ductus Arteriosus (PDA) or *in utero* DA Closure in the Mouse (n=28)						
Gene	**Name**	**Year**	**PMID [Ref]**	**Phenotype**	**Secondary Phenotypes**	**Type**	**Background**
Ptger4	Prostanoid receptor EP4	1997	9363893 (108)	PDA and neonatal death	PDA associated pulmonary edema	Global constitutive KO	129/SvEv
		1998	9600059 (109)	PDA and some neonatal death	PDA associated congestion of pulmonary arteries, shrunken disorganized alveolar structure, and dilation of left ventricle and pulmonary arteries	Global constitutive KO	129/Ola + C57BL/6 mixed
		2004	15354288 (110)	PDA and neonatal death	PDA associated congestion of pulmonary arteries	Floxed Mouse	129/SvEvTac + C57BL/6 mixed
Ntf3	Neurotrophin 3	1996	8841198 (469)	Premature DA closure *in utero* and at birth, and neonatal death (100%)	Atrial and ventricular septal defects, tetralogy of Fallot, valvular defects, general cardiac malformations	Global constitutive KO	C57BL/6 + CJ7 mixed
Tfap2b	Transcription factor AP2 beta	1997	9271117 (449)	PDA and neonatal death noted by Gelb (unpublished) Ivey 2008	Polycystic kidney disease which lead to apoptosis of the kidney epithelium	Global Constitutive KO	C57BL/6
		2018	29804851 (450)	Delayed closure of the DA	Renal Malfunction	Global Constitutive KO (CRISPR)	C57Bl/6
Gja5/ Gja1	Connexin 40/ Connexin 43	1999	10969038 (471)	Premature DA closure at E18.5 and neonatal death 100%	All embryos had persisting interventricular foramen, while many had persisting foramen primum and subcutaneous edema	Global constitutive KO	129/Sv + C57BL/6 mixed
Foxc1	Forkhead box C1, Mesenchymal forkhead 1, Mesenchymal/mesodermal forkhead 1	1999	10479458 (452)	PDA and perinatal death	Interruptions and coarctations of the aortic arch, VSDs, valve defects, thin myocardium, prenatal death	Global constitutive double KO	129 x BlackSwiss mixed (451, 498)
Ptgs1/ Ptgs2 dKO	Cyclooxygenase 1 / Cyclooxygenase 2	2000	10944235 (106)	PDA and neonatal death		Global constitutive KO	CD1 WT
		2001	11158594 (107)	PDA and 100% neonatal death in the dKO, partial phenotypes in the COX-2 -/- ;COX-1 +/-		Global constitutive KO	129/Ola + C57BL/6 mixed (239, 499)
		2002	12189249 (195)			Global constitutive KO	129/Ola + C57BL/6 mixed
Ptgs1	Cyclooxygenase 1	1995	8521478 (499)	No DA phenotype	Reduced indomethacin-induced gastric ulceration, reduced platelet aggregation and inflammatory response to arachidonic acid	Global constitutive KO	129 + C57BL/6 mixed
		2006	16732282 (225)	PDA and some neonatal death	Defects in both renal and reproductive development	Global constitutive KO (loss of function)	129S6/SvEvTac + C57BL/6 mixed
Ptgs2	Cyclooxygenase 2	2002	12189249 (195)	PDA or *in utero* constriction or depending on dosing regimen	Delayed birth (in Cox-1 KO)	Pharmacologic inhibition model	129/Ola + C57BL/6 mixed
Hpgd	15-Prostaglandin Dehydrogenase	2002	11821873 (23)	PDA and neonatal death	PDA associated congestive heart failure	Global constitutive KO	C57BL/6
Myh11	Myosin heavy chain 11	2000	10854329 (437)	Delayed DA closure (6h instead of 3h)	Generally defective SMC function resulting in failure to evacuate bladders, etc.	Global constitutive KO	C57BL/6 (500)
Myocd	Myocardin	2008	18188448 (111)	PDA and neonatal death in 100% of KO	Dramatic decrease in SMC contractile potential and neural crest derived SMC differentiation	Conditional constitutive KO	SV129 + C57BL/6 mixed + described

				mice			crosses (501)
Gpc3	Glypican 3	2009	19733558 (447)	PDA in a single replicate	Delayed coronary plexus formation and various cardiovascular defects including VSDs, common atrioventricular canal, double outlet right ventricle, and coronary artery fistulas	Global constitutive KO	C57Bl/6
Itga2b	Integrin alpha 2b	2010	19966813 (462)	PDA and neonatal death in 31% of KO mice	dysfunctional platelets and associated tendancy towards hemorrhage	Global constitutitve KO (loss of function)	C57BL/6J (502, 503)
Itga5/ Itgav	Integrins alpha 5 and alpha v	2010	20570943 (457)	PDA in 90% of KO mice surviving to 10-20 weeks and potential neonatal death of the remaining 50% of litters	Varying degrees of embryonic lethality dependent on genotype	Conditional constitutive KO	C57Bl/6 N7 or 129S4:C57Bl/6
Jag1	Jagged 1	2010	21068062 (440)	PDA and neonatal death	Defects in contractile SMC differentiation in the DA and surrounding great arteries	Conditional constitutive KO	129Sv + C57BL/6 mixed (445, 504)
Nfe2	Nuclear factor, erythroid 2	2010	19966813 (462)	PDA and neonatal death in 70% of KO mice	PDA associated pulmonary hypertension, internal hemorrhage into peritoneal cavity, wall of urinary bladder, and frequently in GI tract, brain, testes, pericardium, and mouth	Global constitutitve KO	129/Sv + C57BL/6 (502, 503)
Slco2a1	Prostaglandin trasnporter	2010	20083684 (430)	PDA and neonatal death in both KO and Hypomorph	PDA associated congestive heart failure	Global constitutitve KO	129Sv + C57BL/6 mixed
Smarca4	SWI/SNF Brahma Brg1	2011	21518954 (459)	PDA and neonatal death in 30-40% of KO mice	Cardiovascular and intestinal defects relating to SMC gene expression and death	Conditional constitutive KO	Sv129 + C57BL/6 mixed
Ilk	Integrin linked kinase	2011	21778429 (456)	PDA and neonatal death	Extreme dilated thoracic aortic aneurysms (~50% of abdominal cavity)	Conditional constitutive KO	SV129 + C57BL/6 mixed
Ctnnb1	Wnt-beta catenin	2013	23382837 (435)	PDA and neonatal death	Melanoblasts are found in locations you would normally expect neural crest derived SMCs such as in the DA media, dilation of left atria, thrombus formation in dilated atrium	Conditional constitutive dominant positive	C57BL/6 (435, 505)
Hand2	Heart and neural crest derivatives expressed protein 2	2013	23449628 (455)	PDA and neonatal death	VSD, skeletal hypoplasties, and various malformations of the digits	Global constitutive partial chromosomal duplication	C57Bl/10J
Asxl2	Additional sex combs like 2	2014	24860998 (461)	PDA and neonatal death	Low birth weight, thickened compact myocardium in the left ventricle, membranous ventricular septal defect, atrioventricular stenosis	Global constitutive KO	C57BL/6
Gdf2/ Bmp10	Bone morphogenetic protein 9 and 10	2015	26056270 (417)	Reopening of the DA on P4 and subsequent death	Decrease in DA wall thickness and matrix deposition	Global constitutive KO with antibody treatment	C57BL6/J (506)
Matr3	Matrin 3	2015	25574029 (454)	PDA and neonatal death in 12% of heterzygotes	Homozygotes die preimplantation. Heterozygotes show cardiac defects including subaortic VSD and DORV, BAV, and CoA	Global constitutive KO	129/SvJ + C57BL/6J or FVB/N + C57BL/6J
Notch3/ Notch2	Notch receptor 3 and 2	2015	26453897 (442)	PDA and neonatal death	Decrease in contractile gene expression and SMC development	Notch3 global constitutive KO, Notch2 conditional constitutive KO	C57BL/6 (507, 508)
Rbpj	Recombination signal binding protein for immunoglobulin kappa J	2015	26742650 (446)	PDA and neonatal death	Decrease in contractile SMC gene expression	Conditional constitutive KO	C57BL/6 mixed (509, 510)

	region						
Lox	Lysyl oxidase	2017	28550176 (418)	Tortuosity in 100% of DAs, PDA in 22%, and neonatal death	Abnormal outflow tract formation, thoracic aortic aneurysm and dissection, ruptured diaphragms, impaired airways	Global constitutive KO	129/SvJ + C57BL/6 mixed (511)
Fbln1	Fibulin 1	2020	32640908 (458)	PDA in 100% of KO mice	Hypoplastic intimal thickening of DA	Global constitutive KO	C57Bl/6

Table S1: Genetic Models of PDA or *in utero* DA Closure in the Mouse. Mouse models were identified by literature search. Gene names presented are official mouse gene symbol and may vary from names given in individual publications. Due to the emergent importance of strain to PDA phenotypes, strain information about each given mouse model was referenced. dKO – double knockout

Table S2 **Human Single-Gene Syndromes Associated with PDA (n=224)**

Gene/ Locus	Gene/Locus name	Gene/ Locus MIM number	location	Phenotype	MIM number	Pattern	Reference	PMID
ABCA3	ATP-binding cassette-3	601615	16p13.3	Surfactant metabolism dysfunction, pulmonary, 3	610921	AR	Kunig et al. (2007)	17719949
ABCC9	ATP-binding cassette, subfamily C, member 9 (sulfonylurea receptor 2)	601439	12p12.1	Hypertrichotic osteochondrodysplasia (Cantu syndrome)	239850	AD	Harakalova et al (2012)	22610116
							Scurr et al. (2011)	21344641
ACAD9	Acyl-CoA dehydrogenase family, member 9	611103	3q21.3	Mitochondrial complex I deficiency, nuclear type 20	611126	AR	Dewulf et al (2016)	27233227
ACTA2	Actin, alpha-2, smooth muscle, aorta	102620	10q23.31	Multisystemic smooth muscle dysfunction syndrome	613834	AD	Milewicz et al. (2010)	20734336
				Moyamoya disease 5	614042		Guo et al (2007)	17994018
				Aortic aneurysm, familial thoracic 6	611788	AD	Guo et al (2007)	17994018
ACTB	Actin, beta	102630	7p22.1	Baraitser-Winter syndrome 1	243310	AD	Cuvertino et al (2017)	29220674
							Verloes et al (2015)	25052316
ACVR1	Activin A Receptor, Type I	102576	2q24.1	Fibrodysplasia ossificans progressiva	135100	AD	Kaplan et al (2015)	26097044
ADAMTS10	A disintegrin-like and metalloproteinase with thrombospondin type 1 motif, 10	608990	19p13.2	Weill-Marchesani syndrome 1, recessive	277600	AR	Faivre et al. (2003)	14598350
ADAMTS3	A Disintegrin-like and metalloproteinase with thrombospondin type 1 motif, 3	605011	4q13.3	Hennekam lymphangiectasia-lymphedema syndrome 3	618154	AR	Scheuerle et al (2018)	30450763
ADAT3	Adenosine deaminase, t-RNA- specific-3	615302	19p13.3	Syndromic form of intellectual disability?	615286	AR	Thomas et al (2019)	31687266
AFF4	AF4/FMR2 family, member 4	604417	5q31.1	CHOPS syndrome	616368	AD	Izumi et al. (2015)	25730767
ALDH18A1	Aldehyde dehydrogenase 18 family, member A1 (1-pyrroline-5-carboxylate synthetase)	138250	10q24.1	Cutis laxa, autosomal recessive, type IIIA	219150	AR	Fischer et al (2014)	24913064
ALG12	Dolichyl-P-mannose:Man-7-GlcNAc-2-PP-dolichyl-alpha-6- mannosyltransferase	607144	22q13.33	Congenital disorder of glycosylation, type Ig	607143	AR	Kranz et al. (2007)	17506107
ALG8	Alg8, S. cerevisiae, homolog of	608103	11q14.1	Congenital disorder of glycosylation, type Ih	608104	AR	Schollen et al. (2004)	15235028
AMER1	APC membrane recruitment protein 1	300647	Xq11.2	Osteopathia striata with cranial sclerosis	300373	XLD	Perdu et al (2011)	20950377
AMMECR1	Alport syndrome, mental retardation, midface hypoplasia, and elliptocytosis chromosomal region gene 1	300195	Xq23	Midface hypoplasia, hearing impairment, elliptocytosis, and nephrocalcinosis	300990	XLR	Basel-Vanagaite et al. (2017)	28089922
ANKS6	Ankyrin repeat and sterile alpha motif domains-containing protein 6	615370	9q22.33	Nephronophthisis 16	615382	AR	Hoff et al (2013)	23793029
ARHGAP31	Rho GTPase-activating protein 31	610911	3q13.32-q13.33	Adams-Oliver syndrome 1	100300	AD	Lin et al (1998)	9823488
							Deeken and Caplan et al (1970)	5536130
ARID1B	AT-rich interaction domain-containing protein 1B	614556	6q25.3	Coffin-Siris syndrome 1	135900	AD	Poyhonen et al (2004)	15057123
							Kellermayer et al (2007)	17523151
ARX	Aristaless-related homeobox, X-linked	300382	Xp21.3	Lissencephaly, X-linked 2	300215	X-link	Ogata et al (2000)	10982975
				Hydranencephaly with abnormal genitalia				
ASCC1	Activating signal cointegrator 1 complex, subunit 1	614215	10q22.1	?Spinal muscular atrophy with congenital bone fractures 2	616867	AR	Knierim et al. (2016)	26924529
ATP6V1E1	ATPase, H+ transporting, V1 subunit E1	108746	22q11.21	Cutis laxa, autosomal recessive, type IIC	617402	AR	Alazami et al (2016)	27023906
ATR	Ataxia-telangiectasia and Rad3-related (FRAP-related protein-1)	601215	3q23	Seckel syndrome 1	210600	AR	Rappen et al (1993)	8413337
				?Cutaneous telangiectasia and cancer syndrome, familial	614564	AD		

ATXN7	Ataxin 7	607640	3p14.1	Spinocerebellar ataxia 7	164500	AD	Whitney et al (2007)	17254003
B3GLCT	Beta 3-glucosyltransferase	610308	13q12.3	Peters-plus syndrome	261540	AR	Reis et al. (2008	18798333
B4GALT7	Beta-1,4-galactosyltransferase 7	604327	5q35.3	Ehlers-Danlos syndrome, spondylodysplastic type, 1	130070	AR	Payet (1975)	1221956
B9D2	B9 domain-containing protein 2	611951	19q13.2	Joubert syndrome 34	614175	AR	Bachmann-Gagescu et al (2015)	26092869
				?Meckel syndrome 10				
BCOR	BCL6 corepressor	300485	Xp11.4	Microphthalmia, syndromic 2	300166	XLD	Hilton et al (2009)	19367324
BMPR2	Bone Morphogenetic Protein Receptor Type II	600799	2q33.1-q33.2	Pulmonary arterial hypertension, pulmonary vascular obstructive disease, PDA, atrial and ventricular septal defects, partial anomalous pulmonary venous return, transposition of the great arteries, atrioventricular canal, rare lesions with systemic to pulmonary shunt		AD	Roberts et al (2004)	15358693
C12orf57	Chromosome 12 open reading frame 57	615140	12p13.31	Temtamy syndrome	218340	AR	Talisetti et al (2003)	14564155
C2CD3	C2 calcium-dependent domain-containing protein 3	615944	11q13.4	Orofaciodigital syndrome XIV	615948	AR	Boczek et al (2018)	30097616
CACNA1C	Calcium channel, voltage-dependent, L type, alpha 1C subunit	114205	12p13.33	Timothy syndrome	601005	AD	Splawski et al. (2004)	15454078
CCDC22	Coiled-coil domain-containing protein 22	300859	Xp11.23	Ritscher-Schinzel syndrome 2	300963	XLR	Voineagu et al. (2012)	21826058
CD96	CD96 antigen	606037	3q13.1-q13.2	C syndrome	211750	AD	Haaf et al. (1991)	1746609
CDC42	Cell division cycle 42 (GTP-binding protein, 25kD)	116952	1p36.12	Takenouchi-Kosaki syndrome	616737	AD	Takenouchi et al. (2015)	26386261
							Martinelli et al. (2018)	29394990
CDK10	Cyclin-Dependent Kinase 10	603464	16q24.3	Al Kaissi syndrome	617694	AR	Guen et al (2017)	29130579
CDT1	Chromatin licensing and DNA replication factor 1	605525	16q24.3	Meier-Gorlin syndrome 4	613804	AR	Guernsey et al (2011)	21358631
CECR	Cat eye syndrome	115470	22q11	Cat eye syndrome	115470	AD	Denavit et al (2004)	15658620
CEP120	Centrosomal protein, 120kD	613446	5q13.2	Short-rib thoracic dysplasia 13 with or without polydactyly	616300	AR	Shaheen et al (2015)	25361962
CHD4	Chromodomain helicase DNA-binding protein-4	603277	12p13.31	Sifrim-Hitz-Weiss syndrome	617159	AD	Weiss et al (2016)	27616479
CHD7	Chromodomain helicase DNA binding protein 7	608892	8q12.2	Hypogonadotropic hypogonadism 5 with or without anosmia	612370	AD	Jongmans et al. (2006)	16155193
				CHARGE syndrome	214800	AD		
CHRM3	Cholinergic receptor, muscarinic, 3	118494	1q43	?Prune belly syndrome	100100	AR	Yoshida et al (1995)	7737585
CITED2	CBP/p300-Interacting Transactivator, With GLU/ASP-Rich C-Terminal Domain, 2	602937	6q24.1	Atrial septal defect 8, Ventricular septal defect 2	614433, 614431	AD	Liu et al (2017)	28687891
CLMP	Coxsackievirus- and adenovirus receptor-like membrane protein	611693	11q24.1	Congenital short bowel syndrome	615237	AR	Hasosah et al. (2008)	18209785
COL18A1	Collagen XVIII, alpha-1 polypeptide	120328	21q22.3	Knobloch syndrome, type 1	267750	AR	Wilson et al (1998)	9677068
COLEC10	Collectin 10	607620	8q24.12	3MC syndrome 3	248340	AR	Chinen & Naritomi et al (1995)	
COQ4	Coenzyme Q4, S. cerevisiae, homolog of	612898	9q34.11	Coenzyme Q10 deficiency, primary, 7	616276	AR	Brea-Calvo et al. (2015)	25658047
CREBBP	CREB binding protein	600140	16p13.3	Rubinstein-Taybi syndrome 1	180849	AD	Kanjilal et al. (1992)	1404300
							Stevens and Bhakta (1995)	8599359
CRELD1	CYSTEINE-RICH PROTEIN WITH EGF-LIKE DOMAINS 1	607170	3p25.3	Allelic variant-ATRIOVENTRICULAR SEPTAL DEFECT, SUSCEPTIBILITY TO, 2	606217	AD	Maslen et al. (2006)	17036335
CTCF	CCCTC-binding factor	604167	16q22.1	Intellectual disability, autosomal dominant 21	615502	AD	Gregor et al (2013)	23746550

CTU2	Cytosolic thiouridylase, subunit 2	617057	16q24.3	Microcephaly, facial dysmorphism, renal agenesis, and ambiguous genitalia syndrome	618142	AR	Shaheen et al., 2016	27480277
CUX1	Cut-like homeobox 1	116896	7q22.1	Global developmental delay with or without impaired intellectual development	618330	AD	Platzer et al (2018)	30014507
DER22t11-22	Emanuel syndrome (supernumerary der(22)t(11;22) syndrome)	609029	22q11.2	Emanuel syndrome	609029		Carter et al (2009)	19606488
DHCR24	24-dehydrocholesterol reductase	606418	1p32.3	Desmosterolosis	602398	AR	Andersson et al (2002)	12457401
DHCR7	Delta-7-dehydrocholesterol reductase	602858	11q13.4	Smith-Lemli-Opitz syndrome	270400	AR	Opitz et al., 1987	3322013
							Cunniff et al. 1997	9024557
							Kelley, 1998	9683618
DICER1	Dicer, Drosophila, homolog of, 1	606241	14q32.13	Pleuropulmonary blastoma	601200	AD	Foulkes et al (2011)	21882293
DIP2B	Disco-Interacting Protein 2 Homolog B	611379	12q13.12	Intellectual disability, FRA12A type	136630	AD	Berg et al (2000)	10955484
DPM1	Dolichyl-phosphate mannosyltransferase 1, catalytic subunit	603503	20q13.13	Congenital disorder of glycosylation, type Ie	608799	AR	Kim et al. (2000)	10642597
DTNA	Dystobrevin, alpha (dystrophin-related protein 3)	601239	18q12.1	Left ventricular noncompaction 1, with or without congenital heart defects	604169	AD	Ichida et al. (2001)	11238270
DVL3	Dishevelled 3 (homologous to Drosophila dsh)	601368	3q27.1	Robinow syndrome, autosomal dominant 3	616894	AD	White et al. (2016)	26924530
DYNC2LI1	Dynein, cytoplasmic 2, light intermediate chain 1	617083	2p21	Short-rib thoracic dysplasia 15 with polydactyly	617088	AR	Niceta et al. (2018)	28857138
ECE1	Endothelin converting enzyme 1	600423	1p36.12	?Hirschsprung disease, cardiac defects, and autonomic dysfunction	613870	AD	Hofstra et al. (1999)	9915973
ECHS1	Enoyl-CoA Hydratase, Short-Chain, 1, Mitochondrial	602292	10q26.3	Mitochondrial short-chain enoyl-CoA hydratase 1 deficiency	616277	AR	Nair et al (2016)	27221955
EED	Embryonic ectoderm development protein, mouse, homolog of	605984	11q14.2	Cohen-Gibson syndrome	617561	AD	Cooney et al. (2017)	27868325
EFTUD2	Elongation factor Tu GTP-binding domain-containing 2	603892	17q21.31	Mandibulofacial dysostosis, Guion-Almeida type	610536	AD	Vincent et al. (2016)	25790162
ELN	Elastin	130160	7q11.23	Williams-Beuren syndrome		AD	Figueroa et al. (2008)	18941598
EOGT	EGF domain-specific O-linked N-acetylglucosamine transferase	614789	3p14.1	Adams-Oliver syndrome 4	615297	AR	Shaheen et al (2013)	23522784
ESCO2	Establishment of cohesion 1, S. cerevisiae, homolog of, 2	609353	8p21.1	Roberts syndrome	268300	AR	Goh et al. (2010)	20101700
EVC	EVC Ciliary Complex Subunit 1	604831	4p16.2	Ellis-van Creveld syndrome	225500	AR	Vaughan et al. (2000)	11376442
EXT2	Exostosin Glycosyltransferase 2	608210	11p11.2	Exostoses, multiple, type 2	133701	AD	Gentile et al. (2019)	30288735
				Seizures, scoliosis, and macrocephaly syndrome	616682	AR		
F5	Coagulation factor V (proaccelerin, labile factor)	612309	1q24.2	Thrombophilia due to activated protein C resistance	188055	AD	Gorbe et al. (1999)	10066036
FANCI	FANCI gene	611360	15q26.1	Fanconi anemia, complementation group I	609053	AR	Savage et al (2015)	26590883
FBN1	Fibrillin-1	134797	15q21.1	Weill-Marchesani syndrome 2, dominant	608328	AD	Faivre et al. (2003)	14598350
FBN2	Fibrillin-2	612570	5q23.3	Contractural arachnodactyly, congenital	121050	AD	Viljoen et al (1994)	7815423
FGFR2	Fibroblast growth factor receptor-2 (bacteria-expressed kinase)	176943	10q26.13	Saethre-Chotzen syndrome	101400	AD	Okamoto et al (2016)	30358290
FKBP14	FK506-binding protein 14	614505	7p14.3	Ehlers-Danlos syndrome, kyphoscoliotic type, 2	614557	AR	Aldeeri et al. (2014)	24773188
FLNA	Filamin A, alpha (actin-binding protein-280)	300017	Xq28	Congenital short bowel syndrome	300048	XLR	FitzPatrick et al. (1997)	9279759
				Intestinal	300048	XLR	FitzPatrick	9279759

				pseudoobstruction, neuronal			et al. (1997)	
				Heterotopia, periventricular, 1	300049	XLD	Jefferies et al. (2010)	20014127
FOXC1	Forkhead, Drosophila, homolog-like 7	601090	6p25.3	Axenfeld-Rieger syndrome, type 3	602482	AD	Baruch and Erickson (2001)	11343302
FOXC2	Forkhead box C2	602402	16q24.1	Lymphedema-distichiasis syndrome with renal disease and diabetes mellitus	153400	AD	Johnson et al. (1999)	10086462
				Lymphedema-distichiasis syndrome				
FOXF1	Forkhead box F1	601089	16q24.1	Alveolar capillary dysplasia with misalignment of pulmonary veins	265380	AD	Sen et al (2004)	15520767
							Vassal et al (1998)	9475097
FTO	Fat mass- and obesity-associated gene	610966	16q12.2	Growth delay, developmental delay, facial dysmorphism	612938	AR	Daoud et al. (2016)	26378117
G6PC3	Glucose-6-phosphatase, catalytic, 3	611045	17q21.31	Neutropenia, severe congenital 4, autosomal recessive	612541	AR	Banka et al. (2011)	20717171
				Dursun syndrome				
GATA4	GATA-binding protein-4	600576	8p23.1	Tetralogy of Fallot	187500	AD	Yang et al (2012)	22101736
				Atrioventricular septal defect 4	614430	AD		
				Atrial septal defect 2	607941	AD		
				?Testicular anomalies with or without congenital heart disease	615542	AD		
				Ventricular septal defect 1	614429	AD		
GATA5	GATA-binding protein 5	611496	20q13.33	Congenital heart defects, multiple types, 5	617912	AD; AR	Hempel et al (2017)	28180938
GATA6	GATA-binding protein-6	601656	18q11.2	Persistent truncus arteriosus	217095		Kodo et al. (2009)	19666519
				Pancreatic agenesis and congenital heart defects	600001	AD	Yorifuji et al. (1994)	8071961
GFI1B	Growth factor-independent 1B	604383	9q34.13	Bleeding disorder, platelet-type, 17	187900	AD; AR	Ferreira et al (2017)	28041820
GJA1	Gap junction protein, alpha-1, 43kD (connexin 43)	121014	6q22.31	Hypoplastic left heart syndrome 1	241550	AR	Brekke et al (1953)	13050604
GLI3	GLI-Kruppel family member GLI3 (oncogene GLI3)	165240	7p14.1	Pallister-Hall syndrome	146510	AD	Hall et al. (1980)	7211952
GLIS3	GLIS family zinc finger protein 3	610192	9p24.2	Diabetes mellitus, neonatal, with congenital hypothyroidism	610199	AR	Dimitri et al (2015)	26259131
GPC3	Glypican 3	300037	Xq26.2	Simpson-Golabi-Behmel syndrome, type 1	312870	XLR	Yano et al. (2011)	20950395
HBHR	Alpha-thalassemia/intellectual disability syndrome, type 1	141750	16pter-p13.3	Alpha-thalassemia/intellectual disability syndrome, type 1	141750	AD	Borochovitz et al. (1970)	5433640
							Gibbons et al (1995)	7726225
HCCS	Holocytochrome c synthase (cytochrome c heme-lyase)	300056	Xp22.2	Linear skin defects with multiple congenital anomalies 1	309801	XLD	Prepeluh et al (2018)	30068298
HPGD	Hydroxyprostaglandin dehydrogenase 15-(NAD)	601688	4q34.1	Hypertrophic osteoarthropathy, primary, autosomal recessive 1	259100	AR	Uppal et al (2008)	18500342
				Digital clubbing, isolated congenital	119900	AR	Sinha et al. (1997)	9402870
				Cranioosteoarthropathy	259100	AR		
HRAS	Harvey rat sarcoma viral (v-Ha-ras) oncogene homolog	190020	11p15.5	Schimmelpenning-Feuerstein-Mims syndrome, somatic mosaic	163200		Rijntes-Jacobs et al (2010)	20949522
IGBP1	Immunoglobulin-binding protein 1	300139	Xq13.1	Corpus callosum, agenesis of, intellectual disability, ocular coloboma and micrognathia	300472	XLR	Graham et al (2003)	14556245
IGF2	Insulin-like growth factor-2, or somatomedin A	147470	11p15.5	?Growth restriction, severe, with distinctive facies	616489	AD	Begemann et al. (2015)	26154720
IRX5	Iroquois homeo box protein 5	606195	16q12.2	Hamamy syndrome	611174	AR	Bonnard et al. (2012)	22581230
							Hamamy et al. (2007)	17230486

ISL1	Islet 1	600366	5q11.1	PDA, ventricular septal defect		AD	Ma et al (2019)	30390123
JAG1	Jagged 1	601920	20p12.2	Tetralogy of Fallot	187500	AD	Sánchez-Angulo et al (1997)	9410541
				Alagille syndrome 1	118450	AD		
				?Deafness, congenital heart defects, and posterior embryotoxon	617992			
KAOGS	Kagami-Ogata syndrome	608149	14q32	Kagami-Ogata syndrome	608149	AD	Sutton and Shaffer (2000)	10951461
KAT6A	K(lysine) acetyltransferase 6A	601408	8p11.21	Intellectual disability, autosomal dominant 32	616268	AD	Tham et al. (2015)	25728777
							Millan et al. (2016)	27133397
KAT6B	Lysine acetyltransferase 6B	605880	10q22.2	Genitopatellar syndrome	606170	AD	Brugha et al (2011)	21412151
KCNH1	Potassium voltage-gated channel, subfamily H, member 1 (ether-a-go-go, drosophila, homolog of)	603305	1q32.2	Zimmermann-Laband syndrome 1	135500	AD	Robertson et al. (1998)	9674908
KCNJ8	Potassium inwardly rectifying channel subfamily J member 8	600935	12p12.1	Hypertrichotic osteochondrodysplasia (Cantu syndrome)		AD	Grange et al. (2019)	31828977
KMT2A	Lysine-Specific Methyl Transferase 2A	159555	11q23.3	Wiedemann-Steiner syndrome	605130	AD	Min Ko et al (2016)	27777327
KMT2D	Lysine (K)-specific methyltransferase 2D	602113	12q13.12	Kabuki syndrome 1	147920	AD	Niikawa et al (1988)	3067577
KRAS	Kirsten rat sarcoma-2 viral (v-Ki-ras2) oncogene homolog	190070	12p12.1	Schimmelpenning-Feuerstein-Mims syndrome, somatic mosaic	163200		Rijntes-Jacobs et al (2010)	20949522
				Noonan syndrome 3	609942	AD	Kratz et al. (2009)	19396835
KYNU	Kynureninase	605197	2q22.2	Vertebral, cardiac, renal, and limb defects syndrome 2	617661	AR	Shi et al. (2017)	28792876
LARS2	Leucyl-tRNA synthetase, mitochondrial	604544	3p21.31	?Hydrops, lactic acidosis, and sideroblastic anemia	617021	AR	Riley et al. (2016)	26537577
LIFR	Leukemia inhibitory factor receptor	151443	5p13.1	Stuve-Wiedemann syndrome/Schwartz-Jampel type 2 syndrome	601559	AR	Raas-Rothschild et al (2003)	12910496
LMNA	Lamin A/C	150330	1q22	Restrictive dermopathy, lethal	275210	AR	Bokenkamp et al. (2011)	21915271
MAP3K7	Mitogen-activated protein kinase kinase kinase 7	602614	6q15	Frontometaphyseal dysplasia 2	617137	AD	Morava et al. (2003)	12503106
MASP1	Mannan-binding lectin serine protease-1 (C4/C2 activating component of Ra-reactive factor)	600521	3q27.3	3MC syndrome 1	257920	AR	Rooryck et al., 2011	21258343
MATR3	Matrin 3	164015	5q31.2	Developmental delay, left ventricular outflow tract defects, bicuspid aortic valve, coarctation of the aorta, PDA		AD	Quintero-Rivera et al (2015)	25574029
MECP2	Methyl-CpG-binding protein-2	300005	Xq28	Intellectual disability, X-linked syndromic, Lubs type	300260	XLR	Belligni et al. (2010)	20503343
MED12	Mediator of RNA polymerase II transcription, subunit 12, S. cerevisiae, homolog of	300188	Xq13.1	Opitz-Kaveggia syndrome	305450	XLR	Kato et al (1994)	7802020
MED13L	Mediator complex subunit 13-like	608771	12q24.21	Transposition of the great arteries, dextro-looped 1	608808	AD	Asadollahi et al (2017)	28645799
				Intellectual disability and distinctive facial features with or without cardiac defects	616789	AD		
MEGF8	Multiple epidermal growth factor-like domains 8	604267	19q13.2	Carpenter syndrome 2	614976	AR	Twigg et al., 2012	23063620
MEF2C	MADS Box Transcription Enhancer Factor 2, Polypeptide C	600662	5q14.3	Intellectual disability, stereotypic movements, epilepsy, and/or cerebral malformations	613443	AD	Qiao et al (2017)	29104469
MID1	Midline-1	300552	Xp22.2	Opitz GBBB syndrome, type I	300000	XLR	Winter et al (2003)	12545276
MKKS	McKusick-Kaufman syndrome gene	604896	20p12.2	Mckusick-kaufman Syndrome	236700	AR	Slavotinek et al (2015)	20301675
MKS1	MKS1 gene	609883	17q22	Meckel syndrome 1	249000	AR	Salonen et al (1984)	6486167
MRPS16	Mitochondrial ribosomal protein S16	609204	10q22.2	Combined oxidative phosphorylation	610498	AR	Miller et al. (2004)	15505824

				deficiency 2				
MUSK	Receptor tyrosine kinase MuSK	601296	9q31.3	Myasthenic syndrome, congenital, 9, associated with acetylcholine receptor deficiency	616325	AR	Maselli et al (2010)	20371544
MYBPC3	Myosin-Binding Protein C, Cardiac	600958	11p11.2	Cardiomyopathy, dilated, 1MM	615396	AD	Wessels et al (2014)	25335496
MYCN	Oncogene NMYC	164840	2p24.3	Feingold syndrome 1	164280	AD	Frydman et al. (1997)	9268091
MYH11	Myosin, heavy polypeptide-11, smooth muscle	160745	16p13.11	Aortic aneurysm, familial thoracic 4	132900	AD	Glancy et al (2001)	11249915
MYH3	Myosin, heavy polypeptide-3, skeletal muscle, embryonic	160720	17p13.1	Contractures, pterygia, and variable skeletal fusions syndrome 1A	178110	AD	Carapito et al. (2016)	27381093
MYH7	Myosin, Heavy Chain 7	160760	14q11.2	Left ventricular noncompaction	613426	AD	Hirono et al (2020)	32183154
MYRF	Myelin regulatory factor	608329	11q12.2	Cardiac-urogenital syndrome	618280	AD	Pinz et al. (2018)	29446546
NCAPG2	Non-SMC condensin II complex subunit G2	608532	7q36.3	Khan-Khan-Katsanis syndrome	618460	AR	Khan et al. (2019)	30609410
NEK8	Never in mitosis gene A-related kinase 8	609799	17q11.2	?Nephronophthisis 9	613824		Rajagopalan et al (2016)	26697755
				Renal-hepatic-pancreatic dysplasia 2	615415	AR		
NFIX	Nuclear factor I/X (CCAAT-binding transcription factor)	164005	19p13.13	Marshall-Smith syndrome	602535	AD	Shaw et al. (2010)	16531739
NHS	NHS gene	300457	Xp22.2-p22.1	Cataract 40, X-linked	302200	X-link	Coccia et al. (2009)	19414485
NKX2-5	NK2 homeobox-5 gene	600584	5q35.1	Hypoplastic left heart syndrome 2	614435	AD	Brekke et al (1953)	13050604
				Ventricular septal defect 3	614432	AD	Peng et al. (2010)	21110066
				Tetralogy of Fallot	187500	AD	Pauli et al (1999)	10398271
NKX2-6	NK2, Drosophila, homolog of, 6	611770	8p21.2	Conotruncal heart malformations	217095		Kodo et al. (2009)	19666519
				Persistent truncus arteriosus				
NMLFS	Nablus mask-like facial syndrome (chromosome 8q22.1 deletion syndrome)	608156	8q22.1	Nablus mask-like facial syndrome	608156	AD	Barber et al. (2008)	17940555
NONO	NON-POU DOMAIN-CONTAINING OCTAMER-BINDING PROTEIN	300084	Xq13.1	Intellectual disability, X-linked, syndromic 34	300967	X link	Scott et al (2017)	27550220
NOTCH1	Notch receptor 1	190198	9q34.3	Aortic valve disease 1	109730	AD	Stittrich et al (2014)	25132448
				Adams-Oliver syndrome 5	616028	AD		
NOTCH2	Notch, Drosophila, homolog of, 2	600275	1p12	Hajdu-Cheney syndrome	102500	AD	Rosser et al. (1996)	8723560
NOTCH3	Notch, Drosophila, homolog of, 3	600276	19p13.12	Lateral meningocele syndrome	130720	AD	Gripp et al (2015)	25394726
NPHP3	Nephrocystin 3	608002	3q22.1	Meckel syndrome 7	267010	AR	Bergmann et al. (2008)	18371931
				Renal-hepatic-pancreatic dysplasia 1	208540	AR		
				Nephronophthisis 3	604387	AR		
NR2F2	Nuclear Receptor Sub-family 2, Group F, Member 2	107773	15q26.2	Congenital heart defects, multiple types, 4	615779	AD	Upadia et al (2018)	29663647
NRAS	Neuroblastoma RAS viral (v-ras) oncogene homolog	164790	1p13.2	Schimmelpenning-Feuerstein-Mims syndrome, somatic mosaic	163200		Rijntes-Jacobs et al (2010)	20949522
NSD1	Nuclear receptor binding SET domain protein 1	606681	5q35.3	Leukemia, acute myeloid	601626	Som.; AD	Nagai et al (2005)	12676901
				Sotos syndrome 1	117550	AD	Kanemoto et al. (2006)	16329110
PACS1	Phosphofurin acidic cluster sorting protein 1	607492	11q13.1-q13.2	Schuurs-Hoeijmakers syndrome	615009	AD	Martinez-Monseny et al. (2018)	30113927
PEX1	Peroxisome biogenesis factor-1	602136	7q21.2	Peroxisome biogenesis disorder 1A (Zellweger)	214100	AR	Bowen et al (1964)	14169466
PEX19	Peroxisome biogenesis factor 19 (peroxisomal farnesylated protein)	600279	1q23.2	Peroxisome biogenesis disorder 12A (Zellweger)	614886	AR	Mohamed et al. (2010)	20683989
PHGDH	Phosphoglycerate dehydrogenase	606879	1p12	Neu-Laxova syndrome 1	256520	AR	Manning et al (2004)	14994231
PIGA	Phosphatidylinositol glycan, class A	311770	Xp22.2	Multiple congenital anomalies-hypotonia-seizures syndrome 2	300868	XLR	Johnston et al (2012)	22305531

PIGN	Phosphatidylinositol glycan, class N	606097	18q21.33	Multiple congenital anomalies-hypotonia-seizures syndrome 1	614080	AR	Maydan et al. (2011)	21493957
PIGT	Phosphatidylinositol glycan, class T	610272	20q13.12	Multiple congenital anomalies-hypotonia-seizures syndrome 3	615398	AR	Nakashima et al. (2014)	24906948
PKS	Pallister-Killian syndrome	601803	12p	Pallister-Killian syndrome	601803	Som.	Schinzel et al (1991)	2002482
POLR1A	Polymerase I, RNA, subunit A	616404	2p11.2	Acrofacial dysostosis, Cincinnati type	616462	AD	Weaver et al. (2015)	25913037
PORCN	Porcupine, Drosophila, homolog of	300651	Xp11.23	Focal dermal hypoplasia	305600	XLD	Irvine et al (1996)	8882775
POU1F1	POU domain, class 1, transcription factor 1 (Pit1, growth hormone factor 1)	173110	3p11.2	Pituitary hormone deficiency, combined, 1	613038	AD; AR	De Zegher et al. (1995)	7593413
PPCS	Phosphopantothenoylcysteine synthetase	609853	1p34.2	Cardiomyopathy, dilated, 2C	618189	AR	Iuso et al (2018)	29754768
PPP1CB	Protein phosphatase-1, catalytic subunit, beta isoform	600590	2p23.2	Noonan syndrome-like disorder with loose anagen hair 2	617506	AD	Bertola et al. (2017)	28211982
PRDM6	PR domain-containing protein 6	616982	5q13.2	Patent ductus arteriosus 3	617039	AD	Lynch et al. (1965)	5897316 27716515
PSMD12	Proteasome 26S subunit, non-ATPase, 12	604450	17q24.2	Stankiewicz-Isidor syndrome	617516	AD	Kury et al. (2017)	28132691
PTPN11	Protein tyrosine phosphatase, nonreceptor-type, 11	176876	12q24.13	Noonan syndrome 1	163950	AD	Noonan (1968)	4386970
RAB23	Ras-associated protein RAB23	606144	6p12.1-p11.2	Carpenter syndrome	201000	AR	Alessandri et al. (2010)	20358613
RBP4	Retinol-binding protein-4, interstitial	180250	10q23.33	Retinal dystrophy, iris coloboma, and comedogenic acne syndrome	615147	AR	Cukras et al (2012)	23189188
RMND5A	Required For Meiotic Nuclear Division 5 Homolog A	618964	2p11.2	Giant occipitoparietal encephaloceles			Vogel et al (2012)	22681319
RNF110	Ring finger protein 110 (zinc finger protein-144)	600346	17q12	Turnpenny-Fry syndrome	618371	AD	Turnpenny et al., 2018	30343942
RPL11	Ribosomal protein L11	604175	1p36.11	Diamond-Blackfan anemia 7	612562	AD	Gerrard et al (2013)	23718193
RPL5	Ribosomal protein L5	603634	1p22.1	Diamond-Blackfan anemia 6	612561	AD	Gazda et al (2008)	19061985
RPS26	Ribosomal protein S26	603701	12q13.2	Diamond-Blackfan anemia 10	613309	AD	Handler et al. (2009)	19816270
SALL1	Sal-like 1	602218	16q12.1	Townes-Brocks syndrome 1	107480	AD	Kohlhase et al (2007)	20301618
				Townes-Brocks branchiootorenal-like syndrome				
SAMD9	Sterile alpha motif domain-containing protein 9	610456	7q21.2	MIRAGE syndrome	617053	AD	Narumi et al (2016)	27182967
SEMA3E	Semaphorin 3E	608166	7q21.11	?CHARGE syndrome	214800	AD	Alazami et al. (2008)	18553515
SF3B4	Splicing factor 3B, subunit 4	605593	1q21.2	Acrofacial dysostosis 1, Nager type	154400	AD	Petit et al. (2014)	24003905
SH3PXD2B	SH3 AND PX Domains-Containing Protein 2B	613293	5q35.1	Frank-ter Haar syndrome	249420	AR	Saeed et al (2011)	21453629
SIK3	Salt-inducible kinase 3	614776	11q23.3	?Spondyloepimetaphyseal dysplasia, Krakow type	618162	AR	Csukasi et al. (2018)	30232230
SKI	Avian sarcoma viral (v-ski) oncogene homolog	164780	1p36.33-p36.32	Shprintzen-Goldberg syndrome	182212	AD	Greally et al (1998)	9508238
SLC25A24	Solute carrier family 25 (mitochondrial carrier, phosphate carrier), member 24	608744	1p13.3	Fontaine progeroid syndrome	612289	AD	Gorlin et al. (1960)	13851313
SLC26A2	Solute carrier family 26 (sulfate transporter), member 2 (diastrophic dysplasia sulfate transporter)	606718	5q32	Diastrophic dysplasia	222600	AR	De la Chapelle et al. (1972)	4644462
				De la Chapelle dysplasia	256050	AR		
SLC29A3	Solute carrier family 29 (nucleoside transporter), member 3	612373	10q22.1	Histiocytosis-lymphadenopathy plus syndrome	602782	AR	Rossbach et al (2006)	16155931
SLC35A3	Solute Carrier Family 35 (UDP-N-Acetylglucosamine Transporter), Member 3	605632	1p21.2	Arthrogryposis, intellectual disability, and seizures	615553	AR	Edmondson et al (2017)	28777481
SLCO2A1	Solute carrier organic anion transporter family, member 2A1	601460	3q22.1-q22.2	Hypertrophic osteoarthropathy, primary, autosomal recessive 2	614441	AR	Zhang et al (2012)	22197487
							Chang et al (2010)	20083684
SMAD3	Mothers against decapentaplegic, Drosophila, homolog of, 3	603109	15q22.33	Loeys-Dietz syndrome 3	613795	AD	Van de Laar et al. (2012)	22167769
SMAD4	Mothers against decapentaplegic, Drosophila,	600993	18q21.2	Myhre syndrome	139210	AD	Caputo et al. (2012)	22243968

	homolog of, 4							
SMC3	Structural maintenance of chromosomes 3	606062	10q25.2	Cornelia de Lange syndrome 3	610759	AD	Gil-Rodríguez et al (2015)	25655089
SMN1	Survival of motor neuron 1, telomeric	600354	5q13.2	Spinal Muscle Atrophy 1	253300	AR	Rudnik-Schoneborn et al (2008)	18662980
SNRPB	Small nuclear ribonucleoprotein polypeptides B and B1	182282	20p13	Cerebrocostomandibular syndrome	117650	AD	Tooley et al (2016)	26971886
SOX17	SRY-box 17	610928	8q11.23	Vesicoureteral reflux 3	613674	AD	Gimelli et al (2010)	20960469
SOX2	SRY (sex determining region Y)-box 2	184429	3q26.33	Optic nerve hypoplasia and abnormalities of the central nervous system	206900	AD	Bardakjian and Schneider (2005)	15578584
				Microphthalmia, syndromic 3				
SPECC1L	Sperm antigen with calponin homology and coiled-coil domains 1-like	614140	22q11.23	Opitz GBBB syndrome, type II	145410	AD	Opitz et al. (1969)	
				Hypertelorism, Teebi type	145420	AD	Tsai et al (2002)	12439902
STAMBP	STAM binding protein	606247	2p13.1	Microcephaly-capillary malformation syndrome	614261	AR		
STRA6	Stimulated by retinoic acid 6, mouse, homolog of	610745	15q24.1	Microphthalmia, syndromic 9	601186	AR	Segel et al (2009)	19839040
				Microphthalmia, isolated, with coloboma 8			Pasutto et al. (2007)	17273977
TAB2	TAK1-Binding Protein 2	605101	6q25.1	Congenital heart defects, nonsyndromic, 2	614980	AD	Ackerman et al (2016)	27452334
TALDO1	Transaldolase-1	602063	11p15.5	Transaldolase deficiency	606003	AR	Eyaid et al. (2013)	23315216
TBC1D32	TBC1 DOMAIN FAMILY, MEMBER 32	615867	6q22.31	Allelic variant-VARIANT OF UNKNOWN SIGNIFICANCE			Adly et al. (2014)	24285566
TBX1	T-box 1	602054	22q11.21	Velocardiofacial syndrome	192430	AD	McElhinney et al (2001)	11731631
				Digeorge syndrome	188400	AD	Fukushima et al (1992)	
				Conotruncal anomaly face syndrome	217095		Matsuoka et al (1998)	9737780
TBX2	T-box 2	600747	17q23.2	Vertebral anomalies and variable endocrine and T-cell dysfunction	618223	AD	Liu et al. (2018)	29726930
TBX4	T-Box Transcription Factor 4	601719	17q23.2	Ischiocoxopodopatellar syndrome with or without pulmonary arterial hypertension	147891	AD	Galambos et al (2019)	31151956
TBX5	T-box 5	601620	12q24.21	Holt-Oram syndrome	142900	AD	Glauser et al. (1989)	2766565
TFAP2B	Transcription factor AP-2 beta (activating enhancer-binding protein 2 beta)	601601	6p12.3	Patent ductus arteriosus 2	617035	AD	Khetyar et al. (2008)	18752453
				Char syndrome	169100	AD	Davidson (1993)	8326495
TGFBR1	Transforming growth factor, beta receptor I (activin A receptor type II-like kinase, 53kD)	190181	9q22.33	{Multiple self-healing squamous epithelioma, susceptibility to}	132800	AD	Loeys et al (2005)	15731757
				Loeys-Dietz syndrome 1	609192	AD	Sheikhzadeh et al. (2014)	24344637
TGFBR2	Transforming growth factor, beta receptor II, 70-80kD	190182	3p24.1	Loeys-Dietz syndrome 2	610168	AD	Loeys et al. (2006)	16928994
THOC6	THO complex subunit 6	615403	16p13.3	Beaulieu-Boycott-Innes syndrome	613680	AR	Boycott et al. (2010)	20503307
TKT	Transketolase	606781	3p21.1	Short stature, developmental delay, and congenital heart defects	617044	AR	Boyle et al. (2016)	27259054
TMCO1	Transmembrane and coiled-coil domains protein 1	614123	1q24.1	cerebrofaciothoracic dysplasia	213980	AR	Cilliers et al. (2007)	17351359
TMEM126B	Transmembrane protein 126B	615533	11q14.1	Mitochondrial complex I deficiency, nuclear type 29	618250	AR	Alston et al (2016)	27374774
TMEM94	Transmembrane protein 94	618163	17q25.1	Intellectual developmental disorder with cardiac defects and dysmorphic facies	618316	AR	Stephen et al. (2018)	30526868
TP63	Tumor protein p63 (tumor protein p73-like)	603273	3q28	Hay-Wells syndrome	106260	AD	Sutton et al. (2009)	19676059
TRAF7	TNF receptor-associated factor 7	606692	16p13.3	Cardiac, facial, and digital anomalies with developmental delay	618164	AD	Tokita et al. (2018)	29961569
TRIP4	Thyroid hormone receptor interactor 4	604501	15q22.31	Spinal muscular atrophy with congenital bone	616866	AR	Knierim et al. (2016)	26924529

				fractures 1				
TRRAP	Transformation/transcription domain-associated protein	603015	7q22.1	Developmental delay with or without dysmorphic facies and autism	618454	AD	Cogne et al. (2019)	30827496
TSFM	Ts translation elongation factor, mitochondrial	604723	12q14.1	Combined oxidative phosphorylation deficiency 3	610505	AR	Smeitink et al. (2006)	17033963
UBR1	Ubiquitin-Protein Ligase E3 Component N-Recognin 1	605981	15q15.2	Johanson-Blizzard syndrome	243800	AR	Fallahi et al (2011)	20556423
USP18	Ubiquitin-specific protease 18	607057	22q11.21	Pseudo-TORCH syndrome 2	617397	AR	Meuwissen et al., 2016	27325888
USP9X	Ubiquitin-specific protease-9, X chromosome (Drosophila fat facets related, X-linked)	300072	Xp11.4	Intellectual disability, X-linked 99, syndromic, female-restricted	300968	XLD	Reijnders et al. (2016)	26833328
VANGL1	Vang-like 1	610132	1p13.1	Caudal regression syndrome	600145	AD	Finer et al (1978)	657575
VPS33A	Vacuolar protein sorting 33, yeast, homolog of, A	610034	12q24.31	Mucopolysaccharidosis-plus syndrome	617303	AR	Kondo et al. (2017)	28013294
WAC	WW domain-containing adaptor with coiled-coil region	615049	10p12.1	Desanto-Shinawi syndrome	616708	AD	Wentzel et al (2011)	21522184
WDR35	WD repeat-containing protein 35	613602	2p24.1	Cranioectodermal dysplasia 2	613610	AR	Bacino et al. (2012)	22987818
WNT3	Wingless-type MMTV integration site family, member 3	165330	17q21.31-q21.32	?Tetra-amelia syndrome 1	273395	AR	Zimmer et al (1985)	4076260
WSHC5	WASH complex, subunit 5	610657	8q24.13	Ritscher-Schinzel syndrome 1	220210	AR	Leonardi et al (2001)	11484200
WT1	WT1 Transcription Factor	607102	11p13	Ambiguous genitalia with absence of gonadal dysgenesis and kidney disease			Köhler et al (2004)	15191353
XRCC2	X-ray repair, complementing defective, repair in Chinese hamster cells-2	600375	7q36.1	?Fanconi anemia, complementation group U	617247	AR	Shamseldin et al. (2012)	22232082
YY1AP1	YY1 associated protein 1	607860	1q22	Grange syndrome	602531	AR	Grange et al (1998)	9489789
ZEB2	Zinc finger E box-binding homeobox 2	605802	2q22.3	Mowat-Wilson syndrome	235730	AD	Wakamatsu et al. (2001)	11279515
							Strenge et al. (2007)	17567886
ZIC3	Zic family, member 3	300265	Xq26.3	Heterotaxy, visceral, 1, X-linked	306955	XLR	Mathias et al. (1987)	3674105
ZNF148	Zinc finger protein-148	601897	3q21.2	Global developmental delay, absent or hypoplastic corpus callosum, and dysmorphic facies	617260	AD	Stevens et al. (2016)	27964749

Brackets, "[ ]", indicate "nondiseases," mainly genetic variations that lead to apparently abnormal laboratory test values (e.g., dysalbuminemic euthyroidal hyperthyroxinemia). Braces, "{ }", indicate mutations that contribute to susceptibility to multifactorial disorders (e.g., diabetes, asthma) or to susceptibility to infection (e.g., malaria). A question mark, "?", before the phenotype name indicates that the relationship between the phenotype and gene is provisional. More details about this relationship are provided in the comment field of the map and in the gene and phenotype OMIM entries.

Table S2. **Human single-gene syndromes associated with PDA.** The OMIM database was searched for genes which complied with three major criteria: association with a single-gene syndrome, a database association with PDA, and available references linking to a human PDA phenotype. OMIM searches were limited to single-gene syndromes and made use of both the 'and' command and exhaustive combinations of the terms 'patent,' 'ductus,' 'arteriosus,' 'arterial duct', and 'Botalli". References were validated or compiled manually. Additional online resources including GeneCards, Human Phenotype Ontology, DisGeNET, FindZebra, GeneReviews and UniProtKB were then used to validate the exhaustive nature of the OMIM list with novel genes added. Some genes associated with PDA in genetic syndrome databases (**Table 1**) could not be verified by primary sources (e.g. DDX11, EZH2, TXNL4A, SUCLG1, ZNF462, MAF, and others). These examples may represent clinical syndromes associated with multiple genes where only one gene is clearly linked to PDA, or syndromes belonging to a class of disorders where PDA is a feature of one specific gene and genotype-phenotype association. This list is limited by the databases used to assemble it and should not be considered exhaustive.

Table S3	Chromosomal Deletions, Duplications, and Additions Associated with PDA in the Human (N=15)							
Gene/ Locus	**Gene/ Locus name**	**MIM number**	**Cytogenetic location**	**Phenotype**	**Phenotype MIM number**	**Inheritance**	**Reference**	**PMID**
DEL10q26	Chromosome 10q26 deletion syndrome	609625	10q26	Chromosome 10q26 deletion syndrome	609625	AD	Tanabe et al. (1999)	10530074
							Yatsenko et al. (2009)	19558528
DEL14q11q22	Chromosome 14q11-q22 deletion syndrome	613457	14q11-q22	Chromosome 14q11-q22 deletion syndrome	613457	Isolated cases	Shapira et al. (1994)	7977460
							Zahir et al. (2007)	17545556
DEL17q23.1q23.2	Chromosome 17q23.1-q23.2 deletion syndrome	613355	17q23.1-q23.2	Chromosome 17q23.1-q23.2 deletion syndrome	613355	Isolated cases	Ballif et al. (2010)	20206336
DEL18q	Chromosome 18q deletion syndrome	601808	18q	Chromosome 18q deletion syndrome	601808	AD	Versacci et al. (2005)	16100728
DEL1q41q42	Chromosome 1q41-q42 deletion syndrome	612530	1q41-q42	Chromosome 1q41-q42 deletion syndrome	612530	Isolated cases	Filges et al. (2010)	20358614
DEL22q11.2	Chromosome 22q11.2 deletion syndrome, distal	611867	22q11.2	Chromosome 22q11.2 deletion syndrome, distal	611867	PH	Rauch et al (2005)	15831592
DEL3pterp25	3p- syndrome (chromosome 3pter-p25 deletion syndrome)	613792	3pter-p25	3p- syndrome	613792	AD	Nienhaus et al (1992)	1481811
DEL3q29	Chromosome 3q29 microdeletion syndrome	609425	3q29	Chromosome 3q29 microdeletion syndrome	609425	Isolated cases	Li et al (2009)	19460468
DEL6pter	Chromosome 6pter-p24 deletion syndrome	612582	6pter-p24	Chromosome 6pter-p24 deletion syndrome	612582	Isolated cases	DeScipio et al. (2005)	15704124
DEL6q24q25	Chromosome 6q24-q25 deletion syndrome	612863	6q24-q25	Chromosome 6q25-q25 deletion syndrome	612863	PH	Caselli et al (2007)	17512813
DEL8q13	Mesomelia-synostoses syndrome (Chromosome 8q13 deletion syndrome)	600383	8q13	Mesomelia-synostoses syndrome	600383	AD	Day-Salvatore & McLean et al (1998)	9856555
DEL9p	Chromosome 9p deletion syndrome	158170	9p	Chromosome 9p deletion syndrome	158170	AD	Alfi et al. (1973)	4541805
							Swinkels et al. (2008)	18452192
DER22t11-22	Emanuel syndrome (supernumerary der(22)t(11;22) syndrome)	609029	22q11.2	Emanuel syndrome	609029	Inherited chromosomal imbalance	Carter et al (2009)	19606488
DUP7q11.23	Chromosome 7q11.23 duplication syndrome	609757	7q11.23	Chromosome 7q11.23 duplication syndrome	609757	AD	Van der Aa et al. (2009)	19249392
EYA4	Eyes Absent 4	603550	6q23.2-q24.1	Microcephaly, short stature, PDA, sensorineural hearing loss		AD	Dutrannoy et al (2009)	19576303

Table S3. **Chromosomal deletions, duplications, and additions associated with PDA in the human**. The OMIM database was searched for genes which complied with three major criteria: association with a single-gene syndrome, a database association with PDA, and available references linking to a human PDA phenotype. OMIM searches were limited to single-gene syndromes and made use of both the 'and' command and exhaustive combinations of the terms 'patent,' 'ductus,' 'arteriosus,' 'arterial duct', and 'Botalli". References were validated or compiled manually. Additional online resources including GeneCards, Human Phenotype Ontology, DisGeNET, FindZebra, GeneReviews and UniProtKB were then used to validate the exhaustive nature of the OMIM list with novel genes added.

Table S4	Mouse Model Genes Associated with Single-Gene PDA Syndromes in Humans (n=10 Genes)							
Gene/ Locus	**Gene/Locus name**	**Gene/ Locus MIM number**	**Cytogenetic location**	**Phenotype**	**MIM number**	**Inheritance**	**Reference**	**PMID**
FOXC1	Forkhead, Drosophila, homolog-like 7	601090	6p25.3	Axenfeld-Rieger syndrome, type 3	602482	AD	Baruch and Erickson (2001)	11343302
*GJA1**	Gap junction protein, alpha-1, 43kD (connexin 43)	121014	6q22.31	Hypoplastic left heart syndrome 1	241550	AR	Brekke et al (1953)	13050604
GPC3	Glypican 3	300037	Xq26.2	Simpson-Golabi-Behmel syndrome, type 1	312870	XLR	Yano et al. (2011)	20950395
HPGD	Hydroxyprostaglandin dehydrogenase 15-(NAD)	601688	4q34.1	Hypertrophic osteoarthropathy, primary, autosomal recessive 1	259100	AR	Uppal et al (2008)	18500342
				Digital clubbing, isolated congenital	119900	AR	Sinha et al. (1997)	9402870
				Craniooosteoarthropathy	259100	AR		
JAG1	Jagged 1	601920	20p12.2	Tetralogy of Fallot	187500	AD	Sánchez-Angulo et al (1997)	9410541
				Alagille syndrome 1	118450	AD		
				?Deafness, congenital heart defects, and posterior embryotoxon	617992			
MATR3	Matrin 3	164015	5q31.2	Developmental delay, left ventricular outflow tract defects, bicuspid aortic valve, coarctation of the aorta, PDA		AD	Quintero-Rivera et al (2015)	25574029
MYH11	Myosin, heavy polypeptide-11, smooth muscle	160745	16p13.11	Aortic aneurysm, familial thoracic 4	132900	AD	Glancy et al (2001)	11249915
NOTCH2	Notch, Drosophila, homolog of, 2	600275	1p12	Hajdu-Cheney syndrome	102500	AD	Rosser et al. (1996)	8723560
NOTCH3	Notch, Drosophila, homolog of, 3	600276	19p13.12	Lateral meningocele syndrome	130720	AD	Gripp et al (2015)	25394726
SLCO2A1	Solute carrier organic anion transporter family, member 2A1	601460	3q22.1-q22.2	Hypertrophic osteoarthropathy, primary, autosomal recessive 2	614441	AR	Zhang et al (2012)	22197487
							Chang et al (2010)	20083684
TFAP2B	Transcription factor AP-2 beta (activating enhancer-binding protein 2 beta)	601601	6p12.3	Char syndrome	169100	AD	Khetyar et al. (2008)	18752453
							Davidson (1993)	8326495

*While a mouse model does exist for this gene, it is not of PDA, but premature DA closure. This gene was included as it is likely still relevant for both human and mouse DA biology

Table S4: Mouse Model Genes Associated with Single-Gene PDA Syndromes in Humans. Our list of genetic mouse models of PDA was compared to our OMIM generated list of human single gene syndromes associated with PDA. This resulted in the identification of 10 mouse models of PDA which have associated single-gene syndromes in humans. Additionally, one gene was found to have a human single-gene syndrome associated with PDA and a mouse model in which the DA closes prematurely *in utero.*

Table S5 **GO, KEGG, and UP Keywords Common Between Human PDA Syndromes and Mouse Models of PDA**

GO Biological Process - Overlap: 57/137 Common, 41.6%	Human Count[1]	Human p Value	Mouse Count	Mouse p Value
GO:0000122~negative regulation of transcription from RNA polymerase II promoter	41	2.01E-15	8	7.37E-05
GO:0001568~blood vessel development	6	1.12E-04	4	1.59E-04
GO:0001569~patterning of blood vessels	4	5.22E-03	2	5.81E-02
GO:0001570~vasculogenesis	6	7.08E-04	4	1.39E-04
GO:0001658~branching involved in ureteric bud morphogenesis	5	1.93E-03	3	2.32E-03
GO:0001701~in utero embryonic development	16	1.63E-08	5	9.52E-04
GO:0001756~somitogenesis	5	1.46E-03	2	8.04E-02
GO:0001822~kidney development	7	7.85E-04	4	9.36E-04
GO:0001947~heart looping	14	5.86E-13	3	3.84E-03
GO:0001974~blood vessel remodeling	7	2.67E-06	3	1.87E-03
GO:0003007~heart morphogenesis	4	7.61E-03	3	4.09E-03
GO:0003151~outflow tract morphogenesis	9	1.01E-07	3	2.93E-03
GO:0003184~pulmonary valve morphogenesis	4	2.26E-04	2	1.63E-02
GO:0003281~ventricular septum development	4	5.22E-03	2	5.53E-02
GO:0006351~transcription, DNA-templated	43	4.12E-04	11	2.35E-04
GO:0006355~regulation of transcription, DNA-templated	33	2.56E-03	11	1.09E-03
GO:0006357~regulation of transcription from RNA polymerase II promoter	12	2.54E-02	5	2.69E-03
GO:0007219~Notch signaling pathway	10	1.58E-05	5	3.38E-05
GO:0007507~heart development	30	1.10E-23	9	2.96E-09
GO:0007512~adult heart development	4	5.24E-04	3	2.54E-04
GO:0008284~positive regulation of cell proliferation	19	2.88E-05	10	5.29E-08
GO:0008285~negative regulation of cell proliferation	14	1.68E-03	8	1.14E-06
GO:0009887~organ morphogenesis	7	1.12E-03	3	1.15E-02
GO:0009948~anterior/posterior axis specification	3	1.92E-02	2	3.24E-02
GO:0010468~regulation of gene expression	5	3.85E-02	3	7.68E-02
GO:0010628~positive regulation of gene expression	14	3.11E-05	7	2.22E-05
GO:0010862~positive regulation of pathway-restricted SMAD protein phosphorylation	4	2.29E-02	2	6.93E-02
GO:0030154~cell differentiation	11	7.07E-02	5	2.74E-02
GO:0030199~collagen fibril organization	4	1.31E-02	2	5.67E-02
GO:0030308~negative regulation of cell growth	6	1.91E-02	3	1.49E-02
GO:0030324~lung development	13	1.94E-10	3	1.46E-02
GO:0030335~positive regulation of cell migration	8	9.16E-03	3	3.66E-02
GO:0030513~positive regulation of BMP signaling pathway	6	4.07E-05	5	2.25E-07
GO:0030900~forebrain development	4	2.05E-02	3	7.26E-03
GO:0032924~activin receptor signaling pathway	4	9.98E-04	2	2.07E-02
GO:0035050~embryonic heart tube development	6	8.48E-07	2	3.38E-02
GO:0035116~embryonic hindlimb morphogenesis	4	5.22E-03	3	1.10E-03
GO:0035909~aorta morphogenesis	5	1.65E-05	2	2.22E-02
GO:0042127~regulation of cell proliferation	6	8.69E-02	5	3.38E-04
GO:0042475~odontogenesis of dentin-containing tooth	4	3.26E-02	3	3.96E-03
GO:0042493~response to drug	8	9.23E-02	4	1.37E-02
GO:0042733~embryonic digit morphogenesis	11	1.87E-09	2	9.41E-02
GO:0043066~negative regulation of apoptotic process	14	5.48E-03	4	5.12E-02
GO:0043410~positive regulation of MAPK cascade	7	5.71E-04	3	1.05E-02
GO:0045669~positive regulation of osteoblast differentiation	8	1.05E-05	5	3.01E-06
GO:0045892~negative regulation of transcription, DNA-templated	22	1.58E-06	4	5.41E-02
GO:0045893~positive regulation of transcription, DNA-templated	38	6.23E-18	11	5.15E-09
GO:0045944~positive regulation of transcription from RNA polymerase II promoter	45	1.38E-13	11	8.70E-07
GO:0048844~artery morphogenesis	6	5.40E-06	3	6.31E-04
GO:0051145~smooth muscle cell differentiation	4	5.24E-04	2	2.66E-02
GO:0055010~ventricular cardiac muscle tissue morphogenesis	6	1.35E-05	2	4.10E-02
GO:0060038~cardiac muscle cell proliferation	4	5.24E-04	3	2.88E-04
GO:0060045~positive regulation of cardiac muscle cell proliferation	6	6.92E-06	2	3.38E-02
GO:0060389~pathway-restricted SMAD protein phosphorylation	3	1.14E-02	2	1.92E-02
GO:0060982~coronary artery morphogenesis	3	3.22E-03	2	1.34E-02
GO:0072017~distal tubule development	3	4.76E-04	2	4.47E-03
GO:0097070~ductus arteriosus closure	4	1.98E-05	4	5.92E-08
GO Cellular Component - Overlap: 9/24 Common, 37.5%	**Count**	**p Value**	**Count**	**p Value**
GO:0000790~nuclear chromatin	9	2.17E-03	3	3.89E-02
GO:0005578~proteinaceous extracellular matrix	7	9.95E-02	3	6.95E-02
GO:0005634~nucleus	94	1.97E-05	16	6.09E-03
GO:0005654~nucleoplasm	71	1.97E-10	9	3.48E-03
GO:0005667~transcription factor complex	14	5.33E-07	3	5.16E-02
GO:0005737~cytoplasm	78	1.48E-02	14	8.57E-02
GO:0005925~focal adhesion	9	9.43E-02	5	1.88E-03
GO:0016020~membrane	43	1.16E-03	15	6.11E-02
GO:0043234~protein complex	13	3.83E-03	6	1.47E-03

GO Molecular Function - Overlap: 12/25 Common, 48.0%	Count	p Value	Count	p Value
GO:0000977~RNA polymerase II regulatory region sequence-specific DNA binding	11	2.63E-04	3	4.56E-02
GO:0001077~transcriptional activator activity, RNA polymerase II core promoter proximal region sequence-specific binding	12	1.71E-04	4	8.15E-03
GO:0001105~RNA polymerase II transcription coactivator activity	6	8.56E-05	3	1.82E-03
GO:0003677~DNA binding	36	1.28E-03	7	5.92E-02
GO:0003682~chromatin binding	27	2.57E-12	4	3.44E-02
GO:0003700~transcription factor activity, sequence-specific DNA binding	34	8.24E-08	5	4.53E-02
GO:0003713~transcription coactivator activity	9	1.18E-02	5	1.60E-04
GO:0005515~protein binding	154	1.35E-10	16	3.20E-04
GO:0008134~transcription factor binding	13	2.17E-04	6	1.59E-04
GO:0043565~sequence-specific DNA binding	26	5.82E-09	5	1.55E-02
GO:0044212~transcription regulatory region DNA binding	18	1.21E-09	3	5.01E-02
GO:0046982~protein heterodimerization activity	13	1.28E-02	4	4.41E-02
KEGG Pathway - Overlap: 10/15 Common, 66.7%	**Count**	**p Value**	**Count**	**p Value**
hsa04320:Dorso-ventral axis formation	4	9.48E-03	2	4.46E-02
hsa04330:Notch signaling pathway	6	1.07E-03	4	8.42E-05
hsa04810:Regulation of actin cytoskeleton	9	2.18E-02	3	5.58E-02
hsa04919:Thyroid hormone signaling pathway	11	1.68E-05	4	1.02E-03
hsa05200:Pathways in cancer	14	1.19E-02	5	4.55E-03
hsa05205:Proteoglycans in cancer	12	4.14E-04	4	5.32E-03
hsa05206:MicroRNAs in cancer	12	7.09E-03	4	1.24E-02
hsa05213:Endometrial cancer	4	5.34E-02	2	9.07E-02
hsa05410:Hypertrophic cardiomyopathy (HCM)	5	3.89E-02	3	8.75E-03
hsa05412:Arrhythmogenic right ventricular cardiomyopathy (ARVC)	4	9.73E-02	4	2.15E-04
UP_Keywords - Overlap: 11/29 Common, 37.9%	**Count**	**p Value**	**Count**	**p Value**
Activator	33	6.73E-13	8	6.34E-06
Calcium	15	8.37E-02	5	1.58E-02
Developmental protein	28	3.02E-06	6	5.35E-03
Differentiation	14	2.58E-02	4	4.05E-02
EGF-like domain	9	3.95E-03	5	1.36E-04
Metal-binding	67	3.51E-06	8	9.76E-02
Notch signaling pathway	5	2.07E-03	4	2.36E-05
Nucleus	93	4.70E-08	12	1.09E-02
Phosphoprotein	140	1.12E-12	15	3.82E-02
Transcription	66	3.43E-13	11	3.07E-05
Transcription regulation	64	1.06E-12	11	2.31E-05

[1]Number of genes identified within each term

Table S5: GO, KEGG, and UP Keywords Common Between Human PDA Syndromes and Mouse Models of PDA. Our list of genetic mouse models of PDA and our OMIM generated list of human single gene syndromes associated with PDA were assessed for predicted biological terms using Gene Ontology Biological Process, Cellular Component, and Molecular Function as well as KEGG Pathway analysis and UniProt Keywords. Resulting terms, counts, and p-values are reported. P-Value in this context refers to the probability that a given number of genes out of the total n genes in a list annotates to a particular GO term, based on the proportion of genes in the genome annotated to that particular GO term.

Chapter 4

PGE_2 SIGNALING THROUGH EP_4 MEDIATES AN UNEXPECTED DEVELOPMENTAL ROLE IN DA MATURATION ESSENTIAL FOR ESTABLISHING THE CONTRACTILE PROPERTIES AND REMODELING POTENTIAL REQUIRED FOR DA CLOSURE AFTER BIRTH

Adapted with permission from: Michael T. Yarboro, Naoko Boatwright, M.S., Deanna C. Sekulich, Chris Hooper, Ting Wong, Pharm.D., Stanley D. Poole, M.S., Courtney D. Berger, P.A., Alexus J. Brown, Chris Jetter, M.S., Jennifer M. S. Sucre, M.D., Elaine L. Shelton, Ph.D., and Jeff Reese, M.D. (2023) A Novel Role for PGE_2-EP_4 in the Developmental Programing of the Mouse Ductus Arteriosus: Consequences for Vessel Maturation and Function. DOI:10.1152/ajpheart.00294.2023

Abstract:

Fetal DA patency requires vasodilatory signaling via the PGE_2 receptor EP_4. However, in humans and mice, disrupted PGE_2-EP_4 signaling *in utero* causes unexpected PDA after birth, suggesting another role for EP_4 during development. We used EP_4 KO mice and acute versus chronic pharmacologic approaches to investigate EP_4 signaling in DA development and function. Expression analyses identified EP_4 as the primary EP receptor in the DA from mid-gestation to term; inhibitor studies verified EP_4 as the primary dilator during this period. Chronic antagonism recapitulated the EP_4 KO phenotype and revealed a narrow developmental window when EP_4 stimulation is required for postnatal DA closure. Myography studies indicate that despite reduced contractile properties, the EP_4 KO DA maintains an intact

O_2 response. In newborns, hyperoxia constricted the EP_4 KO DA but survival was not improved and permanent remodeling was disrupted. Vasomotion and increased NO sensitivity in the EP_4 KO DA suggest incomplete DA development. Analysis of DA maturity markers confirmed a partially immature EP_4 KO DA phenotype. Together, our data suggest that EP_4 signaling in late gestation plays a key developmental role in establishing a functional term DA. When disrupted in EP_4 KO mice, the postnatal DA exhibits signaling and contractile properties characteristic of an immature DA including impairments in the first, muscular phase of DA closure, in addition to known abnormalities in the second permanent remodeling phase.

Introduction:

The DA is a fetal vessel which shunts blood past the lungs *in utero* to protect the developing pulmonary vasculature and direct freshly oxygenated blood from the placenta into the systemic circulation. While the DA is essential during fetal development, its postnatal closure is critical for circulatory transition to neonatal life. DA constriction is an elegant cascade of biological processes requiring acute changes in vascular tone, fluidity in cell phenotypes, and both prenatal and postnatal structural remodeling (1, 2). Frequently, disruptions in these genetic, environmental, and developmental processes result in failure of the DA to close, termed PDA. PDA comprises ~10% of congenital heart defect cases in the US (29) and is disproportionately common amongst preterm (64% at 27-28 weeks) and very preterm infants (87% at 24 weeks) (31). Adverse outcomes related to PDA can be severe, especially in preterm and low-birth weight neonates (38).

Prostaglandin signaling plays a critical role in the development and function of the DA. Prostaglandin precursors produced by the cyclooxygenase enzymes, COX-1 and -2 are

converted to PGE_2 by specific PGE synthases. PGE_2 actions are mediated by a family of G-protein coupled receptors, including the PGE receptors EP1, 2, 3, and 4 which have diverse cellular distribution and functions (168, 213, 256, 512). PGE_2 has potent vasodilatory effects on the DA and is clinically used to maintain DA patency after birth in newborns with cyanotic congenital heart lesions. Conversely, COX inhibitors are used to induce constriction of hemodynamically significant PDAs in preterm infants (38). EP_4 is the primary prostanoid receptor expressed in both the rat (146) and human (263, 264) DA and is upregulated compared to surrounding vessels (114, 265). After birth, initiation of respiration results in increased O_2 tension and the initial constriction of the DA through mechanisms that are not fully understood (1, 2, 25, 513, 514). High levels of HPGD expression in the newly inflated lungs rapidly metabolizes circulating PGE_2, removing a dilatory signal and furthering constriction (23, 24).

The importance of developmental timing in fetal PGE_2 signaling was first supported by observations that maternal exposure to COX inhibitors, given as a tocolytic to arrest preterm labor, results in *fetal DA constriction* after 30-32 weeks of gestation, but not earlier in pregnancy (45, 46). In contrast, mothers who received COX inhibitors as tocolytics during late- but not mid-gestation had an increased risk of PDA in their offspring (47). This maturation-dependent response was confirmed pharmacologically in mice (195-197) and COX-1;COX-2 double KO mice were generated which consistently produced a PDA phenotype coupled with congestive heart failure and early neonatal death (106, 107). In addition, three separate EP_4 KO mouse models have been produced (108-110), all of which exhibit PDA and neonatal death with high penetrance, confirming the importance of the PGE_2-EP_4 receptor signaling axis in the DA. However, the COX double KO and EP_4 KO models are considered “paradoxical PDAs” since the removal of a vasodilatory signaling pathway would be expected to result in DA

constriction rather than PDA (272). These findings suggest that PGE_2-EP_4 signaling may play a secondary developmental role in the DA, beyond acute regulation of DA tone. While significant research has shown alterations in gene expression (113) and matrix biology of the EP_4 KO DA (146, 147, 375, 396, 477), a complete mechanistic explanation for their PDA phenotype has proven elusive.

Here, we utilized pharmacological inhibition studies (Protocols for the specific timing of different inhibitors provided in **Figure 1**), pressurized myography of isolated vessels, primary culture methods, and survival studies to assess the role of EP_4 in DA development and function. Specifically, we set out to determine the developmental window in which EP_4 is critical for proper DA development, and whether the EP_4 KO DA resulted from impaired contractile potential, biomechanical properties, and or deficient O_2 response. We hypothesized that PGE_2-EP_4 signaling mediates a time-dependent developmental program essential for establishing the contractile properties and O_2-sensing capabilities necessary to close the mature DA.

Results:

EP_4 is the Primary Mediator of Prostanoid Signaling in the DA:

To determine the magnitude and timing of PGE receptor expression, RT-qPCR was performed on D15-19 DAs for the four prostanoid receptor genes *Ptger1*, *Ptger2*, *Ptger3*, and *Ptger4* (EP1, 2, 3 and 4 respectively) (**Figure 2A**). EP_4 was significantly upregulated at D16 and maintained this upregulation into the postnatal period. Cell-specific localization of *Ptger4* transcripts revealed low levels of EP_4 expression in the D19 pulmonary artery and Ao, but strong expression in the medial layer of the DA (**Figure 2B**). *Ptger4* expression persisted in the

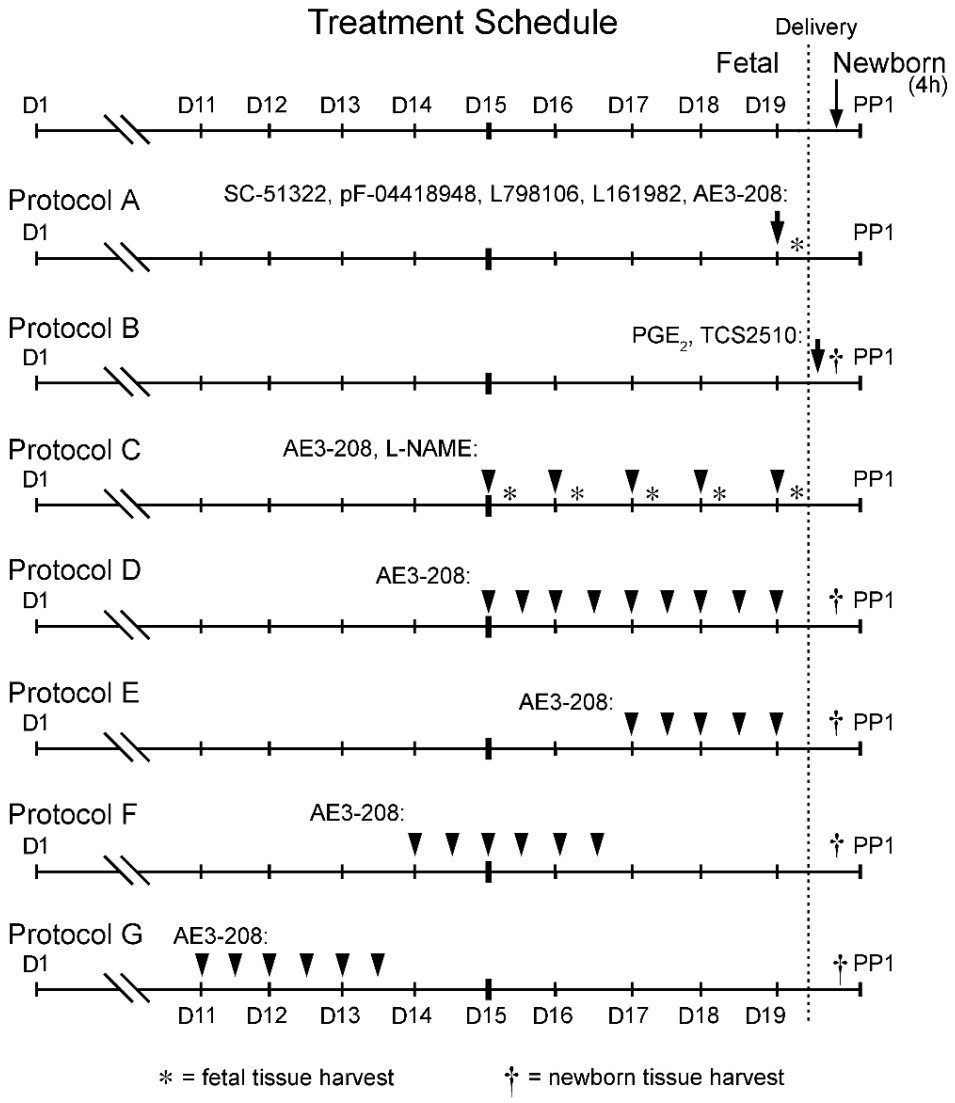

Figure 1. Drug treatment protocols. Pregnant dams were treated with selective agonists to the prostaglandin E receptors EP_1 (SC-51322), EP_2 (pF-04418948), EP_3 (L798,106), and EP_4 (L161,982, ONO-AE3-208), a selective agonist to EP_4 (TCS2510), PGE_2, or an inhibitor of NO synthase (L-NAME) on the indicated days of gestation [Day (D)1 = presence of vaginal plug]. Fetal exposure studies: ***Protocol A*** examined the effect of acute EP receptor antagonism on the *in utero* DA, with DA scoring 4hrs after maternal i.p. administration. Neonatal injection studies: ***Protocol B*** examined the effect of postnatal EP receptor stimulation on DA constriction, with drugs being administered to offspring 30 min after delivery and DA scoring 4hrs later. Maternal gavage studies: ***Protocol C*** examined how inhibition of EP_4 or NO synthase affected fetal DA patency on select days of pregnancy. Drugs were administered the morning of the indicated day and DA patency assessed 4hrs later. Chronic gavage studies: ***Protocol D*** examined the effect of chronically inhibiting EP_4 signaling over a defined window of pregnancy. Mice were delivered via caesarean section on the morning of D19 with their DAs scored 4hrs later. This approach was repeated during discrete windows in ***Protocols E, F, and G***. PP1, postpartum *day* 1.

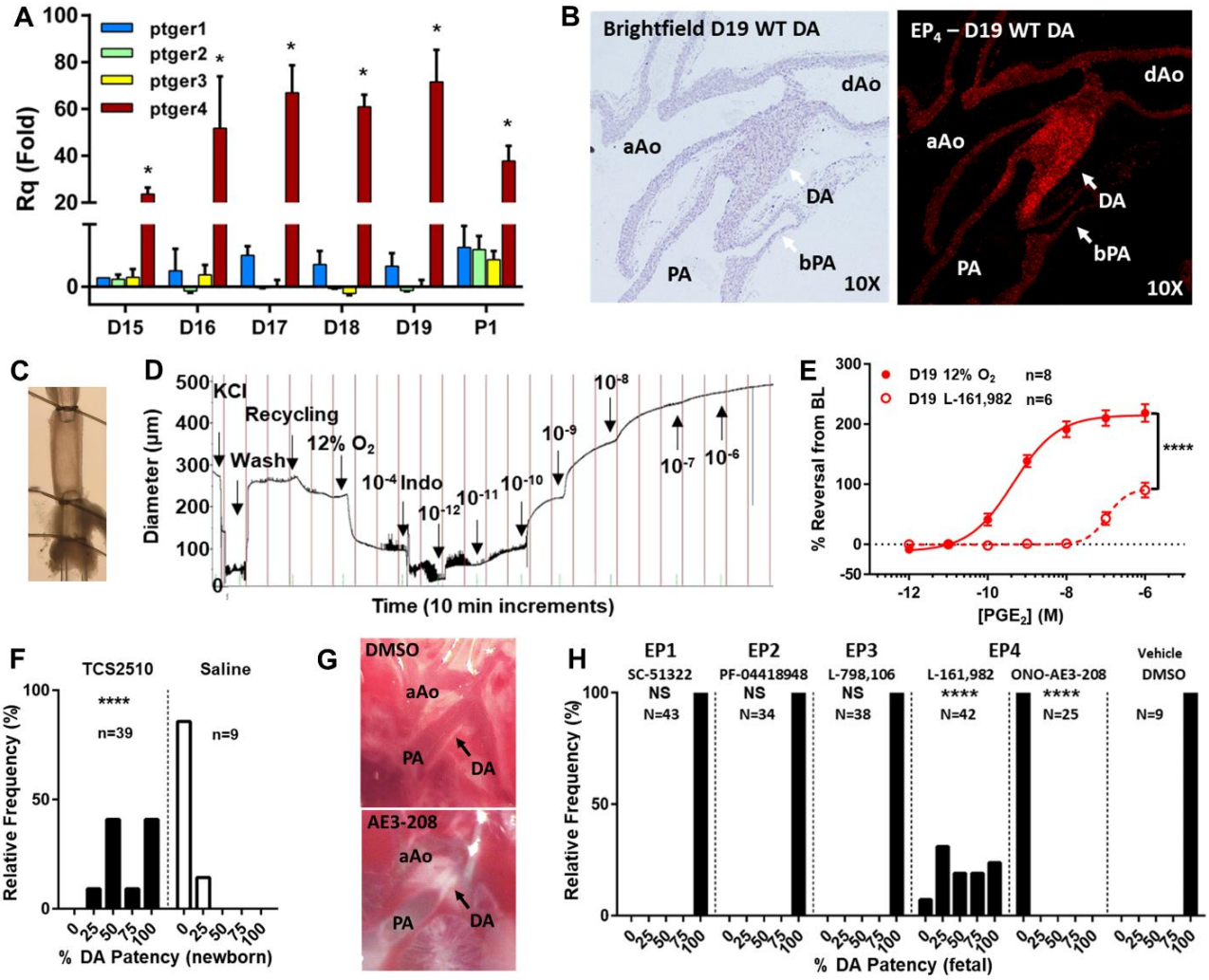

Figure 2. EP_4 is the predominant EP receptor in the mouse DA. A) Time course of EP receptor expression in the DA. *Ptger4* expression increased with advancing gestation compared to D15 ($p<0.05$; Kruskal-Wallis) and was significantly greater than individual EP subtypes at each gestational stage (*, $p<0.05$; Kruskal-Wallis) (n=3 biological replicates). **B**) Localization of *Ptger4* (EP_4) expression in the DA and outflow tracts by RNA Scope. **C**) Cannulated *ex vivo* preparation of D19 CD1 WT DA for vessel myography. **D**) Representative tracing of a PGE_2 concentration response curve (CRC) and **E**) cumulative response curves of EP_4-inhibited and control DAs following O_2-induced pre-constriction, demonstrating the potent and EP_4-predominant effects of PGE_2 on the isolated DA. **F**) *In vivo* studies demonstrate a shift in neonatal DA patency rates in response to injections of the selective EP_4 agonist TCS2510, resulting in PDA. **G**) Representative images of DA patency in response to selective EP receptor antagonists, scored on a 5-point non-continuous scale, showing 100% patency (top) and 0% patency (bottom). **H**) *In utero* exposure to selective EP receptor antagonists resulted in fetal DA constriction in response to two selective EP_4 antagonists, but not to EP_1 EP_2, or EP_3 antagonists. AE3-208 was used in subsequent EP_4 inhibitor studies due to its increased potency and DA effects. ****, $p<0.001$ compared to control (**E**) or vehicle (**F**, **H**) (**A**, Kruskal-Wallis; **E**, 2-way ANOVA; **F**, **H**, χ^2) (DA- ductus arteriosus, aAo- ascending aorta, dAo- descending aorta, PA- pulmonary artery, bPA- branch pulmonary artery).

medial and endothelial layers of the closed DA on postpartum day 1 (**Figure 3**). Because EP_4 null mice unexpectedly have a PDA phenotype, the role of EP_4 in mediating acute DA tone was assessed through pressurized vessel myography (**Figure 4**). Isolated WT vessels (**Figure 2C**) exposed to increasing concentrations of PGE_2 (**Figure 2D**) or the selective EP_4 agonist TCS2510 (**Figure 5A**) displayed a potent concentration-dependent vasodilatory response. This effect was significantly attenuated by pretreatment with a selective EP_4 antagonist (L-161,982) (**Figure 2E**). Direct injection of L-161,982 into the fetal intraperitoneal compartment (**Figure 5B-E**) also caused DA constriction, suggesting that EP_4 mediates PGE_2's acute vasodilatory effects in the fetal DA. To determine the role of EP_4 on DA tone *in vivo*, the EP_4 agonist TCS2510 was administered to newborn pups following delivery (**Protocol B, Figure 1**). After 4hrs, DA closure was impaired in treated animals resulting in PDA (**Figure 2F**), similar to the effects of PGE_2 infusion in newborn infants. To determine the *in vivo* contributions of other EP receptors, DA patency was scored in fetuses 4h after maternal injection with a selective EP receptor antagonist (**Protocol A, Figure 1**). While antagonism of EP1, 2, and 3 had no detectable effect on fetal DA caliber, antagonism of EP_4 led to significant constriction of the DA (**Figure 2G-H**). Constriction of the fetal DA by AE3-208 was more extensive than by L-161,982, thus AE3-208 was used for all subsequent EP_4 antagonist experiments. Collectively, these data suggest that EP_4 is the primary prostanoid receptor expressed in the DA and that it mediates the vasodilatory effects of PGE_2.

***The Acute Role of EP_4 in the DA is Dependent on Developmental Timing*:**

To determine when EP_4 gains a significant role as a vasodilator in the developing DA, dams were given a single dose of the AE3-208 selective EP_4 antagonist on different days of

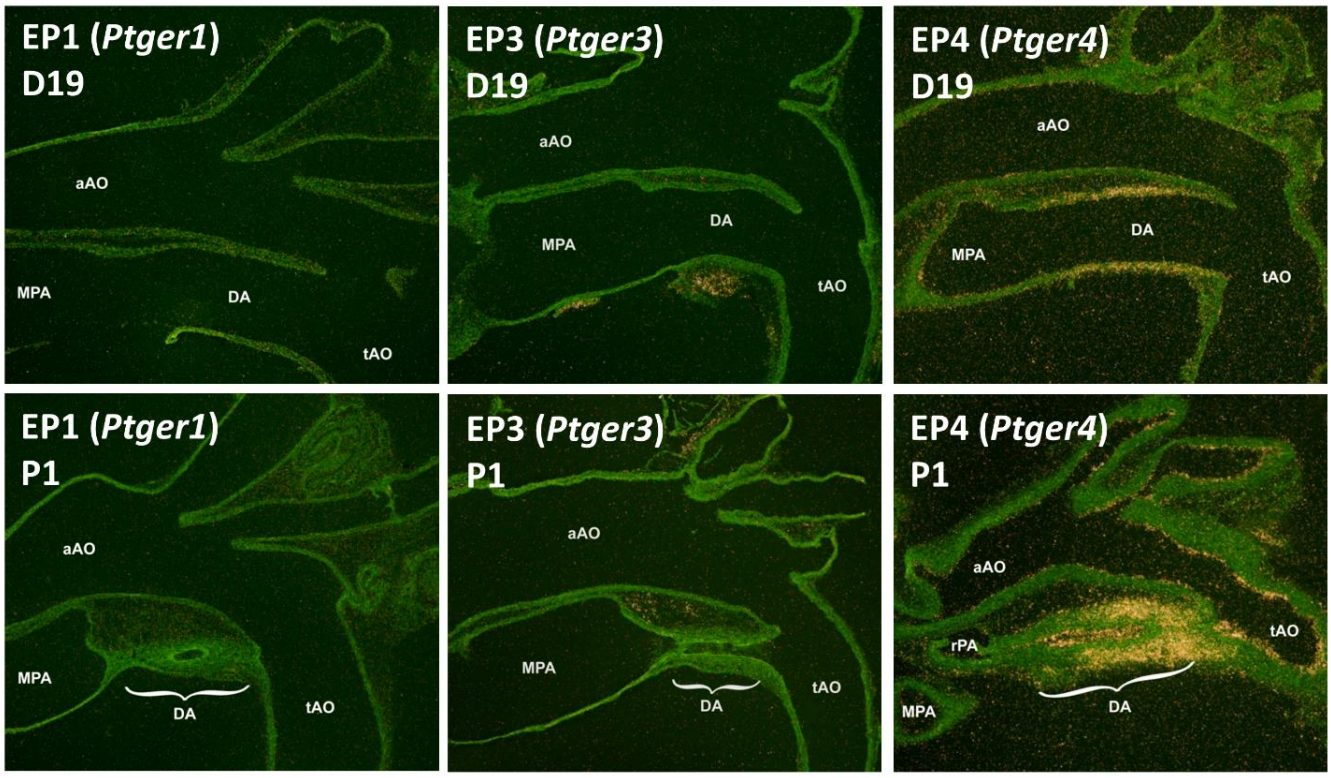

Figure 3. *Ptger4* expression is strongly localized to the medial and intimal layers of the patent fetal and closed postnatal (P1) DA. *In situ* hybridization of D19 (upper panel) and P1 (lower panel) outflow tracts radiolabeled for *Ptger1*, *Ptger3*, and *Ptger4*. Due to undetectable expression levels in initial PCR experiments, *Ptger2* was not assessed via *in situ* hybridization (DA- ductus arteriosus, aAo- ascending aorta, tAo- transverse aorta, MPA- main pulmonary artery).

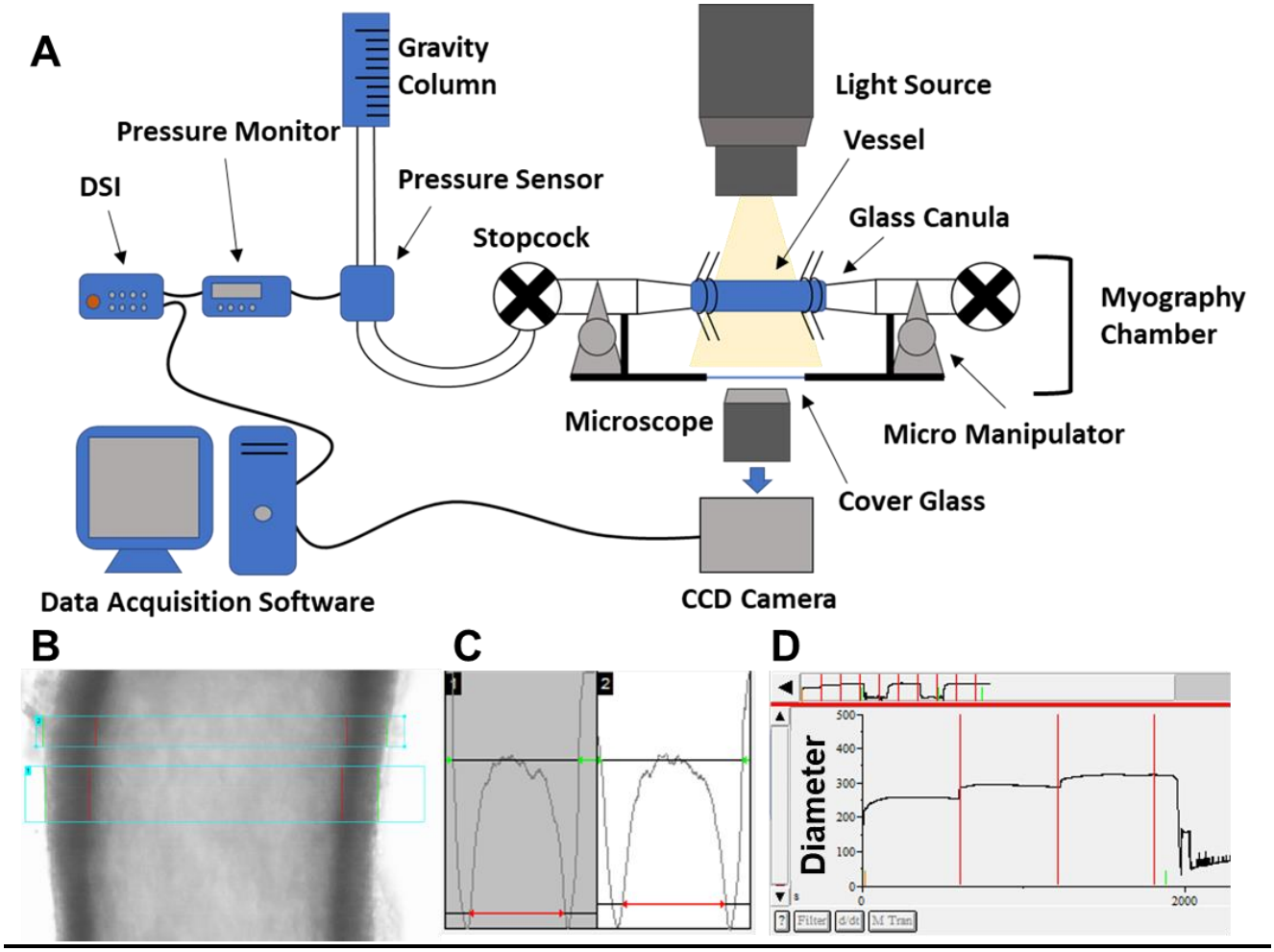

Figure 4. Use of pressurized vessel myography to assess the mouse DA. A) Fresh DA tissue is excised in cold deoxygenated Kreb's solution to minimize O_2-mediated constriction and tissue degradation. The DA is then mounted on glass micropipettes in a specialized myography chamber, its lumen pressurized via gravity column, and superfused with Kreb's solution at physiological temperature, isotonicity, and fetal pO_2. **B)** The DA is visualized and recorded on an inverted light microscope with video and pressure recordings synthesized via Ionwizard data acquisition software (IonOptix). **C)** Ionwizard creates a greyscale map of the vessel and automatically detects the vessel lumen (red) and outer wall (green). **D)** This is recorded as a tracing of lumen diameter (μm) and pressure over time, allowing the monitoring of vasoconstriction and dilation in response to various stimuli.

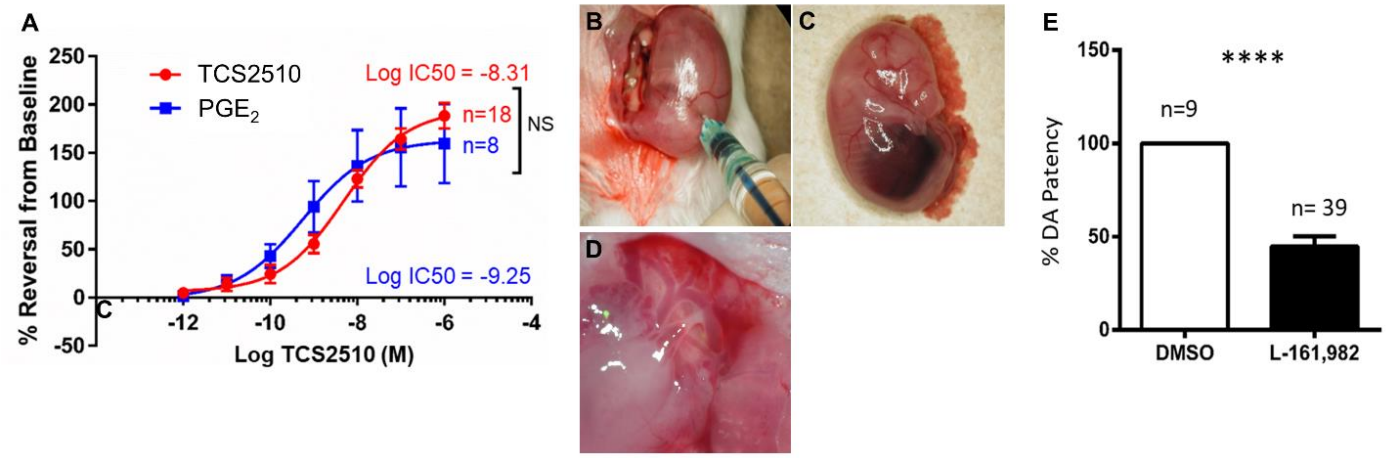

Figure 5. Selective antagonism of EP_4 constricts the DA *in utero*. **A**) CRC of PGE_2 and the selective EP_4 receptor agonist (TCS2510) indicating that the vasodilatory effects of PGE_2 are primarily accounted for by EP_4 stimulation. **B**) Due to limited information on the transplacental passage of EP receptor antagonists, a selective EP_4 antagonist (L-161,982; 100mg/kg) mixed with Chicago Blue B dye (Sigma) to enhance visualization was directly administered into the fetal abdominal cavity via transuterine i.p. injection. Exteriorized uterine horns were returned to the maternal abdominal cavity and dams were briefly allowed to ambulate. **C**) Representative image of post-injection pup showing blue labeling in the peritoneal cavity. **D**) Representative image of outflow tracts of accurately injected fetus demonstrating constricted DA at 30-40 minutes after fetal i.p. injection. **E**) Comparison of DA patency demonstrating a significant fetal DA constriction following EP_4 antagonism compared to vehicle-injected fetuses. ****, $p<0.001$. (**A**, 2-way ANOVA; **B,** *t*-test).

pregnancy (**Protocol C, Figure 1**). Antagonism of EP_4 was found to have little effect on D15 and D16, more significant effects on D17, and complete *in utero* DA constriction on D18 and D19 (**Figure 6A**). Corresponding myography studies comparing PGE_2 concentration response curves (CRCs) in the term (D19) and premature (D15) DA revealed a significantly diminished response in the premature DA (**Figure 6B**). In a parallel experiment, an NO synthase inhibitor (L-NAME) given to dams on different days of pregnancy revealed significant effects on DA tone on D15 and D16, but not on D17-19 of gestation (**Figure 6C**). Together, these data suggest that NO is the primary dilator in the fetal DA until D17 when PGE_2 acting via EP_4 begins to subsume this role (**Figure 6D**).

EP_4 is Indispensable for DA Development from D17-19:

Chronic pharmacological inhibition of the EP_4 receptor during discrete windows of pregnancy was used to mimic the EP_4 KO phenotype in order to determine when EP_4 signaling serves in a developmental role. First, we observed that dams given the selective EP_4 antagonist AE3-208 from D15-19 of pregnancy (**Protocol D, Figure 1**) had pups with varying degrees of PDA at 4h of age compared to fully closed DAs in vehicle-treated mice (**Figure 7**). The PDA phenotype in offspring exposed to chronic pharmacological inhibition was more pronounced in C57BL/6J than CD1 mice or mice with a mixed genetic background (**Figure 7A, B**). Similarly, attempts to cross the EP_4 null allele (B6.129S6-*Ptger4*$^{tm1.2Matb}$) into CD1 mice resulted in increased survival of KO mice at weaning (**Figure 7C**) and loss of the PDA phenotype (**Figure 7D**). While EP_4 KO (B6;129-*Ptger4*^{tm1Sna}) mice were found at the expected Mendelian ratio at the time of birth (20 KO, 24 WT, 47 Het), at the time of weaning both EP_4 KO models on either a C57BL/6J (4 KO, 142 WT, 188 Het) or CD1 (50 KO, 118 WT, 197 Het)

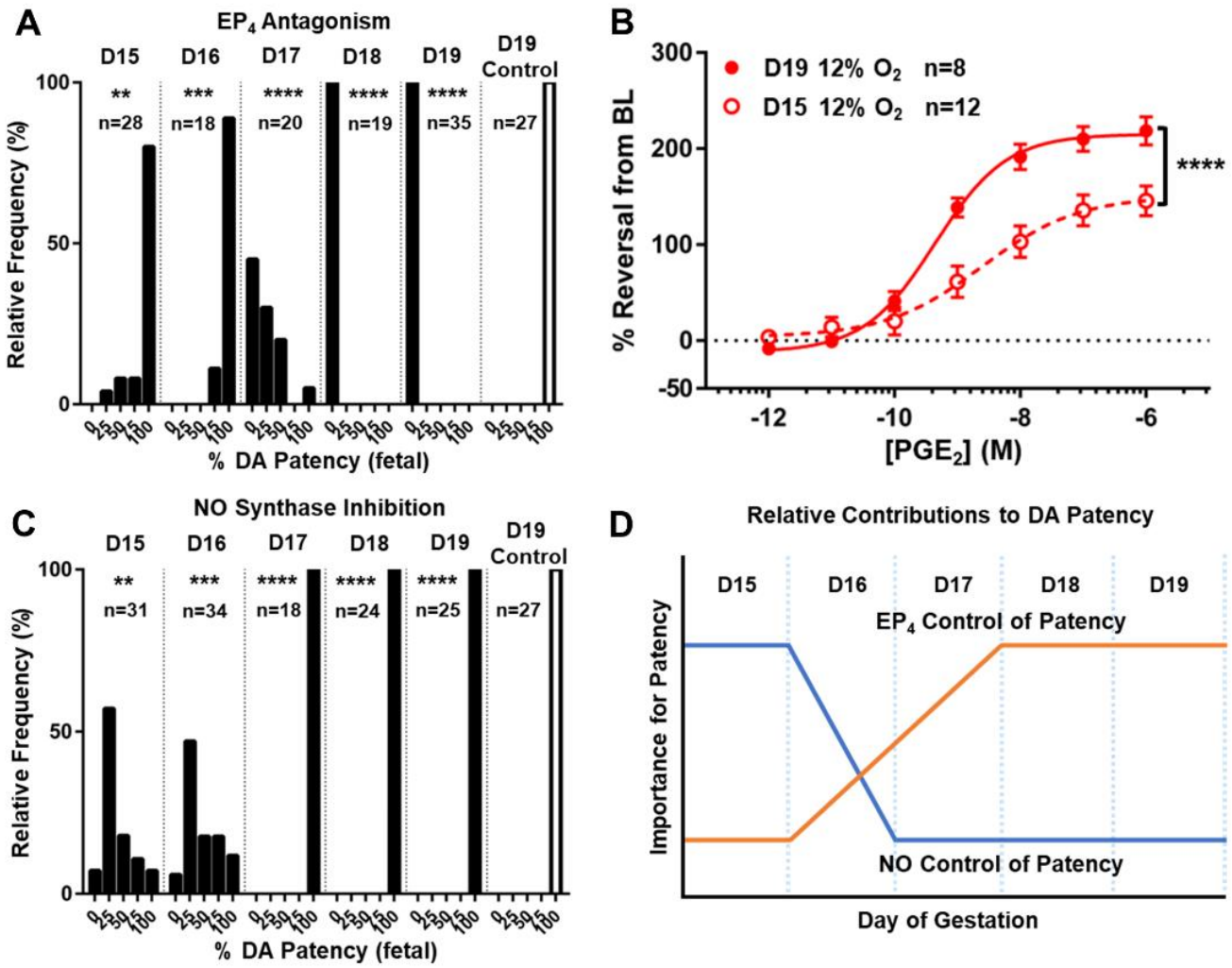

Figure 6. The role of EP_4 in DA patency is dependent on gestational timing. A) Response of the *in vivo* fetal DA to a selective EP_4 antagonist demonstrates late DA constriction and a gestational stage-specific shift in sensitivity of the developing DA to disruption of PGE_2-EP_4 signaling between D16-17 of pregnancy. **B**) Cumulative PGE_2 response curves similarly show that the pre-constricted *ex vivo* immature D15 DA is significantly less sensitive to PGE_2 exposure compared to D19 DAs. **C**) In contrast, the response of the *in vivo* fetal DA to a selective NO synthase antagonist showed limited effects in late gestation but significant fetal DA constriction at immature time points. **D**) Schematic diagram depicting reciprocal shifts in DA dependence on PGE_2-EP_4 and NO signaling for patency with advancing gestation. **, $p<0.01$; ***, $p<0.005$; ****, $p<0.001$ compared to controls (**A**, **C**) or between gestations (**B**) (**B**, 2-way ANOVA) (DA- ductus arteriosus, NO- nitric oxide).

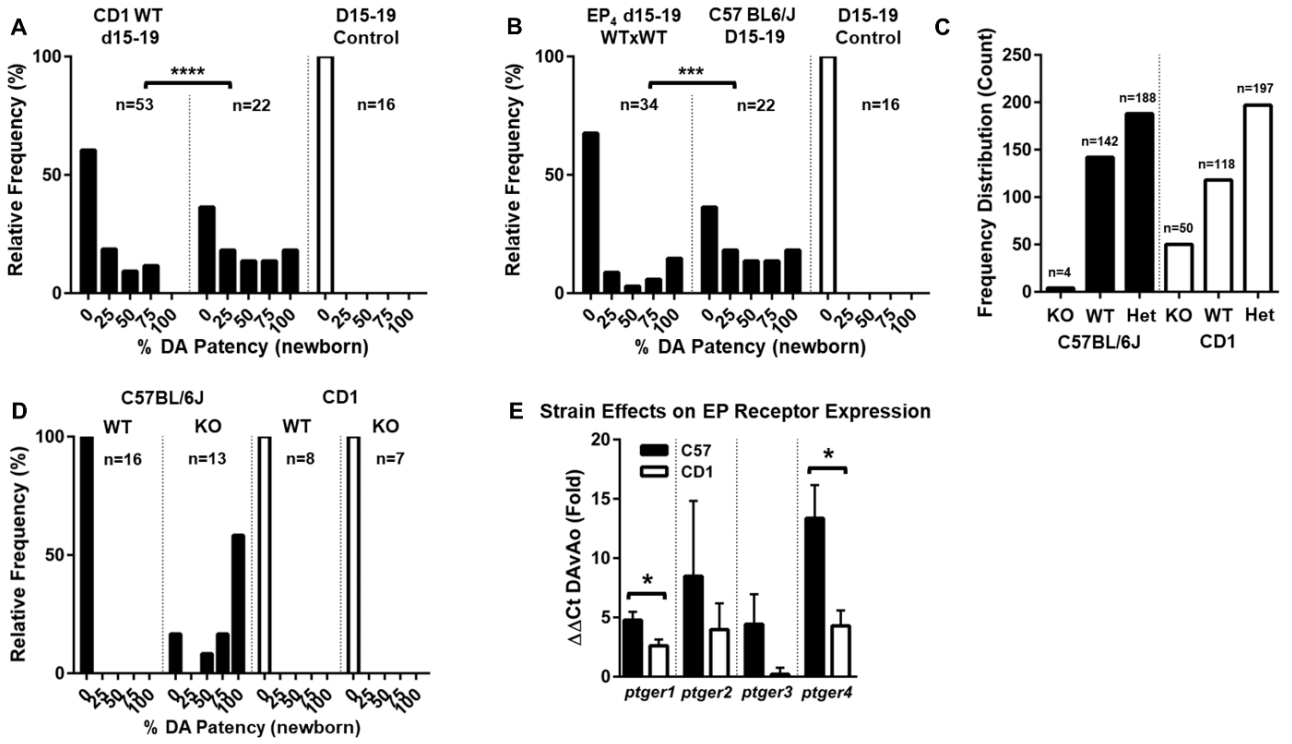

Figure 7. Mouse strain has an effect on EP receptor expression and function. A) Response of the neonatal DA to chronic EP_4 antagonist exposure during D15-D19 of gestation demonstrating different rates of failed DA closure (PDA) at 4h of age in C57BL/6J mice compared to CD1 WT. **B**) Response of the neonatal DA to chronic EP_4 antagonist exposure during D15-D19 of gestation demonstrating that offspring of WT dams on the mixed genetic background of our EP_4 colony (left graph) did not increase the PDA phenotype compared to offspring of C57BL6/J dams (right graph) despite all KO pups dying of PDA. **C**) Frequency distribution of KO mice of different backgrounds that survived to weaning in our colony. While neither group displayed the expected Mendelian distribution, KOs on a CD1 background survive at a much higher rate than on a C57BL/6J background. **D**) Differing levels of PDA in KO mice from different background strains. **E**) RT-qPCR analyzing the effects of mouse strain on relative EP receptor expression between DA and Ao indicated CD1 mice trend towards decreased expression of all EP receptors, *Ptger1* and *Ptger4* significantly. (n=3 biological replicates) *, $p<0.05$; ***, $p<0.005$; ****, $p<0.001$. (**A**, **B**, **D**, χ^2; **E**, *t*-test).

background were no longer Mendelian, consistent with neonatal death. Though post-neonatal losses of KO mice on the CD1 background still occurred, they were significantly less severe. These findings may be related to strain-specific differences in EP receptor expression (**Figure 7E**).

Next, we compared chronic pharmacological EP_4 inhibition during three shorter windows (D11-13, D14-16, and D17-19) (**Protocols E**, **F**, and **G, Figure 1**), revealing that drug treatment over the D14-16 window had no effect on postnatal DA closure at 4h of age, whereas inhibition from D17-19 resulted in significant DA patency compared to control and a phenotype that recapitulated the EP_4 KO (**Figure 8A**). Pups similarly grew weak and dusky after birth, occasionally succumbing near 4hr of age (**Figure 8B**). Inhibition during the D11-13 window revealed an EP_4-dependent neonatal death phenotype independent of PDA, likely representing drug effects that are off-target or not specific to DA function (**Figure 8C**). Together, these data show that EP_4 plays a temporal role in DA development during the D17-19 window which is indispensable for accomplishing postnatal DA closure (**Figure 8D**).

EP_4 Plays a Non-Matrix Role in Migratory Potential of DA VSMCs:

EP_4 signaling contributes to cell migration and invasion in various tissues (310, 515, 516). Specifically, EP_4-activated EPAC1 has been shown to promote SMC migration independent of matrix or proliferation in the rat DA (477). To determine if EP_4 plays a role in the VSMC migration that leads to DA closure (28, 517-519) in the mouse, we utilized a primary culture model. Low-passage VSMCs were cultured from explants of term mouse DA and Ao,

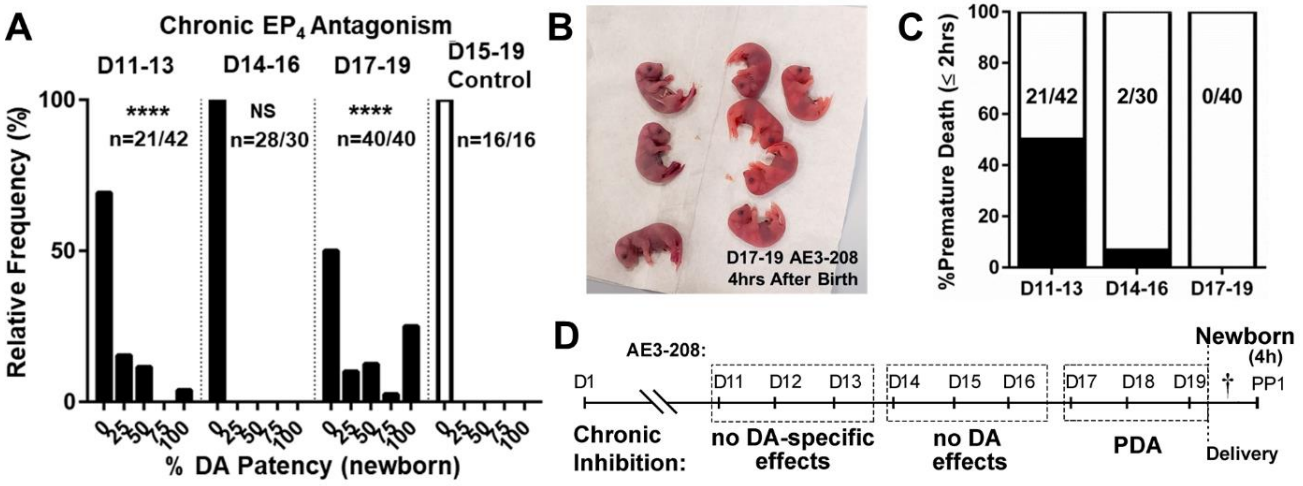

Figure 8. EP_4 is critical during the D17-19 window for proper postnatal DA function. A) Response of the neonatal DA to chronic EP_4 antagonist exposure during discrete gestational windows demonstrating increased rates of failed DA closure at 4h of age when drug was given over the late- but not mid-gestational window (n values represent animals surviving to 2hrs after birth/ total animals assessed). **B**) Representative image of a litter of chronically EP_4 inhibited offspring (D17-19), some of whom exhibited a dusky appearance frequently associated with PDA. **C**) Chronic exposure to the EP_4 antagonist during D11-13 of gestation resulted in significant postnatal mortality associated with apnea, the need for constant stimulation, and early demise, suggesting that increased PDA rates among some D11-13 survivors (n values represent animals surviving to 2hrs after birth/ total animals assessed) (**A**) were related to non-specific effects unrelated to DA status. Thus, while acute exposure to an EP_4 antagonist (AE3-208) resulted in fetal DA constriction (Figures **2H**, **3A**), prolonged exposure to the same drug produced PDA in newborns, but only in the late gestational window (**D**) (n values superimposed on columns). ****, $p<0.001$ compared to control (**A**, χ^2) (DA-ductus arteriosus).

shown to express mature muscle markers in >99% of cells (**Figure 9A**), and subjected to treated scratch assays (**Figure 9B**). DA cells that were wounded and incubated for 24hrs migrated faster than Ao cells in the scratch assay. EP_4 antagonism with AE3-208 had a

significant negative effect on wound healing and cell migration rates in DA but not Ao cells, suggesting that EP_4 does contribute to the migratory potential of DA VSMCs and that this effect is vessel specific (**Figure 9C-D**).

Deletion of EP_4 Results in Altered Signaling Characteristics in the DA:

To assess the functional consequences of EP_4 deletion in determining key aspects of DA signaling, we utilized pressurized vessel myography. Isolated EP_4 KO (B6.129S6-*Ptger4*$^{tm1.2Matb}$) DAs were mounted and their response to different vasoactive stimuli were interrogated (**Figure 10A**). Unexpectedly, EP_4 KO DAs showed significant constriction in response to PGE_2 exposure in both non-pre-constricted and pre-constricted states when endogenous PG and NO synthesis were suppressed (**Figure 10B-C**). These findings stand in contrast to the strong dilation normally induced by PGE_2 in the DA of most species. The unanticipated contractile response of EP_4 KO DAs to PGE_2 may be related to reduction in the vasodilatory EP_2 receptor combined with the loss of EP_4, and preservation of EP_1 and EP_3 receptor expression, which typically mediate vasoconstrictive responses (**Figure 11**). To test this, we administered PGE_2 to EP_4 KO and WT vessels before and after the administration of selective EP_1 and EP_3 receptor antagonists **(Figure 12A)**. Whereas blocking EP_1 and EP_3 had no effect on WT PGE_2-induced vasodilation, PGE_2-induced vasoconstriction in the EP_4 KO was completely mitigated **(Figure 12B)**. This might also be explained by shifting receptor affinity or receptor density amongst the remaining EP receptors, as EP_4 is known to drive a positive feedback loop of PGE_2 production (297). Further still, the change in downstream

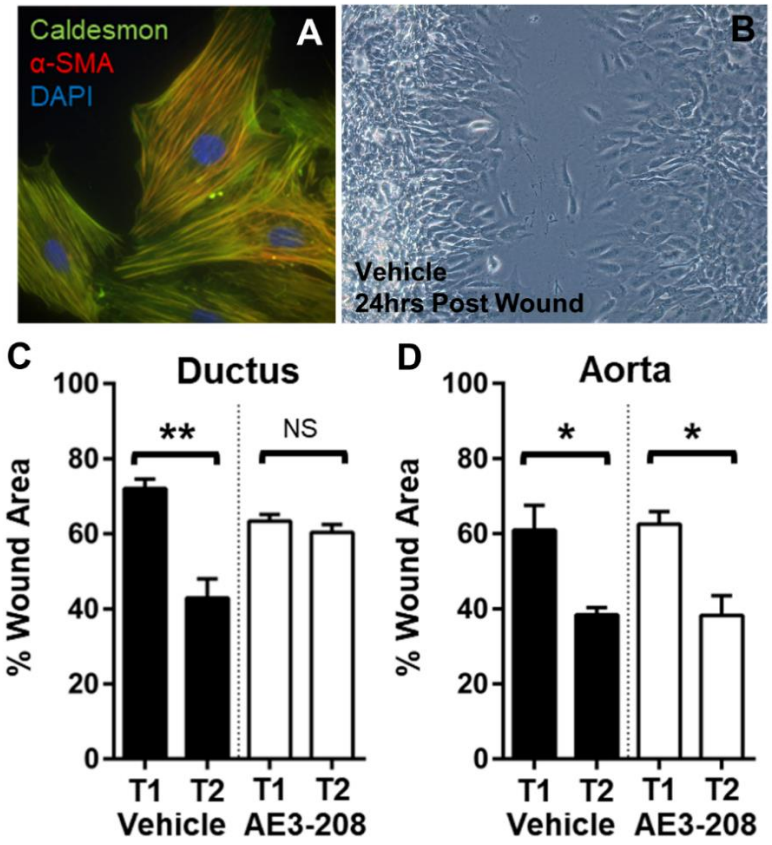

Figure 9. EP_4 antagonism disrupts cell migration in DA SMCs but not AO SMCs. A) Primary cultured P3 DA SMCs labeled with markers for mature VSMCs demonstrated typical SMC characteristics after low passage. **B**) Scratch assay studies demonstrated intact cell migration in a field of DA SMCs 24hrs post wounding. **C**) Cumulative results representing the response of vehicle- versus EP_4 selective antagonist-treated ductus and **D**) aorta SMCs to wound healing, suggesting that DA SMC, but not AO SMC, migration is dependent on EP_4 signaling *in vitro*. [T1=0hrs post wound, T2=24hrs post wound; %wound area determined as average % of 3 visual fields with 3 technical replicates and 3 biological replicates each]. *, $p<0.05$, **, $p<0.01$ compared to T1 baseline. (**C**, **D**, *t*-test).

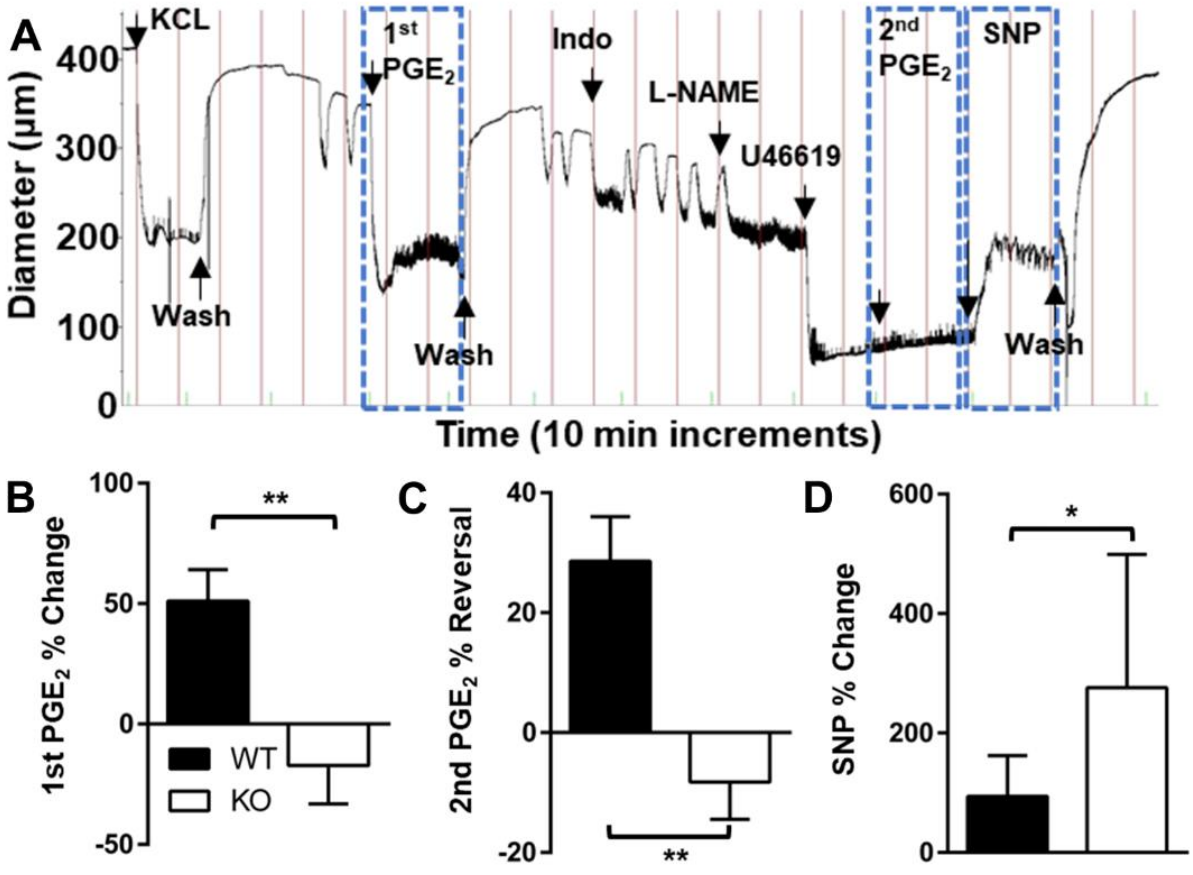

Figure 10. The PDA of EP_4 KO mice exhibits an unexpected contractile response to PGE_2. A) Representative tracing of an isolated EP_4 KO DA exposed to various stimuli demonstrating unexpected PGE-induced vasoconstriction (10^{-6} M), but appropriate contractile response to the thromboxane mimetic U46619 (10^{-5} M) and vasodilatory response to the NO-donor SNP (10^{-5} M). **B**, **C**) Cumulative results in wild type (WT) littermate DAs demonstrate the typical PGE_2-mediated vasodilatory response in comparison to PGE_2-induced constriction in EP_4 KO DAs under baseline (**B**) and U46619-pre-constricted (**C**) conditions (done in the presence of 10^{-5} M indomethacin and 10^{-4} M L-NAME to inhibit endogenous PGE_2 and NO production). **D**) Subsequent exposure of the pre-constricted and PGE_2- and NO-inhibited DA to SNP resulted in greater DA dilation in EP_4 KO than WT DAs (WT n=13, KO n=13 **B**, **C**, **D**). *, $p<0.05$, **, $p<0.01$ compared to WT. (**B**, **C**, **D**, *t*-test).

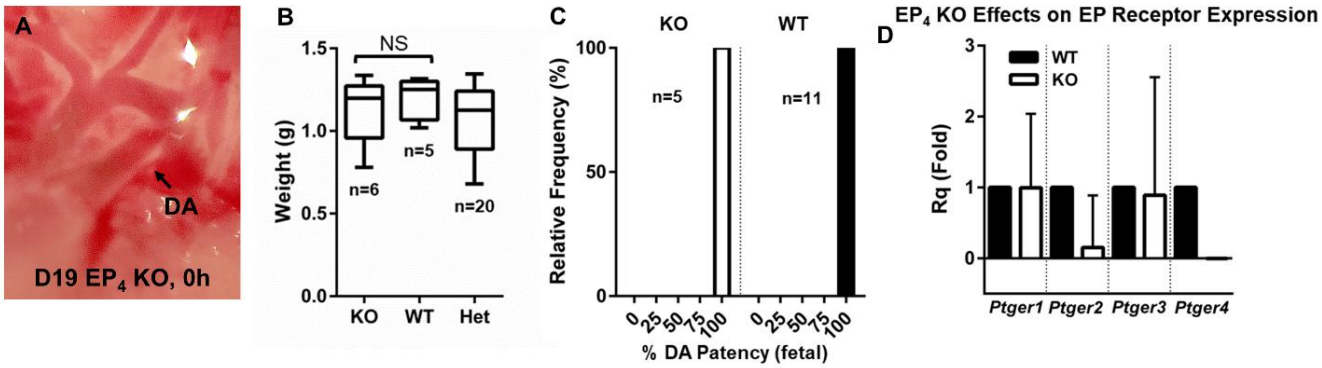

Figure 11. Effects of an EP_4 KO allele on fetal mice. A) Representative EP_4 KO DA demonstrating that size and position of the outflow tracts are consistent with WT anatomy **B**) Weights of representative KO pups and their WT littermates at birth were not significantly different, suggesting that differences in DA diameter (Fig. **7D**) are not related to body size. **C**) EP_4 KO and WT littermates were blindly scored for percent patency on D17 of gestation. All DAs were patent regardless of genotype, ruling out fetal DA constriction as a consequence of deleting the EP_4 vasodilatory receptor. **D**) RT-qPCR assessment of the effects of *Ptger4* deletion on EP receptor expression in the DA, revealing no significant compensation by *Ptger1*, *Ptger2*, or *Ptger3* in the absence of *Ptger4* (n=3 biological replicates) (**B**, *t*-test) (DA-ductus arteriosus).

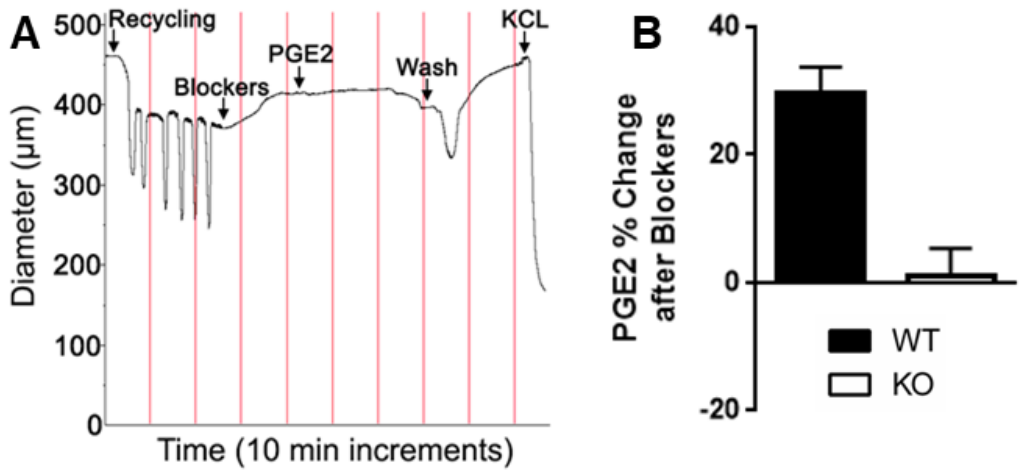

Figure 12. Antagonism of EP_1 and EP_3 disrupts PGE_2-mediated vasoconstriction in the EP_4 KO DA. A) Representative tracing of an isolated EP_4 KO DA exposed to selective antagonists of EP_1 and EP_3 followed by single high dose PGE_2 (10^{-6} M). **B**) Percent change of PGE_2-mediated response following administration of selective antagonists revealing an unaffected dilatory response in WT DA and essentially no response in EP_4 KO DA.

signaling resulting from the absence of EP_4 may affect the contractile apparatus of the DA but was not addressed in the present studies. EP_4 KO (B6.129S6-*Ptger4*$^{tm1.2Matb}$) DAs also showed an enhanced vasodilatory response to the NO donor sodium SNP suggesting that altered vascular effects are not limited to the prostanoid pathway (**Figure 10D**) and may have NO-dominant regulation similar to the preterm DA (**Figure 6C**, **D**).

Deletion of EP_4 Results in Altered DA Vasoconstrictive Properties:

To further interrogate the impact of EP_4 loss, we examined dynamic responses of the isolated DA in a second EP_4 KO model (B6;129-*Ptger4*^{tm1Sna}) (**Figure 13A**). The DA of WT offspring demonstrated consistent pressure-induced tone (myogenic response) during pressure ramps at the start of each study, while littermate EP_4 KO (B6;129-*Ptger4*^{tm1Sna}) DAs showed little or no myogenic response (**Figure 13B-C**). EP_4 KO (B6;129-*Ptger4*^{tm1Sna}) DAs had significantly greater lumen diameter, nearly twice that of WT littermates, at each pressure step (**Figure 13D**). Both of these findings are consistent with a decrease in basal DA tone. We did not observe that the DA of EP_4 KO mice was physically larger, as the DA was appropriately proportioned to the Ao and pulmonary artery during dissection (**Figure 11A**) and EP_4 KO pups were no larger than WT littermates (**Figure 11B**). To test whether this reduction in tone corresponded with decreased vasconstrictive potential, EP_4 KO (B6;129-*Ptger4*^{tm1Sna}) DAs were exposed to different vasoactive stimuli. EP_4 KO DAs exhibited decreases in KCl- and U46619-induced vasoconstriction compared to WT littermates, suggesting the loss of EP_4 adversely impacts voltage-gated and agonist-induced vasoconstrictive pathways in the DA

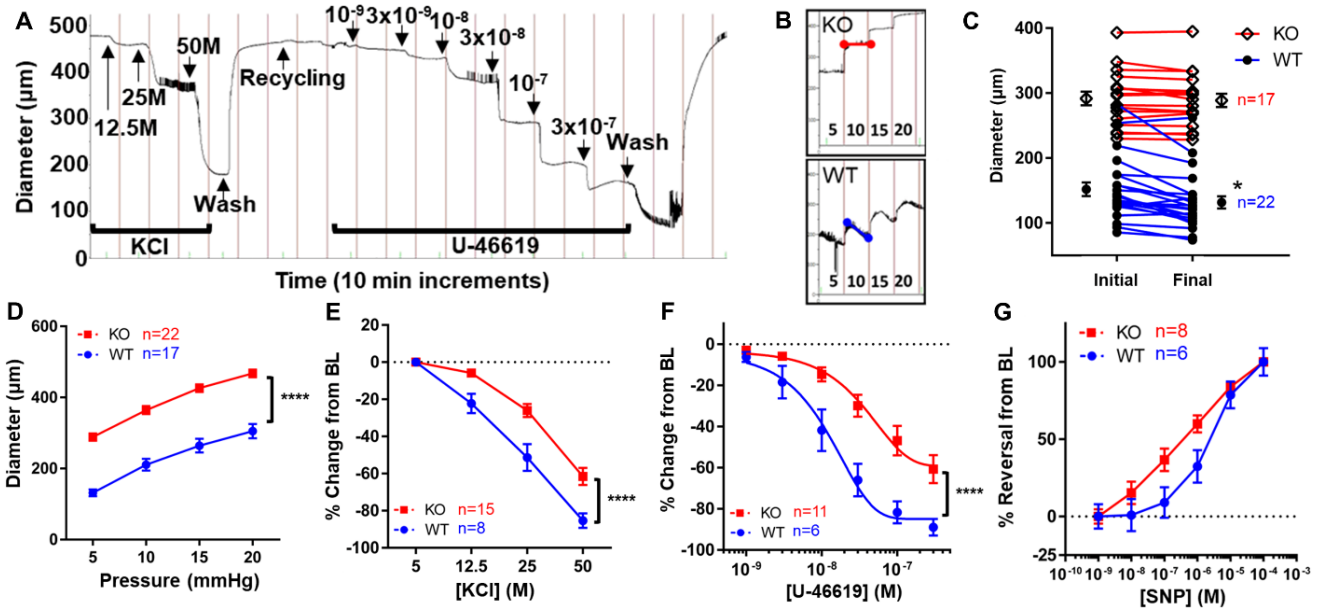

Figure 13. The PDA of EP_4 KO mice exhibits impaired responses to multiple stimuli. A) Representative tracing of an isolated EP_4 KO DA in response to U46619 contractile stimuli. **B**) Representative tracings of pressure-induced tone (myogenic response) during initial pressure ramps in EP_4 KO and WT littermate vessels, and **C**) plot showing impaired myogenic response in EP_4 KO DAs (10-15mm step). **D**) Compared to WT littermates, the *ex vivo* EP_4 KO DA was consistently noted to have larger diameter at each pressure step, **E**) reduced contractile response to membrane depolarization under high KCl conditions, **F**) reduced contraction in response to the thromboxane receptor agonist U46619, and **G**) enhanced vasodilatory response to SNP. *, $p<0.05$; ****, $p<0.0001$. (**C**, ANOVA; **D**, **E**, **F**, **G**, 2-way ANOVA).

(**Figure 13E-F**). Interestingly, the EP_4 KO DA also showed an increased trend in responsiveness to SNP, consistent with a continued importance for NO as a vasodilator in the KO DA (**Figure 13G**), similar to premature WT DAs (**Figure 6C**, **D**)

Deletion of EP_4 Does Not Impair the DA Response to O_2 But Reveals a Premature Phenotype:

Pressurized vessel myography was used to assess the *ex vivo* response of the EP_4 KO DA to O_2. Contrary to expectation, EP_4 KO (B6;129-*Ptger4*^{tm1Sna}) DAs exhibited no deficits in the O_2-induced DA contractile response compared to WT (**Figure 14A**, **B**). Of interest, both KO models exhibited highly regular patterns of rhythmic constrictions and dilations with a peak-peak length of ~10s (**Figure 14B**). This activity is consistent with vasomotion, a spontaneous oscillation in vessel tone or diameter noted in various vascular beds, which has only been previously described in the DA of premature (D15) mice (347, 520) .

To determine whether the seemingly intact O_2 response of the *ex vivo* KO DA could effectively constrict the DA *in vivo,* we tested the effects of hyperoxia on DA closure and survival. Incubating EP_4 KO (B6;129-*Ptger4*^{tm1Sna}) pups in a hyperoxic chamber (~70% O_2) for 4hrs lead to significant constriction of the EP_4 KO DA (**Figure 14C**). In other experiments, EP_4 KO pups were fostered to CD1 WT mothers in hyperoxia chambers (~70% O_2) for 24hrs or 48hrs. Despite a significant constriction of the KO DA at 24hrs (**Figure 14D**), pup survival was not significantly increased (**Figure 14F**). Incompletely constricted DAs were noted among the few surviving KO pups at 48hrs, but their small DA lumens dilated when mounted for myography, consistent with failed permanent remodeling despite muscular constriction after

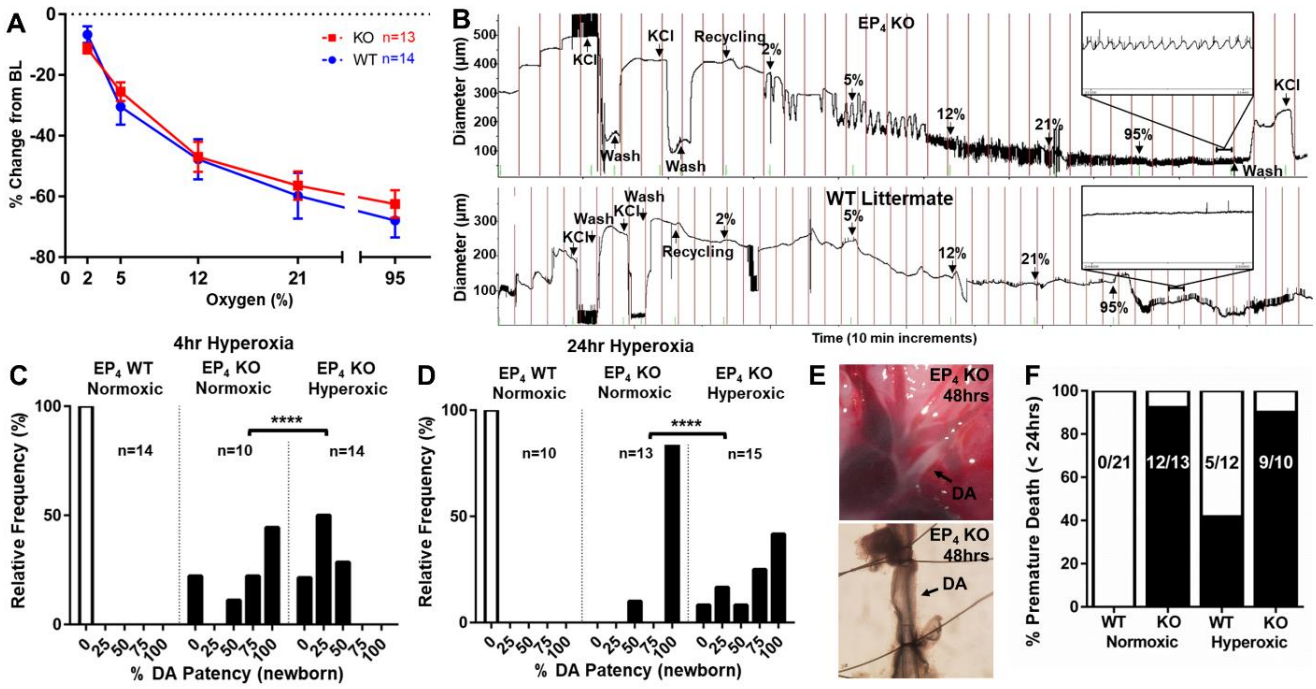

Figure 14. The PDA of EP_4 KO mice responds effectively to O_2 but display an immature phenotype. A) No difference was noted between *ex vivo* WT littermate and EP_4 KO DAs after exposure to increasing O_2 concentrations. **B**) Despite their similar degrees of constriction, EP_4 KO DAs were consistently observed to have O_2-induced vasomotion (see inset, **B**), a characteristic of premature DAs which was not observed in WT littermate DAs (**B**, bottom panel). **C**) *In vivo* studies to test O_2-induced DA constriction showed that short-term (4h) and **D)** long-term (24hr) exposure to hyperoxia lead to significant constriction of the EP_4 KO DA. **E**) Surviving EP_4 KO offspring exposed to hyperoxia for 48h had constricted DAs that failed to remodel (top) and were easily reopened with minimal pressure once mounted in myography chambers (bottom). **F**) Hyperoxia failed to increase survival in EP_4 KO pups (n values superimposed on columns). ****, $p<0.001$ (DA- ductus arteriosus). (**A**, 2-way ANOVA; **C**, **D**, χ^2).

extended O_2 exposure (**Figure 14E**). Together, these data suggest that impaired O_2-induced DA constriction is likely not the cause of PDA in these neonates, and that hyperoxia can only partially rescue this phenotype.

The isolated DA of WT preterm fetal mice typically has a blunted *ex vivo* response to increasing O_2 tension compared to term (201, 347). Interestingly, EP_4 KO (B6;129-*Ptger4*^{tm1Sna}) DAs displayed intact O_2-induced DA constriction similar to term vessels, but also consistently demonstrated contraction-associated vasomotion, a reliable characteristic of isolated preterm mouse DAs. Despite an incomplete understanding of DA maturation and a paucity of developmental markers, we examined a select group of genes with known gestation-specific changes in the DA (114, 117, 424). Similar to the mixed O_2 response phenotype, EP_4 KO (B6;129-*Ptger4*^{tm1Sna}) DAs shared a mature gene expression profile for some DA regulatory genes (*Tfap2b*, *IL15*, *Kcnma1*, *Kcnmb1*) but an immature profile for other DA-associated genes (*Pcp4*, *Rgs5*, *Des*) compared to WT littermates (**Figure 15**) (Primers in **Table S1**).

Discussion:

In this study we establish the acute role of EP_4 as the primary EP receptor in the DA and primary regulator of DA tone in late gestation. We also provide new evidence for the chronic role of EP_4 as a critical regulator of DA development and maturity.

Previous studies have determined that EP_4 is the primary EP receptor in the DA of rats (146), rabbits (258), lambs (259, 260), pigs (261, 262), baboons (260), and humans (263, 264) and that EP_4 is differentially expressed between DA and Ao in both mice (114), rodents, and humans (265). We found that EP_4 expression rose over gestation and was limited to the media

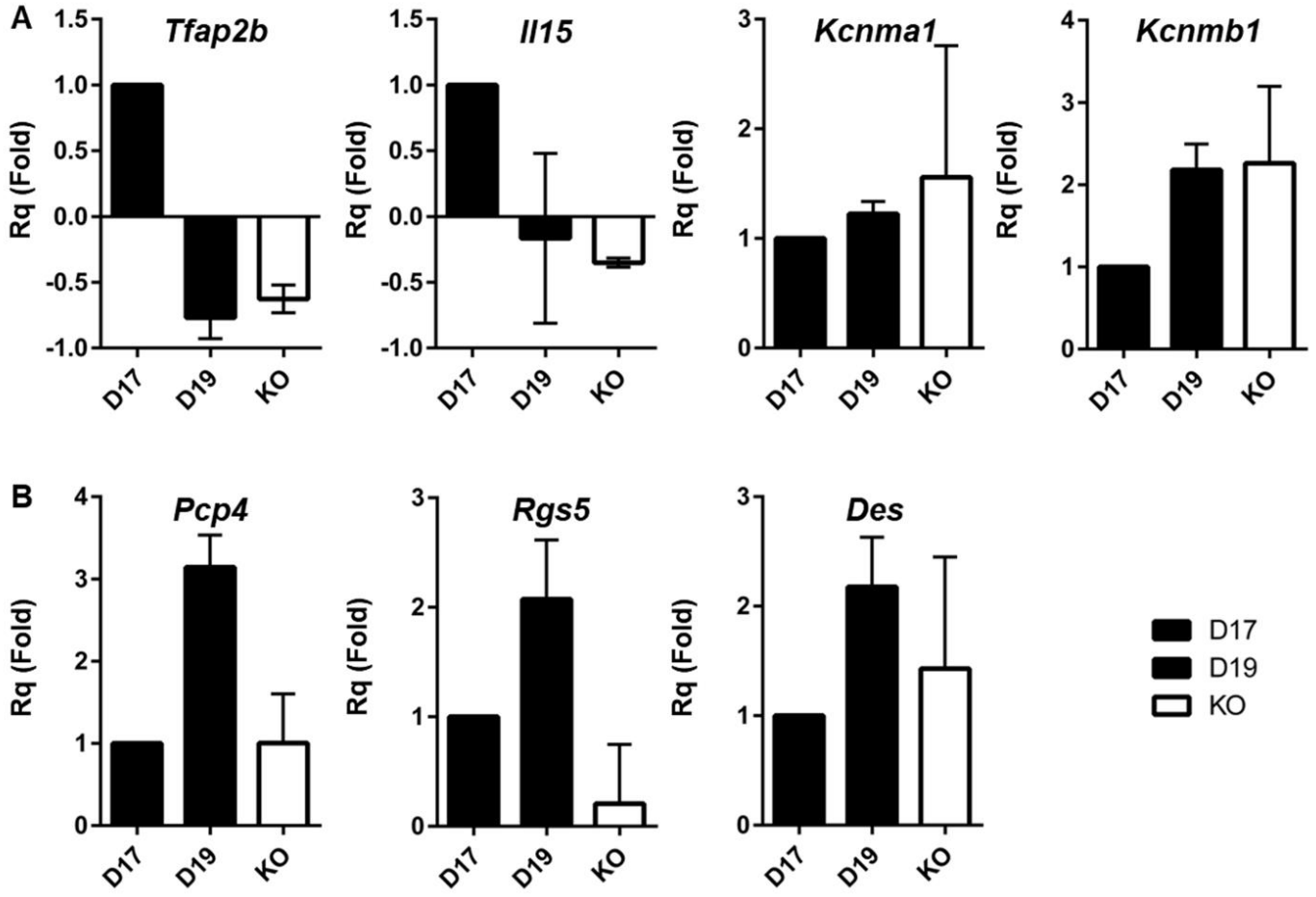

Figure 15: Analysis of maturity markers reveal complexities of DA development. RT-qPCR of a set of maturity markers in term (D19) EP_4 KO DA tissue revealed that **A**) while some markers aligned well with the late gestation D19 DA suggesting vessel maturity, **B**) others were better aligned with the D17 DA consistent with an immature DA phenotype. Primer information provided (**Table S1**) (n=3 biological replicates)**.**

and intima of the DA, reflecting the human expression pattern (264). Decreasing expression of EP_4 in the neonatal period, which we observed in both C57BL/6J and CD1 mice, has also been reported (258). The acute role of PGE as a dilator of the DA is also well established in rodents (108, 176, 181, 182) and used therapeutically for neonates born with ductus-dependent congenital cardiac defects (175, 521-524). That said, the importance of PGE_2 for DA tone seems to change throughout gestation. It was previously shown that PGE_2 is more critical for DA patency in late-gestation as opposed to mid-gestation whereas NO is more critical in mid-gestation (198-201). Our results show a gradual shift in these signals' role in tone in the mouse DA, with a discernable plateau on D17.

While the acute role of PGE_2-EP_4 in mediating DA tone is fairly straightforward, the chronic role of these signals in the DA has been a source of confusion and speculation. Multiple reports suggest that indomethacin tocolysis is associated with postnatal PDA (47, 183-191), although this has not been a consistent finding (192-194). This discrepancy is likely due to variations in the timing, dosage, and length of tocolytic treatments. In general tocolytic treatments later in pregnancy (47, 185), closer to delivery (188), with higher dosage (190), or longer duration (189, 190) promote PDA. Incidence aside, tocolysis has also been associated with failed pharmacological treatment and an increased need for ligation (47, 186, 187, 189, 191). These details offer insight into the role of PGE_2 in DA development. The recapitulation of a PDA phenotype in mice with chronic COX inhibition solidified the importance of PGE_2 in late- but not mid-gestation (196, 197). Despite the fact that KO models have been produced for all prostaglandin receptors (266-271), only EP_4 KO mice have a PDA phenotype, and all global EP_4 KO models have PDA (108-110). But it is counterintuitive that disruption of PGE_2-EP_4, a vasodilatory interaction in the DA, would result in a failure to constrict the DA of either tocolytic-exposed infants or KO mice. This discrepancy has been referred to as the "paradoxical PDA"

(272) and suggests that EP_4 has a distinct chronic role in DA development unrelated to the acute mediation of DA tone. Our group and others have proposed the existence of a developmental or transcriptional program that is necessary for establishing the mature, functional DA (111, 402, 440, 456, 525) with PGE_2 considered as a potential regulator (196, 197). We found that antagonizing EP_4 from D17-D19 was sufficient to produce PDA. This corresponds with rising EP_4 expression and a shift in dependence on PGE_2-EP_4 signaling for DA patency both on D17. This is likely the gestational point at which the PGE_2-EP_4-driven developmental program becomes active and begins to prepare the DA for constriction and remodeling after birth.

It remains unclear what PGE_2-EP_4 signaling does in the DA to prepare it for closure and remodeling. Microarray analysis of the EP_4 KO DA found differential expression of genes associated with SMC phenotypes (113). These genes could be grouped into those affecting function of the contractile apparatus, migration, growth, and vascular tone. However, these changes in expression are likely linked to shifting proportions of particular phenotypes within the SMC population. Notably, α7 integrin, Myocardin, and Myh11, genes associated with the contractile SMC phenotype (128), are downregulated in the KO (113). Similarly, matrix metalloproteases genes, associated with the synthetic SMC phenotype (128), are upregulated in the KO (113). These data suggest that PGE_2-EP_4 contributes to establishing the phenotypic characteristics of the SMC population in the maturing DA required for both contraction and remodeling, though it should be noted there are many markers of SMC phenotype that did not significantly change in the KO DA (127-129) or in other transcriptional assessments of the murine DA (265, 424). This may partially explain our observation of decreased tone and decreased responsiveness of the EP_4 KO DA to constrictive stimuli. SMC migration plays a key role in the permanent closure and fibromuscular remodeling of the DA (144, 517-519). During

development, VSMCs migrate inward from the media, cross the increasingly fenestrated IEL, and relocate into the subendothelial space where they form a neointima of radially realigned SMCs (375) in preparation for postnatal closure. In larger species, including humans, this includes the formation of large intimal cushions (28, 144) which facilitate occlusion of the constricting DA after birth. EP_4 has been shown to promote PKA-independent SMC migration via EPAC1 (*Rapgef3*) in the rat DA (477), supporting our finding of a DA-specific effect of EP_4 antagonism on SMC migration. Extensive studies demonstrate the role of EP_4 stimulation in directing extracellular matrix composition in support of this process. EP_4 stimulation has been shown to promote hyaluronic acid production leading to increased SMC migration (146). This is exacerbated by the inhibitor effects of EP_4 stimulation on elastogenesis, supporting fenestration of the IEL (396).

Given this context, it is a surprising but logical finding that hyperoxia-treated EP_4 KO DAs were able to constrict but not remodel, in contrast to our original hypothesis. Recent studies have identified genes associated with remodeling of the mouse DA after birth that could be important for understanding remodeling deficits in the EP_4 KO (125) but transcriptional analysis of post-birth KO DAs are not available for comparison. Interestingly, recent studies into the PRDM6 KO mouse model revealed both decreased EP_4 expression and an inability to constrict in response to O_2 (112). At first, these results appear to contradict our findings, but previous studies of D15 DA found a partially intact O_2 response, indicating that the DA's O_2 sensing mechanism begins development before EP_4 begins its developmental role. It is still unclear what factors regulate EP_4 expression and timing in the DA, but PRDM6 is a known transcriptional repressor and AP2 binding sites are present in the EP_4 promoter suggesting Tfap2b may play a role. It is worth noting that neonatal death in hyperoxia treated animals may be related to other non-DA requirements for EP_4 during development, as is

evident in our pups administered EP_4 antagonists from D11-D14. However, unlike these pups, who die very early after birth with respiratory distress, death in hyperoxia treated animals seems to correlate with a gradual reopening of the DA between 4 and 48hrs. While this doesn't prove death is caused by PDA, it does suggest it.

Since the potential roles for EP_4 in DA development are so diverse, we believe our data provides a novel conceptual framework to consider the KO phenotype in terms of DA maturity, with EP_4 KO DAs more comparable to vessels from D17 or earlier. Previous myography studies of premature mouse DAs have shown decreased responsiveness to KCl and PGE_2, as well as the presence of vasomotion (520) all of which were present in EP_4 KO DAs. Additionally, the absence of effects of EP_4 deletion on *in utero* patency could result from maintenance of NO-mediated dilation into late gestation. On the other hand, previous studies have indicated that immature DAs have a diminished O_2 response (61), unlike the EP_4 KO. This nuance coincides with our finding that three of seven maturity markers were more similar to premature vessels while four were more similar to mature vessels. Thus, the EP_4 KO DA appears to have an immature phenotype, but only with regard to distinct pathways. This immature phenotype is characterized in the KO DA by impairments in the first, muscular phase of DA closure, as well as previously described abnormalities in the second phase of permanent remodeling.

One limitation of this study, and use of mice to investigate PGE_2-EP_4 in general, is strain variation. Attempts to cross the EP_4 KO allele onto a CD1 background resulted in a loss of the PDA phenotype. A similar loss of the EP_4-associated PDA phenotype while outcrossing has been reported (526, 527) and initial characterization of the EP_4 KO on a mixed genetic background revealed an attenuated phenotype with successive generations of outcrossing (108). Similarly, attempts to induce a reliable PDA phenotype via pharmacological antagonism

of the EP_4 receptor were successful in C57BL/6J mice, but were less effective in CD1 mice. Additionally, WT littermates from our EP_4 KO colony were no more susceptible to pharmacologic antagonism of EP_4 than C57BL/6J WTs, indicating that these are strain-specific effects, not a result of genetic drift within our colony. A relative decrease in EP receptor expression levels in CD1 compared to C57BL/6J DAs may be a possible explanation. Clearly, strain variation in EP expression was significant enough to alter susceptibility to PDA phenotypes. It is unclear what compensatory mechanisms maintain DA patency *in utero* and prepare the DA to function after birth. Our study was not designed to address the role that strain variation plays in the DA. Future studies utilizing KO mice will need to be aware of the effects of background strain on PDA phenotype and outcomes.

Another limitation is the use of passaged primary SMCs to explore cell migration in the DA. Due to the size of the mouse DA, disaggregation of cells from tissue, or studies of unpassaged primary cells could not yield the quantity of cells necessary for our studies. While the loss of phenotype is a common consequence of culturing primary cells with FBS or for multiple passages (528, 529), we tried to minimize these concerns by utilizing low passage cells and serum starvation prior to experiments, similar to other DA SMC studies (477, 517-519, 530, 531). We found migratory differences between cultured DA and Ao cells, suggesting that some degree of tissue-specific identity was maintained. More thorough analyses of cultured DA SMCs in the future should utilize immortalized cells to minimize phenotypic drift, and always include a biologically matched Ao control.

Conclusion:

In summary, our findings suggest that PGE_2-EP_4 signaling plays a crucial developmental role for the proper maturation and function of the term DA that is distinct from PGE's widely known role in acute control of DA vasomotor tone. Similar to premature infants suffering PDA, EP_4 KO mice are delivered without experiencing this late gestational surge of EP_4 expression and stimulation which guides expression of critical SMC genes, cell migration, and changes to ECM necessary for DA closure and remodeling at birth. As such, the EP_4 KO DA is likely not a mature vessel with a single mechanistic defect, or a wholly immature vessel, but a partially matured vessel capable of weak transient constriction and incapable of permanently remodeling. This likely results from the disruption of a PGE_2-EP_4-mediated developmental program essential for defining DA identity. Further exploration of EP_4 function and DA development will likely hold key insights on the process of DA maturation relevant for human health.

Supplemental Tables:

Table S1	**Maturity Marker Taqman Primer List**			
Gene Symbol	**Gene Name**	**Taqman Assay ID**	**Assay Location**	**Amplicon Length**
Des	desmin	Mm00802455_m1	697	92
Il15	interleukin 15	Mm00434210_m1	607	73
Kcnma1	potassium large conductance calcium-activated channel, subfamily M, alpha member 1	Mm01268569_m1	1410	86
Kcnmb1	potassium large conductance calcium-activated channel, subfamily M, beta member 1	Mm00466621_m1	650	75
Pcp4	Purkinje cell protein 4	Mm00500973_m1	234	86
Ptger1	prostaglandin E receptor 1 (subtype EP1)	Mm00443098_g1	1247	85
Ptger2	prostaglandin E receptor 2 (subtype EP2)	Mm00436051_m1	1697	73
Ptger3	prostaglandin E receptor 3 (subtype EP3)	Mm01316856_m1	952	79
Ptger4	prostaglandin E receptor 4 (subtype EP4)	Mm00436053_m1	1500	70
Rgs5	regulator of G-protein signaling 5	Mm00654112_m1	464	150
Tfap2b	transcription factor AP-2 beta	Mm00493468_m1	1373	87

Chapter 5

FINAL DISCUSSION, CONCLUSIONS, FUTURE DIRECTIONS

Introduction:

DA closure and the transition to neonatal life is an incredibly complex developmental process which requires many diverse biological mechanisms to act in concert. At the center of this process, the function of a few pathways act to coordinate the others. The end result is complete remodeling of the circulatory system, establishing the adult pattern and enabling the first adaptation of a new life.

The first key steps in the process of DA closure occur in late gestation, with a dramatic remodeling program that converts the DA from a normal muscular artery to one resembling a diseased atherosclerotic artery (144, 149, 153, 154). This Remodeling phase is characterized by a breakdown in proper matrix production, migration of VSMCs, and the formation of intimal thickening. In most vessels this would be pathological, but in the DA it represents a process of maturation. We found that EP_4 expression increased dramatically between D15 and D17, corresponding with *in utero* remodeling during late gestation. In support of this concept, prior reports have already linked EP_4 to parts of this remodeling program. EP4 has been shown to disrupt the crosslinking of elastin in the vasculature leading to several forms of vascular pathologies (131, 141, 143). Decreased or disordered elastin cross linking prevents maintenance of the IEL leading to fenestrations (120, 143, 396). EP_4 activation promotes both the AC-mediated production of hyaluronic acid (146), as well as the AC-independent, EPAC-dependent promotion of cell migration (477). Deposited hyaluronic acid swells with water,

producing matrix rich gaps between cells which facilitate the migration of VSMCs (146, 151, 153, 517) and potentially the separation of endothelial cells from the fragmented IEL (135). VSMCs then migrate into the subendothelial space and form an organized layer of radially realigned contractile VSMCs (136, 153, 375). This intimal thickening is absent in the EP_4 KO DA (146). Key to all aspects of this remodeling program is the presence of a migratory, secretory, synthetic subpopulation of VSMCs which then undergo a contractile transition in preparation for delivery. Microarray analysis revealed that key markers of contractile VSMCs were downregulated in the EP_4 KO DA while markers of synthetic VSMCs were increased (113). This suggests that EP_4 may not just act as an acute vasodilator after birth, but may even be responsible for establishing the contractile potential of the DA. We found that the EP_4 KO DA had reduced responses to contractile stimuli and reduced basal tone, which could be explained by a reduced VSMC population. Similarly, we found multiple markers of DA maturity were reduced in the KO DA, suggesting that disrupting EP_4 disrupts the phenotypic characteristics of the VSMC population. Curiously, an overall decrease in contractile potential does not translate to the O_2 signaling pathway, which we discovered was comparable to WT *ex vivo* and intact *in vivo*. Despite the induction of DA closure via hyperoxia in the EP_4 KO, permanent remodeling does not seem to have occurred, and the DA could still be reopened after 48hrs. This further emphasizes the importance of the mid-gestational remodeling step in preparation for DA closure, and illustrates that without EP_4, the DA remains an immature vessel incapable of fully constricting or permanently remodeling. In the end, DA closure is composed of three major processes: mid-gestational remodeling, acute functional constriction after birth, and permanent anatomic remodeling. Thorough examination has revealed that the PDA phenotype of the EP_4 KO DA does not result from the failure of one of these, but all three.

Throughout this dissertation, I have argued that the process of DA closure is contingent on a highly ordered developmental program, and that this developmental program is dependent on EP_4. Originally, we set out to define this program, envisaging a simple cascade of factors critical for VSMC contraction downstream of EP_4 activation. Biology, as in life, seems never so simple or forthcoming. While we fell short of defining the exact transcripts and pathways which compose this developmental program, we have shown that it exists. More critically, we have shown that its activation is contingent on EP_4, specifically during late gestation. What follows are my final thoughts and conclusions on the role of EP_4 in DA closure, and some future directions that may bring us closer to more complete mechanistic answers. A thorough understanding of prostaglandin signaling has revealed itself to be critical for addressing the clinical concerns posed by the DA. It is the aim of this chapter to discuss powerful questions of DA biology that may give way to powerful solutions to DA complications.

The Transcriptional Landscape of the DA Suggests a Developmental Program:

Chapters 2 and 3 of this dissertation sought to establish the foundations of a developmental program in the DA by interrogating the transcriptional landscape of the vessel. Based on the state of the literature when this project was envisioned, these studies were both necessary and their findings provide a deep and nuanced understanding of what identifies the DA that was not available beforehand. This much needed context identified key transcripts upregulated in the DA across species and timepoints, which mouse models of PDA may be relevant for human health, and provided the first resource of sequencing data from human DA tissue (265, 424). Since the publication of these works, multiple labs have published transcriptional and genetic analyses of the DA. Microarray analysis of human vessels revealed that patent DAs have increased expression of second heart field related genes like ISL1, and

decreased expression of differentiated smooth muscle markers JAG1 and calponin compared to their closing counterparts (124). Another study utilized extraction of VSMCs from human DA tissue harvested during surgery to repair congenital heart defects. RNAseq was then performed on isolated cells following 96hr culture in either hypoxic or hyperoxic conditions (514, 532). 1344 genes were found to have significant differential expression between normoxia and hypoxia, including two associated with syndromic PDA in humans (CREB and histone acetyltransferase P300) and several associated with mitochondrial redox reactions. Due to SMC de-differentiation in culture and a strong selection bias towards synthetic VSMCs, cultured DA cells are likely a suboptimal place to start for transcriptional analysis of the DA and no substitute for native tissue. It is also unsurprising that hypoxia would affect mitochondrial transcripts in any cells, especially DA cells. Finally, the first sequencing data from the mouse DA revealed that key differences in matrix and cytoskeletal proteins occur during the process of DA closure (125). Two recent mouse models of PDA have been reported: Vimentin (125) and PRDM6 (112), which we helped to characterize. While these studies have continued to add to our understanding of the DA transcriptome, the true identification of a developmental program has proven elusive, but the following proposed studies could potentially answer several key questions. Our concerns are identifying transcripts that change between mid-gestation and term, and possibly including postnatal DA closure. Comparison to an index tissue such as Ao may be required to isolate DA-specific developmental changes from the transcriptional changes of the developing outflow tracts. Finally, because VSMC phenotype seems to play such a critical role in DA remodeling and closure, single cell sequencing should be used to allow the identification of cell subpopulations. Three primary questions would guide this study: what genes define the DA from surrounding tissues, what genes comprise the developmental program of the DA, and do distinct sub-populations of VSMCs play a role in this

developmental program. To satisfy these factors, I would perform single cell RNAseq on tissue from a minimum of three timepoints: D16 preterm, D19 term, P1 post-delivery. Initial analysis would determine genes differentially expressed between DA and Ao samples which define the DA from surrounding tissue. Sub-populations of VSMCs would be defined agnostically via available software tools. Individual transcriptional profiles for these groups would then be assessed for their contribution to the differential expression of genes between DA and Ao, testing the hypothesis that a single sub-population is responsible for initiating the developmental program. Finally, individual sub-populations would be assessed for genes that are differentially expressed over time, specifically between mid-gestation and term, suggesting they play a role in DA development. This last group would likely provide the most complete list of genes involved in the developmental program of the DA. Once a library of candidate effectors whose expression shifts between mid-gestation and term is constructed, comparison to the EP_4 KO DA, either via sequencing or qRT-PCR of specific transcripts, can validate which aspects of a putative developmental program that EP_4 is responsible for. While I have stressed the role of EP_4 as a regulator of this developmental program here, it is likely not the core regulator. This is likely a transcription factor which regulates the expression of *Ptger4*, and other key conserved DA genes such as *Abcc9*, *Kcnma1*, and *Pde1c*, or mature VSMC genes such as *Myh11* and *Cnn1*. *Tfap2b* has been suggested as a master DA regulator (265, 391) and *Tfap2b* KO mice die with a PDA (450). Regardless, a better understanding of this program would help to identify the key pathways controlling DA function.

PGE_2-EP_4 Plays an Essential Role in Permanent Closure and Remodeling of the DA:

Perhaps the most important finding in chapter 4 is that hyperoxia-induced closure of the EP_4 KO DA resulted in failure to permanently close and remodel. Permanent closure and

remodeling is a fascinating part of DA biology that has remained mechanistically elusive. Histological studies of DA from the 1970s and 80s defined the structural hallmarks of permanent closure as fibrosis and necrosis (126, 134, 153, 154). Further, it is clear from these studies that PDA and lack of permanent closure is strongly associated with failure to undergo mid-gestational remodeling. Specifically, in histological studies of PDA, vessels are often found with intact IEL, lack of intimal thickening, and less of the vascular oddities found in the vessel wall, such as disorganized medial elastin (though this varies in dogs with hereditary PDA (126, 137)), and cytolytic necrosis (134). Yokoyama et al. have studied at length the contributions of EP_4 to the mid-gestational remodeling events that prepare the DA for closure. What is unclear is the exact way these changes facilitate permanent DA closure and remodeling. Specifically, alterations in elastin crosslinking and hyaluronic acid production facilitate movement of DA VSMCs into the subendothelial space (146, 375, 396, 477). These VSMCs then undergo radial reorientation and it is unclear why. It is possible that this orientation allows the VSMCs to load force on the axis between the vessel wall and the lumen. Essentially, once the DA undergoes its O_2-mediated acute constriction, the opposing walls of the DA lumen are brought close enough in proximity to interact. Endothelial cells begin to lose orientation because of their separation from both the IEL and the shear stress of hemodynamically significant luminal flow. These cells then undergo rapid apoptosis and/or necrosis allowing VSMCs to form intermediate junctions across the lumen which can then be loaded. These VSMCs may then either further constrict, causing a two-stage constriction, or act as static inward anchors for the outer wall once the acute O_2-mediated constriction abates. This could explain why the EP_4 KO DA failed to stay closed after O_2-induced constriction. Without the formation of radially realigned VSMCs in the lumen following intimal thickening, it is possible the KO DA was incapable of stabilizing its initial contraction. There are several ways this could be assessed as

a mechanism of DA closure. The first is static fluorescent microscopy. Sections of actively closing DAs could be taken and labeled for endothelial markers such as VE cadherin or PECAM1 as well as muscle markers such as Myh11 or caldesmon. Observing a rapid decrease in or displacement of endothelial markers in the closing lumen could suggest muscle-muscle association plays a role in permanent closure. This could be augmented by staining for desmin or other proteins associated with the formation of intermediate junctions or muscle-muscle contacts. We had initially planned to attempt fluorescent labeling of muscle proteins in mounted whole DA explants using transgenic mouse models. If this could be achieved with an acceptable level of temporal and spatial resolution, it may be possible to observe the formation of these bonds as an explanted DA closes on its mounts. I have attempted to culture whole mounted DA explants overnight in a normoxic incubator and found that a media-submerged DA was entirely capable of constricting itself shut and remodeling against a pressure head. Using isolated DAs with superfusion would allow for complete control of O_2 concentration and the activation/inhibition of various pathways to observe their contributions. If this is the case, then EP_4 is largely responsible for late gestational remodeling, maintenance of DA patency in late gestation, and permanent closure and remodeling of the DA.

The Oxygen Sensing Mechanisms of the DA Develop Independent of EP_4:

I initially predicted that the EP_4 KO DA would have a significantly depleted O_2 response *ex vivo*. I attempted several different O_2 concentration response curve protocols thinking I had to be doing something wrong, but each time the results were the same. There is no difference between WT and KO in terms of O_2 response *ex vivo* and studies utilizing hyperoxia proved that EP_4 KO pups could constrict their DAs *in vivo*. This is potentially very significant for what it can tell us about the O_2 sensing mechanism of the DA. There is still vigorous debate within the

field as to which O_2 sensing mechanism likely mediates DA constriction after birth (347, 354, 362, 364, 476). As previously outlined, there are several mechanisms of shifting the balance of contractile machinery in a VSMC to facilitate constriction or dilation. Some of these mechanisms are independent of each other while some are dependent. For example, direct activation of MLCK via phosphorylation bypasses calmodulin, and therefore can increase VSMC constriction in a Ca^{2+}-independent manner. If we could determine which of these components seem to have decreased effectiveness constricting the EP_4 KO DA, we may be able to isolate the particular mechanism which mediates the intact O_2 response. Pharmacological inhibitors are available for many of the proteins involved in this process. Calyculin and microcystin-LR can be used to inhibit MLCP (533, 534), U-73122 can be used to inhibit PLC (535), heparin can be used to modestly inhibit IP3Rs (536), etc. Myography studies of O_2 concentration response curves utilizing different combinations of these inhibitors could procedurally determine which pathways are still active in the EP_4 KO DA and therefore essential for the DA O_2 response. It was initially our goal to use mass spectrometry-based detection of isoprostanes, qRT-PCR of endothelin expression, and luciferase assays of DA explants to determine if there were deficits of O_2 response. Now, knowing that the EP_4 KO DA has an intact O_2 response these assays could be used to determine if all of these pathways are still active, and potentially eliminate a potential mechanism. For each of these mechanisms, if no difference is detected between KO and WT, we can determine whether that particular O_2 sensing mechanism is not functional in the EP_4 KO DA and is not required for an intact O_2 response. To detect isoprostane production, specifically 8-iso-$PGF_2\alpha$, whole EP_4 KO and WT DAs would be explanted to serum free media and incubated using a gradient of O_2 concentrations in a tri-gas incubator (2%, 5%, 12%, 21%, and 95%). After an hour, media would be collected and subjected to stable isotope dilution assay of gas chromatography and

mass spectrometry. We have previously used this technique to characterize prostaglandin metabolites in the DA (347). Expression of ET1A is a critical component of the CYP450-mediated oxygen sensing mechanism in the DA. Performing qRT-PCR on DA tissue isolated from EP_4 KO and WT littermates before birth (O_2 naïve) and 4hrs after birth (O_2 exposed) would allow us to determine if EP_4 KO DA expresses the required machinery for this form of oxygen sensing at birth, and determine whether that change is induced by O_2 exposure. Finally, reactive oxygen species production, specifically the production of H_2O_2, is a reliable indicator of mitochondrial activity and a potential mediator of O_2 sensing in the DA. Cultured DA VSMCs from EP_4 KO and WT littermates would be cultured in hypoxic conditions (5% O_2) and once confluent, cultured in hyperoxia (21% O_2) for 4hrs. H_2O_2 production would be detected via luminescent H_2O_2 detector. While it is possible that all of these O_2 sensing mechanisms are active in the EP_4 KO DA, a reduction in one compared to WT would indicate that mechanism is not required for DA O_2 mediated constriction.

PGE_2-EP_4 is Likely Essential for Establishing the Mature Contractile VSMCs of the DA:

Previous microarray analyses of the EP_4 KO DA have found decreases in transcripts associated with mature contractile VSMCs (113). We found that EP_4 KO DAs had reduced basal tone and diminished constrictive potential in response to contractile stimuli. While it is possible that this represents the downregulation of a specific pathway or mechanism within the VSMCs, it is more likely that a shift in VSMC phenotype has resulted in a decrease in contractile VSMCs in the DA. This could be partially assessed through the use of single cell RNAsequencing. Alternatively, using the lists of transcripts provided by the prior microarray study of EP_4 KO DA and the many papers outlining variations in VSMC phenotype, an *in situ* hybridization based system could be used to examine the prevalence and distribution of

synthetic and contractile VSMCs in the KO DA over development based on the expression pattern of transcripts associated with VSMC phenotype. While individual markers do not provide a robust method for identifying VSMC phenotypes, systems such as RNAscope can now be multiplexed to allow for visualizing multiple expression patterns. The use of commercially available spatial transcriptomics techniques would allow us to detect expression levels of known markers of VSMC phenotype, while preserving information about cell localization, and allowing discovery of new patterns of transcription within the DA. Using an *in situ* hybridization, imaging-based form of spatial transcriptomics could allow us to profile thousands of genes, with more genes meaning more rounds of hybridization, meaning more time, and more potential for tissue degradation or errors. For our purposes, a large library of transcripts identified in our prior microarray work, or relevant for VSMCs, endothelial cells, or neural crest cells, could be assayed across a late gestational time course of outflow tract explants from EP_4 KO and WT littermates. Data from the WT littermates alone would be powerful for determining the presence and activity of VSMC sub-populations within the DA. Comparison to the EP_4 KO would allow us to determine exactly what portions of these cell populations are EP_4-dependent, and the timing of their activity. While there are limitations to the use of cultured DA VSMCs as a proxy for native DA cells, they provide the perfect test bed for assessing a factor's role in determining cell phenotype. We showed that EP_4 contributed to cell migration in cultured DA VSMCs, something that has also been shown in cultured rat DA cells (146). Exposing cultured DA VSMCs to selective EP_4 agonists such as TCS2510, or antagonists such as AE3-208, then subjecting those cells to either qRT-PCR of select markers or sequencing could tell us whether EP_4 activation is actually responsible for driving expression of contractile transcripts in the DA. It is somewhat counterintuitive that EP_4 could drive both cell migration, a process requiring synthetic VSMC phenotype, and differentiation

toward the contractile fate. Though this could be possible through the differential expression of downstream pathway constituents. Some mouse models of PDA reported either a decrease in VSMCs or contractile VSMCs present in the medial layer of the DA (456). This suggests that the EP_4 KO DA may suffer from a paucity of VSMCs which impair its contractile potential. In order to test this, I would perform BrdU integration-based proliferation assays of both cultured EP_4 KO DA VSMCs and *in vivo* DA. For both experiments, administration of BrdU would be followed by an incubation period to allow BrdU to integrate into replicating DNA and detection of signal via fluorescent microscopy. Proliferation would also be quantified through the counting of immunolabeled cells in cryosections of excised DA tissue. Anti-calponin and anti-caldesmon antibodies would identify VSMCs while anti-Ki-67 antibody would identify proliferating cells to be counted. Comparisons between EP_4 KO and WT would reveal if KO VSMCs have a deficit in proliferative potential.

The Mechanism Through Which PGE_2-EP_4 Directs DA Development Remains Unclear:

EP_4 activation has been shown to drive diverse processes in the DA, which is relatively unsurprising given its wide range of potential downstream pathways. EP_4 acts primarily through the $G_s\alpha$ G-protein and leads to vasodilation through the stimulation of cAMP. This cAMP has been shown to be primarily produced through the AC6 isoform of adenylyl cyclase (147). EP_4 activation has also been shown to drive cell migration in the DA via EPAC activation in an adenylyl cyclase-independent manner (477). Despite this, it is still unclear exactly which downstream pathways mediate certain aspects of EP_4 activity. If EP_4 does in fact drive transcriptional changes associated with contractile smooth muscle, or vessel maturity as we found, does it do this through CREB or ICER (168)? Does ERK signaling play a role in EP_4-mediated development? What about the transactivation of receptor tyrosine kinases? Many of

these mechanistic questions could be answered by the use of selective agonists and antagonists on cultured DA VSMCs, such as whether certain processes are AC-dependent or PKA-dependent. That said, to truly determine the contributions of these specific pathways to DA remodeling and closure, perhaps the most definitive method would be to create a series of transgenic mouse lines with targeted mutations in specific regions of the receptor. For instance, swapping critical residues to prevent the association of $G_s\alpha$ G proteins, or excising the portion of the N-terminal tail that facilitate binding to EPRAP and the inactivation of NF-κB and MEK. While this would have proven a massive undertaking a decade ago, now with the use of CRISPR Cas9 and similar techniques it would prove a somewhat less massive undertaking. Once created though, these constructs could be used to answer many critical questions about EP_4 outside of the DA.

Another option to differentiate between the multiple downstream pathways of the EP_4 receptor is through the creation of chimeric EP_4 receptors using segments from other prostanoid receptors with varying functions. These chimeric receptors could then be coded into plasmids and transfected into cultured primary EP_4 KO DA VSMCs via electroporation. Since these cells lack a functional EP_4 receptor, we can be sure that our chimeric construct is responsible for observed effects. Compared to a simple targeted mutation strategy, wherein the bases encoding specific residues necessary for the interaction of the EP_4 receptor and its G proteins or other proteins would be replaced by substitution, preventing said interaction, chimeric receptors may offer more stability and support normal trafficking of the receptor to the plasma membrane. Experimental design should feature the removal of an EP_4-mediated effect by the use of a chimeric receptor lacking a particular interaction, and restoration of said action through the use of a receptor stripped of all interactions but that one. For example, to determine whether EP_4 mediates VSMC migration through an adenylyl cyclase-mediated

mechanism, a chimeric receptor should be created using the mouse EP_4 receptor with the residues comprising the first intracellular loop being replaced by the residues encoding the first intracellular loop of the EP_3 receptor which lacks an interaction with the $G_s\alpha$ G protein. If $G_s\alpha$-activated adenylyl cyclase mediates migration, we would expect migration to decrease or cease. To validate this, we would then use a chimeric receptor stripped of all interactions but the $G_s\alpha$ interaction of the first intracellular loop. This could be accomplished by replacing the residues comprising the intracellular C-terminal tail with those of the EP_2 receptor, which is incapable of interacting with the $G_i\alpha$ G protein, EPRAP, or undergoing desensitization and internalization-mediated by β-arrestin. Use of this receptor should restore migration if it is adenylyl cyclase-mediated. Because ERK/AKT signaling may be activated by either the $G_i\alpha$ G protein or transactivation of receptor tyrosine kinases such as EGFR by the release of cSRC following internalization by β-arrestin, these constructs will require more thought. To prevent interaction with $G_i\alpha$ a chimeric receptor would replace the membrane-adjacent residues of the C-terminal tail which interact with $G_i\alpha$ with those of the EP_2 receptor. To disrupt internalization of the receptor and subsequent release of cSRC without disrupting the binding of EPRAP, it may be easier to substitute the C-terminal tail residues GRK phosphorylates to initiate desensitization and internalization. Migration could be assessed through the use of wound healing or Boyden chamber assays. Boyden chamber assays should utilize endothelial conditioned media to promote migration, mimicking conditions in the DA. The major limitation to this approach is that the EP_4 KO PDA phenotype is composed of many tissue-wide processes which cannot currently be modeled in culture. Because questions of vascular development rely heavily on the tissue environment of the vessel to define a particular cell's niche, it becomes increasingly complex to try and reduce these to culture testable processes.

Detecting interactions between the EP_4 receptor and its downstream signaling proteins could also help determine what pathways are active in the DA. Co-immunoprecipitation of the EP_4 receptor could be used to detect interactions with $G_s\alpha$ and $G_i\alpha$ G proteins, β-arrestin, or EPRAP. WT DA explants taken from D16 mice, before EP_4 begins to affect development, and D19 mice, while EP_4 is driving development, would allow us to determine what downstream signals are interacting with EP_4, and if this changes in a developmentally relevant way. Proteins pulled down in the assay would be denatured and separated on a western blot to determine the number and size of interacting proteins. Co-immunoprecipitation would rely on the use of an EP_4 antibody to pull down the receptor and its interacting partners, although EP_4 antibodies are notoriously promiscuous and not considered reliable within the field. This does raise the potential of pulling down the small number of EP_1, EP_2, and EP_3 receptors expressed in the DA. This is further complicated by the potential of pulling down dimerized EP receptors, which means the detection of other EP receptors may occur intentionally. Whereas my other proposed approaches rely on detecting differences in known downstream interactions with EP_4, this approach does offer the potential of discovering new, potentially DA-specific protein interactions with EP_4.

While co-immunoprecipitation may depend on reliable and selective antibodies, bioluminescence resonance energy transfer (BRET) assays could be conducted with fusion proteins instead. Luciferase or fluorescent tags could be added to non-disruptive sites on the EP_4 receptor and proteins with potential interactions: $G_s\alpha$ and $G_i\alpha$ G proteins, β-arrestin, or EPRAP. Fusion proteins could be induced in cultured EP_4 KO DA VSMCs similar to the aforementioned chimeric proteins. When an interaction between labeled fusion proteins occurs, Förster resonance energy transfer (FRET) occurs, allowing detection of a new fluorescent signal via fluorescent microscopy. This would allow us to determine, in real time, in

live cells, what proteins are interacting with EP_4 in cultured DA VSMCs. That said, the generated fusion proteins for $G_s\alpha$ and $G_i\alpha$ G proteins, β-arrestin, or EPRAP, would not be expressed under their native promoters, ignoring the transcriptional level of regulation. Additionally, native untagged versions of these proteins would still be expressed, competing for interactions with tagged receptors and decreasing signal.

EP_4 is one of the most frequently dysregulated genes in metastatic cancers (537-539), and plays significant roles in maintaining the barrier function of the intestinal epithelium as well as the skin. The development of mouse models, chimeric EP receptors, and BRET-ready fusion proteins to determine exactly when a specific downstream pathway of the EP_4 receptor is active would be invaluable in assessing DA biology as well as other EP receptor related conditions.

References

1. **Crockett SL, Berger CD, Shelton EL, and Reese J**. Molecular and mechanical factors contributing to ductus arteriosus patency and closure. *Congenit Heart Dis* 14: 15-20, 2019.
2. **Ovali F**. Molecular and Mechanical Mechanisms Regulating Ductus Arteriosus Closure in Preterm Infants. *Front Pediatr* 8: 516, 2020.
3. **Bergwerff M, DeRuiter MC, and Gittenberger-de Groot AC**. Comparative anatomy and ontogeny of the ductus arteriosus, a vascular outsider. *Anat Embryol (Berl)* 200: 559-571, 1999.
4. **Johansen K**. 9 Air Breathing in Fishes**This chapter was written while the author was supported by grants GB 7166 from the National Science Foundation and HE 12071 from the National Institutes of Health. In: *Fish Physiology*, edited by Hoar WS, and Randall DJAcademic Press, 1970, p. 361-411.
5. **Kolesova H, Lametschwandtner A, and Rocek Z**. The evolution of amphibian metamorphosis: insights based on the transformation of the aortic arches of Pelobates fuscus (Anura). *J Anat* 210: 379-393, 2007.
6. **O'Donoghue C H**. A Note on the Ductus Caroticus and Ductus Arteriosus and their Distribution in the Reptilia. *J Anat* 51: 137-149, 1917.
7. **Jacobs K, Goy SK, and Dzialowski EM**. Morphology of the embryonic and hatchling American alligator ductus arteriosi and implications for embryonic cardiovascular shunting. *J Morphol* 273: 186-194, 2012.
8. **Agren P, Cogolludo AL, Kessels CG, Perez-Vizcaino F, De Mey JG, Blanco CE, and Villamor E**. Ontogeny of chicken ductus arteriosus response to oxygen and vasoconstrictors. *Am J Physiol Regul Integr Comp Physiol* 292: R485-496, 2007.
9. **Belanger C, Copeland J, Muirhead D, Heinz D, and Dzialowski EM**. Morphological changes in the chicken ductus arteriosi during closure at hatching. *Anat Rec (Hoboken)* 291: 1007-1015, 2008.
10. **Smith GC**. The pharmacology of the ductus arteriosus. *Pharmacol Rev* 50: 35-58, 1998.
11. **Fishman AP, DeLaney RG, and Laurent P**. Circulatory adaptation to bimodal respiration in the dipnoan lungfish. *J Appl Physiol (1985)* 59: 285-294, 1985.
12. **Dzialowski EM**. Comparative physiology of the ductus arteriosus among vertebrates. *Semin Perinatol* 42: 203-211, 2018.
13. **Kirby ML, and Waldo KL**. Neural crest and cardiovascular patterning. *Circ Res* 77: 211-215, 1995.
14. **Hutson MR, and Kirby ML**. Neural crest and cardiovascular development: a 20-year perspective. *Birth Defects Res C Embryo Today* 69: 2-13, 2003.
15. **Pfaltzgraff ER, Shelton EL, Galindo CL, Nelms BL, Hooper CW, Poole SD, Labosky PA, Bader DM, and Reese J**. Embryonic domains of the aorta derived from diverse origins exhibit distinct properties that converge into a common phenotype in the adult. *J Mol Cell Cardiol* 69: 88-96, 2014.
16. **Wang X, Chen D, Chen K, Jubran A, Ramirez A, and Astrof S**. Endothelium in the pharyngeal arches 3, 4 and 6 is derived from the second heart field. *Dev Biol* 421: 108-117, 2017.
17. **Mortola JP**. Gas exchange in avian embryos and hatchlings. *Comp Biochem Physiol A Mol Integr Physiol* 153: 359-377, 2009.
18. **Ardran G, Dawes GS, Prichard MM, Reynolds SR, and Eyatt DG**. The effect of ventilation of the foetal lungs upon the pulmonary circulation. *J Physiol* 118: 12-22, 1952.
19. **Dawes GS**. Pulmonary circulation in the foetus and new-born. *Br Med Bull* 22: 61-65, 1966.
20. **Lakshminrusimha S**. The pulmonary circulation in neonatal respiratory failure. *Clin Perinatol* 39: 655-683, 2012.
21. **Heymann MA, and Rudolph AM**. Control of the ductus arteriosus. *Physiol Rev* 55: 62-78, 1975.
22. **Longo LD**. Carbon monoxide: effects on oxygenation of the fetus in utero. *Science* 194: 523-525, 1976.
23. **Coggins KG, Latour A, Nguyen MS, Audoly L, Coffman TM, and Koller BH**. Metabolism of PGE2 by prostaglandin dehydrogenase is essential for remodeling the ductus arteriosus. *Nat Med* 8: 91-92, 2002.
24. **Roizen JD, Asada M, Tong M, Tai HH, and Muglia LJ**. Preterm birth without progesterone withdrawal in 15-hydroxyprostaglandin dehydrogenase hypomorphic mice. *Mol Endocrinol* 22: 105-112, 2008.

25. **Stoller JZ, Demauro SB, Dagle JM, and Reese J**. Current Perspectives on Pathobiology of the Ductus Arteriosus. *J Clin Exp Cardiolog* 8: 2012.
26. **Burggren WW**. The Persistence of a Patent Ductus Arteriosus in an Adult Specimen of the Tortoise Testudo graeca. *Copeia* 1976: 405-407, 1976.
27. **Gillam-Krakauer M, and Mahajan K**. Patent Ductus Arteriosus. In: *StatPearls [Internet]*. Treasure Island (FL): StatPearls Publishing, 2023.
28. **Tada T, and Kishimoto H**. Ultrastructural and histological studies on closure of the mouse ductus arteriosus. *Acta Anat (Basel)* 139: 326-334, 1990.
29. **van der Linde D, Konings EE, Slager MA, Witsenburg M, Helbing WA, Takkenberg JJ, and Roos-Hesselink JW**. Birth prevalence of congenital heart disease worldwide: a systematic review and meta-analysis. *J Am Coll Cardiol* 58: 2241-2247, 2011.
30. **Clyman RI, Couto J, and Murphy GM**. Patent ductus arteriosus: are current neonatal treatment options better or worse than no treatment at all? *Semin Perinatol* 36: 123-129, 2012.
31. **Gillam-Krakauer M, and Reese J**. Diagnosis and Management of Patent Ductus Arteriosus. *Neoreviews* 19: e394-e402, 2018.
32. **Koch J, Hensley G, Roy L, Brown S, Ramaciotti C, and Rosenfeld CR**. Prevalence of spontaneous closure of the ductus arteriosus in neonates at a birth weight of 1000 grams or less. *Pediatrics* 117: 1113-1121, 2006.
33. **Martin JA, Hamilton BE, Osterman MJ, Curtin SC, and Matthews TJ**. Births: final data for 2013. *Natl Vital Stat Rep* 64: 1-65, 2015.
34. **Matthews TJ, MacDorman MF, and Thoma ME**. Infant Mortality Statistics From the 2013 Period Linked Birth/Infant Death Data Set. *Natl Vital Stat Rep* 64: 1-30, 2015.
35. **Stoll BJ, Hansen NI, Bell EF, Walsh MC, Carlo WA, Shankaran S, Laptook AR, Sanchez PJ, Van Meurs KP, Wyckoff M, Das A, Hale EC, Ball MB, Newman NS, Schibler K, Poindexter BB, Kennedy KA, Cotten CM, Watterberg KL, D'Angio CT, DeMauro SB, Truog WE, Devaskar U, Higgins RD, Eunice Kennedy Shriver National Institute of Child H, and Human Development Neonatal Research N**. Trends in Care Practices, Morbidity, and Mortality of Extremely Preterm Neonates, 1993-2012. *JAMA* 314: 1039-1051, 2015.
36. **Patel RM, Kandefer S, Walsh MC, Bell EF, Carlo WA, Laptook AR, Sanchez PJ, Shankaran S, Van Meurs KP, Ball MB, Hale EC, Newman NS, Das A, Higgins RD, Stoll BJ, Eunice Kennedy Shriver National Institute of Child H, and Human Development Neonatal Research N**. Causes and timing of death in extremely premature infants from 2000 through 2011. *N Engl J Med* 372: 331-340, 2015.
37. **Snyers D, Lefebvre C, Viellevoye R, and Rigo V**. [Late preterm : high risk newborns despite appearances]. *Rev Med Liege* 75: 105-110, 2020.
38. **Hammerman C**. Patent ductus arteriosus. Clinical relevance of prostaglandins and prostaglandin inhibitors in PDA pathophysiology and treatment. *Clin Perinatol* 22: 457-479, 1995.
39. **Reese J, Veldman A, Shah L, Vucovich M, and Cotton RB**. Inadvertent relaxation of the ductus arteriosus by pharmacologic agents that are commonly used in the neonatal period. *Semin Perinatol* 34: 222-230, 2010.
40. PATENT ductus arteriosus and maternal rubella. *J Am Med Assoc* 150: 419, 1952.
41. **Toizumi M, Motomura H, Vo HM, Takahashi K, Pham E, Nguyen HA, Le TH, Hashizume M, Ariyoshi K, Dang DA, Moriuchi H, and Yoshida LM**. Mortality associated with pulmonary hypertension in congenital rubella syndrome. *Pediatrics* 134: e519-526, 2014.
42. **Toizumi M, Do CGT, Motomura H, Do TN, Fukunaga H, Iijima M, Le NN, Nguyen HT, Moriuchi H, and Yoshida LM**. Characteristics of Patent Ductus Arteriosus in Congenital Rubella Syndrome. *Sci Rep* 9: 17105, 2019.
43. **Forsey JT, Elmasry OA, and Martin RP**. Patent arterial duct. *Orphanet J Rare Dis* 4: 17, 2009.
44. **Krichenko A, Benson LN, Burrows P, Moes CA, McLaughlin P, and Freedom RM**. Angiographic classification of the isolated, persistently patent ductus arteriosus and implications for percutaneous catheter occlusion. *Am J Cardiol* 63: 877-880, 1989.
45. **Moise KJ, Jr.** Effect of advancing gestational age on the frequency of fetal ductal constriction in association with maternal indomethacin use. *Am J Obstet Gynecol* 168: 1350-1353, 1993.

46. **Vermillion ST, Scardo JA, Lashus AG, and Wiles HB**. The effect of indomethacin tocolysis on fetal ductus arteriosus constriction with advancing gestational age. *Am J Obstet Gynecol* 177: 256-259; discussion 259-261, 1997.
47. **Norton ME, Merrill J, Cooper BA, Kuller JA, and Clyman RI**. Neonatal complications after the administration of indomethacin for preterm labor. *N Engl J Med* 329: 1602-1607, 1993.
48. **Engelstad HJ, Roghair RD, Calarge CA, Colaizy TT, Stuart S, and Haskell SE**. Perinatal outcomes of pregnancies complicated by maternal depression with or without selective serotonin reuptake inhibitor therapy. *Neonatology* 105: 149-154, 2014.
49. **Dakshinamurti S**. Pathophysiologic mechanisms of persistent pulmonary hypertension of the newborn. *Pediatr Pulmonol* 39: 492-503, 2005.
50. **Alwan S, and Friedman JM**. Safety of selective serotonin reuptake inhibitors in pregnancy. *CNS Drugs* 23: 493-509, 2009.
51. **Croen LA, Grether JK, Yoshida CK, Odouli R, and Hendrick V**. Antidepressant use during pregnancy and childhood autism spectrum disorders. *Arch Gen Psychiatry* 68: 1104-1112, 2011.
52. **Chambers CD, Johnson KA, Dick LM, Felix RJ, and Jones KL**. Birth outcomes in pregnant women taking fluoxetine. *N Engl J Med* 335: 1010-1015, 1996.
53. **Chambers CD, Hernandez-Diaz S, Van Marter LJ, Werler MM, Louik C, Jones KL, and Mitchell AA**. Selective serotonin-reuptake inhibitors and risk of persistent pulmonary hypertension of the newborn. *N Engl J Med* 354: 579-587, 2006.
54. **Levin DL, Mills LJ, and Weinberg AG**. Hemodynamic, pulmonary vascular, and myocardial abnormalities secondary to pharmacologic constriction of the fetal ductus arteriosus. A possible mechanism for persistent pulmonary hypertension and transient tricuspid insufficiency in the newborn infant. *Circulation* 60: 360-364, 1979.
55. **Hooper CW, Delaney C, Streeter T, Yarboro MT, Poole S, Brown N, Slaughter JC, Cotton RB, Reese J, and Shelton EL**. Selective serotonin reuptake inhibitor exposure constricts the mouse ductus arteriosus in utero. *Am J Physiol Heart Circ Physiol* 311: H572-581, 2016.
56. **Clyman RI, Ballard PL, Sniderman S, Ballard RA, Roth R, Heymann MA, and Granberg JP**. Prenatal administration of betamethasone for prevention of patient ductus arteriosus. *J Pediatr* 98: 123-126, 1981.
57. **Waffarn F, Siassi B, Cabal LA, and Schmidt PL**. Effect of antenatal glucocorticoids on clinical closure of the ductus arteriosus. *Am J Dis Child* 137: 336-338, 1983.
58. **Doyle LW, Kitchen WH, Ford GW, Rickards AL, Lissenden JV, and Ryan MM**. Effects of antenatal steroid therapy on mortality and morbidity in very low birth weight infants. *J Pediatr* 108: 287-292, 1986.
59. **Eronen M, Kari A, Pesonen E, and Hallman M**. The effect of antenatal dexamethasone administration on the fetal and neonatal ductus arteriosus. A randomized double-blind study. *Am J Dis Child* 147: 187-192, 1993.
60. **Shelton EL, Waleh N, Plosa EJ, Benjamin JT, Milne GL, Hooper CW, Ehinger NJ, Poole S, Brown N, Seidner S, McCurnin D, Reese J, and Clyman RI**. Effects of antenatal betamethasone on preterm human and mouse ductus arteriosus: comparison with baboon data. *Pediatr Res* 84: 458-465, 2018.
61. **Vucovich MM, Cotton RB, Shelton EL, Goettel JA, Ehinger NJ, Poole SD, Brown N, Wynn JL, Paria BC, Slaughter JC, Clark RH, Rojas MA, and Reese J**. Aminoglycoside-mediated relaxation of the ductus arteriosus in sepsis-associated PDA. *Am J Physiol Heart Circ Physiol* 307: H732-740, 2014.
62. **Adams HR, Goodman FR, and Weiss GB**. Alteration of contractile function and calcium ion movements in vascular smooth muscle by gentamicin and other aminoglycoside antibiotics. *Antimicrob Agents Chemother* 5: 640-646, 1974.
63. **Descotes J, and Evreux JC**. Cardiac depressant effects of some recent aminoglycoside antibiotics. *J Antimicrob Chemother* 7: 197-200, 1981.
64. **Belus A, and White E**. Effects of antibiotics on the contractility and Ca2+ transients of rat cardiac myocytes. *Eur J Pharmacol* 412: 121-126, 2001.
65. **Cotton RB, Hazinski TA, Morrow JD, Roberts LJ, Zeldin DC, Lindstrom DP, Lappalainen U, Law AB, and Steele S**. Cimetidine does not prevent lung injury in newborn premature infants. *Pediatr Res* 59: 795-800, 2006.

66. **Cotton RB, Shah LP, Poole SD, Ehinger NJ, Brown N, Shelton EL, Slaughter JC, Baldwin HS, Paria BC, and Reese J**. Cimetidine-associated patent ductus arteriosus is mediated via a cytochrome P450 mechanism independent of H2 receptor antagonism. *J Mol Cell Cardiol* 59: 86-94, 2013.
67. **Thebaud B, Michelakis E, Wu XC, Harry G, Hashimoto K, and Archer SL**. Sildenafil reverses O2 constriction of the rabbit ductus arteriosus by inhibiting type 5 phosphodiesterase and activating BK(Ca) channels. *Pediatr Res* 52: 19-24, 2002.
68. **Toyoshima K, Momma K, Imamura S, and Nakanishi T**. In vivo dilatation of the postnatal ductus arteriosus by atrial natriuretic peptide in the rat. *Neonatology* 92: 139-144, 2007.
69. **Liu H, Manganiello V, Waleh N, and Clyman RI**. Expression, activity, and function of phosphodiesterases in the mature and immature ductus arteriosus. *Pediatr Res* 64: 477-481, 2008.
70. **Johnston PG, Gillam-Krakauer M, Fuller MP, and Reese J**. Evidence-based use of indomethacin and ibuprofen in the neonatal intensive care unit. *Clin Perinatol* 39: 111-136, 2012.
71. **Patel J, Roberts I, Azzopardi D, Hamilton P, and Edwards AD**. Randomized double-blind controlled trial comparing the effects of ibuprofen with indomethacin on cerebral hemodynamics in preterm infants with patent ductus arteriosus. *Pediatr Res* 47: 36-42, 2000.
72. **Merritt TA, White CL, Coen RW, Friedman WF, Gluck L, and Rosenberg M**. Preschool assessment of infants with a patent ductus arteriosus: comparison of ligation and indomethacin therapy. *Am J Dis Child* 136: 507-512, 1982.
73. **Lago P, Bettiol T, Salvadori S, Pitassi I, Vianello A, Chiandetti L, and Saia OS**. Safety and efficacy of ibuprofen versus indomethacin in preterm infants treated for patent ductus arteriosus: a randomised controlled trial. *Eur J Pediatr* 161: 202-207, 2002.
74. **Su PH, Chen JY, Su CM, Huang TC, and Lee HS**. Comparison of ibuprofen and indomethacin therapy for patent ductus arteriosus in preterm infants. *Pediatr Int* 45: 665-670, 2003.
75. **Pezzati M, Vangi V, Biagiotti R, Bertini G, Cianciulli D, and Rubaltelli FF**. Effects of indomethacin and ibuprofen on mesenteric and renal blood flow in preterm infants with patent ductus arteriosus. *J Pediatr* 135: 733-738, 1999.
76. **Grosfeld JL, Chaet M, Molinari F, Engle W, Engum SA, West KW, Rescorla FJ, and Scherer LR, 3rd**. Increased risk of necrotizing enterocolitis in premature infants with patent ductus arteriosus treated with indomethacin. *Ann Surg* 224: 350-355; discussion 355-357, 1996.
77. **Clyman RI**. Recommendations for the postnatal use of indomethacin: an analysis of four separate treatment strategies. *J Pediatr* 128: 601-607, 1996.
78. **Schmidt B, Davis P, Moddemann D, Ohlsson A, Roberts RS, Saigal S, Solimano A, Vincer M, Wright LL, and Trial of Indomethacin Prophylaxis in Preterms I**. Long-term effects of indomethacin prophylaxis in extremely-low-birth-weight infants. *N Engl J Med* 344: 1966-1972, 2001.
79. **Knight DB**. The treatment of patent ductus arteriosus in preterm infants. A review and overview of randomized trials. *Semin Neonatol* 6: 63-73, 2001.
80. **Cooke L, Steer P, and Woodgate P**. Indomethacin for asymptomatic patent ductus arteriosus in preterm infants. *Cochrane Database Syst Rev* 2003: CD003745, 2003.
81. **Nagaraj HS, Sandhu AS, Cook LN, Buchino JJ, and Groff DB**. Gastrointestinal perforation following indomethacin therapy in very low birth weight infants. *J Pediatr Surg* 16: 1003-1007, 1981.
82. **Grosfeld JL, Cheu H, Schlatter M, West KW, and Rescorla FJ**. Changing trends in necrotizing enterocolitis. Experience with 302 cases in two decades. *Ann Surg* 214: 300-306; discussion 306-307, 1991.
83. **Corff KE, and Sekar KC**. Clinical considerations for the pharmacologic management of patent ductus arteriosus with cyclooxygenase inhibitors in premature infants. *J Pediatr Pharmacol Ther* 12: 147-157, 2007.
84. **Weisz DE, More K, McNamara PJ, and Shah PS**. PDA ligation and health outcomes: a meta-analysis. *Pediatrics* 133: e1024-1046, 2014.
85. **Teixeira LS, Shivananda SP, Stephens D, Van Arsdell G, and McNamara PJ**. Postoperative cardiorespiratory instability following ligation of the preterm ductus arteriosus is related to early need for intervention. *J Perinatol* 28: 803-810, 2008.

86. **Jain A, Sahni M, El-Khuffash A, Khadawardi E, Sehgal A, and McNamara PJ**. Use of targeted neonatal echocardiography to prevent postoperative cardiorespiratory instability after patent ductus arteriosus ligation. *J Pediatr* 160: 584-589 e581, 2012.
87. **Ulrich TJB, Hansen TP, Reid KJ, Bingler MA, and Olsen SL**. Post-ligation cardiac syndrome is associated with increased morbidity in preterm infants. *J Perinatol* 38: 537-542, 2018.
88. **Harting MT, Blakely ML, Cox CS, Jr., Lantin-Hermoso R, Andrassy RJ, and Lally KP**. Acute hemodynamic decompensation following patent ductus arteriosus ligation in premature infants. *J Invest Surg* 21: 133-138, 2008.
89. **Pereira KD, Webb BD, Blakely ML, Cox CS, Jr., and Lally KP**. Sequelae of recurrent laryngeal nerve injury after patent ductus arteriosus ligation. *Int J Pediatr Otorhinolaryngol* 70: 1609-1612, 2006.
90. **Thach BT**. Recurrent laryngeal nerve injury during patent ductus ligation: can this common complication be reduced? *J Perinatol* 30: 371-372, 2010.
91. **Sathanandam SK, Gutfinger D, O'Brien L, Forbes TJ, Gillespie MJ, Berman DP, Armstrong AK, Shahanavaz S, Jones TK, Morray BH, Rockefeller TA, Justino H, Nykanen DG, and Zahn EM**. Amplatzer Piccolo Occluder clinical trial for percutaneous closure of the patent ductus arteriosus in patients >/=700 grams. *Catheter Cardiovasc Interv* 96: 1266-1276, 2020.
92. **Serrano RM, Madison M, Lorant D, Hoyer M, and Alexy R**. Comparison of 'post-patent ductus arteriosus ligation syndrome' in premature infants after surgical ligation vs. percutaneous closure. *J Perinatol* 40: 324-329, 2020.
93. **Tomasulo CE, Gillespie MJ, Munson D, Demkin T, O'Byrne ML, Dori Y, Smith CL, Rome JJ, and Glatz AC**. Incidence and fate of device-related left pulmonary artery stenosis and aortic coarctation in small infants undergoing transcatheter patent ductus arteriosus closure. *Catheter Cardiovasc Interv* 96: 889-897, 2020.
94. **Bruckheimer E, Steiner K, Barak-Corren Y, Slanovic L, Levinzon M, Lowenthal A, Amir G, Dagan T, and Birk E**. The Amplatzer duct occluder (ADOII) and Piccolo devices for patent ductus arteriosus closure: a large single institution series. *Front Cardiovasc Med* 10: 1158227, 2023.
95. **Liu J, Gao L, Tan HL, Zheng QH, Liu L, and Wang Z**. Transcatheter closure through single venous approach for young children with patent ductus arteriosus: A retrospective study of 686 cases. *Medicine (Baltimore)* 97: e11958, 2018.
96. **Mashally S, Nield LE, McNamara PJ, Martins FF, El-Khuffash A, Jain A, and Weisz DE**. Late oral acetaminophen versus immediate surgical ligation in preterm infants with persistent large patent ductus arteriosus. *J Thorac Cardiovasc Surg* 156: 1937-1944, 2018.
97. **Aygun A, Poryo M, Wagenpfeil G, Wissing A, Ebrahimi-Fakhari D, Zemlin M, Gortner L, and Meyer S**. Birth weight, Apgar scores and gentamicin were associated with acute kidney injuries in VLBW neonates requiring treatment for patent ductus arteriosus. *Acta Paediatr* 108: 645-653, 2019.
98. **Lamy M, De Grouchy J, and Schweisguth O**. Genetic and non-genetic factors in the etiology of congenital heart disease: a study of 1188 cases. *Am J Hum Genet* 9: 17-41, 1957.
99. **Polani PE, and Campbell M**. Factors in the causation of persistent ductus arteriosus. *Ann Hum Genet* 24: 343-357, 1960.
100. **Lavoie PM, Pham C, and Jang KL**. Heritability of bronchopulmonary dysplasia, defined according to the consensus statement of the national institutes of health. *Pediatrics* 122: 479-485, 2008.
101. **Bhandari V, Zhou G, Bizzarro MJ, Buhimschi C, Hussain N, Gruen JR, and Zhang H**. Genetic contribution to patent ductus arteriosus in the premature newborn. *Pediatrics* 123: 669-673, 2009.
102. **Mani A, Meraji SM, Houshyar R, Radhakrishnan J, Mani A, Ahangar M, Rezaie TM, Taghavinejad MA, Broumand B, Zhao H, Nelson-Williams C, and Lifton RP**. Finding genetic contributions to sporadic disease: a recessive locus at 12q24 commonly contributes to patent ductus arteriosus. *Proc Natl Acad Sci U S A* 99: 15054-15059, 2002.
103. **Khau Van Kien P, Mathieu F, Zhu L, Lalande A, Betard C, Lathrop M, Brunotte F, Wolf JE, and Jeunemaitre X**. Mapping of familial thoracic aortic aneurysm/dissection with patent ductus arteriosus to 16p12.2-p13.13. *Circulation* 112: 200-206, 2005.

104. **Mani A, Radhakrishnan J, Farhi A, Carew KS, Warnes CA, Nelson-Williams C, Day RW, Pober B, State MW, and Lifton RP**. Syndromic patent ductus arteriosus: evidence for haploinsufficient TFAP2B mutations and identification of a linked sleep disorder. *Proc Natl Acad Sci U S A* 102: 2975-2979, 2005.
105. **Waleh N, Hodnick R, Jhaveri N, McConaghy S, Dagle J, Seidner S, McCurnin D, Murray JC, Ohls R, and Clyman RI**. Patterns of gene expression in the ductus arteriosus are related to environmental and genetic risk factors for persistent ductus patency. *Pediatr Res* 68: 292-297, 2010.
106. **Reese J, Paria BC, Brown N, Zhao X, Morrow JD, and Dey SK**. Coordinated regulation of fetal and maternal prostaglandins directs successful birth and postnatal adaptation in the mouse. *Proc Natl Acad Sci U S A* 97: 9759-9764, 2000.
107. **Loftin CD, Trivedi DB, Tiano HF, Clark JA, Lee CA, Epstein JA, Morham SG, Breyer MD, Nguyen M, Hawkins BM, Goulet JL, Smithies O, Koller BH, and Langenbach R**. Failure of ductus arteriosus closure and remodeling in neonatal mice deficient in cyclooxygenase-1 and cyclooxygenase-2. *Proc Natl Acad Sci U S A* 98: 1059-1064, 2001.
108. **Nguyen M, Camenisch T, Snouwaert JN, Hicks E, Coffman TM, Anderson PA, Malouf NN, and Koller BH**. The prostaglandin receptor EP4 triggers remodelling of the cardiovascular system at birth. *Nature* 390: 78-81, 1997.
109. **Segi E, Sugimoto Y, Yamasaki A, Aze Y, Oida H, Nishimura T, Murata T, Matsuoka T, Ushikubi F, Hirose M, Tanaka T, Yoshida N, Narumiya S, and Ichikawa A**. Patent ductus arteriosus and neonatal death in prostaglandin receptor EP4-deficient mice. *Biochem Biophys Res Commun* 246: 7-12, 1998.
110. **Schneider A, Guan Y, Zhang Y, Magnuson MA, Pettepher C, Loftin CD, Langenbach R, Breyer RM, and Breyer MD**. Generation of a conditional allele of the mouse prostaglandin EP4 receptor. *Genesis* 40: 7-14, 2004.
111. **Huang J, Cheng L, Li J, Chen M, Zhou D, Lu MM, Proweller A, Epstein JA, and Parmacek MS**. Myocardin regulates expression of contractile genes in smooth muscle cells and is required for closure of the ductus arteriosus in mice. *J Clin Invest* 118: 515-525, 2008.
112. **Zou M, Mangum KD, Magin JC, Cao HH, Yarboro MT, Shelton EL, Taylor JM, Reese J, Furey TS, and Mack CP**. Prdm6 drives ductus arteriosus closure by promoting ductus arteriosus smooth muscle cell identity and contractility. *JCI Insight* 8: 2023.
113. **Gruzdev A, Nguyen M, Kovarova M, and Koller BH**. PGE2 through the EP4 receptor controls smooth muscle gene expression patterns in the ductus arteriosus critical for remodeling at birth. *Prostaglandins Other Lipid Mediat* 97: 109-119, 2012.
114. **Shelton EL, Ector G, Galindo CL, Hooper CW, Brown N, Wilkerson I, Pfaltzgraff ER, Paria BC, Cotton RB, Stoller JZ, and Reese J**. Transcriptional profiling reveals ductus arteriosus-specific genes that regulate vascular tone. *Physiol Genomics* 46: 457-466, 2014.
115. **Costa M, Barogi S, Socci ND, Angeloni D, Maffei M, Baragatti B, Chiellini C, Grasso E, and Coceani F**. Gene expression in ductus arteriosus and aorta: comparison of birth and oxygen effects. *Physiol Genomics* 25: 250-262, 2006.
116. **Yokoyama U, Sato Y, Akaike T, Ishida S, Sawada J, Nagao T, Quan H, Jin M, Iwamoto M, Yokota S, Ishikawa Y, and Minamisawa S**. Maternal vitamin A alters gene profiles and structural maturation of the rat ductus arteriosus. *Physiol Genomics* 31: 139-157, 2007.
117. **Jin MH, Yokoyama U, Sato Y, Shioda A, Jiao Q, Ishikawa Y, and Minamisawa S**. DNA microarray profiling identified a new role of growth hormone in vascular remodeling of rat ductus arteriosus. *J Physiol Sci* 61: 167-179, 2011.
118. **Liu NM, Yokota T, Maekawa S, Lu P, Zheng YW, Taniguchi H, Yokoyama U, Kato T, and Minamisawa S**. Transcription profiles of endothelial cells in the rat ductus arteriosus during a perinatal period. *PLoS One* 8: e73685, 2013.
119. **Bokenkamp R, van Brempt R, van Munsteren JC, van den Wijngaert I, de Hoogt R, Finos L, Goeman J, Groot AC, Poelmann RE, Blom NA, and DeRuiter MC**. Dlx1 and Rgs5 in the ductus arteriosus: vessel-specific genes identified by transcriptional profiling of laser-capture microdissected endothelial and smooth muscle cells. *PLoS One* 9: e86892, 2014.

120. **Hsieh YT, Liu NM, Ohmori E, Yokota T, Kajimura I, Akaike T, Ohshima T, Goda N, and Minamisawa S**. Transcription profiles of the ductus arteriosus in Brown-Norway rats with irregular elastic fiber formation. *Circ J* 78: 1224-1233, 2014.
121. **Goyal R, Goyal D, Longo LD, and Clyman RI**. Microarray gene expression analysis in ovine ductus arteriosus during fetal development and birth transition. *Pediatr Res* 80: 610-618, 2016.
122. **Akaike T, Shinjo S, Ohmori E, Kajimura I, Goda N, and Minamisawa S**. Transcriptional profiles in the chicken ductus arteriosus during hatching. *PLoS One* 14: e0214139, 2019.
123. **Mueller PP, Drynda A, Goltz D, Hoehn R, Hauser H, and Peuster M**. Common signatures for gene expression in postnatal patients with patent arterial ducts and stented arteries. *Cardiol Young* 19: 352-359, 2009.
124. **Saito J, Kojima T, Tanifuji S, Kato Y, Oka S, Ichikawa Y, Miyagi E, Tachibana T, Asou T, and Yokoyama U**. Transcriptome Analysis Reveals Differential Gene Expression between the Closing Ductus Arteriosus and the Patent Ductus Arteriosus in Humans. *J Cardiovasc Dev Dis* 8: 2021.
125. **Salvador J, Hernandez GE, Ma F, Abrahamson CW, Pellegrini M, Goldman R, Ridge KM, and Iruela-Arispe ML**. Transcriptional Evaluation of the Ductus Arteriosus at the Single-Cell Level Uncovers a Requirement for Vim (Vimentin) for Complete Closure. *Arterioscler Thromb Vasc Biol* 42: 732-742, 2022.
126. **Gittenberger-de Groot AC, Strengers JL, Mentink M, Poelmann RE, and Patterson DF**. Histologic studies on normal and persistent ductus arteriosus in the dog. *J Am Coll Cardiol* 6: 394-404, 1985.
127. **Owens GK, Kumar MS, and Wamhoff BR**. Molecular regulation of vascular smooth muscle cell differentiation in development and disease. *Physiol Rev* 84: 767-801, 2004.
128. **Rensen SS, Doevendans PA, and van Eys GJ**. Regulation and characteristics of vascular smooth muscle cell phenotypic diversity. *Neth Heart J* 15: 100-108, 2007.
129. **Beamish JA, He P, Kottke-Marchant K, and Marchant RE**. Molecular regulation of contractile smooth muscle cell phenotype: implications for vascular tissue engineering. *Tissue Eng Part B Rev* 16: 467-491, 2010.
130. **Liu C, Zhu P, Wang W, Li W, Shu Q, Chen ZJ, Myatt L, and Sun K**. Inhibition of lysyl oxidase by prostaglandin E2 via EP2/EP4 receptors in human amnion fibroblasts: Implications for parturition. *Mol Cell Endocrinol* 424: 118-127, 2016.
131. **Hiromi T, Yokoyama U, Kurotaki D, Mamun A, Ishiwata R, Ichikawa Y, Nishihara H, Umemura M, Fujita T, Yasuda S, Minami T, Goda M, Uchida K, Suzuki S, Takeuchi I, Masuda M, Breyer RM, Tamura T, and Ishikawa Y**. Excessive EP4 Signaling in Smooth Muscle Cells Induces Abdominal Aortic Aneurysm by Amplifying Inflammation. *Arterioscler Thromb Vasc Biol* 40: 1559-1573, 2020.
132. **Tada T, Wakabayashi T, Nakao Y, Ueki R, Ogawa Y, Inagawa A, Shibata T, and Kishimoto H**. Human ductus arteriosus. A histological study on the relation between ductal maturation and gestational age. *Acta Pathol Jpn* 35: 23-34, 1985.
133. **Langille BL**. Arterial remodeling: relation to hemodynamics. *Can J Physiol Pharmacol* 74: 834-841, 1996.
134. **Gittenberger-de Groot AC, van Ertbruggen I, Moulaert AJ, and Harinck E**. The ductus arteriosus in the preterm infant: histologic and clinical observations. *J Pediatr* 96: 88-93, 1980.
135. **De Reeder EG, Girard N, Poelmann RE, Van Munsteren JC, Patterson DF, and Gittenberger-De Groot AC**. Hyaluronic acid accumulation and endothelial cell detachment in intimal thickening of the vessel wall. The normal and genetically defective ductus arteriosus. *Am J Pathol* 132: 574-585, 1988.
136. **de Reeder EG, Poelmann RE, van Munsteren JC, Patterson DF, and Gittenberger-de Groot AC**. Ultrastructural and immunohistochemical changes of the extracellular matrix during intimal cushion formation in the ductus arteriosus of the dog. *Atherosclerosis* 79: 29-40, 1989.
137. **Buchanan JW**. Morphology of the ductus arteriosus in fetal and neonatal dogs genetically predisposed to patent ductus arteriosus. *Birth Defects Orig Artic Ser* 14: 349-360, 1978.
138. **Gittenberger-de Groot AC**. Persistent ductus arteriosus: most probably a primary congenital malformation. *Br Heart J* 39: 610-618, 1977.
139. **Chuaqui B, Piwonka G, and Farru O**. [The wall in persistent ductus arteriosus (author's transl)]. *Virchows Arch A Pathol Anat Histol* 372: 315-324, 1977.

140. **Gittenberger-de Groot AC, Moulaert AJ, and Hitchcock JF**. Histology of the persistent ductus arteriosus in cases of congenital rubella. *Circulation* 62: 183-186, 1980.
141. **Sauvage M, Osborne-Pellegrin M, Deslandes-Le Flohic F, and Jacob MP**. Influence of elastin gene polymorphism on the elastin content of the aorta: A study in 2 strains of rat. *Arterioscler Thromb Vasc Biol* 19: 2308-2315, 1999.
142. **Kota L, Osborne-Pellegrin M, Schulz H, Behmoaras J, Coutard M, Gong M, and Hubner N**. Quantitative genetic basis of arterial phenotypes in the Brown Norway rat. *Physiol Genomics* 30: 17-25, 2007.
143. **Bokenkamp R, Gittenberger-De Groot AC, Van Munsteren CJ, Grauss RW, Ottenkamp J, and Deruiter MC**. Persistent ductus arteriosus in the Brown-Norway inbred rat strain. *Pediatr Res* 60: 407-412, 2006.
144. **Toda T, Tsuda N, Takagi T, Nishimori I, Leszczynski D, and Kummerow F**. Ultrastructure of developing human ductus arteriosus. *J Anat* 131: 25-37, 1980.
145. **de Reeder EG, van Munsteren CJ, Poelmann RE, Patterson DF, and Gittenberger-de Groot AC**. Changes in distribution of elastin and elastin receptor during intimal cushion formation in the ductus arteriosus. *Anat Embryol (Berl)* 182: 473-480, 1990.
146. **Yokoyama U, Minamisawa S, Quan H, Ghatak S, Akaike T, Segi-Nishida E, Iwasaki S, Iwamoto M, Misra S, Tamura K, Hori H, Yokota S, Toole BP, Sugimoto Y, and Ishikawa Y**. Chronic activation of the prostaglandin receptor EP4 promotes hyaluronan-mediated neointimal formation in the ductus arteriosus. *J Clin Invest* 116: 3026-3034, 2006.
147. **Yokoyama U, Minamisawa S, Katayama A, Tang T, Suzuki S, Iwatsubo K, Iwasaki S, Kurotani R, Okumura S, Sato M, Yokota S, Hammond HK, and Ishikawa Y**. Differential regulation of vascular tone and remodeling via stimulation of type 2 and type 6 adenylyl cyclases in the ductus arteriosus. *Circ Res* 106: 1882-1892, 2010.
148. **Yokoyama U, Minamisawa S, and Ishikawa Y**. Regulation of vascular tone and remodeling of the ductus arteriosus. *J Smooth Muscle Res* 46: 77-87, 2010.
149. **Slomp J, van Munsteren JC, Poelmann RE, de Reeder EG, Bogers AJ, and Gittenberger-de Groot AC**. Formation of intimal cushions in the ductus arteriosus as a model for vascular intimal thickening. An immunohistochemical study of changes in extracellular matrix components. *Atherosclerosis* 93: 25-39, 1992.
150. **Slomp J, Gittenberger-de Groot AC, Koteliansky VE, Glukhova MA, Bogers AJ, and Poelmann RE**. Cytokeratin expression in human arteries pertinent to intimal thickening formation in the ductus arteriosus. *Differentiation* 61: 305-311, 1997.
151. **Yoder MJ, Baumann FG, Grover-Johnson NM, Brick I, and Imparato AM**. A morphological study of early cellular changes in the closure of the rabbit ductus arteriosus. *Anat Rec* 192: 19-39, 1978.
152. **Mensah B**. Ligamentum arteriosum: Muscular and contractile. *Anat Rec (Hoboken)* 306: 409-421, 2023.
153. **Toda T, Leszczynski DE, and Kummerow FA**. Morphological evidence of endogenous lipid production in swine ductus vasculature. *Atherosclerosis* 37: 325-330, 1980.
154. **Toda T, Leszczynski DE, and Kummerow FA**. Degenerative changes in endothelial and smooth muscle cells from aging swine ductus arteriosus and venosus. *Am J Anat* 160: 37-49, 1981.
155. **Nass J, Terglane J, and Gerke V**. Weibel Palade Bodies: Unique Secretory Organelles of Endothelial Cells that Control Blood Vessel Homeostasis. *Front Cell Dev Biol* 9: 813995, 2021.
156. **Rafieian-Kopaei M, Setorki M, Doudi M, Baradaran A, and Nasri H**. Atherosclerosis: process, indicators, risk factors and new hopes. *Int J Prev Med* 5: 927-946, 2014.
157. **Webb RC**. Smooth muscle contraction and relaxation. *Adv Physiol Educ* 27: 201-206, 2003.
158. **Chalovich JM, and Eisenberg E**. Inhibition of actomyosin ATPase activity by troponin-tropomyosin without blocking the binding of myosin to actin. *J Biol Chem* 257: 2432-2437, 1982.
159. **Miller DD, Hamada A, Clark MT, Adejare A, Patil PN, Shams G, Romstedt KJ, Kim SU, Intrasuksri U, McKenzie JL, and et al.** Synthesis and alpha 2-adrenoceptor effects of substituted catecholimidazoline and catecholimidazole analogues in human platelets. *J Med Chem* 33: 1138-1144, 1990.
160. **He WQ, Qiao YN, Zhang CH, Peng YJ, Chen C, Wang P, Gao YQ, Chen C, Chen X, Tao T, Su XH, Li CJ, Kamm KE, Stull JT, and Zhu MS**. Role of myosin light chain kinase in regulation of basal blood pressure and maintenance of salt-induced hypertension. *Am J Physiol Heart Circ Physiol* 301: H584-591, 2011.

161. **Somlyo AP, and Somlyo AV**. Signal transduction and regulation in smooth muscle. *Nature* 372: 231-236, 1994.
162. **Kamm KE, and Stull JT**. Dedicated myosin light chain kinases with diverse cellular functions. *J Biol Chem* 276: 4527-4530, 2001.
163. **Somlyo AP, and Somlyo AV**. Ca2+ sensitivity of smooth muscle and nonmuscle myosin II: modulated by G proteins, kinases, and myosin phosphatase. *Physiol Rev* 83: 1325-1358, 2003.
164. **Kamm KE, and Stull JT**. The function of myosin and myosin light chain kinase phosphorylation in smooth muscle. *Annu Rev Pharmacol Toxicol* 25: 593-620, 1985.
165. **Karaki H, Ozaki H, Hori M, Mitsui-Saito M, Amano K, Harada K, Miyamoto S, Nakazawa H, Won KJ, and Sato K**. Calcium movements, distribution, and functions in smooth muscle. *Pharmacol Rev* 49: 157-230, 1997.
166. **Sakurada S, Takuwa N, Sugimoto N, Wang Y, Seto M, Sasaki Y, and Takuwa Y**. Ca2+-dependent activation of Rho and Rho kinase in membrane depolarization-induced and receptor stimulation-induced vascular smooth muscle contraction. *Circ Res* 93: 548-556, 2003.
167. **Wu X, Somlyo AV, and Somlyo AP**. Cyclic GMP-dependent stimulation reverses G-protein-coupled inhibition of smooth muscle myosin light chain phosphate. *Biochem Biophys Res Commun* 220: 658-663, 1996.
168. **Konya V, Marsche G, Schuligoi R, and Heinemann A**. E-type prostanoid receptor 4 (EP4) in disease and therapy. *Pharmacol Ther* 138: 485-502, 2013.
169. **Syrovatkina V, Alegre KO, Dey R, and Huang XY**. Regulation, Signaling, and Physiological Functions of G-Proteins. *J Mol Biol* 428: 3850-3868, 2016.
170. **Kurzrok R, and Lieb CC**. Biochemical Studies of Human Semen. II. The Action of Semen on the Human Uterus. *Proceedings of the Society for Experimental Biology and Medicine* 28: 268-272, 1930.
171. **v. Euler US**. Über die Spezifische Blutdrucksenkende Substanz des Menschlichen Prostata- und Samenblasensekretes. *Klinische Wochenschrift* 14: 1182-1183, 1935.
172. **Bergstrom S, Duner H, von EU, Pernow B, and Sjovall J**. Observations on the effects of infusion of prostaglandin E in man. *Acta Physiol Scand* 45: 145-151, 1959.
173. **Van D, Beerthuis RK, Nugteren DH, and Vonkeman H**. The Biosynthesis of Prostaglandins. *Biochim Biophys Acta* 90: 204-207, 1964.
174. **Elliott RB, and Starling MB**. The effect of prostaglandin $F_{2\alpha}$ in the closure of the ductus arteriosus. *Prostaglandins* 2: 399-403, 1972.
175. **Coceani F, and Olley PM**. The response of the ductus arteriosus to prostaglandins. *Can J Physiol Pharmacol* 51: 220-225, 1973.
176. **Sharpe GL, Thalme B, and Larsson KS**. Studies on closure of the ductus arteriosus. XI. Ductal closure in utero by a prostaglandin synthetase inhibitor. *Prostaglandins* 8: 363-368, 1974.
177. **Friedman WF, Hirschklau MJ, Printz MP, Pitlick PT, and Kirkpatrick SE**. Pharmacologic closure of patent ductus arteriosus in the premature infant. *N Engl J Med* 295: 526-529, 1976.
178. **Clyman RI**. Ontogeny of the ductus arteriosus response to prostaglandins and inhibitors of their synthesis. *Semin Perinatol* 4: 115-124, 1980.
179. **Momma K, Uemura S, Nishihara S, and Ota Y**. Dilatation of the ductus arteriosus by prostaglandins and prostaglandin's precursors. *Pediatr Res* 14: 1074-1077, 1980.
180. **Smith GC, Coleman RA, and McGrath JC**. Characterization of dilator prostanoid receptors in the fetal rabbit ductus arteriosus. *J Pharmacol Exp Ther* 271: 390-396, 1994.
181. **Sharpe GL, and Larsson KS**. Studies on closure of the ductus arteriosus. X. In vivo effect of prostaglandin. *Prostaglandins* 9: 703-719, 1975.
182. **Janatova T, Jarkovska D, Hruda J, Samanek M, and Ostadal B**. Effect of the administration of prostaglandins (PGE2) in the early postnatal period on closure of the ductus arteriosus in the laboratory rat. *Physiol Bohemoslov* 38: 201-206, 1989.
183. **Atad J, Lissak A, Rofe A, and Abramovici H**. Patent ductus arteriosus after prolonged treatment with indomethacin during pregnancy: case report. *Int J Gynaecol Obstet* 25: 73-76, 1987.
184. **Moise KJ, Jr., Huhta JC, Sharif DS, Ou CN, Kirshon B, Wasserstrum N, and Cano L**. Indomethacin in the treatment of premature labor. Effects on the fetal ductus arteriosus. *N Engl J Med* 319: 327-331, 1988.

185. **Gerson A, Abbasi S, Johnson A, Kalchbrenner M, Ashmead G, and Bolognese R**. Safety and efficacy of long-term tocolysis with indomethacin. *Am J Perinatol* 7: 71-74, 1990.
186. **Eronen M, Pesonen E, Kurki T, Teramo K, Ylikorkala O, and Hallman M**. Increased incidence of bronchopulmonary dysplasia after antenatal administration of indomethacin to prevent preterm labor. *J Pediatr* 124: 782-788, 1994.
187. **Hammerman C, Glaser J, Kaplan M, Schimmel MS, Ferber B, and Eidelman AI**. Indomethacin tocolysis increases postnatal patent ductus arteriosus severity. *Pediatrics* 102: E56, 1998.
188. **Souter D, Harding J, McCowan L, O'Donnell C, McLeay E, and Baxendale H**. Antenatal indomethacin--adverse fetal effects confirmed. *Aust N Z J Obstet Gynaecol* 38: 11-16, 1998.
189. **Suarez VR, Thompson LL, Jain V, Olson GL, Hankins GD, Belfort MA, and Saade GR**. The effect of in utero exposure to indomethacin on the need for surgical closure of a patent ductus arteriosus in the neonate. *Am J Obstet Gynecol* 187: 886-888, 2002.
190. **Cordero L, Nankervis CA, Gardner D, and Giannone PJ**. The effects of indomethacin tocolysis on the postnatal response of the ductus arteriosus to indomethacin in extremely low birth weight infants. *J Perinatol* 27: 22-27, 2007.
191. **Soraisham AS, Dalgleish S, and Singhal N**. Antenatal indomethacin tocolysis is associated with an increased need for surgical ligation of patent ductus arteriosus in preterm infants. *J Obstet Gynaecol Can* 32: 435-442, 2010.
192. **Loe SM, Sanchez-Ramos L, and Kaunitz AM**. Assessing the neonatal safety of indomethacin tocolysis: a systematic review with meta-analysis. *Obstet Gynecol* 106: 173-179, 2005.
193. **Rovers JFJ, Thomissen IJC, Janssen LCE, Lingius S, Wieland BV, Dieleman JP, Niemarkt HJ, and van Runnard Heimel PJ**. The relationship between antenatal indomethacin as a tocolytic drug and neonatal outcomes: a retrospective cohort study. *J Matern Fetal Neonatal Med* 34: 2945-2951, 2021.
194. **Turan OM, Driscoll C, Cetinkaya-Demir B, Gabbay-Benziv R, Turan S, Kopelman JN, and Harman C**. Prolonged early antenatal indomethacin exposure is safe for fetus and neonate(). *J Matern Fetal Neonatal Med* 34: 167-176, 2021.
195. **Loftin CD, Trivedi DB, and Langenbach R**. Cyclooxygenase-1-selective inhibition prolongs gestation in mice without adverse effects on the ductus arteriosus. *J Clin Invest* 110: 549-557, 2002.
196. **Reese J, Anderson JD, Brown N, Roman C, and Clyman RI**. Inhibition of cyclooxygenase isoforms in late- but not midgestation decreases contractility of the ductus arteriosus and prevents postnatal closure in mice. *Am J Physiol Regul Integr Comp Physiol* 291: R1717-1723, 2006.
197. **Reese J, Waleh N, Poole SD, Brown N, Roman C, and Clyman RI**. Chronic in utero cyclooxygenase inhibition alters PGE2-regulated ductus arteriosus contractile pathways and prevents postnatal closure. *Pediatr Res* 66: 155-161, 2009.
198. **Clyman RI, Waleh N, Black SM, Riemer RK, Mauray F, and Chen YQ**. Regulation of ductus arteriosus patency by nitric oxide in fetal lambs: the role of gestation, oxygen tension, and vasa vasorum. *Pediatr Res* 43: 633-644, 1998.
199. **Momma K, and Toyono M**. The role of nitric oxide in dilating the fetal ductus arteriosus in rats. *Pediatr Res* 46: 311-315, 1999.
200. **Richard C, Gao J, LaFleur B, Christman BW, Anderson J, Brown N, and Reese J**. Patency of the preterm fetal ductus arteriosus is regulated by endothelial nitric oxide synthase and is independent of vasa vasorum in the mouse. *Am J Physiol Regul Integr Comp Physiol* 287: R652-660, 2004.
201. **Reese J, O'Mara PW, Poole SD, Brown N, Tolentino C, Eckman DM, and Aschner JL**. Regulation of the fetal mouse ductus arteriosus is dependent on interaction of nitric oxide and COX enzymes in the ductal wall. *Prostaglandins Other Lipid Mediat* 88: 89-96, 2009.
202. **Coceani F, Bodach E, White E, Bishai I, and Olley PM**. Prostaglandin I2 is less relaxant than prostaglandin E2 on the lamb ductus arteriosus. *Prostaglandins* 15: 551-556, 1978.
203. **Clyman RI, Mauray F, Roman C, and Rudolph AM**. PGE2 is a more potent vasodilator of the lamb ductus arteriosus than is either PGI2 or 6 keto PGF1alpha. *Prostaglandins* 16: 259-264, 1978.

204. **Burke JE, and Dennis EA**. Phospholipase A2 structure/function, mechanism, and signaling. *J Lipid Res* 50 Suppl: S237-242, 2009.
205. **Kramer RM, Checani GC, Deykin A, Pritzker CR, and Deykin D**. Solubilization and properties of Ca2+-dependent human platelet phospholipase A2. *Biochim Biophys Acta* 878: 394-403, 1986.
206. **Clark JD, Lin LL, Kriz RW, Ramesha CS, Sultzman LA, Lin AY, Milona N, and Knopf JL**. A novel arachidonic acid-selective cytosolic PLA2 contains a Ca(2+)-dependent translocation domain with homology to PKC and GAP. *Cell* 65: 1043-1051, 1991.
207. **Kramer RM, Roberts EF, Manetta J, and Putnam JE**. The Ca2(+)-sensitive cytosolic phospholipase A2 is a 100-kDa protein in human monoblast U937 cells. *J Biol Chem* 266: 5268-5272, 1991.
208. **Ghosh M, Tucker DE, Burchett SA, and Leslie CC**. Properties of the Group IV phospholipase A2 family. *Prog Lipid Res* 45: 487-510, 2006.
209. **Bonventre JV, Huang Z, Taheri MR, O'Leary E, Li E, Moskowitz MA, and Sapirstein A**. Reduced fertility and postischaemic brain injury in mice deficient in cytosolic phospholipase A2. *Nature* 390: 622-625, 1997.
210. **Uozumi N, Kume K, Nagase T, Nakatani N, Ishii S, Tashiro F, Komagata Y, Maki K, Ikuta K, Ouchi Y, Miyazaki J, and Shimizu T**. Role of cytosolic phospholipase A2 in allergic response and parturition. *Nature* 390: 618-622, 1997.
211. **Uozumi N, and Shimizu T**. Roles for cytosolic phospholipase A2alpha as revealed by gene-targeted mice. *Prostaglandins Other Lipid Mediat* 68-69: 59-69, 2002.
212. **Murakami M, Shimbara S, Kambe T, Kuwata H, Winstead MV, Tischfield JA, and Kudo I**. The functions of five distinct mammalian phospholipase A2S in regulating arachidonic acid release. Type IIa and type V secretory phospholipase A2S are functionally redundant and act in concert with cytosolic phospholipase A2. *J Biol Chem* 273: 14411-14423, 1998.
213. **Yokoyama U, Iwatsubo K, Umemura M, Fujita T, and Ishikawa Y**. The prostanoid EP4 receptor and its signaling pathway. *Pharmacol Rev* 65: 1010-1052, 2013.
214. **Smith WL, Garavito RM, and DeWitt DL**. Prostaglandin endoperoxide H synthases (cyclooxygenases)-1 and -2. *J Biol Chem* 271: 33157-33160, 1996.
215. **Smith WL**. Prostanoid biosynthesis and mechanisms of action. *Am J Physiol* 263: F181-191, 1992.
216. **Park GY, and Christman JW**. Involvement of cyclooxygenase-2 and prostaglandins in the molecular pathogenesis of inflammatory lung diseases. *Am J Physiol Lung Cell Mol Physiol* 290: L797-805, 2006.
217. **O'Banion MK**. Prostaglandin E2 synthases in neurologic homeostasis and disease. *Prostaglandins Other Lipid Mediat* 91: 113-117, 2010.
218. **Lin LL, Wartmann M, Lin AY, Knopf JL, Seth A, and Davis RJ**. cPLA2 is phosphorylated and activated by MAP kinase. *Cell* 72: 269-278, 1993.
219. **Murakami M, Kambe T, Shimbara S, and Kudo I**. Functional coupling between various phospholipase A2s and cyclooxygenases in immediate and delayed prostanoid biosynthetic pathways. *J Biol Chem* 274: 3103-3115, 1999.
220. **Laneuville O, Breuer DK, Xu N, Huang ZH, Gage DA, Watson JT, Lagarde M, DeWitt DL, and Smith WL**. Fatty acid substrate specificities of human prostaglandin-endoperoxide H synthase-1 and -2. Formation of 12-hydroxy-(9Z, 13E/Z, 15Z)- octadecatrienoic acids from alpha-linolenic acid. *J Biol Chem* 270: 19330-19336, 1995.
221. **Capdevila JH, Morrow JD, Belosludtsev YY, Beauchamp DR, DuBois RN, and Falck JR**. The catalytic outcomes of the constitutive and the mitogen inducible isoforms of prostaglandin H2 synthase are markedly affected by glutathione and glutathione peroxidase(s). *Biochemistry* 34: 3325-3337, 1995.
222. **Kulmacz RJ, and Wang LH**. Comparison of hydroperoxide initiator requirements for the cyclooxygenase activities of prostaglandin H synthase-1 and -2. *J Biol Chem* 270: 24019-24023, 1995.
223. **Landino LM, Crews BC, Timmons MD, Morrow JD, and Marnett LJ**. Peroxynitrite, the coupling product of nitric oxide and superoxide, activates prostaglandin biosynthesis. *Proc Natl Acad Sci U S A* 93: 15069-15074, 1996.
224. **Wan S, and Coveney PV**. A comparative study of the COX-1 and COX-2 isozymes bound to lipid membranes. *J Comput Chem* 30: 1038-1050, 2009.

225. **Yu Y, Fan J, Chen XS, Wang D, Klein-Szanto AJ, Campbell RL, FitzGerald GA, and Funk CD**. Genetic model of selective COX2 inhibition reveals novel heterodimer signaling. *Nat Med* 12: 699-704, 2006.
226. **Spencer AG, Woods JW, Arakawa T, Singer, II, and Smith WL**. Subcellular localization of prostaglandin endoperoxide H synthases-1 and -2 by immunoelectron microscopy. *J Biol Chem* 273: 9886-9893, 1998.
227. **Otto JC, and Smith WL**. The orientation of prostaglandin endoperoxide synthases-1 and -2 in the endoplasmic reticulum. *J Biol Chem* 269: 19868-19875, 1994.
228. **Otto JC, and Smith WL**. Photolabeling of prostaglandin endoperoxide H synthase-1 with 3-trifluoro-3-(m-[125I]iodophenyl)diazirine as a probe of membrane association and the cyclooxygenase active site. *J Biol Chem* 271: 9906-9910, 1996.
229. **Han JW, Sadowski H, Young DA, and Macara IG**. Persistent induction of cyclooxygenase in p60v-src-transformed 3T3 fibroblasts. *Proc Natl Acad Sci U S A* 87: 3373-3377, 1990.
230. **Evett GE, Xie W, Chipman JG, Robertson DL, and Simmons DL**. Prostaglandin G/H synthase isoenzyme 2 expression in fibroblasts: regulation by dexamethasone, mitogens, and oncogenes. *Arch Biochem Biophys* 306: 169-177, 1993.
231. **DeWitt DL, and Meade EA**. Serum and glucocorticoid regulation of gene transcription and expression of the prostaglandin H synthase-1 and prostaglandin H synthase-2 isozymes. *Arch Biochem Biophys* 306: 94-102, 1993.
232. **Kujubu DA, Reddy ST, Fletcher BS, and Herschman HR**. Expression of the protein product of the prostaglandin synthase-2/TIS10 gene in mitogen-stimulated Swiss 3T3 cells. *J Biol Chem* 268: 5425-5430, 1993.
233. **Jones DA, Carlton DP, McIntyre TM, Zimmerman GA, and Prescott SM**. Molecular cloning of human prostaglandin endoperoxide synthase type II and demonstration of expression in response to cytokines. *J Biol Chem* 268: 9049-9054, 1993.
234. **Mancini JA, O'Neill GP, Bayly C, and Vickers PJ**. Mutation of serine-516 in human prostaglandin G/H synthase-2 to methionine or aspirin acetylation of this residue stimulates 15-R-HETE synthesis. *FEBS Lett* 342: 33-37, 1994.
235. **Yamagata K, Andreasson KI, Kaufmann WE, Barnes CA, and Worley PF**. Expression of a mitogen-inducible cyclooxygenase in brain neurons: regulation by synaptic activity and glucocorticoids. *Neuron* 11: 371-386, 1993.
236. **Neeraja S, Sreenath AS, Reddy PR, and Reddanna P**. Expression of cyclooxygenase-2 in rat testis. *Reprod Biomed Online* 6: 302-309, 2003.
237. **Harris RC, McKanna JA, Akai Y, Jacobson HR, Dubois RN, and Breyer MD**. Cyclooxygenase-2 is associated with the macula densa of rat kidney and increases with salt restriction. *J Clin Invest* 94: 2504-2510, 1994.
238. **Murakami M, Matsumoto R, Austen KF, and Arm JP**. Prostaglandin endoperoxide synthase-1 and -2 couple to different transmembrane stimuli to generate prostaglandin D2 in mouse bone marrow-derived mast cells. *J Biol Chem* 269: 22269-22275, 1994.
239. **Morham SG, Langenbach R, Loftin CD, Tiano HF, Vouloumanos N, Jennette JC, Mahler JF, Kluckman KD, Ledford A, Lee CA, and Smithies O**. Prostaglandin synthase 2 gene disruption causes severe renal pathology in the mouse. *Cell* 83: 473-482, 1995.
240. **Bingham CO, 3rd, Murakami M, Fujishima H, Hunt JE, Austen KF, and Arm JP**. A heparin-sensitive phospholipase A2 and prostaglandin endoperoxide synthase-2 are functionally linked in the delayed phase of prostaglandin D2 generation in mouse bone marrow-derived mast cells. *J Biol Chem* 271: 25936-25944, 1996.
241. **Reddy ST, and Herschman HR**. Prostaglandin synthase-1 and prostaglandin synthase-2 are coupled to distinct phospholipases for the generation of prostaglandin D2 in activated mast cells. *J Biol Chem* 272: 3231-3237, 1997.
242. **Kuwata H, Nakatani Y, Murakami M, and Kudo I**. Cytosolic phospholipase A2 is required for cytokine-induced expression of type IIA secretory phospholipase A2 that mediates optimal cyclooxygenase-2-dependent delayed prostaglandin E2 generation in rat 3Y1 fibroblasts. *J Biol Chem* 273: 1733-1740, 1998.

243. **Naraba H, Murakami M, Matsumoto H, Shimbara S, Ueno A, Kudo I, and Oh-ishi S**. Segregated coupling of phospholipases A2, cyclooxygenases, and terminal prostanoid synthases in different phases of prostanoid biosynthesis in rat peritoneal macrophages. *J Immunol* 160: 2974-2982, 1998.
244. **Ueno N, Murakami M, Tanioka T, Fujimori K, Tanabe T, Urade Y, and Kudo I**. Coupling between cyclooxygenase, terminal prostanoid synthase, and phospholipase A2. *J Biol Chem* 276: 34918-34927, 2001.
245. **Ueno N, Takegoshi Y, Kamei D, Kudo I, and Murakami M**. Coupling between cyclooxygenases and terminal prostanoid synthases. *Biochem Biophys Res Commun* 338: 70-76, 2005.
246. **Ricciotti E, and FitzGerald GA**. Prostaglandins and inflammation. *Arterioscler Thromb Vasc Biol* 31: 986-1000, 2011.
247. **Kudo I, and Murakami M**. Prostaglandin E synthase, a terminal enzyme for prostaglandin E2 biosynthesis. *J Biochem Mol Biol* 38: 633-638, 2005.
248. **Kennedy I, Coleman RA, Humphrey PP, Levy GP, and Lumley P**. Studies on the characterisation of prostanoid receptors: a proposed classification. *Prostaglandins* 24: 667-689, 1982.
249. **Coleman RA, Grix SP, Head SA, Louttit JB, Mallett A, and Sheldrick RL**. A novel inhibitory prostanoid receptor in piglet saphenous vein. *Prostaglandins* 47: 151-168, 1994.
250. **Honda A, Sugimoto Y, Namba T, Watabe A, Irie A, Negishi M, Narumiya S, and Ichikawa A**. Cloning and expression of a cDNA for mouse prostaglandin E receptor EP2 subtype. *J Biol Chem* 268: 7759-7762, 1993.
251. **Coleman RA, Smith WL, and Narumiya S**. International Union of Pharmacology classification of prostanoid receptors: properties, distribution, and structure of the receptors and their subtypes. *Pharmacol Rev* 46: 205-229, 1994.
252. **Nishigaki N, Negishi M, Honda A, Sugimoto Y, Namba T, Narumiya S, and Ichikawa A**. Identification of prostaglandin E receptor 'EP2' cloned from mastocytoma cells EP4 subtype. *FEBS Lett* 364: 339-341, 1995.
253. **Breyer RM, Davis LS, Nian C, Redha R, Stillman B, Jacobson HR, and Breyer MD**. Cloning and expression of the rabbit prostaglandin EP4 receptor. *Am J Physiol* 270: F485-493, 1996.
254. **Woodward DF, Jones RL, and Narumiya S**. International Union of Basic and Clinical Pharmacology. LXXXIII: classification of prostanoid receptors, updating 15 years of progress. *Pharmacol Rev* 63: 471-538, 2011.
255. **Alfranca A, Iniguez MA, Fresno M, and Redondo JM**. Prostanoid signal transduction and gene expression in the endothelium: role in cardiovascular diseases. *Cardiovasc Res* 70: 446-456, 2006.
256. **Sugimoto Y, and Narumiya S**. Prostaglandin E receptors. *J Biol Chem* 282: 11613-11617, 2007.
257. **Yang T, and Du Y**. Distinct roles of central and peripheral prostaglandin E2 and EP subtypes in blood pressure regulation. *Am J Hypertens* 25: 1042-1049, 2012.
258. **Fan FL, Zhu S, Chen LH, Zou YL, Fan LH, Kang JH, Ma AQ, and Guan YF**. Role of prostaglandin E and its receptors in the process of ductus arteriosus maturation and functional closure in the rabbit. *Clin Exp Pharmacol Physiol* 37: 574-580, 2010.
259. **Smith GC, Wu WX, Nijland MJ, Koenen SV, and Nathanielsz PW**. Effect of gestational age, corticosteroids, and birth on expression of prostanoid EP receptor genes in lamb and baboon ductus arteriosus. *J Cardiovasc Pharmacol* 37: 697-704, 2001.
260. **Waleh N, Kajino H, Marrache AM, Ginzinger D, Roman C, Seidner SR, Moss TJ, Fouron JC, Vazquez-Tello A, Chemtob S, and Clyman RI**. Prostaglandin E2--mediated relaxation of the ductus arteriosus: effects of gestational age on g protein-coupled receptor expression, signaling, and vasomotor control. *Circulation* 110: 2326-2332, 2004.
261. **Bhattacharya M, Asselin P, Hardy P, Guerguerian AM, Shichi H, Hou X, Varma DR, Bouayad A, Fouron JC, Clyman RI, and Chemtob S**. Developmental changes in prostaglandin E(2) receptor subtypes in porcine ductus arteriosus. Possible contribution in altered responsiveness to prostaglandin E(2). *Circulation* 100: 1751-1756, 1999.
262. **Bouayad A, Bernier SG, Asselin P, Hardy P, Bhattacharya M, Quiniou C, Fouron JC, Guerguerian AM, Varma DR, Clyman RI, and Chemtob S**. Characterization of PGE2 receptors in fetal and newborn ductus arteriosus in the pig. *Semin Perinatol* 25: 70-75, 2001.
263. **Leonhardt A, Glaser A, Wegmann M, Schranz D, Seyberth H, and Nusing R**. Expression of prostanoid receptors in human ductus arteriosus. *Br J Pharmacol* 138: 655-659, 2003.

264. **Rheinlaender C, Weber SC, Sarioglu N, Strauss E, Obladen M, and Koehne P**. Changing expression of cyclooxygenases and prostaglandin receptor EP4 during development of the human ductus arteriosus. *Pediatr Res* 60: 270-275, 2006.
265. **Yarboro MT, Durbin MD, Herington JL, Shelton EL, Zhang T, Ebby CG, Stoller JZ, Clyman RI, and Reese J**. Transcriptional profiling of the ductus arteriosus: Comparison of rodent microarrays and human RNA sequencing. *Semin Perinatol* 42: 212-220, 2018.
266. **Sugimoto Y, Yamasaki A, Segi E, Tsuboi K, Aze Y, Nishimura T, Oida H, Yoshida N, Tanaka T, Katsuyama M, Hasumoto K, Murata T, Hirata M, Ushikubi F, Negishi M, Ichikawa A, and Narumiya S**. Failure of parturition in mice lacking the prostaglandin F receptor. *Science* 277: 681-683, 1997.
267. **Murata T, Ushikubi F, Matsuoka T, Hirata M, Yamasaki A, Sugimoto Y, Ichikawa A, Aze Y, Tanaka T, Yoshida N, Ueno A, Oh-ishi S, and Narumiya S**. Altered pain perception and inflammatory response in mice lacking prostacyclin receptor. *Nature* 388: 678-682, 1997.
268. **Ushikubi F, Segi E, Sugimoto Y, Murata T, Matsuoka T, Kobayashi T, Hizaki H, Tuboi K, Katsuyama M, Ichikawa A, Tanaka T, Yoshida N, and Narumiya S**. Impaired febrile response in mice lacking the prostaglandin E receptor subtype EP3. *Nature* 395: 281-284, 1998.
269. **Hizaki H, Segi E, Sugimoto Y, Hirose M, Saji T, Ushikubi F, Matsuoka T, Noda Y, Tanaka T, Yoshida N, Narumiya S, and Ichikawa A**. Abortive expansion of the cumulus and impaired fertility in mice lacking the prostaglandin E receptor subtype EP(2). *Proc Natl Acad Sci U S A* 96: 10501-10506, 1999.
270. **Matsuoka T, Hirata M, Tanaka H, Takahashi Y, Murata T, Kabashima K, Sugimoto Y, Kobayashi T, Ushikubi F, Aze Y, Eguchi N, Urade Y, Yoshida N, Kimura K, Mizoguchi A, Honda Y, Nagai H, and Narumiya S**. Prostaglandin D2 as a mediator of allergic asthma. *Science* 287: 2013-2017, 2000.
271. **Okada Y, Hara A, Ma H, Xiao CY, Takahata O, Kohgo Y, Narumiya S, and Ushikubi F**. Characterization of prostanoid receptors mediating contraction of the gastric fundus and ileum: studies using mice deficient in prostanoid receptors. *Br J Pharmacol* 131: 745-755, 2000.
272. **Ivey KN, and Srivastava D**. The paradoxical patent ductus arteriosus. *J Clin Invest* 116: 2863-2865, 2006.
273. **Lincoln TM, and Cornwell TL**. Intracellular cyclic GMP receptor proteins. *FASEB J* 7: 328-338, 1993.
274. **Vaandrager AB, and de Jonge HR**. Signalling by cGMP-dependent protein kinases. *Mol Cell Biochem* 157: 23-30, 1996.
275. **Ruiz-Velasco V, Zhong J, Hume JR, and Keef KD**. Modulation of Ca2+ channels by cyclic nucleotide cross activation of opposing protein kinases in rabbit portal vein. *Circ Res* 82: 557-565, 1998.
276. **Francis SH, Noblett BD, Todd BW, Wells JN, and Corbin JD**. Relaxation of vascular and tracheal smooth muscle by cyclic nucleotide analogs that preferentially activate purified cGMP-dependent protein kinase. *Mol Pharmacol* 34: 506-517, 1988.
277. **Lincoln TM, Cornwell TL, and Taylor AE**. cGMP-dependent protein kinase mediates the reduction of Ca2+ by cAMP in vascular smooth muscle cells. *Am J Physiol* 258: C399-407, 1990.
278. **Hei YJ, MacDonell KL, McNeill JH, and Diamond J**. Lack of correlation between activation of cyclic AMP-dependent protein kinase and inhibition of contraction of rat vas deferens by cyclic AMP analogs. *Mol Pharmacol* 39: 233-238, 1991.
279. **White RE, Kryman JP, El-Mowafy AM, Han G, and Carrier GO**. cAMP-dependent vasodilators cross-activate the cGMP-dependent protein kinase to stimulate BK(Ca) channel activity in coronary artery smooth muscle cells. *Circ Res* 86: 897-905, 2000.
280. **Haynes J, Jr., Robinson J, Saunders L, Taylor AE, and Strada SJ**. Role of cAMP-dependent protein kinase in cAMP-mediated vasodilation. *Am J Physiol* 262: H511-516, 1992.
281. **Kannan MS, and Johnson DE**. Modulation of nitric oxide-dependent relaxation of pig tracheal smooth muscle by inhibitors of guanylyl cyclase and calcium activated potassium channels. *Life Sci* 56: 2229-2238, 1995.
282. **Trongvanichnam K, Mitsui-Saito M, Ozaki H, and Karaki H**. Effects of chronic oral administration of levcromakalim on in vitro contractile responses of arterial smooth muscle. *Eur J Pharmacol* 303: 39-45, 1996.
283. **Yamakage M, Hirshman CA, and Croxton TL**. Sodium nitroprusside stimulates Ca2+ -activated K+ channels in porcine tracheal smooth muscle cells. *Am J Physiol* 270: L338-345, 1996.

284. **Zhou XB, Ruth P, Schlossmann J, Hofmann F, and Korth M**. Protein phosphatase 2A is essential for the activation of Ca2+-activated K+ currents by cGMP-dependent protein kinase in tracheal smooth muscle and Chinese hamster ovary cells. *J Biol Chem* 271: 19760-19767, 1996.
285. **Tewari K, and Simard JM**. Sodium nitroprusside and cGMP decrease Ca2+ channel availability in basilar artery smooth muscle cells. *Pflugers Arch* 433: 304-311, 1997.
286. **Furukawa K, Tawada Y, and Shigekawa M**. Regulation of the plasma membrane Ca2+ pump by cyclic nucleotides in cultured vascular smooth muscle cells. *J Biol Chem* 263: 8058-8065, 1988.
287. **Clapp LH, and Gurney AM**. Modulation of calcium movements by nitroprusside in isolated vascular smooth muscle cells. *Pflugers Arch* 418: 462-470, 1991.
288. **Baines RJ, Brown C, Ng LL, and Boarder MR**. Angiotensin II-stimulated phospholipase C responses of two vascular smooth muscle-derived cell lines. Role of cyclic GMP. *Hypertension* 28: 772-778, 1996.
289. **Xia C, Bao Z, Yue C, Sanborn BM, and Liu M**. Phosphorylation and regulation of G-protein-activated phospholipase C-beta 3 by cGMP-dependent protein kinases. *J Biol Chem* 276: 19770-19777, 2001.
290. **Moustafa A, Sakamoto KQ, and Habara Y**. Nitric oxide stimulates IP3 production via a cGMP/ PKG-dependent pathway in rat pancreatic acinar cells. *Jpn J Vet Res* 59: 5-14, 2011.
291. **Hoshi T, Garber SS, and Aldrich RW**. Effect of forskolin on voltage-gated K+ channels is independent of adenylate cyclase activation. *Science* 240: 1652-1655, 1988.
292. **Brown AM, and Birnbaumer L**. Ion channels and G proteins. *Hosp Pract (Off Ed)* 24: 189-193, 198, 202-184, 1989.
293. **Garber SS, Hoshi T, and Aldrich RW**. Interaction of forskolin with voltage-gated K+ channels in PC12 cells. *J Neurosci* 10: 3361-3368, 1990.
294. **Lee MR, Li L, and Kitazawa T**. Cyclic GMP causes Ca2+ desensitization in vascular smooth muscle by activating the myosin light chain phosphatase. *J Biol Chem* 272: 5063-5068, 1997.
295. **Stock A, Booth S, and Cerundolo V**. Prostaglandin E2 suppresses the differentiation of retinoic acid-producing dendritic cells in mice and humans. *J Exp Med* 208: 761-773, 2011.
296. **Bos JL**. Epac: a new cAMP target and new avenues in cAMP research. *Nat Rev Mol Cell Biol* 4: 733-738, 2003.
297. **Faour WH, Gomi K, and Kennedy CR**. PGE(2) induces COX-2 expression in podocytes via the EP(4) receptor through a PKA-independent mechanism. *Cell Signal* 20: 2156-2164, 2008.
298. **Xin X, Majumder M, Girish GV, Mohindra V, Maruyama T, and Lala PK**. Targeting COX-2 and EP4 to control tumor growth, angiogenesis, lymphangiogenesis and metastasis to the lungs and lymph nodes in a breast cancer model. *Lab Invest* 92: 1115-1128, 2012.
299. **Hsu HH, Lin YM, Shen CY, Shibu MA, Li SY, Chang SH, Lin CC, Chen RJ, Viswanadha VP, Shih HN, and Huang CY**. Prostaglandin E2-Induced COX-2 Expressions via EP2 and EP4 Signaling Pathways in Human LoVo Colon Cancer Cells. *Int J Mol Sci* 18: 2017.
300. **Nam J, Kwon B, Yoon Y, and Choe J**. PGE2 stimulates COX-2 expression via EP2/4 receptors and acts in synergy with IL-1β in human follicular dendritic cell-like cells. *European Journal of Inflammation* 16: 2058739218796386, 2018.
301. **Desai S, April H, Nwaneshiudu C, and Ashby B**. Comparison of agonist-induced internalization of the human EP2 and EP4 prostaglandin receptors: role of the carboxyl terminus in EP4 receptor sequestration. *Mol Pharmacol* 58: 1279-1286, 2000.
302. **Foudi N, Kotelevets L, Gomez I, Louedec L, Longrois D, Chastre E, and Norel X**. Differential reactivity of human mammary artery and saphenous vein to prostaglandin E(2) : implication for cardiovascular grafts. *Br J Pharmacol* 163: 826-834, 2011.
303. **Kobayashi K, Murata T, Hori M, and Ozaki H**. Prostaglandin E2-prostanoid EP3 signal induces vascular contraction via nPKC and ROCK activation in rat mesenteric artery. *Eur J Pharmacol* 660: 375-380, 2011.
304. **Leduc M, Breton B, Gales C, Le Gouill C, Bouvier M, Chemtob S, and Heveker N**. Functional selectivity of natural and synthetic prostaglandin EP4 receptor ligands. *J Pharmacol Exp Ther* 331: 297-307, 2009.

305. **Fujino H, Xu W, and Regan JW**. Prostaglandin E2 induced functional expression of early growth response factor-1 by EP4, but not EP2, prostanoid receptors via the phosphatidylinositol 3-kinase and extracellular signal-regulated kinases. *J Biol Chem* 278: 12151-12156, 2003.
306. **Pozzi A, Yan X, Macias-Perez I, Wei S, Hata AN, Breyer RM, Morrow JD, and Capdevila JH**. Colon carcinoma cell growth is associated with prostaglandin E2/EP4 receptor-evoked ERK activation. *J Biol Chem* 279: 29797-29804, 2004.
307. **Fujino H, and Regan JW**. EP(4) prostanoid receptor coupling to a pertussis toxin-sensitive inhibitory G protein. *Mol Pharmacol* 69: 5-10, 2006.
308. **Samson SC, Khan AM, and Mendoza MC**. ERK signaling for cell migration and invasion. *Front Mol Biosci* 9: 998475, 2022.
309. **Lavoie H, Gagnon J, and Therrien M**. ERK signalling: a master regulator of cell behaviour, life and fate. *Nat Rev Mol Cell Biol* 21: 607-632, 2020.
310. **Rao R, Redha R, Macias-Perez I, Su Y, Hao C, Zent R, Breyer MD, and Pozzi A**. Prostaglandin E2-EP4 receptor promotes endothelial cell migration via ERK activation and angiogenesis in vivo. *J Biol Chem* 282: 16959-16968, 2007.
311. **Nishigaki N, Negishi M, and Ichikawa A**. Two Gs-coupled prostaglandin E receptor subtypes, EP2 and EP4, differ in desensitization and sensitivity to the metabolic inactivation of the agonist. *Mol Pharmacol* 50: 1031-1037, 1996.
312. **Bastepe M, and Ashby B**. Identification of a region of the C-terminal domain involved in short-term desensitization of the prostaglandin EP4 receptor. *Br J Pharmacol* 126: 365-371, 1999.
313. **Ludwig A, Ehlert JE, Flad HD, and Brandt E**. Identification of distinct surface-expressed and intracellular CXC-chemokine receptor 2 glycoforms in neutrophils: N-glycosylation is essential for maintenance of receptor surface expression. *J Immunol* 165: 1044-1052, 2000.
314. **Takayama K, Sukhova GK, Chin MT, and Libby P**. A novel prostaglandin E receptor 4-associated protein participates in antiinflammatory signaling. *Circ Res* 98: 499-504, 2006.
315. **Minami M, Shimizu K, Okamoto Y, Folco E, Ilasaca ML, Feinberg MW, Aikawa M, and Libby P**. Prostaglandin E receptor type 4-associated protein interacts directly with NF-kappaB1 and attenuates macrophage activation. *J Biol Chem* 283: 9692-9703, 2008.
316. **Regard JB, Sato IT, and Coughlin SR**. Anatomical profiling of G protein-coupled receptor expression. *Cell* 135: 561-571, 2008.
317. **Zaslona Z, Serezani CH, Okunishi K, Aronoff DM, and Peters-Golden M**. Prostaglandin E2 restrains macrophage maturation via E prostanoid receptor 2/protein kinase A signaling. *Blood* 119: 2358-2367, 2012.
318. **Grigsby PL, Sooranna SR, Adu-Amankwa B, Pitzer B, Brockman DE, Johnson MR, and Myatt L**. Regional expression of prostaglandin E2 and F2alpha receptors in human myometrium, amnion, and choriodecidua with advancing gestation and labor. *Biol Reprod* 75: 297-305, 2006.
319. **Huang SK, Fisher AS, Scruggs AM, White ES, Hogaboam CM, Richardson BC, and Peters-Golden M**. Hypermethylation of PTGER2 confers prostaglandin E2 resistance in fibrotic fibroblasts from humans and mice. *Am J Pathol* 177: 2245-2255, 2010.
320. **Breyer MD, Davis L, Jacobson HR, and Breyer RM**. Differential localization of prostaglandin E receptor subtypes in human kidney. *Am J Physiol* 270: F912-918, 1996.
321. **Morimoto K, Sugimoto Y, Katsuyama M, Oida H, Tsuboi K, Kishi K, Kinoshita Y, Negishi M, Chiba T, Narumiya S, and Ichikawa A**. Cellular localization of mRNAs for prostaglandin E receptor subtypes in mouse gastrointestinal tract. *Am J Physiol* 272: G681-687, 1997.
322. **Matsumoto Y, Nakanishi Y, Yoshioka T, Yamaga Y, Masuda T, Fukunaga Y, Sono M, Yoshikawa T, Nagao M, Araki O, Ogawa S, Goto N, Hiramatsu Y, Breyer RM, Fukuda A, and Seno H**. Epithelial EP4 plays an essential role in maintaining homeostasis in colon. *Sci Rep* 9: 15244, 2019.
323. **Regan JW**. EP2 and EP4 prostanoid receptor signaling. *Life Sci* 74: 143-153, 2003.
324. **Negishi M, Sugimoto Y, and Ichikawa A**. Prostanoid receptors and their biological actions. *Prog Lipid Res* 32: 417-434, 1993.

325. **Stillman BA, Audoly L, and Breyer RM**. A conserved threonine in the second extracellular loop of the human EP2 and EP4 receptors is required for ligand binding. *Eur J Pharmacol* 357: 73-82, 1998.
326. **Margan D, Borota A, Mracec M, and Mracec M**. 3D homology model of the human prostaglandin E2 receptor EP4 subtype. *Rev Roum Chim* 57: 39-44, 2012.
327. **Fox JJ, Ziegler JW, Ivy DD, Halbower AC, Kinsella JP, and Abman SH**. Role of nitric oxide and cGMP system in regulation of ductus arteriosus tone in ovine fetus. *Am J Physiol* 271: H2638-2645, 1996.
328. **Chen K, Pittman RN, and Popel AS**. Nitric oxide in the vasculature: where does it come from and where does it go? A quantitative perspective. *Antioxid Redox Signal* 10: 1185-1198, 2008.
329. **Bredt DS, Hwang PM, and Snyder SH**. Localization of nitric oxide synthase indicating a neural role for nitric oxide. *Nature* 347: 768-770, 1990.
330. **Beasley D**. Interleukin 1 and endotoxin activate soluble guanylate cyclase in vascular smooth muscle. *Am J Physiol* 259: R38-44, 1990.
331. **Wood KS, Buga GM, Byrns RE, and Ignarro LJ**. Vascular smooth muscle-derived relaxing factor (MDRF) and its close similarity to nitric oxide. *Biochem Biophys Res Commun* 170: 80-88, 1990.
332. **Nozaki K, Moskowitz MA, Maynard KI, Koketsu N, Dawson TM, Bredt DS, and Snyder SH**. Possible origins and distribution of immunoreactive nitric oxide synthase-containing nerve fibers in cerebral arteries. *J Cereb Blood Flow Metab* 13: 70-79, 1993.
333. **Coceani F, Kelsey L, and Seidlitz E**. Occurrence of endothelium-derived relaxing factor--nitric oxide in the lamb ductus arteriosus. *Can J Physiol Pharmacol* 72: 82-88, 1994.
334. **Lacza Z, Pankotai E, Csordas A, Gero D, Kiss L, Horvath EM, Kollai M, Busija DW, and Szabo C**. Mitochondrial NO and reactive nitrogen species production: does mtNOS exist? *Nitric Oxide* 14: 162-168, 2006.
335. **Lacza Z, Pankotai E, and Busija DW**. Mitochondrial nitric oxide synthase: current concepts and controversies. *Front Biosci (Landmark Ed)* 14: 4436-4443, 2009.
336. **Carvajal JA, Germain AM, Huidobro-Toro JP, and Weiner CP**. Molecular mechanism of cGMP-mediated smooth muscle relaxation. *J Cell Physiol* 184: 409-420, 2000.
337. **Coceani F, Kelsey L, Seidlitz E, Marks GS, McLaughlin BE, Vreman HJ, Stevenson DK, Rabinovitch M, and Ackerley C**. Carbon monoxide formation in the ductus arteriosus in the lamb: implications for the regulation of muscle tone. *Br J Pharmacol* 120: 599-608, 1997.
338. **Francis SH, and Corbin JD**. Structure and function of cyclic nucleotide-dependent protein kinases. *Annu Rev Physiol* 56: 237-272, 1994.
339. **Shibata M, Ichioka S, and Kamiya A**. Nitric oxide modulates oxygen consumption by arteriolar walls in rat skeletal muscle. *Am J Physiol Heart Circ Physiol* 289: H2673-2679, 2005.
340. **Cabrales P, Tsai AG, and Intaglietta M**. Nitric oxide regulation of microvascular oxygen exchange during hypoxia and hyperoxia. *J Appl Physiol (1985)* 100: 1181-1187, 2006.
341. **Milne GL, Yin H, Brooks JD, Sanchez S, Jackson Roberts L, 2nd, and Morrow JD**. Quantification of F2-isoprostanes in biological fluids and tissues as a measure of oxidant stress. *Methods Enzymol* 433: 113-126, 2007.
342. **Janssen LJ**. Isoprostanes: an overview and putative roles in pulmonary pathophysiology. *Am J Physiol Lung Cell Mol Physiol* 280: L1067-1082, 2001.
343. **Cracowski JL, and Durand T**. Cardiovascular pharmacology and physiology of the isoprostanes. *Fundam Clin Pharmacol* 20: 417-427, 2006.
344. **Belik J, Gonzalez-Luis GE, Perez-Vizcaino F, and Villamor E**. Isoprostanes in fetal and neonatal health and disease. *Free Radic Biol Med* 48: 177-188, 2010.
345. **van der Sterren S, and Villamor E**. Contractile effects of 15-E2t-isoprostane and 15-F2t-isoprostane on chicken embryo ductus arteriosus. *Comp Biochem Physiol A Mol Integr Physiol* 159: 436-444, 2011.
346. **Jankov RP, Luo X, Cabacungan J, Belcastro R, Frndova H, Lye SJ, and Tanswell AK**. Endothelin-1 and O2-mediated pulmonary hypertension in neonatal rats: a role for products of lipid peroxidation. *Pediatr Res* 48: 289-298, 2000.

347. **Chen JX, O'Mara PW, Poole SD, Brown N, Ehinger NJ, Slaughter JC, Paria BC, Aschner JL, and Reese J**. Isoprostanes as physiological mediators of transition to newborn life: novel mechanisms regulating patency of the term and preterm ductus arteriosus. *Pediatr Res* 72: 122-128, 2012.
348. **Weir EK, Lopez-Barneo J, Buckler KJ, and Archer SL**. Acute oxygen-sensing mechanisms. *N Engl J Med* 353: 2042-2055, 2005.
349. **Post JM, Hume JR, Archer SL, and Weir EK**. Direct role for potassium channel inhibition in hypoxic pulmonary vasoconstriction. *Am J Physiol* 262: C882-890, 1992.
350. **Weir EK, and Archer SL**. The mechanism of acute hypoxic pulmonary vasoconstriction: the tale of two channels. *FASEB J* 9: 183-189, 1995.
351. **Yuan XJ, Tod ML, Rubin LJ, and Blaustein MP**. Contrasting effects of hypoxia on tension in rat pulmonary and mesenteric arteries. *Am J Physiol* 259: H281-289, 1990.
352. **Michelakis ED, Hampl V, Nsair A, Wu X, Harry G, Haromy A, Gurtu R, and Archer SL**. Diversity in mitochondrial function explains differences in vascular oxygen sensing. *Circ Res* 90: 1307-1315, 2002.
353. **Madden JA, Vadula MS, and Kurup VP**. Effects of hypoxia and other vasoactive agents on pulmonary and cerebral artery smooth muscle cells. *Am J Physiol* 263: L384-393, 1992.
354. **Dunham-Snary KJ, Hong ZG, Xiong PY, Del Paggio JC, Herr JE, Johri AM, and Archer SL**. A mitochondrial redox oxygen sensor in the pulmonary vasculature and ductus arteriosus. *Pflugers Arch* 468: 43-58, 2016.
355. **Hong Z, Kutty S, Toth PT, Marsboom G, Hammel JM, Chamberlain C, Ryan JJ, Zhang HJ, Sharp WW, Morrow E, Trivedi K, Weir EK, and Archer SL**. Role of dynamin-related protein 1 (Drp1)-mediated mitochondrial fission in oxygen sensing and constriction of the ductus arteriosus. *Circ Res* 112: 802-815, 2013.
356. **Tristani-Firouzi M, Reeve HL, Tolarova S, Weir EK, and Archer SL**. Oxygen-induced constriction of rabbit ductus arteriosus occurs via inhibition of a 4-aminopyridine-, voltage-sensitive potassium channel. *J Clin Invest* 98: 1959-1965, 1996.
357. **McMurtry IF, Davidson AB, Reeves JT, and Grover RF**. Inhibition of hypoxic pulmonary vasoconstriction by calcium antagonists in isolated rat lungs. *Circ Res* 38: 99-104, 1976.
358. **Harder DR, Madden JA, and Dawson C**. Hypoxic induction of Ca2+-dependent action potentials in small pulmonary arteries of the cat. *J Appl Physiol (1985)* 59: 1389-1393, 1985.
359. **Michelakis E, Rebeyka I, Bateson J, Olley P, Puttagunta L, and Archer S**. Voltage-gated potassium channels in human ductus arteriosus. *Lancet* 356: 134-137, 2000.
360. **Fay FS**. Guinea pig ductus arteriosus. I. Cellular and metabolic basis for oxygen sensitivity. *Am J Physiol* 221: 470-479, 1971.
361. **Reeve HL, Tolarova S, Nelson DP, Archer S, and Weir EK**. Redox control of oxygen sensing in the rabbit ductus arteriosus. *J Physiol* 533: 253-261, 2001.
362. **Michelakis ED, Rebeyka I, Wu X, Nsair A, Thebaud B, Hashimoto K, Dyck JR, Haromy A, Harry G, Barr A, and Archer SL**. O2 sensing in the human ductus arteriosus: regulation of voltage-gated K+ channels in smooth muscle cells by a mitochondrial redox sensor. *Circ Res* 91: 478-486, 2002.
363. **Wu GR, Jing S, Momma K, and Nakanishi T**. The effect of vitamin A on contraction of the ductus arteriosus in fetal rat. *Pediatr Res* 49: 747-754, 2001.
364. **Baragatti B, Ciofini E, Scebba F, Angeloni D, Sodini D, Luin S, Ratto GM, Ottaviano V, Pagni E, Paolicchi A, Nencioni S, and Coceani F**. Cytochrome P-450 3A13 and endothelin jointly mediate ductus arteriosus constriction to oxygen in mice. *Am J Physiol Heart Circ Physiol* 300: H892-901, 2011.
365. **Coceani F, Kelsey L, and Seidlitz E**. Evidence for an effector role of endothelin in closure of the ductus arteriosus at birth. *Can J Physiol Pharmacol* 70: 1061-1064, 1992.
366. **Coceani F, Liu Y, Seidlitz E, Kelsey L, Kuwaki T, Ackerley C, and Yanagisawa M**. Endothelin A receptor is necessary for O(2) constriction but not closure of ductus arteriosus. *Am J Physiol* 277: H1521-1531, 1999.
367. **Taniguchi T, Azuma H, Okada Y, Naiki H, Hollenberg MD, and Muramatsu I**. Endothelin-1-endothelin receptor type A mediates closure of rat ductus arteriosus at birth. *J Physiol* 537: 579-585, 2001.
368. **Baragatti B, and Coceani F**. Arachidonic acid epoxygenase and 12(S)-lipoxygenase: evidence of their concerted involvement in ductus arteriosus constriction to oxygen. *Can J Physiol Pharmacol* 89: 329-334, 2011.

369. **Coceani F, Armstrong C, and Kelsey L**. Endothelin is a potent constrictor of the lamb ductus arteriosus. *Can J Physiol Pharmacol* 67: 902-904, 1989.
370. **Coceani F, and Kelsey L**. Endothelin-1 release from the lamb ductus arteriosus: are carbon monoxide and nitric oxide regulatory agents? *Life Sci* 66: 2613-2623, 2000.
371. **Takizawa T, Horikoshi E, Shen MH, Masaoka T, Takagi H, Yamamoto M, Kasai K, and Arishima K**. Effects of TAK-044, a nonselective endothelin receptor antagonist, on the spontaneous and indomethacin- or methylene blue-induced constriction of the ductus arteriosus in rats. *J Vet Med Sci* 62: 505-509, 2000.
372. **Shen J, Nakanishi T, Gu H, Miyagawa-Tomita S, Wu GR, Momma K, and Nakazawa M**. The role of endothelin in oxygen-induced contraction of the ductus arteriosus in rabbit and rat fetuses. *Heart Vessels* 16: 181-188, 2002.
373. **Coceani F, Kelsey L, Seidlitz E, and Korzekwa K**. Inhibition of the contraction of the ductus arteriosus to oxygen by 1-aminobenzotriazole, a mechanism-based inactivator of cytochrome P450. *Br J Pharmacol* 117: 1586-1592, 1996.
374. **Loftin CD, Tiano HF, and Langenbach R**. Phenotypes of the COX-deficient mice indicate physiological and pathophysiological roles for COX-1 and COX-2. *Prostaglandins Other Lipid Mediat* 68-69: 177-185, 2002.
375. **Yokoyama U**. Prostaglandin E-mediated molecular mechanisms driving remodeling of the ductus arteriosus. *Pediatr Int* 57: 820-827, 2015.
376. **Lloyd TR, and Beekman RH, 3rd**. Clinically silent patent ductus arteriosus. *Am Heart J* 127: 1664-1665, 1994.
377. **Reller MD, Rice MJ, and McDonald RW**. Review of studies evaluating ductal patency in the premature infant. *J Pediatr* 122: S59-62, 1993.
378. **Yu VY**. Patent ductus arteriosus in the preterm infant. *Early Hum Dev* 35: 1-14, 1993.
379. **Bokenkamp R, DeRuiter MC, van Munsteren C, and Gittenberger-de Groot AC**. Insights into the pathogenesis and genetic background of patency of the ductus arteriosus. *Neonatology* 98: 6-17, 2010.
380. **Grange DK, Lorch SM, Cole PL, and Singh GK**. Cantu syndrome in a woman and her two daughters: Further confirmation of autosomal dominant inheritance and review of the cardiac manifestations. *Am J Med Genet A* 140: 1673-1680, 2006.
381. **Harakalova M, van Harssel JJ, Terhal PA, van Lieshout S, Duran K, Renkens I, Amor DJ, Wilson LC, Kirk EP, Turner CL, Shears D, Garcia-Minaur S, Lees MM, Ross A, Venselaar H, Vriend G, Takanari H, Rook MB, van der Heyden MA, Asselbergs FW, Breur HM, Swinkels ME, Scurr IJ, Smithson SF, Knoers NV, van der Smagt JJ, Nijman IJ, Kloosterman WP, van Haelst MM, van Haaften G, and Cuppen E**. Dominant missense mutations in ABCC9 cause Cantu syndrome. *Nat Genet* 44: 793-796, 2012.
382. **Grange DK, Nichols CG, and Singh GK**. *Cantu Syndrome and Related Disorders*. Seattle (WA): University of Washington, 2014.
383. **Waleh N, Barrette AM, Dagle JM, Momany A, Jin C, Hills NK, Shelton EL, Reese J, and Clyman RI**. Effects of Advancing Gestation and Non-Caucasian Race on Ductus Arteriosus Gene Expression. *J Pediatr* 167: 1033-1041 e1032, 2015.
384. **Boczek NJ, Miller EM, Ye D, Nesterenko VV, Tester DJ, Antzelevitch C, Czosek RJ, Ackerman MJ, and Ware SM**. Novel Timothy syndrome mutation leading to increase in CACNA1C window current. *Heart Rhythm* 12: 211-219, 2015.
385. **Ushikubi F, Sugimoto Y, Ichikawa A, and Narumiya S**. Roles of prostanoids revealed from studies using mice lacking specific prostanoid receptors. *Jpn J Pharmacol* 83: 279-285, 2000.
386. **Fujino T, Yuhki K, Yamada T, Hara A, Takahata O, Okada Y, Xiao CY, Ma H, Karibe H, Iwashima Y, Fukuzawa J, Hasebe N, Kikuchi K, Narumiya S, and Ushikubi F**. Effects of the prostanoids on the proliferation or hypertrophy of cultured murine aortic smooth muscle cells. *Br J Pharmacol* 136: 530-539, 2002.
387. **Satoda M, Zhao F, Diaz GA, Burn J, Goodship J, Davidson HR, Pierpont ME, and Gelb BD**. Mutations in TFAP2B cause Char syndrome, a familial form of patent ductus arteriosus. *Nat Genet* 25: 42-46, 2000.
388. **Zhao F, Weismann CG, Satoda M, Pierpont ME, Sweeney E, Thompson EM, and Gelb BD**. Novel TFAP2B mutations that cause Char syndrome provide a genotype-phenotype correlation. *Am J Hum Genet* 69: 695-703, 2001.

389. **Schneider DJ, and Moore JW**. Patent ductus arteriosus. *Circulation* 114: 1873-1882, 2006.
390. **Khetyar M, Syrris P, Tinworth L, Abushaban L, and Carter N**. Novel TFAP2B mutation in nonsyndromic patent ductus arteriosus. *Genet Test* 12: 457-459, 2008.
391. **Zhao F, Bosserhoff AK, Buettner R, and Moser M**. A heart-hand syndrome gene: Tfap2b plays a critical role in the development and remodeling of mouse ductus arteriosus and limb patterning. *PLoS One* 6: e22908, 2011.
392. **Chen YW, Zhao W, Zhang ZF, Fu Q, Shen J, Zhang Z, Ji W, Wang J, and Li F**. Familial nonsyndromic patent ductus arteriosus caused by mutations in TFAP2B. *Pediatr Cardiol* 32: 958-965, 2011.
393. **Lewis TR, Shelton EL, Van Driest SL, Kannankeril PJ, and Reese J**. Genetics of the patent ductus arteriosus (PDA) and pharmacogenetics of PDA treatment. *Semin Fetal Neonatal Med* 2018.
394. **Rybalkin SD, Rybalkina I, Beavo JA, and Bornfeldt KE**. Cyclic nucleotide phosphodiesterase 1C promotes human arterial smooth muscle cell proliferation. *Circ Res* 90: 151-157, 2002.
395. **Clyman RI**. Mechanisms regulating the ductus arteriosus. *Biol Neonate* 89: 330-335, 2006.
396. **Yokoyama U, Minamisawa S, Shioda A, Ishiwata R, Jin MH, Masuda M, Asou T, Sugimoto Y, Aoki H, Nakamura T, and Ishikawa Y**. Prostaglandin E2 inhibits elastogenesis in the ductus arteriosus via EP4 signaling. *Circulation* 129: 487-496, 2014.
397. **Bouayad A, Kajino H, Waleh N, Fouron JC, Andelfinger G, Varma DR, Skoll A, Vazquez A, Gobeil F, Jr., Clyman RI, and Chemtob S**. Characterization of PGE2 receptors in fetal and newborn lamb ductus arteriosus. *Am J Physiol Heart Circ Physiol* 280: H2342-2349, 2001.
398. **Kajino H, Taniguchi T, Fujieda K, Ushikubi F, and Muramatsu I**. An EP4 receptor agonist prevents indomethacin-induced closure of rat ductus arteriosus in vivo. *Pediatr Res* 56: 586-590, 2004.
399. **Momma K, Toyoshima K, Takeuchi D, Imamura S, and Nakanishi T**. In vivo reopening of the neonatal ductus arteriosus by a prostanoid EP4-receptor agonist in the rat. *Prostaglandins Other Lipid Mediat* 78: 117-128, 2005.
400. **Momma K, Toyoshima K, Takeuchi D, Imamura S, and Nakanishi T**. In vivo constriction of the fetal and neonatal ductus arteriosus by a prostanoid EP4-receptor antagonist in rats. *Pediatr Res* 58: 971-975, 2005.
401. **de Reeder EG, Gittenberger-de Groot AC, van Munsteren JC, Poelmann RE, Patterson DF, and Keirse MJ**. Distribution of prostacyclin synthase, 6-keto-prostaglandin F1 alpha, and 15-hydroxy-prostaglandin dehydrogenase in the normal and persistent ductus arteriosus of the dog. *Am J Pathol* 135: 881-887, 1989.
402. **Ivey KN, Sutcliffe D, Richardson J, Clyman RI, Garcia JA, and Srivastava D**. Transcriptional regulation during development of the ductus arteriosus. *Circ Res* 103: 388-395, 2008.
403. **Coceani F**. Control of the ductus arteriosus--a new function for cytochrome P450, endothelin and nitric oxide. *Biochem Pharmacol* 48: 1315-1318, 1994.
404. **Momma K, Toyoshima K, Imamura S, and Nakanishi T**. In vivo dilation of fetal and neonatal ductus arteriosus by inhibition of phosphodiesterase-5 in rats. *Pediatr Res* 58: 42-45, 2005.
405. **Toyoshima K, Momma K, Imamura S, and Nakanishi T**. In vivo dilatation of the fetal and postnatal ductus arteriosus by inhibition of phosphodiesterase 3 in rats. *Biol Neonate* 89: 251-256, 2006.
406. **Chan S, and Yan C**. PDE1 isozymes, key regulators of pathological vascular remodeling. *Curr Opin Pharmacol* 11: 720-724, 2011.
407. **Cai Y, Nagel DJ, Zhou Q, Cygnar KD, Zhao H, Li F, Pi X, Knight PA, and Yan C**. Role of cAMP-phosphodiesterase 1C signaling in regulating growth factor receptor stability, vascular smooth muscle cell growth, migration, and neointimal hyperplasia. *Circ Res* 116: 1120-1132, 2015.
408. **Carvalho T, Cardarelli S, Giorgi M, Lenzi A, Isidori AM, and Naro F**. Phosphodiesterases Expression during Murine Cardiac Development. *Int J Mol Sci* 22: 2021.
409. **Goyal R, and Clyman RI**. Response to Coceani et al. *Pediatr Res* 82: 175, 2017.
410. **Coceani F, Scebba F, and Angeloni D**. Ductus arteriosus: gene profile for fetal maturation versus postnatal closure. *Pediatr Res* 82: 174, 2017.
411. **Cahan P, Ahmad AM, Burke H, Fu S, Lai Y, Florea L, Dharker N, Kobrinski T, Kale P, and McCaffrey TA**. List of lists-annotated (LOLA): a database for annotation and comparison of published microarray gene lists. *Gene* 360: 78-82, 2005.

412. **Cahan P, Rovegno F, Mooney D, Newman JC, St Laurent G, 3rd, and McCaffrey TA**. Meta-analysis of microarray results: challenges, opportunities, and recommendations for standardization. *Gene* 401: 12-18, 2007.
413. **Tseng GC, Ghosh D, and Feingold E**. Comprehensive literature review and statistical considerations for microarray meta-analysis. *Nucleic Acids Res* 40: 3785-3799, 2012.
414. **Eidem HR, Ackerman WEt, McGary KL, Abbot P, and Rokas A**. Gestational tissue transcriptomics in term and preterm human pregnancies: a systematic review and meta-analysis. *BMC Med Genomics* 8: 27, 2015.
415. **Hughes DA, Kircher M, He Z, Guo S, Fairbrother GL, Moreno CS, Khaitovich P, and Stoneking M**. Evaluating intra- and inter-individual variation in the human placental transcriptome. *Genome Biol* 16: 54, 2015.
416. **Manoli T, Gretz N, Grone HJ, Kenzelmann M, Eils R, and Brors B**. Group testing for pathway analysis improves comparability of different microarray datasets. *Bioinformatics* 22: 2500-2506, 2006.
417. **Levet S, Ouarne M, Ciais D, Coutton C, Subileau M, Mallet C, Ricard N, Bidart M, Debillon T, Faravelli F, Rooryck C, Feige JJ, Tillet E, and Bailly S**. BMP9 and BMP10 are necessary for proper closure of the ductus arteriosus. *Proc Natl Acad Sci U S A* 112: E3207-3215, 2015.
418. **Staiculescu MC, Kim J, Mecham RP, and Wagenseil JE**. Mechanical behavior and matrisome gene expression in the aneurysm-prone thoracic aorta of newborn lysyl oxidase knockout mice. *Am J Physiol Heart Circ Physiol* 313: H446-H456, 2017.
419. **Hamrick SEG, Sallmon H, Rose AT, Porras D, Shelton EL, Reese J, and Hansmann G**. Patent Ductus Arteriosus of the Preterm Infant. *Pediatrics* 146: 2020.
420. **Siegel RE**. Galen's experiments and observations on pulmonary blood flow and respiration. *The American Journal of Cardiology* 10: 738, 1962.
421. **Cassels DE**. *The Ductus Arteriosus*. Springfield Illinois, USA: Charles C Thomas, 1973.
422. **Hornblad PY**. Embryological observations of the ductus arteriosus in the guinea-pig, rabbit, rat and mouse. Studies on closure of the ductus arteriosus. IV. *Acta Physiol Scand* 76: 49-57, 1969.
423. **Phifer-Rixey M, and Nachman MW**. Insights into mammalian biology from the wild house mouse Mus musculus. *Elife* 4: 2015.
424. **Yarboro MT, Gopal SH, Su RL, Morgan TM, and Reese J**. Mouse models of patent ductus arteriosus (PDA) and their relevance for human PDA. *Dev Dyn* 251: 424-443, 2022.
425. **Vane JR, Bakhle YS, and Botting RM**. Cyclooxygenases 1 and 2. *Annu Rev Pharmacol Toxicol* 38: 97-120, 1998.
426. **Kulmacz RJ**. Regulation of cyclooxygenase catalysis by hydroperoxides. *Biochem Biophys Res Commun* 338: 25-33, 2005.
427. **Sinha GP, Curtis P, Haigh D, Lealman GT, Dodds W, and Bennett CP**. Pachydermoperiostosis in childhood. *Br J Rheumatol* 36: 1224-1227, 1997.
428. **Eling TE, and Anderson MW**. Studies on the biosynthesis, metabolism and transport of prostaglandins by the lung. *Agents Actions* 6: 543-546, 1976.
429. **Hawkins HJ, Wilson AG, Anderson MW, and Eling TE**. Uptake and metabolism of prostaglandins by isolated perfused lung: species comparisons and the role of plasma protein binding. *Prostaglandins* 14: 251-259, 1977.
430. **Chang HY, Locker J, Lu R, and Schuster VL**. Failure of postnatal ductus arteriosus closure in prostaglandin transporter-deficient mice. *Circulation* 121: 529-536, 2010.
431. **Zhang Z, Xia W, He J, Zhang Z, Ke Y, Yue H, Wang C, Zhang H, Gu J, Hu W, Fu W, Hu Y, Li M, and Liu Y**. Exome sequencing identifies SLCO2A1 mutations as a cause of primary hypertrophic osteoarthropathy. *Am J Hum Genet* 90: 125-132, 2012.
432. **Pipes GC, Creemers EE, and Olson EN**. The myocardin family of transcriptional coactivators: versatile regulators of cell growth, migration, and myogenesis. *Genes Dev* 20: 1545-1556, 2006.
433. **Parmacek MS**. Myocardin-related transcription factors: critical coactivators regulating cardiovascular development and adaptation. *Circ Res* 100: 633-644, 2007.
434. **Ji Y, Hao H, Reynolds K, McMahon M, and Zhou CJ**. Wnt Signaling in Neural Crest Ontogenesis and Oncogenesis. *Cells* 8: 2019.

435. **Yajima I, Colombo S, Puig I, Champeval D, Kumasaka M, Belloir E, Bonaventure J, Mark M, Yamamoto H, Taketo MM, Choquet P, Etchevers HC, Beermann F, Delmas V, Monassier L, and Larue L**. A subpopulation of smooth muscle cells, derived from melanocyte-competent precursors, prevents patent ductus arteriosus. *PLoS One* 8: e53183, 2013.
436. **Kim HS, Aikawa M, Kimura K, Kuro-o M, Nakahara K, Suzuki T, Katoh H, Okamoto E, Yazaki Y, and Nagai R**. Ductus arteriosus. Advanced differentiation of smooth muscle cells demonstrated by myosin heavy chain isoform expression in rabbits. *Circulation* 88: 1804-1810, 1993.
437. **Morano I, Chai GX, Baltas LG, Lamounier-Zepter V, Lutsch G, Kott M, Haase H, and Bader M**. Smooth-muscle contraction without smooth-muscle myosin. *Nat Cell Biol* 2: 371-375, 2000.
438. **Glancy DL, Wegmann M, and Dhurandhar RW**. Aortic dissection and patent ductus arteriosus in three generations. *Am J Cardiol* 87: 813-815, A819, 2001.
439. **Pannu H, Tran-Fadulu V, Papke CL, Scherer S, Liu Y, Presley C, Guo D, Estrera AL, Safi HJ, Brasier AR, Vick GW, Marian AJ, Raman CS, Buja LM, and Milewicz DM**. MYH11 mutations result in a distinct vascular pathology driven by insulin-like growth factor 1 and angiotensin II. *Hum Mol Genet* 16: 2453-2462, 2007.
440. **Feng X, Krebs LT, and Gridley T**. Patent ductus arteriosus in mice with smooth muscle-specific Jag1 deletion. *Development* 137: 4191-4199, 2010.
441. **Sanchez-Angulo JI, Benitez-Roldan A, Castro-Fernandez A, and Ruiz-Campos J**. [Alagille syndrome and isolated persistent ductus arteriosus]. *Gastroenterol Hepatol* 20: 418-421, 1997.
442. **Baeten JT, Jackson AR, McHugh KM, and Lilly B**. Loss of Notch2 and Notch3 in vascular smooth muscle causes patent ductus arteriosus. *Genesis* 53: 738-748, 2015.
443. **Rosser EM, Mann NP, Hall CM, and Winter RM**. Serpentine fibula syndrome: expansion of the phenotype with three affected siblings. *Clin Dysmorphol* 5: 105-113, 1996.
444. **Gripp KW, Robbins KM, Sobreira NL, Witmer PD, Bird LM, Avela K, Makitie O, Alves D, Hogue JS, Zackai EH, Doheny KF, Stabley DL, and Sol-Church K**. Truncating mutations in the last exon of NOTCH3 cause lateral meningocele syndrome. *Am J Med Genet A* 167A: 271-281, 2015.
445. **Holtwick R, Gotthardt M, Skryabin B, Steinmetz M, Potthast R, Zetsche B, Hammer RE, Herz J, and Kuhn M**. Smooth muscle-selective deletion of guanylyl cyclase-A prevents the acute but not chronic effects of ANP on blood pressure. *Proc Natl Acad Sci U S A* 99: 7142-7147, 2002.
446. **Krebs LT, Norton CR, and Gridley T**. Notch signal reception is required in vascular smooth muscle cells for ductus arteriosus closure. *Genesis* 54: 86-90, 2016.
447. **Ng A, Wong M, Viviano B, Erlich JM, Alba G, Pflederer C, Jay PY, and Saunders S**. Loss of glypican-3 function causes growth factor-dependent defects in cardiac and coronary vascular development. *Dev Biol* 335: 208-215, 2009.
448. **Yano S, Baskin B, Bagheri A, Watanabe Y, Moseley K, Nishimura A, Matsumoto N, and Ray PN**. Familial Simpson-Golabi-Behmel syndrome: studies of X-chromosome inactivation and clinical phenotypes in two female individuals with GPC3 mutations. *Clin Genet* 80: 466-471, 2011.
449. **Moser M, Pscherer A, Roth C, Becker J, Mucher G, Zerres K, Dixkens C, Weis J, Guay-Woodford L, Buettner R, and Fassler R**. Enhanced apoptotic cell death of renal epithelial cells in mice lacking transcription factor AP-2beta. *Genes Dev* 11: 1938-1948, 1997.
450. **Wang J, Ji W, Zhu D, Wang W, Chen Y, Zhang Z, and Li F**. Tfap2b mutation in mice results in patent ductus arteriosus and renal malformation. *J Surg Res* 227: 178-185, 2018.
451. **Winnier GE, Hargett L, and Hogan BL**. The winged helix transcription factor MFH1 is required for proliferation and patterning of paraxial mesoderm in the mouse embryo. *Genes Dev* 11: 926-940, 1997.
452. **Winnier GE, Kume T, Deng K, Rogers R, Bundy J, Raines C, Walter MA, Hogan BL, and Conway SJ**. Roles for the winged helix transcription factors MF1 and MFH1 in cardiovascular development revealed by nonallelic noncomplementation of null alleles. *Dev Biol* 213: 418-431, 1999.
453. **Baruch AC, and Erickson RP**. Axenfeld-Rieger anomaly, hypertelorism, clinodactyly, and cardiac anomalies in sibs with an unbalanced translocation der(6)t(6;8). *Am J Med Genet* 100: 187-190, 2001.
454. **Quintero-Rivera F, Xi QJ, Keppler-Noreuil KM, Lee JH, Higgins AW, Anchan RM, Roberts AE, Seong IS, Fan X, Lage K, Lu LY, Tao J, Hu X, Berezney R, Gelb BD, Kamp A, Moskowitz IP, Lacro RV, Lu W, Morton CC,**

Gusella JF, and Maas RL. MATR3 disruption in human and mouse associated with bicuspid aortic valve, aortic coarctation and patent ductus arteriosus. *Hum Mol Genet* 24: 2375-2389, 2015.
455. **Tamura M, Hosoya M, Fujita M, Iida T, Amano T, Maeno A, Kataoka T, Otsuka T, Tanaka S, Tomizawa S, and Shiroishi T**. Overdosage of Hand2 causes limb and heart defects in the human chromosomal disorder partial trisomy distal 4q. *Hum Mol Genet* 22: 2471-2481, 2013.
456. **Shen D, Li J, Lepore JJ, Anderson TJ, Sinha S, Lin AY, Cheng L, Cohen ED, Roberts JD, Jr., Dedhar S, Parmacek MS, and Gerszten RE**. Aortic aneurysm generation in mice with targeted deletion of integrin-linked kinase in vascular smooth muscle cells. *Circ Res* 109: 616-628, 2011.
457. **van der Flier A, Badu-Nkansah K, Whittaker CA, Crowley D, Bronson RT, Lacy-Hulbert A, and Hynes RO**. Endothelial alpha5 and alphav integrins cooperate in remodeling of the vasculature during development. *Development* 137: 2439-2449, 2010.
458. **Ito S, Yokoyama U, Nakakoji T, Cooley MA, Sasaki T, Hatano S, Kato Y, Saito J, Nicho N, Iwasaki S, Umemura M, Fujita T, Masuda M, Asou T, and Ishikawa Y**. Fibulin-1 Integrates Subendothelial Extracellular Matrices and Contributes to Anatomical Closure of the Ductus Arteriosus. *Arterioscler Thromb Vasc Biol* 40: 2212-2226, 2020.
459. **Zhang M, Chen M, Kim JR, Zhou J, Jones RE, Tune JD, Kassab GS, Metzger D, Ahlfeld S, Conway SJ, and Herring BP**. SWI/SNF complexes containing Brahma or Brahma-related gene 1 play distinct roles in smooth muscle development. *Mol Cell Biol* 31: 2618-2631, 2011.
460. **Lai HL, and Wang QT**. Additional sex combs-like 2 is required for polycomb repressive complex 2 binding at select targets. *PLoS One* 8: e73983, 2013.
461. **McGinley AL, Li Y, Deliu Z, and Wang QT**. Additional sex combs-like family genes are required for normal cardiovascular development. *Genesis* 52: 671-686, 2014.
462. **Echtler K, Stark K, Lorenz M, Kerstan S, Walch A, Jennen L, Rudelius M, Seidl S, Kremmer E, Emambokus NR, von Bruehl ML, Frampton J, Isermann B, Genzel-Boroviczeny O, Schreiber C, Mehilli J, Kastrati A, Schwaiger M, Shivdasani RA, and Massberg S**. Platelets contribute to postnatal occlusion of the ductus arteriosus. *Nat Med* 16: 75-82, 2010.
463. **Sallmon H, Timme N, Atasay B, Erdeve O, Hansmann G, Singh Y, Weber SC, and Shelton EL**. Current Controversy on Platelets and Patent Ductus Arteriosus Closure in Preterm Infants. *Front Pediatr* 9: 612242, 2021.
464. **Sallmon H, Weber SC, Dirks J, Schiffer T, Klippstein T, Stein A, Felderhoff-Muser U, Metze B, Hansmann G, Buhrer C, Cremer M, and Koehne P**. Association between Platelet Counts before and during Pharmacological Therapy for Patent Ductus Arteriosus and Treatment Failure in Preterm Infants. *Front Pediatr* 6: 41, 2018.
465. **Sallmon H, Weber SC, Huning B, Stein A, Horn PA, Metze BC, Dame C, Buhrer C, Felderhoff-Muser U, Hansmann G, and Koehne P**. Thrombocytopenia in the first 24 hours after birth and incidence of patent ductus arteriosus. *Pediatrics* 130: e623-630, 2012.
466. **Fujioka K, Morioka I, Miwa A, Morikawa S, Shibata A, Yokoyama N, and Matsuo M**. Does thrombocytopenia contribute to patent ductus arteriosus? *Nat Med* 17: 29-30; author reply 30-21, 2011.
467. **Shah NA, Hills NK, Waleh N, McCurnin D, Seidner S, Chemtob S, and Clyman R**. Relationship between circulating platelet counts and ductus arteriosus patency after indomethacin treatment. *J Pediatr* 158: 919-923 e911-912, 2011.
468. **Kumar J, Dutta S, Sundaram V, Saini SS, Sharma RR, and Varma N**. Platelet Transfusion for PDA Closure in Preterm Infants: A Randomized Controlled Trial. *Pediatrics* 143: 2019.
469. **Donovan MJ, Hahn R, Tessarollo L, and Hempstead BL**. Identification of an essential nonneuronal function of neurotrophin 3 in mammalian cardiac development. *Nat Genet* 14: 210-213, 1996.
470. **Reaume AG, de Sousa PA, Kulkarni S, Langille BL, Zhu D, Davies TC, Juneja SC, Kidder GM, and Rossant J**. Cardiac malformation in neonatal mice lacking connexin43. *Science* 267: 1831-1834, 1995.
471. **Kirchhoff S, Kim JS, Hagendorff A, Thonnissen E, Kruger O, Lamers WH, and Willecke K**. Abnormal cardiac conduction and morphogenesis in connexin40 and connexin43 double-deficient mice. *Circ Res* 87: 399-405, 2000.

472. **Marissen J, Erdmann H, Bockenholt K, Hoppenz M, Rausch TK, Hartel C, Herting E, Gopel W, and German Neonatal N**. Aminoglycosides were associated with higher rates of surgical patent ductus arteriosus closure in preterm infants. *Acta Paediatr* 2020.
473. **Hajj H, and Dagle JM**. Genetics of patent ductus arteriosus susceptibility and treatment. *Semin Perinatol* 36: 98-104, 2012.
474. **Reese J, and Laughon MM**. The Patent Ductus Arteriosus Problem: Infants Who Still Need Treatment. *J Pediatr* 167: 954-956, 2015.
475. **Evans N**. Preterm patent ductus arteriosus: A continuing conundrum for the neonatologist? *Semin Fetal Neonatal Med* 20: 272-277, 2015.
476. **Coceani F, and Baragatti B**. Mechanisms for ductus arteriosus closure. *Semin Perinatol* 36: 92-97, 2012.
477. **Yokoyama U, Minamisawa S, Quan H, Akaike T, Suzuki S, Jin M, Jiao Q, Watanabe M, Otsu K, Iwasaki S, Nishimaki S, Sato M, and Ishikawa Y**. Prostaglandin E2-activated Epac promotes neointimal formation of the rat ductus arteriosus by a process distinct from that of cAMP-dependent protein kinase A. *J Biol Chem* 283: 28702-28709, 2008.
478. **Eronen M**. The hemodynamic effects of antenatal indomethacin and a beta-sympathomimetic agent on the fetus and the newborn: a randomized study. *Pediatr Res* 33: 615-619, 1993.
479. **Simon SR, van Zogchel L, Bas-Suarez MP, Cavallaro G, Clyman RI, and Villamor E**. Platelet Counts and Patent Ductus Arteriosus in Preterm Infants: A Systematic Review and Meta-Analysis. *Neonatology* 108: 143-151, 2015.
480. **Richter F, Morton SU, Kim SW, Kitaygorodsky A, Wasson LK, Chen KM, Zhou J, Qi H, Patel N, DePalma SR, Parfenov M, Homsy J, Gorham JM, Manheimer KB, Velinder M, Farrell A, Marth G, Schadt EE, Kaltman JR, Newburger JW, Giardini A, Goldmuntz E, Brueckner M, Kim R, Porter GA, Jr., Bernstein D, Chung WK, Srivastava D, Tristani-Firouzi M, Troyanskaya OG, Dickel DE, Shen Y, Seidman JG, Seidman CE, and Gelb BD**. Genomic analyses implicate noncoding de novo variants in congenital heart disease. *Nat Genet* 52: 769-777, 2020.
481. **Shelton EL, Singh GK, and Nichols CG**. Novel drug targets for ductus arteriosus manipulation: Looking beyond prostaglandins. *Semin Perinatol* 42: 221-227, 2018.
482. **Merscher S, Funke B, Epstein JA, Heyer J, Puech A, Lu MM, Xavier RJ, Demay MB, Russell RG, Factor S, Tokooya K, Jore BS, Lopez M, Pandita RK, Lia M, Carrion D, Xu H, Schorle H, Kobler JB, Scambler P, Wynshaw-Boris A, Skoultchi AI, Morrow BE, and Kucherlapati R**. TBX1 is responsible for cardiovascular defects in velo-cardio-facial/DiGeorge syndrome. *Cell* 104: 619-629, 2001.
483. **Schildmeyer LA, Braun R, Taffet G, Debiasi M, Burns AE, Bradley A, and Schwartz RJ**. Impaired vascular contractility and blood pressure homeostasis in the smooth muscle alpha-actin null mouse. *FASEB J* 14: 2213-2220, 2000.
484. **Fath MA, Mullins RF, Searby C, Nishimura DY, Wei J, Rahmouni K, Davis RE, Tayeh MK, Andrews M, Yang B, Sigmund CD, Stone EM, and Sheffield VC**. Mkks-null mice have a phenotype resembling Bardet-Biedl syndrome. *Hum Mol Genet* 14: 1109-1118, 2005.
485. **Urano T, Shiraki M, Sasaki N, Ouchi Y, and Inoue S**. SLC25A24 as a novel susceptibility gene for low fat mass in humans and mice. *J Clin Endocrinol Metab* 100: E655-663, 2015.
486. **Baragatti B, Sodini D, Uematsu S, and Coceani F**. Role of microsomal prostaglandin E synthase-1 (mPGES1)-derived PGE2 in patency of the ductus arteriosus in the mouse. *Pediatr Res* 64: 523-527, 2008.
487. **Bergwerff M, Gittenberger-de Groot AC, Wisse LJ, DeRuiter MC, Wessels A, Martin JF, Olson EN, and Kern MJ**. Loss of function of the Prx1 and Prx2 homeobox genes alters architecture of the great elastic arteries and ductus arteriosus. *Virchows Arch* 436: 12-19, 2000.
488. **Barrick CJ, Dong A, Waikel R, Corn D, Yang F, Threadgill DW, and Smyth SS**. Parent-of-origin effects on cardiac response to pressure overload in mice. *Am J Physiol Heart Circ Physiol* 297: H1003-1009, 2009.
489. **Dagle JM, Lepp NT, Cooper ME, Schaa KL, Kelsey KJ, Orr KL, Caprau D, Zimmerman CR, Steffen KM, Johnson KJ, Marazita ML, and Murray JC**. Determination of genetic predisposition to patent ductus arteriosus in preterm infants. *Pediatrics* 123: 1116-1123, 2009.

490. **Treszl A, Szabo M, Dunai G, Nobilis A, Kocsis I, Machay T, Tulassay T, and Vasarhelyi B**. Angiotensin II type 1 receptor A1166C polymorphism and prophylactic indomethacin treatment induced ductus arteriosus closure in very low birth weight neonates. *Pediatr Res* 54: 753-755, 2003.
491. **Jan SL, Chan SC, Fu YC, and Lin SJ**. Elastin gene study of infants with isolated congenital ductus arteriosus aneurysm. *Acta Cardiol* 64: 363-369, 2009.
492. **Zhu WL, Li Y, Yan L, Dao J, and Li S**. Maternal and offspring MTHFR gene C677T polymorphism as predictors of congenital atrial septal defect and patent ductus arteriosus. *Mol Hum Reprod* 12: 51-54, 2006.
493. **Rooney SR, Shelton EL, Aka I, Shaffer CM, Clyman RI, Dagle JM, Ryckman K, Lewis TR, Reese J, Van Driest SL, and Kannankeril PJ**. CYP2C9*2 is associated with indomethacin treatment failure for patent ductus arteriosus. *Pharmacogenomics* 20: 939-946, 2019.
494. **Karki R, Pandya D, Elston RC, and Ferlini C**. Defining "mutation" and "polymorphism" in the era of personal genomics. *BMC Med Genomics* 8: 37, 2015.
495. **Dagle JM, Ryckman KK, Spracklen CN, Momany AM, Cotten CM, Levy J, Page GP, Bell EF, Carlo WA, Shankaran S, Goldberg RN, Ehrenkranz RA, Tyson JE, Stoll BJ, Murray JC, Eunice Kennedy Shriver National Institute of Child H, and Human Development Neonatal Research N**. Genetic variants associated with patent ductus arteriosus in extremely preterm infants. *J Perinatol* 39: 401-408, 2019.
496. **Lewis TR, Shelton EL, Van Driest SL, Kannankeril PJ, and Reese J**. Genetics of the patent ductus arteriosus (PDA) and pharmacogenetics of PDA treatment. *Semin Fetal Neonatal Med* 23: 232-238, 2018.
497. **Reese J**. Towards a greater understanding of the ductus arteriosus. *Semin Perinatol* 42: 199-202, 2018.
498. **Kume T, Deng KY, Winfrey V, Gould DB, Walter MA, and Hogan BL**. The forkhead/winged helix gene Mf1 is disrupted in the pleiotropic mouse mutation congenital hydrocephalus. *Cell* 93: 985-996, 1998.
499. **Langenbach R, Morham SG, Tiano HF, Loftin CD, Ghanayem BI, Chulada PC, Mahler JF, Lee CA, Goulding EH, Kluckman KD, Kim HS, and Smithies O**. Prostaglandin synthase 1 gene disruption in mice reduces arachidonic acid-induced inflammation and indomethacin-induced gastric ulceration. *Cell* 83: 483-492, 1995.
500. **Kishihara K, Penninger J, Wallace VA, Kundig TM, Kawai K, Wakeham A, Timms E, Pfeffer K, Ohashi PS, Thomas ML, and et al.** Normal B lymphocyte development but impaired T cell maturation in CD45-exon6 protein tyrosine phosphatase-deficient mice. *Cell* 74: 143-156, 1993.
501. **Long X, Creemers EE, Wang DZ, Olson EN, and Miano JM**. Myocardin is a bifunctional switch for smooth versus skeletal muscle differentiation. *Proc Natl Acad Sci U S A* 104: 16570-16575, 2007.
502. **Shivdasani RA, Rosenblatt MF, Zucker-Franklin D, Jackson CW, Hunt P, Saris CJ, and Orkin SH**. Transcription factor NF-E2 is required for platelet formation independent of the actions of thrombopoietin/MGDF in megakaryocyte development. *Cell* 81: 695-704, 1995.
503. **Emambokus NR, and Frampton J**. The glycoprotein IIb molecule is expressed on early murine hematopoietic progenitors and regulates their numbers in sites of hematopoiesis. *Immunity* 19: 33-45, 2003.
504. **Kiernan AE, Xu J, and Gridley T**. The Notch ligand JAG1 is required for sensory progenitor development in the mammalian inner ear. *PLoS Genet* 2: e4, 2006.
505. **Delmas V, Martinozzi S, Bourgeois Y, Holzenberger M, and Larue L**. Cre-mediated recombination in the skin melanocyte lineage. *Genesis* 36: 73-80, 2003.
506. **Ricard N, Ciais D, Levet S, Subileau M, Mallet C, Zimmers TA, Lee SJ, Bidart M, Feige JJ, and Bailly S**. BMP9 and BMP10 are critical for postnatal retinal vascular remodeling. *Blood* 119: 6162-6171, 2012.
507. **Krebs LT, Xue Y, Norton CR, Sundberg JP, Beatus P, Lendahl U, Joutel A, and Gridley T**. Characterization of Notch3-deficient mice: normal embryonic development and absence of genetic interactions with a Notch1 mutation. *Genesis* 37: 139-143, 2003.
508. **McCright B, Lozier J, and Gridley T**. Generation of new Notch2 mutant alleles. *Genesis* 44: 29-33, 2006.
509. **Han H, Tanigaki K, Yamamoto N, Kuroda K, Yoshimoto M, Nakahata T, Ikuta K, and Honjo T**. Inducible gene knockout of transcription factor recombination signal binding protein-J reveals its essential role in T versus B lineage decision. *Int Immunol* 14: 637-645, 2002.
510. **Tanigaki K, Han H, Yamamoto N, Tashiro K, Ikegawa M, Kuroda K, Suzuki A, Nakano T, and Honjo T**. Notch-RBP-J signaling is involved in cell fate determination of marginal zone B cells. *Nat Immunol* 3: 443-450, 2002.

511. **Hornstra IK, Birge S, Starcher B, Bailey AJ, Mecham RP, and Shapiro SD**. Lysyl oxidase is required for vascular and diaphragmatic development in mice. *J Biol Chem* 278: 14387-14393, 2003.
512. **Vane SJ**. Differential inhibition of cyclooxygenase isoforms: an explanation of the action of NSAIDs. *J Clin Rheumatol* 4: s3-10, 1998.
513. **Clyman RI, Chan CY, Mauray F, Chen YQ, Cox W, Seidner SR, Lord EM, Weiss H, Waleh N, Evans SM, and Koch CJ**. Permanent anatomic closure of the ductus arteriosus in newborn baboons: the roles of postnatal constriction, hypoxia, and gestation. *Pediatr Res* 45: 19-29, 1999.
514. **Bentley RET, Hindmarch CCT, Dunham-Snary KJ, Snetsinger B, Mewburn JD, Thebaud A, Lima PDA, Thebaud B, and Archer SL**. The comprehensive transcriptome of human ductus arteriosus smooth muscle cells (hDASMC). *Data Brief* 40: 107736, 2022.
515. **Ke J, Yang Y, Che Q, Jiang F, Wang H, Chen Z, Zhu M, Tong H, Zhang H, Yan X, Wang X, Wang F, Liu Y, Dai C, and Wan X**. Prostaglandin E2 (PGE2) promotes proliferation and invasion by enhancing SUMO-1 activity via EP4 receptor in endometrial cancer. *Tumour Biol* 37: 12203-12211, 2016.
516. **Osawa K, Umemura M, Nakakaji R, Tanaka R, Islam RM, Nagasako A, Fujita T, Yokoyama U, Koizumi T, Mitsudo K, and Ishikawa Y**. Prostaglandin E(2) receptor EP4 regulates cell migration through Orai1. *Cancer Sci* 111: 160-174, 2020.
517. **Boudreau N, Turley E, and Rabinovitch M**. Fibronectin, hyaluronan, and a hyaluronan binding protein contribute to increased ductus arteriosus smooth muscle cell migration. *Dev Biol* 143: 235-247, 1991.
518. **Clyman RI, Mauray F, and Kramer RH**. Beta 1 and beta 3 integrins have different roles in the adhesion and migration of vascular smooth muscle cells on extracellular matrix. *Exp Cell Res* 200: 272-284, 1992.
519. **Koppel R, and Rabinovitch M**. Regulation of fetal lamb ductus arteriosus smooth muscle cell migration by indomethacin and dexamethasone. *Pediatr Res* 33: 352-358, 1993.
520. **Vucovich M, Ehinger N, Poole SD, Lamb FS, and Reese J**. Spontaneous Rhythmic Contractions (Vasomotion) of the Isolated, Pressurized Ductus Arteriosus of Preterm, but Not Term, Fetal Mice. *EJ Neonatol Res* 2: 13-24, 2012.
521. **Elliott RB, Starling MB, and Neutze JM**. Medical manipulation of the ductus arteriosus. *Lancet* 1: 140-142, 1975.
522. **Olley PM, Coceani F, and Bodach E**. E-type prostaglandins: a new emergency therapy for certain cyanotic congenital heart malformations. *Circulation* 53: 728-731, 1976.
523. **Heymann MA, and Rudolph AM**. Ductus arteriosus dilatation by prostaglandin E1 in infants with pulmonary atresia. *Pediatrics* 59: 325-329, 1977.
524. **Thanopoulos BD, Andreou A, and Frimas C**. Prostaglandin E2 administration in infants with ductus-dependent cyanotic congenital heart disease. *Eur J Pediatr* 146: 279-282, 1987.
525. **Zhang H, Gu S, Al-Sabeq B, Wang S, He J, Tam A, Cifelli C, Mathalone N, Tirgari S, Boyd S, and Heximer SP**. Origin-specific epigenetic program correlates with vascular bed-specific differences in Rgs5 expression. *FASEB J* 26: 181-191, 2012.
526. **Gao Q, Zhan P, Alander CB, Kream BE, Hao C, Breyer MD, Pilbeam CC, and Raisz LG**. Effects of global or targeted deletion of the EP4 receptor on the response of osteoblasts to prostaglandin in vitro and on bone histomorphometry in aged mice. *Bone* 45: 98-103, 2009.
527. **Kraemer MP, Choi H, Reese J, Lamb FS, and Breyer RM**. Regulation of arterial reactivity by concurrent signaling through the E-prostanoid receptor 3 and angiotensin receptor 1. *Vascul Pharmacol* 84: 47-54, 2016.
528. **Moir LM, Ward JP, and Hirst SJ**. Contractility and phenotype of human bronchiole smooth muscle after prolonged fetal bovine serum exposure. *Exp Lung Res* 29: 339-359, 2003.
529. **Asai D, Kawano T, Murata M, Nakashima H, Toita R, and Kang JH**. Effect of Fetal Bovine Serum Concentration on Lysophosphatidylcholine-mediated Proliferation and Apoptosis of Human Aortic Smooth Muscle Cells. *J Oleo Sci* 69: 255-260, 2020.
530. **Lee KJ, Hinek A, Chaturvedi RR, Almeida CL, Honjo O, Koren G, and Benson LN**. Rapamycin-eluting stents in the arterial duct: experimental observations in the pig model. *Circulation* 119: 2078-2085, 2009.

531. **Li M, Ye L, Ye X, Wang S, Zhang H, Liu J, and Hong H**. Hypoxia-induced ARHGAP26 deficiency inhibits the proliferation and migration of human ductus arteriosus smooth muscle cell through activating RhoA-ROCK-PTEN pathway. *J Cell Biochem* 120: 10106-10117, 2019.
532. **Bentley RET, Hindmarch CCT, Dunham-Snary KJ, Snetsinger B, Mewburn JD, Thebaud A, Lima PDA, Thebaud B, and Archer SL**. The molecular mechanisms of oxygen-sensing in human ductus arteriosus smooth muscle cells: A comprehensive transcriptome profile reveals a central role for mitochondria. *Genomics* 113: 3128-3140, 2021.
533. **Gong MC, Cohen P, Kitazawa T, Ikebe M, Masuo M, Somlyo AP, and Somlyo AV**. Myosin light chain phosphatase activities and the effects of phosphatase inhibitors in tonic and phasic smooth muscle. *J Biol Chem* 267: 14662-14668, 1992.
534. **Muranyi A, Derkach D, Erdodi F, Kiss A, Ito M, and Hartshorne DJ**. Phosphorylation of Thr695 and Thr850 on the myosin phosphatase target subunit: inhibitory effects and occurrence in A7r5 cells. *FEBS Lett* 579: 6611-6615, 2005.
535. **Macmillan D, and McCarron JG**. The phospholipase C inhibitor U-73122 inhibits Ca(2+) release from the intracellular sarcoplasmic reticulum Ca(2+) store by inhibiting Ca(2+) pumps in smooth muscle. *Br J Pharmacol* 160: 1295-1301, 2010.
536. **Saleem H, Tovey SC, Molinski TF, and Taylor CW**. Interactions of antagonists with subtypes of inositol 1,4,5-trisphosphate (IP3) receptor. *Br J Pharmacol* 171: 3298-3312, 2014.
537. **Fujino H**. The Roles of EP4 Prostanoid Receptors in Cancer Malignancy Signaling. *Biol Pharm Bull* 39: 149-155, 2016.
538. **Karpisheh V, Joshi N, Zekiy AO, Beyzai B, Hojjat-Farsangi M, Namdar A, Edalati M, and Jadidi-Niaragh F**. EP4 receptor as a novel promising therapeutic target in colon cancer. *Pathol Res Pract* 216: 153247, 2020.
539. **Ye Y, Wang X, Jeschke U, and von Schonfeldt V**. COX-2-PGE(2)-EPs in gynecological cancers. *Arch Gynecol Obstet* 301: 1365-1375, 2020.
540. **Dennis G, Jr., Sherman BT, Hosack DA, Yang J, Gao W, Lane HC, and Lempicki RA**. DAVID: Database for Annotation, Visualization, and Integrated Discovery. *Genome Biol* 4: P3, 2003.
541. **Szklarczyk D, Gable AL, Lyon D, Junge A, Wyder S, Huerta-Cepas J, Simonovic M, Doncheva NT, Morris JH, Bork P, Jensen LJ, and Mering CV**. STRING v11: protein-protein association networks with increased coverage, supporting functional discovery in genome-wide experimental datasets. *Nucleic Acids Res* 47: D607-D613, 2019.
542. **Flinsenberg TW, van der Sterren S, van Cleef AN, Schuurman MJ, Agren P, and Villamor E**. Effects of sex and estrogen on chicken ductus arteriosus reactivity. *Am J Physiol Regul Integr Comp Physiol* 298: R1217-1224, 2010.
543. **Boatwright NH, Sorenson C, Israel S, Yarboro MT, Su R, Tolentino CD, Paria BC, Clark RH, Shelton EL, and Reese J**. Limited contribution of sex and sex hormones to regulation of the mouse ductus arteriosus (DA) and human PDA. *EPAS2022:* 211.220: 2022.
544. **Borges-Lujan M, Gonzalez-Luis GE, Roosen T, Huizing MJ, and Villamor E**. Sex Differences in Patent Ductus Arteriosus Incidence and Response to Pharmacological Treatment in Preterm Infants: A Systematic Review, Meta-Analysis and Meta-Regression. *J Pers Med* 12: 2022.
545. **Villamor E, Borges-Lujan M, and Gonzalez-Luis G**. Association of patent ductus arteriosus with fetal factors and endotypes of prematurity. *Semin Perinatol* 47: 151717, 2023.
546. **Crockett SL, Harris M, Boatwright N, Su RL, Yarboro MT, Berger CD, Shelton EL, Reese J, and Segar JL**. Role of dopamine and selective dopamine receptor agonists on mouse ductus arteriosus tone and responsiveness. *Pediatr Res* 87: 991-997, 2020.
547. **Guan Y, Zhang Y, Wu J, Qi Z, Yang G, Dou D, Gao Y, Chen L, Zhang X, Davis LS, Wei M, Fan X, Carmosino M, Hao C, Imig JD, Breyer RM, and Breyer MD**. Antihypertensive effects of selective prostaglandin E2 receptor subtype 1 targeting. *J Clin Invest* 117: 2496-2505, 2007.
548. **Sun Y, Zhang Y, Zhu Y, Zhang A, Huang S, Yin X, Ding G, Liu M, and Jia Z**. Inhibition of mitochondrial complex-1 restores the downregulation of aquaporins in obstructive nephropathy. *Am J Physiol Renal Physiol* 311: F777-F786, 2016.

549. **Ma X, Aoki T, Tsuruyama T, and Narumiya S**. Definition of Prostaglandin E2-EP2 Signals in the Colon Tumor Microenvironment That Amplify Inflammation and Tumor Growth. *Cancer Res* 75: 2822-2832, 2015.
550. **Li C, Liu X, Liu Y, Zhang E, Medepalli K, Masuda K, Li N, Wikenheiser-Brokamp KA, Osterburg A, Borchers MT, Kopras EJ, Plas DR, Sun J, Franz DN, Capal JK, Mays M, Sun Y, Kwiatkowski DJ, Alayev A, Holz MK, Krueger DA, Siroky BJ, and Yu JJ**. Tuberin Regulates Prostaglandin Receptor-Mediated Viability, via Rheb, in mTORC1-Hyperactive Cells. *Mol Cancer Res* 15: 1318-1330, 2017.
551. **Machwate M, Harada S, Leu CT, Seedor G, Labelle M, Gallant M, Hutchins S, Lachance N, Sawyer N, Slipetz D, Metters KM, Rodan SB, Young R, and Rodan GA**. Prostaglandin receptor EP(4) mediates the bone anabolic effects of PGE(2). *Mol Pharmacol* 60: 36-41, 2001.
552. **Xu S, Zhang Z, Ogawa O, Yoshikawa T, Sakamoto H, Shibasaki N, Goto T, Wang L, and Terada N**. An EP4 antagonist ONO-AE3-208 suppresses cell invasion, migration, and metastasis of prostate cancer. *Cell Biochem Biophys* 70: 521-527, 2014.
553. **Toyoshima K, Takeda A, Imamura S, Nakanishi T, and Momma K**. Constriction of the ductus arteriosus by selective inhibition of cyclooxygenase-1 and -2 in near-term and preterm fetal rats. *Prostaglandins Other Lipid Mediat* 79: 34-42, 2006.
554. **Katsuda S, Okada Y, Nakanishi I, and Tanaka J**. Inhibitory effect of dimethyl sulfoxide on the proliferation of cultured arterial smooth muscle cells: relationship to the cytoplasmic microtubules. *Exp Mol Pathol* 48: 48-58, 1988.
555. **Galvao J, Davis B, Tilley M, Normando E, Duchen MR, and Cordeiro MF**. Unexpected low-dose toxicity of the universal solvent DMSO. *FASEB J* 28: 1317-1330, 2014.

Appendix

MATERIALS AND METHODS

Microarray Meta-Analysis:

Microarray data were obtained from NCBI's Gene Expression Omnibus (GEO) database (**Table 1**). All available studies were considered, but only investigations that included a DA/Ao comparison were selected for analysis. For the array data from Bokenkamp *et al.(119),* values for E21 laser micro-dissected endothelium and smooth muscle cells were pooled. For the array data from Hseih *et al.(120)*, only the F344 control samples were considered. CEL files of selected data sets were evaluated in Partek Genomics Suite version 7.17.1222 (Partek Inc.). All data were normalized using the Robust Multi-Array (RMA) method. One-way ANOVA was used to analyze contrasts of interest, namely vessel type, to generate lists of DEGs between DA and Ao. Permissive DEG lists (fold change ≥1.2) were then separated by increased or decreased DA/Ao expression to generate UP and DOWN lists respectively. A naïve vote counting strategy was used to evaluate consistency between studies. Shared genes between UP lists or DOWN lists from each study were determined using Partek Genomics Suite 6.6 (2016).

RNA-seq Analysis:

Previable (21 - 21 5/7 weeks gestation) tissue samples for human RNA-seq analysis were obtained as previously described (383). Tissues were homogenized in Trizol with the IKA

T10 basic Ultra-Turrax. Total RNA was isolated using the RNeasy Mini kit (Qiagen). RNA quality was assessed using the Agilent 2100 Bioanalyzer. RNA samples with RIN score ≥6.5 were considered for further study. 1 microgram of total RNA was used for library construction using the ScriptSeq Complete Gold Kit (Illumina). The libraries, four biological replicates per vessel type, were sequenced on an Illumina HiSeq 2000 by 100bp pair-end sequencing. RNA-seq data was uploaded to Partek Flow (Partek Inc.). Trimming of raw reads (both ends) was based on a minimum read length of 25 and discarded bases after 85. Trimmed reads were aligned to Human Genome Version 38 (hg38) using STAR – 2.5.3a and quantified to Refseq Transcripts 83 using Partek's E/M method. Aligned counts were FPKM normalized with an offset of 1. Gene specific analysis (GSA) was used to detect DA vs. Ao DEGs. DEGs with an FDR of ≤0.1 and a fold change ≥2 were considered significant. Volcano plot and dendrogram heat map figures were generated using Partek Flow 7.0 (2016).

Comparison of Microarray and RNA-seq DEGs:

Rodent gene symbols were converted to human orthologues using biological Database network (bioDBnet) to identify genes common between microarray and RNA-seq DEG lists. Lists were manually aligned to determine genes differentially expressed in both microarray and RNA-seq analyses. Microarray and RNA-seq gene lists were submitted independently for functional annotation using the Database for Annotation, Visualization, and Integrated Discovery (DAVID). Functional terms from GO Biological Process (BP), GO Cellular Component (CC), GO Molecular Function (MF), Kyoto Encyclopedia of Genes and Genomes (KEGG), and UniProt (UP) Keywords databases were evaluated for similarities. Lists of

functional terms and keywords from each database were then manually aligned. In order to create comparison diagrams, significant terms ($p \leq 0.05$) were chosen based on count (defined as number of genes identified in each term), and ordered by –Log(p value).

Identification of Human Single Gene Syndromes Associated with PDA:

Transgenic models of PDA in mice were identified by literature search (PubMed, Google Scholar) and examination of mouse phenotype repositories (Mouse Phenome Database, Jackson Laboratories; the International Mouse Phenotyping Consortium) using variations of the following search terms: persistent ductus arteriosus, patent ductus arteriosus, patent arterial duct, or ductus Botalli. Data on human genetic syndromes were extracted from the Online Mendelian Inheritance in Man (OMIM) database (Johns Hopkins University) using similar search terms, resulting in over 450 entries. Filtering the results to those with a phenotypic description and known molecular basis yielded approximately 300 entries. This human gene list was cross-referenced to additional open-access phenotype-based databases (Human Phenotype Ontology and the Monarch Initiative, DisGeNET, FindZebra, GeneReviews, GeneCards/MalaCards, UniProtKB) and manually reviewed to generate a non-redundant list of 224 single-gene syndromes associated with PDA. Mouse and human gene lists were compared for similarity. BioDBnet was used as a resource to identify and convert homologues. A curated human gene list (GeneReviews) was used to avoid overfitting of gene comparisons and provide additional clinical insights. PDA-associated genes in mice and human single-gene syndromes were compared by functional annotation (DAVID, Database for Annotation, Visualization, and Integrated Discovery (540)).

Construction of a Protein-Protein Network:

Candidate effectors identified in human single-gene syndromes were assessed for protein-protein interactions (PPI) through STRING functional proteins association network software v11.0 (541). The 224 human genes were input to the STRING database of known and predicted protein-protein interactions, including direct (physical) and indirect (functional) associations. The STRING settings included: 1) full network, 2) all active interaction sources, 3) network edge thickness was set to the confidence score of the PPI, and 4) a minimum interaction score of 0.7, which represents a high confidence level. The resulting network of 219 proteins (nodes) contained 256 interactions (edges) with a PPI enrichment P-value less than 1.0e-16. This network was exported to Cytoscape 3.8.2 for further analysis and visualization. The network was analyzed as an undirected graph and network statistics were generated. Of these, we used betweenness centrality to control node size via continuous mapping. The STRING interaction score was used to control edge thickness, transparency and type (dotted vs solid). In order to visually highlight the strongest associations, solid lines were assigned to interaction scores of 0.9 or higher, and dotted lines to scores less than 0.9. For layout, we used a combination of a forced directed layout on the entire graph as well as yFiles organic edge router. Layout was then manually optimized to minimize label crowding and increase legibility. 71 proteins without high confidence interactions were removed from the graph, resulting in a final network of 148 proteins. The graph was then exported to Adobe Illustrator for final refinements.

Animals:

Animal studies were conducted in accordance with approved standards of the Vanderbilt Institutional Animal Care and Use Committee and the National Institutes of Health. CD1 and C57BL/6J WT mice were acquired at reproductive age from The Jackson Laboratory (Bar Harbor, ME). *Ptger4* (+/-) mouse lines were established with permission from Drs. Breyer (110) and Narumiya (109) (CARD, Kumamoto, Japan) and are henceforth designated B6.129S6-*Ptger4*$^{tm1.2Matb}$ and B6;129-*Ptger4*^{tm1Sna} respectively. Both models were maintained on a C57BL/6J background. The B6.129S6-*Ptger4*$^{tm1.2Matb}$ null allele was crossed onto a CD1 background via 10 generation outcross as previously described (106, 527). KO animals were generated by timed mating of EP_4 (+/-) breeders from 0700-1000hrs with a vaginal plug designated as D1 (days post copulation). All litters were delivered via caesarean section after maternal injection of 0.3mL of 1.25% avertin (2,2,2-tribromoethanol in tert-amyl alcohol, Sigma-Aldrich) and brief isoflurane inhalation to ensure adequate fetal anesthesia, followed by cervical dislocation of the dam. In some studies, one uterine horn of anesthetized D17 pregnant females was briefly exteriorized to permit transuterine injection of selective receptor antagonists into the fetal peritoneal cavity. Dams were allowed to recover and ambulate for 30 min prior to euthanasia. For these experiments, drugs were tinted with Chicago blue B dye to document accurate fetal i.p. administration at the time of necropsy. Comprehensive studies on sex differences in mouse and chick models of PDA (542, 543) do not show evidence of sexual dimorphism. Moreover, there are no sex differences in PDA incidence nor response to pharmacological treatment in preterm infants with PDA (544, 545), thus, no exclusions were made on the basis of sex, and male and female mice were included in all studies at their natural sex distribution which have approximately equal values in our animal colony.

Quantitative real-time RT-PCR:

The DA and similarly-sized Ao segments were collected from whole C57BL/6J litters and pooled by tissue with a minimum of three litters per time point (D15-19). EP_4 KO DA and Ao were collected individually and pooled later for three samples representing a minimum of five litters. RNA was extracted using TRIzol (Life Technologies) and bead homogenization (BeadMill24, Fischer Scientific) with cDNA generated by SuperScript VILO cDNA Synthesis Kit (Invitrogen). RT-qPCR was performed using the StepOne Plus Real-Time PCR System and software, with TaqMan Fam-tagged primers (**Table S1**) and Vim-tagged 18S housekeeping standards (Applied Biosystems). Three technical replicates (ΔΔCT) were utilized. Fold change was calculated by setting D15 *Ptger1* expression (for time course), WT littermate expression (for genotype), D17 expression (for maturity markers) or DA/Ao expression (for strain) as indexed values to 1.

Vessel Myography:

Fetuses were delivered on D19 via terminal caesarean section, their thoracic cavities opened, and submerged in chilled and deoxygenated modified Kreb's buffer (in mM; 109NaCl, 4.7 KCl, 2.5 $CaCl_2 2H_2O$, 0.9 $MgSo_4$, 1.0 KH_2PO_4, 11.1 glucose, 34 $NaHCO_3$ (pH 7.3)) as previously described (546). Fresh DA tissue was excised, mounted in custom myography chambers (University of Vermont), and maintained at 37.5C under deoxygenated conditions. Vasoreactivity of vessels was assessed via pressurized-vessel myography as previously described (201). Vessels were maintained at 5mmHg for 40 min before being raised in 10 min, 5mmHg steps to physiological pressure of 20mmHg. Vessels were then subjected to two 10 min exposures to 50mM KCl under deoxygenated constrictions to verify reactivity and integrity.

Lumen diameter was recorded via inverted light microscope and video capture and analysis (IonOptix). The response to pharmacological agents or changes in gas concentrations were assessed by altering conditions in a 20mL recirculating volume. Studies were performed on a minimum of 6-8 vessels representing at least three litters. Findings are presented as percent change, percent reversal from a pre-constricted baseline, or average lumen diameter.

Inhibitor Studies:

Drugs and compounds were administered to pregnant dams or pups at different gestational time points and with varying methodologies (**Figure 1**)**.** Protocol A and C addressed acute drug effects on the fetal DA, protocol B addressed *acute* effects on the neonatal DA, and protocols D-G addressed *chronic* effects on the fetal DA. In protocol A, selective antagonists of the EP receptors EP_1 (SC-51322, 10mg/kg/dose once (547, 548); i.p.; TOCRIS), EP_2 (PF-04418948, 10mg/kg/dose once; i.p (549); TOCRIS), EP_3 (L-798,106, 5mg/kg/dose once (550); i.p.; TOCRIS), and EP_4 (L-161,982, 100mg/kg/dose once hourly, 4 total (551) (originally 10mg/kg/dose once, 1 total, but increased to 4 total doses due to short *in vivo* half-life); i.p.; TOCRIS; or AE3-208, 10mg/kg/dose once; i.p.; ONO Pharmaceuticals) (400, 552) were administered to CD1 WT dams at 0800 on the morning of D19. Four hours later, pups were delivered via caesarean section, their chests opened, and their DAs visually scored for percent patency by a single observer (M.T.Y. or N.B.) blinded to treatment group, using a 5-point non-continuous scale (0%, 25%, 50%, 75%, 100%) comparing the DA to the main pulmonary artery as previously described (1, 55, 61, 106, 196, 200). Visual scoring renders immediate determination of DA patency and corresponds to measurements from histological scoring (196, 197). Dosage and timing of AE3-208 administration was based on previously published optimization studies (400). The 4h incubation time between drug

administration and DA scoring was based on previous COX inhibitor and EP_4 receptor antagonist studies in pregnant rodents (195, 400, 553) and the 3-6h period of time required for normal DA constriction after birth (366). For protocol B, CD1 WT litters were delivered at 0800 on the morning of D19, resuscitated and maintained on a 37.5C warming pad. At 30m after birth, pups were administered PGE_2 (10ug/kg/dose once hourly, 4 total; 13ul i.p.; TOCRIS) or an EP_4 selective agonist (TCS2510 10ug/kg/dose once hourly, 4 total; 13ul i.p.; TOCRIS). After 4hrs, pups were euthanized via isoflurane inhalation and their DAs scored. Terminal isoflurane exposure was considered to have less effect on vessel diameter than alternative euthanasia methods. In addition, pups in control and treatment groups were treated similarly, minimizing the effect of anesthetic choice. Protocol C utilized C57BL/6J dams administered either an EP_4 selective antagonist (AE3-208, 10mg/kg/dose once; 0.2ml gavage) or a NO synthase inhibitor (L-NAME, 180mg/kg/dose once; 0.2ml gavage; Cayman) at 0800 on the morning of a day of pregnancy (D15-D19). At 4hrs after gavage, pups were delivered via caesarean section and their DAs scored. For protocol D, C57BL/6J dams were administered a selective EP_4 antagonist (AE3-208, 100mg/kg/dose twice daily; 0.2ml gavage) at 0800 and 2000 during discrete windows of pregnancy (D: D15-19, E: D17-19, F: D14-16, G: D11-13). For protocols D and E, a final dose was administered at 0800 on D19. All litters delivered and their DAs were scored at 1200. Pups were delivered via caesarean section, resuscitated, and placed on a warming pad heated to 37.5C. After 4hrs, pups were euthanized and their DAs scored. Those who died in less than 2hrs after birth were excluded from further analysis.

Cultured Primary Cells:

Anesthetized CD1 WT pups were delivered via caesarean section and their DA and Ao tissues quickly explanted via dissection. Breathing pups were excluded and euthanized

humanely. Explants were submerged in Dulbecco's Modified Eagle's Medium (Gibco) supplemented with 10% FBS (Atlanta Biologicals) and 2% penicillin/streptomycin (Gibco) warmed to 37.5C. Explants were further cleaned to remove the endothelium and adventitial layer and cut along their length. These medial layer explants were then transferred to a sterile 12-well culture plate (Denville) with fresh, warmed, media and gently pressed into the plastic of the well. Three explants were cultured per well in copper-lined incubators (HeraCell) at 37.5C and normoxia with 5% CO_2 and frequent media changes (every other day). Explants were allowed to grow until a wide corona of cells was present. Explants were then removed from the well using an aspirating pipette, the cells rinsed three times with cold PBS (Corning) and lifted with 0.25% trypsin (Gibco). *For wound healing assays*, P2 cells were seeded into a new 12-well plate at 500 cells per well and allowed to grow until a uniform monolayer formed. Cells were then serum starved for 24hrs, and scratched with a 200ul pipette tip, rinsed twice with serum free media, and given media supplemented with an EP_4 selective antagonist (AE3-208, 10uM)(552) or DMSO (3ul/ml; Sigma-Aldrich) vehicle control (T1). DMSO concentration was minimized (≤0.3%) to limit adverse effects (554, 555). Images were taken immediately following and 24hrs after wound creation (T2). Images were analyzed with NIH ImageJ software to determine wound closure. *For immunohistochemistry*, P1 cells were seeded into a 4-well glass bottomed chamber slide (Lab-Tek II; Thermo-Fisher) at 1000 cells per well and allowed to attach for 24hrs. Cells were then rinsed with PBS, fixed with 4% PFA (Fisher) for 15 min, rinsed with PBS for 45 min. Cells were blocked for 1hr at room temp (90ml PBS, 10ml goat serum (R&D Systems), 100ul triton x (Thermo-Fisher)). Cells were incubated in Caldesmon (1:100; Abcam) and α-SMA (1:250; Sigma) primary antibodies in goat blocking serum overnight at 4C. Cells were washed for an hour with PBS then incubated in GαR Alexa Fluor 488 (1:2000, green; Abcam) and GαM Alexa Fluor 568 (1:2000, red; Abcam) secondary

antibodies diluted in goat blocking serum with DAPI (0.1ug/ml; Thermo-Fisher) for 3hrs at room temp. Cells were then washed with PBS for 30 min, coverslipped with aqueous mounting media, and imaged with an epifluorescence microscope.

RNA in-situ hybridization:

Anesthetized CD1 WT pups were delivered via caesarean section, their thoracic cavities opened, and their bodies submerged in cold deoxygenated Kreb's buffer. Whole outflow tracts were extracted, fixed in 10% phosphate buffered formalin (Fisher) for 30 min, dehydrated in a 4-point ethanol series (Fisher), cleared for 5 min with xylenes (Fisher), and embedded in paraffin blocks. Microtome sections (~8um) were obtained (Thermo Scientific, Shandon Finesse 325) and floated onto slides.

Fixed paraffin slides containing 8um tissue sections from D19 CD1 WT outflow tracts were pre-treated according to ACD's standard RNAscope protocol (Pretreatment Kit 4, ACD). Target probes against transcripts of murine *Ptger4* (Mm-Ptger4-C3 Mus musculus, transcript variant 1, #441461-C3, ACD) and kit-based (RNAscope Multiplex Fluorescent Reagent Kit v2, ACD) preamplifier, amplifier, and fluorescent labeled probes (Atto 550, Orange, ACD) were subsequently hybridized and results visualized via epifluorescence microscopy. Traditional RNA *in situ* hybridization using ^{35}S-labelled sense and antisense probes for *Ptger1*, *Ptger3*, and *Ptger4* was performed as previously described (106).

Hyperoxia Studies:

Litters produced by EP_4 (+/-) intermatings were delivered via caesarean section, resuscitated, and placed inside a mouse isolation chamber supplemented with humidified medical grade O_2 to a concentration of ~80% O_2. Pups were euthanized via isoflurane inhalation after 4hrs and their DAs scored. For 24 and 48hr studies, pups were delivered as described, then fostered to a CD1 WT dam and maintained in hyperoxia chambers for up to two days. Pups that died in less than 2hrs after birth were excluded from further analysis.